Reports of the Department of Geodetic Science

Report No. 284

ESTIMABILITY AND SIMPLE DYNAMICAL ANALYSES OF RANGE (RANGE-RATE AND RANGE-DIFFERENCE) OBSERVATIONS TO ARTIFICIAL SATELLITES

(NASA-CR-158843) ESTIMABILITY AND SIMPLE DYNAMICAL ANALYSES OF RANGE (RANGE-RATE RANGE-DIFFERENCE) OBSERVATIONS TO ARTIFICIAL SATELLITES (Ohio State Univ. Research Foundation) 286 p HC A13/MF A01 CSCL 22A G3/15

N79-28211

Unclas 29416

Prepared for

National Aeronautics and Space Administration
Goddard Space Flight Center
Greenbelt, Maryland 20770

Grant No. NSG 5265
OSURF Project 711055

The Ohio State University
Research Foundation
Columbus, Ohio 43212

AUG 1979
RECEIVED
NASA STI FACILITY
ACCESS DEPT.

December, 1978

PREFACE

This project is under the supervision of Professor Ivan I. Mueller, Department of Geodetic Science, The Ohio State University, and under the technical direction of Dr. David E. Smith, Code 921, NASA, Goddard Space Flight Center, Greenbelt, Maryland 20771.

This report was submitted to the Graduate School of The Ohio State University as partial fulfillment of the requirements for the Ph.D. degree.

ABSTRACT

The estimable quantities are indicated for simple dynamical analyses of range (range-rate and range-difference) observations to artificial satellites.

The philosophy of the analysis is based on non-Bayesian statistics. Not only no a priori knowledge for the parameters (in terms of probabilities) is assumed, but also the mathematical models are developed with unconditional estimable parameters (avoiding minimum constraints). It is argued that the Bayesian approach might lead to too optimistic results.

In particular, the simulation studies centered around laser range observations to LAGEOS. The capabilities of satellite laser ranging especially in connection with relative station positioning are evaluated. The satellite measurement system under investigation may fall short in precise determinations of the earth's orientation (precession and nutation) and the earth's rotation (UT1) as opposed to systems as Very Long Baseline Interferometry (VLBI) and Lunar Laser Ranging (LLR). Relative station positioning, determination of (differential) polar motion, positioning of stations with respect to the earth's center of mass and determination of the earth's gravity field should be easily realized by Satellite Laser Ranging (SLR). The last two features

should be considered as best (or solely) determinable by SLR in contrast to VLBI and LLR.

ACKNOWLEDGEMENTS

In the first place I wish to express my gratitude to Professor Ivan I. Mueller whose academic guidance during these years greatly deepened my understanding and guaranteed that my years at Ohio State University found, at last, its result in this more tangible product. In this respect, my thanks need to be extended to the other members of the reading committee Professors Richard H. Rapp, Urho A. Uotila and Thomas A. Willke for their valuable suggestions and criticism ensuring that the defense of the dissertation can be called everything but the anticlimax of my stay at the Department of Geodetic Science. It is also this department personified in its faculty, staff and students who have greatly influenced my way of thinking through classes and discussions.

Financial support in the form of a two year fellowship given jointly by the Netherlands' Ministry of Education and Sciences and under the NASA International University Fellowship Program is greatly acknowledged. Especially, the help of Messrs. C.W.J. Wamsteeker and H. W. Magoun in this respect has been very much appreciated. I am also grateful to the extensive computer support provided by the Instruction and Research Computer Center of The Ohio State University and to the extensive financial support from the National Aeronautics and Space Administration, under contracts NGR 36-008-204 and NSG 5265.

The resulting Ohio State University Graduate Research and Teaching Associateships provided an unequaled educational experience.

I am greatly indebted to my wife, Annelies, and my children, Klaasjan and Roderick for their encouragement, love and not in the last place patience which sustained me during my years of study.

Special thanks is extended to Mrs. Linda M. Wright for the excellent typing of the long text with innumerable formulae.

Finally, while recognizing that it is impossible to mention everybody, still these thanks are extended to all of those who made the stay of my family and me in the United States an unforgettable one.

TABLE OF CONTENTS

	Page
PREFACE	ii
ABSTRACT	iii
ACKNOWLEDGEMENTS	v
LIST OF TABLES	xii
LIST OF FIGURES	xv
1. INTRODUCTION	1
1.1 Philosophy of the Investigation	1
1.2 Historical Background	3
1.3 Scope of the Investigation	5
2. REFERENCE FRAMES AND SOME UNDERLYING ASSUMPTIONS	8
2.1 Introduction	8
2.2 The Inertial Reference Frame	10
2.3 The Instantaneous Terrestrial Reference Frame	11
2.4 The Axis of Figure Frame	12
2.5 The Establishment of World Wide and Regional Geodetic Reference Frames	13
3. THE INTERMEDIATE ORBIT	18
3.1 Introduction	18
3.2 Two Dimensional Circular Motion	19
3.2.1 GM (or n) Unknown	19
3.2.2 GM (or n) Known	23
3.3 Three Dimensional Circular Motion	26
3.3.1 GM (or n) Unknown	26
3.3.2 GM (or n) Known	33
3.4 Two Dimensional Elliptic Motion	35
3.4.1 GM (or n) Unknown	35
3.4.2 GM (or n) Known	40

Page

3.5 Three Dimensional Elliptic Motion 40
3.5.1 GM (or n) Unknown 41
3.5.2 GM (or n) Known 43

3.6 Three Dimensional Secularly Perturbed Elliptic Motion 43
3.6.1 GM (or n) and J_2 (or $\dot{\omega}$, $\dot{\Omega}$, n) Unknown 44
3.6.2 GM (or n) and J_2^2 (or $\dot{\omega}$, $\dot{\Omega}$, n) Known 47

3.7 Summary 49

4. ORBIT, OBSERVER AND OBSERVATIONS 52

4.1 Introduction 52
4.2 The Clock Problem 54
4.3 Satellite-, Station- and Earth Parameters 61
4.3.1 Satellite Parameters 61
4.3.2 Station Parameters 62
4.3.3 Earth Parameters 64

4.4 The Circular Intermediate Orbit, Station and Earth Rotation/Orientation Determination from Range Observations 65
4.4.1 Two Dimensional Case with GM (or n) Unknown 65
4.4.2 Two Dimensional Case with GM (or n) Known . . . 66
4.4.3 Three Dimensional Case with GM (or n) Unknown 67
4.4.4 Three Dimensional Case with GM (or n) Known 69
4.4.5 Three Dimensional Case, Alternate Approach . . 70

4.5 The Elliptic Intermediate Orbit, Station and Earth Rotation/Orientation Determination from Range Observations 73
4.5.1 Two Dimensional Case with GM (or n) Unknown 73
4.5.2 Two Dimensional Case with GM (or n) Known . . 75
4.5.3 Three Dimensional Case with GM (or n) Unknown 76
4.5.4 Three Dimensional Case with GM (or n) Known 78

4.6 The Secularly Perturbed Elliptic Intermediate Orbit, Station and Earth Rotation/Orientation Determination from Range Observations 79
4.6.1 GM (or n) and J_2 (or $\dot{\omega}$, $\dot{\Omega}$, n) Unknown 79

Page

4.6.2 GM (or n) and J_2 (or $\dot{\omega}$, $\dot{\Omega}$, n) Known 82

4.7 The Intermediate Orbit, Station and Earth Rotation/Orientation Determination from Range-Rate Observations 84

4.7.1 Three Dimensional Circular Intermediate Orbit 84

4.7.2 Three Dimensional Elliptic Intermediate Orbit 85

4.7.3 Three Dimensional Secularly Perturbed Elliptic Intermediate Orbit 86

4.8 The Intermediate Orbit, Station and Earth Rotation/Orientation Determination from Range-Difference Observations 88

4.9 Summary 89

5. VALIDATION OF AND REFINEMENTS TO THE OBSERVATION MODELS . . . 92

5.1 Introduction 92

5.2 The Influence of Weighting on Parameter Estimation . 93

5.2.1 Strong Weighting or Absolute Constraining of Estimable Parameters 94

5.2.2 Moderate Weighting of Estimable Parameters . . 95

5.2.3 Weighting of Non-Estimable Parameters 100

5.3 Is Kepler's Law a Law? 106

5.4 The Influence of the Gravity Field and Polar Motion on Satellite Orbits 108

5.4.1 Polar Motion 109

5.4.2 Polar Motion and the Gravity Field 113

5.4.3 Estimability of the Potential Coefficients . . 121

5.5 Time, Time Synchronization and Estimability 123

6. NUMERICAL EXPERIMENTS AND RESULTS 125

6.1 Introduction 125

6.2 The Experiments 126

6.2.1 The Satellite and Types of Orbit 126

6.2.2 The Stations and Observation Campaigns 128

6.2.3 Modes of Analysis 133

6.2.4 The Observations and Their Accuracies 136

6.2.5 The Earth 140

6.3 Testing Procedure 141

6.4 Standard Deviations of the Parameters as a Function of the Number of Observations per Pass and the Precision of the Single Range Measurements 144

6.5 Baseline Precision as a Function of the Orbital Geometry (Shape and Length) 145

Page

6.5.1 Long Arc Analysis (1 day, 6 passes, 4 stations) 146
6.5.2 Long Arc Analysis (4-1/2 hours, 2 passes, 4 stations) 148

6.6 Baseline Precision as a Function of the Number of Stations 150
6.6.1 All Stations Observing Each Pass 151
6.6.2 Some Stations Observing Each Pass 152

6.7 Short Arc Mode 154
6.7.1 Short Arc Mode, One Pass at a Time 155
6.7.2 Short Arc Mode, Several Passes at a Time . . . 157
6.7.3 The Influence of Weighting in the Short Arc Mode 161
6.7.4 The Influence of the Cut Off Angle 164

6.8 Geometric Mode 166
6.9 Precision of Parameters Not Directly Related to Station Positioning 169
6.9.1 Length of Day/UT 1 Determination 170
6.9.2 Polar Motion Determination 174

6.10 The Influence of Constraints on GM (and J_2) 177
6.11 Range, Range-Rate and Range-Difference Observations . 185

7. SUMMARY AND CONCLUSIONS 188

APPENDIX A: Differential Formulas in Orbit Determination in the Orbit Plane 193

A.1 Introduction 193
A.2 Geocentric Orbital Coordinates 193
A.3 Kepler's Equation and the Intermediate Variables E and $\dot{E}$ 194
A.3.1 GM (or n) Unknown 195
A.3.2 GM (or n) Known 199
A.3.3 Secular Perturbations due to J_2 (GM and J_2 Known) 203

A.4 Cartesian Orbital Elements and the Intermediate Variables E and $\dot{E}$ 209
A.4.1 Range and Range-Difference Observations . . . 209
A.4.2 Range-Rate Observations 209

A.5 Cartesian Orbital Elements 210
A.5.1 GM (or n) Unknown (Parameters a, e, E_o, n) . . 210
A.5.2 GM (or n) Known (Parameters a, e, E_o) 215
A.5.3 Secular Perturbations due to J_2 (GM and J_2 Known) (Parameters a, e, i, E_o) 219

Page

APPENDIX B: Observation Equations for Range, Range-Rate and Range-Difference Observations 224

B.1 Introduction 224

B.2 Two Dimensional Circular Motion in Case of Range Observations 224

B.2.1 GM (or n) Unknown 224

B.2.2 GM (or n) Known 226

B.3 Three Dimensional Circular Motion in Case of Range Observations 227

B.3.1 GM (or n) Unknown 227

B.3.2 GM (or n) Known 229

B.4 Two Dimensional Elliptic Motion in Case of Range Observations 231

B.4.1 GM (or n) Unknown 231

B.4.2 GM (or n) Known 233

B.5 Three Dimensional Elliptic Motion in Case of Range Observations 236

B.5.1 GM (or n) Unknown 236

B.5.2 GM (or n) Known 239

B.6 Three Dimensional Secularly Perturbed Elliptic Motion in Case of Range Observations 240

B.7 Partial Derivatives in Case of Range-Rate Observations 241

B.8 Range-Difference Observations as Viewed as a Transformation of Range Observations 242

APPENDIX C: Simultaneous Range Observations and the Gram Determinant 247

APPENDIX D: Some Matrix Properties 254

D.1 Differentiation of Rotation Matrices 254

D.2 Inversion of a Differentially Changed Matrix 259

REFERENCES 265

LIST OF TABLES

		Page
3.1	The Relationship between Keplerian Elements and Statevectors for the Various Orbital Models	50
4.1	The Estimable Parameters and Rank Deficiencies of the Measurement Systems: Range, Range-Rate and Range-Difference Observations (Non-Simultaneous)	91
6.1	Station Coordinates and Interstation Distances	129
6.2	Station Configurations	130
6.3	Observable Passes during Two Days	132
6.4	Stations and Their Observable Passes	135
6.5	4 Stations with 1 or 2 Observing Each Pass (1 day, long arc mode)	136
6.6	The Lower and Upper Bounds for the Ratio between the a Posteriori and a Priori Variances-of-Unit-Weight for Large Degrees of Freedom. Testing Level of Significance $\alpha = 5\%$	144
6.7	Long Arc Analysis (1 day, 6 passes, 4 stations) for Circular, Elliptic and Secularly Perturbed Elliptic Orbits. Interstation Distance Recovery with Standard Deviation in cm. No Constraints on GM and J_2. $\sigma_r = 5$ cm, $\Delta t = 60$ sec.	146
6.8	Long Arc Analysis (1 day, 6 passes, 4 stations) for Circular and Elliptic Orbits. Interstation Distance Recovery with Standard Deviation in cm. Constraint on GM (or mean motion). $\sigma_r = 50$ cm, $\Delta t = 60$ sec.	147
6.9	Long Arc Analysis (4-1/2 hours, 2 passes, 4 stations) for Elliptic and Secularly Perturbed Orbits. Interstation Distance Recovery with Standard Deviation in cm. No Constraints on GM and J_2. $\sigma_r = 5$ cm, $\Delta t = 60$ sec.	148

Page

6.10 Long Arc Analysis (4-1/2 hours, 2 passes, 4 stations) for Elliptic Orbit. Interstation Distance Recovery with Standard Deviation in cm. Constraint on GM. σ_r = 5 cm, Δt = 60 sec . 150

6.11 Long Arc Analysis (1 day, 6 passes, 4, 3 and 2 stations) for Circular Orbit. Interstation Distance Recovery with Standard Deviation in cm. No Constraints on GM. σ_r = 5 cm, Δt = 60 sec. 151

6.12 Long Arc Analysis (4-1/2 hours, 2 passes, 4, 3 and 2 stations) for Circular Orbit. Interstation Distance Recovery with Standard Deviation in cm. No Constraints on GM. σ_r = 5 cm, Δt = 60 sec. 152

6.13 Long Arc Analysis (1 day, 6 passes, 4, 2 and 1 stations) for Elliptic Orbit. Interstation Distance Recovery with Standard Deviation in cm. No Constraints on GM. σ_r = 5 cm, Δt = 60 sec. 153

6.14 Short Arc Analysis (2 days, 3 passes, 4 stations) for Elliptic Orbit. Interstation Distance Recovery with Standard Deviation in cm. No Constraints on GM. σ_r = 5 cm, Δt = 60 sec. 156

6.15 Dynamic Analysis for Elliptic Orbit. Interstation Distance Recovery with Standard Deviation in cm. No Constraints on GM. σ_r = 5 cm, Δt = 60 sec. 158

6.16 Short Arc Analysis for Elliptic Orbit (2 days, 2 and 3 pass solutions, 4 stations). Interstation Distance Recovery with Standard Deviations in cm. No Constraint on GM. σ_r = 5 cm, Δt = 60 sec. 160

6.17 Short Arc Analysis for Elliptic Orbit (2 days, 3 pass solution, 4 stations) with Varying Weights on One Station (HO: R, ψ, $\Delta\lambda$). Interstation Distance Recovery with Standard Deviations in cm. No Constraint on GM. σ_r = 5 cm, Δt = 60 sec. 162

6.18 Short Arc Analysis for Elliptic Orbit (2 days, 3 pass solution, 4 stations) with Varying Weights on Two Stations (HO: R, ψ, $\Delta\lambda$ and QU: R, ψ). Interstation Distance Recovery with Standard Deviations in cm. No Constraint on GM. σ_r = 5 cm, Δt = 60 sec. 163

6.19 Short Arc Analysis for Elliptic Orbit (2 days, 3 pass solution, 4 stations) with Varying Weights on Four Stations (HO, QU, SA, UT: R, ψ, $\Delta\lambda$). Interstation Distance Recovery with Standard Deviations in cm. No Constraint on GM. σ_r = 5 cm, Δt = 60 sec. 163

Page

6.20 Short Arc Analysis for Elliptic Orbit (1 pass, 4 stations) with Varying Weights on One Station (HO: R, ψ, $\Delta\lambda$). Interstation Distance, Station, Satellite, and Earth Parameter Recovery. No Constraint on GM. σ_r = 5 cm, Δt = 60 sec. . . 165

6.21 Short Arc Analysis for Elliptic Orbit (half a day, 2 pass solution, 4 stations) with Varying Maximum Zenith Angle. Interstation Distance Recovery with Standard Deviations in cm. No Constraint on GM. σ_r = 5 cm, Δt = 60 sec. 166

6.22 Geometric and Dynamic Analyses. Interstation Distance Recovery with Standard Deviation in cm. (Dynamic Mode: Elliptic Orbit, No Constraints on GM. σ_r = 5 cm, Δt = 60 sec. 168

6.23 Earth's Spin Rate Determinations with Standard Deviations in Arcseconds per Timeseconds. σ_r = 5 cm, Δt = 60 sec. . . 172

6.24 Differential Polar Motion Determinations with Standard Deviations for Latitude and Longitude-Differences (times cotan ψ) in Arcseconds and cm. σ_r = 5 cm, Δt = 60 sec. . . 176

6.25 Long Arc Analysis (Elliptic Orbit) Without and With a Properly Constrained GM. Interstation Distance and Spin Rate Recovery with Standard Deviations in cm and "/sec. σ_r = 5 cm, Δt = 60 sec. 178

6.26 Long Arc Analysis (Elliptic Orbit) with a Wrongly Constrained GM. Interstation Distance and Spin Rate Recovery with Standard Deviation in cm and "/sec. σ_r = 5 cm, Δt = 60 sec. 180

6.27 Short Arc Analysis (Elliptic Orbit) without and with a Wrongly Constrained GM. Interstation Distance Recovery with Standard Deviation in cm. σ_r = 5 cm, Δt = 60 sec. . . 181

6.28 Short Arc Analysis (Elliptic Equatorial Orbit) with a Properly and Wrongly Constrained GM. σ_r = 5 cm, Δt = 60 sec. 184

6.29 Long Arc Analysis (Circular Orbit, 1 day) with Range (σ_r = 5 cm) and Range-Rate Observations ($\sigma_{\dot{r}}$ = 0.1 mm/sec), Δt = 60 sec. 186

6.30 Long Arc Analysis (Circular Orbit, 1 day) with Range, Range-Rate and Range-Difference Observations, Δt = 60 sec. 186

LIST OF FIGURES

		Page
3.1	2-D Circular Motion, Keplerian Elements	19
3.2	2-D Circular Motion, Statevector	20
3.3	3-D Circular Motion, Keplerian Elements and Statevector	27
3.4	2-D Elliptic Motion, Keplerian Elements and Statevector	36
3.5	3-D Elliptic Motion, Keplerian Elements and Statevector	41
4.1	Rotations in a Reference Frame	55
4.2	Two Dimensional Circular Motion	56
4.3	Geocentric Reference Frame	63
4.4	The Equator and Orbit Plane	66
4.5	Three Dimensional Circular Motion	67
4.6	The Celestial Sphere and the Fundamental Triangle of Satellite Geodesy	68
4.7	Two Dimensional Elliptic Motion	73
4.8	Three Dimensional Elliptic Motion	76
5.1	Levelling between Three Stations	101
5.2	Differential Polar Motion	110
5.3	Polar Motion	115
6.1	Ground Tracks of LAGEOS (Two Days)	134
6.2	Range and Range-Rate as a Function of Time	138
6.3	Differential Polar Motion	174

Page

A.1 Keplerian Orbital Geometry 194

C.1 Four Vectors in Three Dimensional Space 248

1. INTRODUCTION

"In the cosmogony favored by the Cartesians the earth elongated at the poles; . . . "

D. J. Struik [1967]

1.1 Philosophy of the Investigation

Although it can be argued to call René Descartes (Cartesius) the inventor of the Cartesian coordinate systems, e.g., in the thirteenth century B.C. the Egyptians are known to have reproduced figures by covering them with a rectangular network [Coolidge, 1940, p. 12], the publication of La Géométrie in 1637 meant a large step forward in the progress of the sciences. Descartes and Fermat can safely be considered the founders of analytic geometry. The application of algebra and analysis to geometry and the reverse, the fact that many problems in analysis have their counterparts in geometry, gave the insight to men in science to accelerate the development of their various fields. Although physics is one of the prime examples, surveyors and geodesists (global surveyors) can be considered as the almost eternal geometry-into-algebra-into-geometry translators. However, the acceptance of the Cartesian coordinate system as the natural algebraic translation of geometrical problems became the cause-célèbre for many investigations in recent years. If at this stage a finger needs to be pointed, it is not only to the geodesist as the Cartesian coordinate follower but also to

his environment (i.e., contractor, employer, client, etc.). One still has to imagine a geodesist, after being asked to supply information concerning the position of a point, who would dare to express the position of this point in anything else than some of the convential coordinates (absolute coordinates are always most welcome!). Many geodetic measurement systems yield only relative positions and then not even expressable in Cartesian coordinates. The geodesist having chosen a particular measurement system (geometry) must realize that he cannot translate certain geometries into any arbitrary algebraic representation. As an example, a surveyor equipped with a level instrument cannot measure heights, only height differences. The nature of the (observational) geometry will dictate the algebra in which it can be translated if it is to preserve uniqueness if one wants to translate this algebra back into geometry. More than once the algebra does not contain the popular Cartesian coordinates. The geodesist can go two ways: inform the contractor of the non-estimability of the required Cartesian coordinates or keep the contractor ignorant but use outside information to work towards the desired product of (Cartesian) coordinates. It is this latter approach which became widely used with the advent of weighted least squares or similar adjustment methods.
This (Bayesian) approach is probably better known as the "the-best-you-can-do" method, its name describing an often heard answer if questions concerning estimability become too pressing. Although the scope of this investigation does not intend to be a fulmination against weighted least squares and its abuse, it still hopes to adhere strictly to the first mentioned approach: investigate a measurement system first from

the non-Bayesian point of view as to accurately pinpoint its deficiencies and contributions in reaching the goals it was designed for. Usage of outside information which is not inherent in the measurements, tends to obscure the contributions. To quote the very first sentence in the earlier mentioned book La Géométrie [Descartes, 1637]:

> Any problem in geometry can easily be reduced "to such terms that a knowledge of the lengths of certain straight lines is sufficient for its construction."

To paraphrase this: never should a geodesist be caught adding outside information because of a lack of sufficient straight lines to construct his Cartesian mathematical model. After all, in the seventeenth century the Cartesian cosmogonists were the ones who favored a prolate earth.

1.2 Historical Background

One does not need to go far back in history to notice the growing awareness among geodesists that one cannot arbitrarily put any parameter at the right hand side of the equality sign in an observation equation. It is probably no coincidence that this question was addressed more and more frequently when three dimensional geodesy made his claim of here-to-stay with the launch of artificial satellites in the late fifties and early sixties. Although much attention to this question was paid in earlier years, e.g., in [Bjerhammer, 1973] one finds a full account of papers published by him between 1948 and 1955, the geodetic interest in estimability was revived after publication of [Rinner, 1966] and [Meissl, 1969] in Europe and some time later after a similar publication by Blaha [1971a] in the United States. Taking the latter as an example (the emphasis of the study was on range measurements to satellites) the

idea expressed therein is to have the mathematical models set up as generally as possible and subsequently, investigate which additional information (inner or minimal constraints) needs to be added to make the originally rank deficient normal matrix just invertable. The contrasting method, also applied to satellite ranging, in [Aardoom, 1970 and 1971] is favored in this investigation: investigate the measurement system in such a way that the mathematical model is directly expressed in (the maximum number of) estimable parameters. The need for finding inner constraints is hereby circumvented: first of all, finding the proper inner constraints is not always an easy task and secondly, the non-estimable quantities (and their variance/covariance matrix) need to be mapped into estimable ones anyway as to make a variance analysis meaningful. For a more theoretical discussion the reader is referred to [Bossler, 1973] or [Grafarend and Schaffrin, 1974]. An application of this reasoning one can find in [Mueller et al., 1975].

Questions concerning estimability in dynamic satellite geodesy were upto recently either ignored, not explicitly stated or tacitly assumed to be known. Some publications as [Brown and Trotter, 1973], [Condon, 1974], [Agreen and Smith, 1975] and [Arur, 1977] do not pursue the above outlined reasoning to its fullest extent, therefore did not clarify the problem. A latest systematic attempt to handle the problem of estimability in satellite geodesy can be found in [Grafarend and Livieratos, 1978] and [Grafarend and Heinz, 1978] which are at the time of this writing (March, 1978) still in print. It is against this historical background that one has to view this investigation.

1.3 Scope of the Investigation

The previous section leads one directly into the scope of the investigation: Using very simple dynamical models, what are in general the future applications of (very precise) range, range-rate and range-difference observations to artificial satellites and in particular of laser range measurements to LAGEOS? A relative precision in the parameters of 10^{-9} is envisioned. Given a set of assumptions, the mathematical models are directly expressed in the maximum number of unconditional estimable parameters. The unconditionality expresses the independence from inner, minimum or any other (over) constraints. The set of parameters does not only include orbital parameters but also parameters concerning the positions of the observing stations and some earth related parameters.

Although mathematically the setup is such that it reflects stationary positions of the observatories and a rigid earth, the maximum allowable time span over which the observations are analyzed, was chosen to be between one hour and one day. A survey of the magnitudes, but in this respect more importantly, the spectra of important dynamical phenomena to be monitored can be found in [Fedorov, 1974]. The approach of considering only short time spans allows the recovery of time variable parameters (moving stations on a non-rigid earth) which are only considered constant during the period under investigation.

The analysis of range, range-rate and range-difference observations to artificial satellites is restricted to very simple dynamical models. Circular, elliptic and secularly perturbed (due to J_2) elliptic orbits have been investigated.

Although the maximum number of estimable parameters forms the essential set for a variance analysis, during this study the quality of

estimability for the various derived parameters are indicated. In many cases, the derived parameters are shown to be the best estimable quantities. At this point it should be noted that the particular choice of estimable parameters is completely arbitrary. The soundness of the mathematical model as derived from observations is reflected by the structure of the weight coefficient matrix of the (estimable) parameters. It is this geometry spanned by observations and parameters on which one's attention should be focussed. Redefinition of parameters does not minimize the estimates of precision or correlation. The correlation for instance is determined by the observational and parametric geometry and nothing else [Leick and Van Gelder, 1975].

Since the investigations centered around deficiency in the orbit/station/earth geometry, treatment of perturbing factors as gravitational perturbations of higher degree and order than J_2, and other perturbations due to atmospheric drag, solar radiation pressure, attraction of the sun and moon, earth and ocean tides, etc. was considered to be beyond the scope of this investigation.

The value of a simulation study which should be characterized by you-get-out-what-you-put-in is also expressed as follows: because of the simplicity of the models the study is one of lower bounds. Given a set of assumptions concerning the model, the precision and frequency of the observations, the variance analysis shows the highest attainable estimates of precision. Especially in those cases where the precision estimates of the recovered parameters are bad or at least marginal the conclusion of the variance analysis will be in view of the influence of the various non-considered perturbing factors: reality can only

be worse. Consequently, the standard deviations can only be larger in reality: a study of lower bounds.

Another aspect of this investigation concerns the question of internal consistency of the observations. A favored approach in (geodetic) data analysis is the initial check for internal consistency of the observations. This often being referred to as the first step adjustment (see e.g., [Baarda, 1968]) deserves the predicate of 'precision evaluation'. A subsequent (second step) adjustment fitting the results of the initial adjustment into a network of (known) data of higher order would (hopefully) deserve the predicate 'accuracy evaluation'.

The validity and necessity of the philosophy outlined in the three sections of this chapter is probably best summed up with the following thought: a satellite geodesist should not have as his caricature a surveyor who successfully computes the coordinates of two bench marks after having measured the distance between them.

2. REFERENCE FRAMES AND SOME UNDERLYING ASSUMPTIONS

"The FIRST problem to be considered is the method employed to describe the relative position of points."

W. Baarda [1975]

2.1 Introduction

Even in the simplest simulation studies which deal with laser range observations to earth orbiting satellites one has almost always to establish several reference frames (i.e., coordinate systems) despite the blindness of this measurement system. Only in the case of simultaneous range observations from at least four stations one can pursue the blindness of the observations into their model. This particular case is usually referred to as the geometric mode of satellite observation analysis (also applicable to simultaneous direction measurements). The validity of a geometric analysis of simultaneous range-difference measurements is unclear to the author.

As soon as one deals with range and direction observations in a non-simultaneous mode or range-rate and range-difference observations in (either the simultaneous or) the non-simultaneous mode the establishment of reference frames in which the positions and motions of the satellite and its observer will be given, becomes an unavoidable fact.

The choice of the reference frames in this study reflects the philosophy that no a priori knowledge is assumed. This refers not only to the non-Bayesian character of the estimation process (no a priori weighting of parameters) but also to the behavior of the reference frames, especially in the past. The positions and motions of the reference frames are only reconstructed from the time span of the available observational data. If one has chosen a reference epoch t_o suitably half way during an observation campaign the change in reference frames is investigated between the epochs marking the beginning and the end of this campaign and is preferably referenced against the position of that particular frame at reference epoch t_o.

The reference frames used in the study can be divided in three categories:

i. inertial frame,

ii. instantaneous terrestrial frame, and

iii. axis of figure frame.

The parameters which will connect the different frames are rotational in nature if it is assumed that the center of mass of the earth is common to all three frames. Consequently, each two frames will be rotationally displaced by three angles. Since the orientation of the frames are not stationary with respect to each other, another three parameters of the angular velocity type are needed in order to transform one frame to another. This modelling of course tacitly assumes that during the interval of observations the rotation angles vary only linearly with time. In general frame i will be related to frame j as follows

$$\overline{x}_j = R(\alpha_o+\dot{\alpha}\Delta t,\ \beta_o+\dot{\beta}\Delta t,\ \gamma_o+\dot{\gamma}\Delta t)\overline{x}_i$$

where α_o, β_o, γ_o are the transformation angles at reference epoch t_o and $\dot{\alpha}$, $\dot{\beta}$, $\dot{\gamma}$ are the corresponding angular velocities assumed to be constant during the observation campaign.

2.2 The Inertial Reference Frame

Preferably, one would describe the equations of motion of a satellite in a pure inertial frame. Because of the motion of the earth around the sun, the motion of the sun in our galaxy, the motion of our galaxy among other galaxies, etc., the reference frame can be called at best a quasi-inertial reference frame.

Various (quasi) inertial frames for the modelling of the orbital equations of motion are used in satellite geodesy. A widely used inertial frame is the frame defined by the mean equinox and equator at a certain epoch, often at 1950.0 or at the beginning of the year. The geocentric coordinates of a satellite in such a frame are not inertial anymore (e.g., because of the motion of the geocenter around the sun) but they have to be corrected for this difference between pure and quasi-inertiality. This is often treated in the form of perturbations. The Smithsonian Astrophysical Laboratory (SAO) refers its inertial frame to the mean equinox of date of 1950.0 but chose the direction of the z-axis to be perpendicular to the equator of date. In the underlying study this principle has been carried one step further: the (quasi) inertial frame adopts not only the equator of date but also the equinox of date. The postfix "of date" refers to the reference epoch t_o which is often chosen about halfway the observation campaign. Precession and

nutation influencing the equinox and equator of date were either neglected (maximum 1 day of observations) or assumed to be corrected for. For instance, the precession in right ascension amounts to about 4 meters per day on earth scale and is therefore not negligible. For more detailed discussions concerning the influence of precession and nutation on satellite orbits the reader is referred to publications as [Kozai, 1960], [Kozai and Kinoshita, 1973], [Lambeck, 1973] and [Kozai, 1974].

2.3 The Instantaneous Terrestrial Reference Frame

The instantaneous terrestrial reference frame is chosen such that its z-axis coincides with the instantaneous spin axis of the earth at all times. If one assumes the separation between the angular momentum vector and the instantaneous rotation axis to be known, the latter can be transformed to the z-axis of the inertial reference frame (section 2.2) at reference epoch t_o. The x-axis of this terrestrial frame will be oriented with respect to the x-axis of the inertial frame by the angle $GAST_o$: the Greenwich Apparent Sidereal Time at reference epoch t_o. The instantaneous terrestrial reference frame rotates with an inertial angular velocity of

$$\omega_e = 7.292\ 115\ 1467 * 10^{-5} \text{ rad/sec}$$

with respect to an inertial frame fixed to the stars. Its angular velocity with respect to the equinox of date is slightly higher because of precession in right ascension.

The frames of this section and section 2.2 are then in its simplest form related through a rotation about the z-axis with an angle of

$(GAST_o + \omega_e \Delta t)$ where Δt denotes the difference between the time of interest (e.g. in case of an observation) and the epoch t_o.

2.4 The Axis of Figure Frame

Although the results of the conference 'On Reference Coordinate Systems for Earth Dynamics' held in Toruń, Poland [Kolaczek and Weiffenbach (eds.), 1974] indicate a preference for a "quasi-earth-fixed" coordinate system which follows the motion of the mantle rather than the crust, still in the underlying study a crust-fixed rather than a mantle-fixed earth reference system has been chosen. Since laser range measurements are the subject of the investigation and they are connected via the observatories directly to the crust, the crust-fixed reference frame seems to be more operational. The orientation of such a crust-fixed system is chosen to be determined by the mass distribution of the earth: the z-axis of this reference frame should coincide at all times with the principal axis of the maximum moment of inertia (axis of figure). Assuming the axis of figure fixed to the crust is a good approximation for short time spans (1 day). Seventy years of latitude observations however indicate a secular motion of the axis of figure [Soler, 1977]. The center of the path (Chandler wobble) of the instantaneous spin axis will be close to the z-axis of this axis of figure frame. As a matter of fact, this is how the C.I.O. pole was defined from the adopted latitudes of some stations, based on latitude observations between 1900 and 1905 [Mueller, 1969, p. 82]. Unfortunately, the closeness between the two other moments of inertia does not provide an accurate physical reason for the orientation of the x- and y-axes (e.g., to

diagonalize the inertial tensor). The precise definition of the orientation of these two axes will become irrelevant as subsequent studies will show. The axis of figure and instantaneous spin axis frames will be connected by either two differentially small rotations [Mueller, 1969, p. 80] or in an alternative way which will be described in more detail in section 5.4.

If one wants to call these transformations polar motion, one has to realize that in this investigation it is meant to be the difference between the positions of the instantaneous spin axis and the (instantaneous) position of the principal axis of the maximum moment of inertia (axis of figure). The more detailed sections of Chapter 5 will reveal that the instantaneous terrestrial frame is the one in which the positions of the observatories will be determined and that the axis of figure frame which has a more crust-fixed character, is the one in which the gravity field of the earth is represented. This assumes that the old practice of setting the spherical harmonic coefficients C_{21} and S_{21} equal to zero is carried on in the future [Newton, 1974]. One might say then that the function of the axis of figure frame is not only to minimize the time variations in the station positions but also to minimize the time variations of the gravity field coefficients.

2.5 The Establishment of World Wide and Regional Geodetic Reference Frames

The plans as laid down in NASA's Earth and Ocean Physics Applications Program [NASA, 1972] called for the establishment of a World Wide Geodetic Reference Frame (WWGRF). The realization of such a frame is required to satisfy geophysical needs to describe phenomena such as continental drift, fault motions, etc. The magnitudes and spectra of

the various dynamic phenomena are such that parameters of 10^{-9} precision (about 3 cm, 0".001, 1 μgal, 1 E, etc.) are required to monitor these phenomena.

To quote from [Baarda, 1975]:

> A geodesist . . . should aim at standard deviations of 5 cm or less in his results. This means a relative precision of 10^{-8} Should the reliability . . . also be included in this figure of 5 cm, then the relative precision should be of the order of 10^{-9}. This, because the analysis of national primary networks or filling-in networks for surveying purposes has shown that the reliability sometimes is of the order 5-10 times the standard deviation."

Although it was beyond the scope of this investigation to check whether this statement is also true for networks which are derived by space-geodetic measurement systems such as Very Long Baseline Interferometry (VLBI), Lunar Laser Ranging (LLR) and Satellite Laser Ranging (SLR) in particular, the 10^{-9} relative precision requirement is sure not too stringent for future geodynamic purposes.

Can the geodesist adopt the average terrestrial frame (as described in section 2.4) as a realization of a WWGRF? If done so, he surely did not answer the question as raised in the quote which heads this chapter.

Think of a WWGRF made up by a polyhedron of points. Two main aspects can be recognized:

a. external (or absolute) motions by the points defining the polyhedron. By external motions is meant that part of the point's movements which is common to all points and takes place with respect to an inertial frame (possibly defined by a polyhedron of quasars). Known (absolute) motions which are common to all points are precession, nutation, earth rotation, polar motion, etc.

An alternative way of describing these motions is as follows: the external motions result in different coordinates of the points of the polyhedron at different epochs, but the coordinates can be brought together with only translational and rotational transformations.

b. internal (or relative) motions by the points defining the polyhedron. By internal motions is meant that part of the point's movements which is not common to all points. Known (relative) motions are continental drift, fault motions, earth and ocean tides, ocean loading effects, etc.

Let the polyhedron which forms such a WWGRF be called a Fundamental Polyhedron (FP). Its realization will be first of all a coordinate free problem. The FP's shape, formed by length ratios and/or angles, and size, determined by a scale factor (e.g., velocity of light) are the essential features to be established first. Problems of optimization from geometrical, statistical and geophysical points of view need to be resolved. Secondly, the description of the absolute motions of the FP requires only then the establishment of a coordinate system which is a much more difficult and intriguing task:

a. The orientation of the FP with respect to the quasars from VLBI measurements, with respect to either the instantaneous spin axis or the axes of figure from satellite observations or with respect to a coordinate system defined by the lunar ephemeris from lunar laser ranging.

b. the position of the FP with respect to the earth's center of mass from satellite or absolute gravity measurements and with respect to the earth-moon barycenter from lunar laser ranging.

In this line of thinking it is easy to foresee that the creation of some sort of an "International Fundamental Polyhedron Service" (IFPS) which has to monitor both the relative and absolute behavior of the FP, may be necessary.

In this investigation the spotlight is mainly on the relative realization of station polyhedrons and to a smaller extent on some absolute aspects of the orientation and position of the station geometry. The relative positioning (size and shape of the station polyhedron) does not require very stringent definitions of any coordinate system: as said earlier, it is a coordinate-free problem. The position of a point can be expressed for example by three distances to three mutually perpendicular planes (Cartesian coordinates), or by three distances to three other points. This last approach can be viewed as a (Cartesian) coordinate-free one and the usefulness of this type of relative point positioning in case of the analysis of similarity transformations can be found in [Leick and Van Gelder, 1975].

The analysis of the distances (baselines) between points form the nucleus around which also other problems as estimability in dynamically analyzed satellite observations are discussed. The line of thought expressed for the establishment of a WWGRF can be similarly applied for regional point positioning: the same distinction between relative and absolute motions can be made. In this report only stations in the United States were examined. This implies that more and more phenomena originally listed as having non-common (relative, internal) motions will now have common (absolute, external) motions if more regional type of polyhedra are considered. If a station polyhedron is

situated on one continental plate, continental drift will become mainly an external motion: translational and rotational transformation models are sufficient to monitor the changes in station positions. These redefinitions of the two types of motions are important when satellite measurements are applied for the establishment of Regional Geodetic Reference Frames (RGRF). A nice example of the establishment of such a RGRF is the readjustment of the North American Datum: the analysis of the contribution of either Doppler or laser satellite observations to the strength of the station geometry might be an easy task as compared to the evaluation of the absolute position of the North American Datum because of the increased burden placed on the coordinate system definition due to its regional character.

Although the contribution of neither laser range nor Doppler measurements to the explicit (re)establishment of a world wide or a local datum are analyzed, the reasoning followed in the subsequent sections is very much influenced by it and tries at the same time to be responsive to the question raised in the quote heading this chapter.

3. THE INTERMEDIATE ORBIT

"Seven elements are required for the complete determination of the motion of a heavenly body in its orbit, . . . "

K. F. Gauss [1857]

3.1 Introduction

In this chapter the analytics involved in simple orbital geometries will be investigated. At each step of the investigation the number of parameters (orbital elements) will be carefully examined.

Two sets of widely used orbital elements will be the subject of examination: the Keplerian orbital elements and the Cartesian orbital elements (statevectors, i.e. position and velocity vector). Special attention will be devoted to the interchangeability of the two sets. The estimability of the orbital elements depending on the various measurement systems will be treated in Chapter 4.

The survey starts with the simple two dimensional circular motion of a particle and will be gradually generalized to the three dimensional elliptic motion and will end with the first order secularly perturbed elliptic motion.

The section from which the quotes heading Chapters 2 and 4 have been taken, mentions the term "Keplermanship" as the art of manipulation of the two-body formulas. In this very sense part of the investigation in this chapter might be characterized by "restricted

Keplermanship": although Kepler's First and Second Law, dealing with the ellipticity of planetary orbits and the equal area swept in equal time by the radius vector, will not be tarnished, the determination of the geocentric gravitational constant GM (in Kepler's Third Law) will not be considered as a fait accompli. The geocentric gravitational constant of the primary body (or the mean motion of the satellite) will be considered both unknown and known. The reasons for this approach is fully explained in sections 5.3 and 6.10.

3.2 Two Dimensional Circular Motion

3.2.1 GM (or n) Unknown

The circular motion of a particle (satellite) in a reference system which origin coincides with the center of the circular orbit can be represented in the following figure

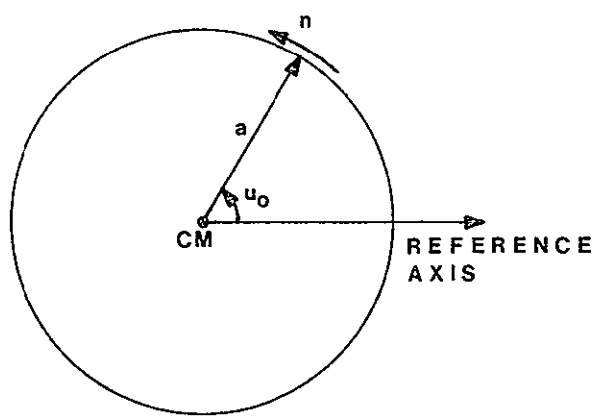

Figure 3.1. 2-D Circular Motion, Keplerian elements

Denoting the radius of the orbit by a, the angle between the radius vector and an inertial reference axis at reference epoch t_o by u_o and the (constant) angular velocity by n one is able to compute at any instant t the position of the satellite from

and

$$u = u_o + n(t-t_o) \tag{3.2-1}$$

Denoting the position and velocity of the satellite by means of a (Cartesian) statevector, one has

$$\bar{x} = \begin{bmatrix} x_\omega \\ y_\omega \end{bmatrix} \tag{3.2-2}$$

and

$$\dot{\bar{x}} = \begin{bmatrix} \dot{x}_\omega \\ \dot{y}_\omega \end{bmatrix} \tag{3.2-3}$$

In a figure,

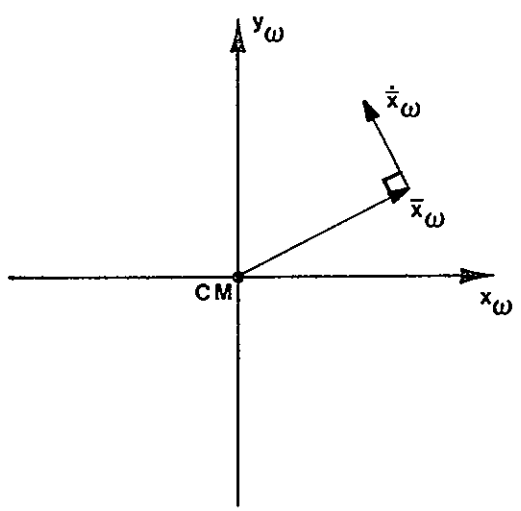

Figure 3.2. 2-D Circular Motion, Statevector

Easily transformation formulas between the Keplerian elements and the statevector can be derived.

$$\bar{x}_\omega = \begin{bmatrix} x_\omega \\ y_\omega \end{bmatrix} = a \begin{bmatrix} \cos[u_o+n(t-t_o)] \\ \sin[u_o+n(t-t_o)] \end{bmatrix} \tag{3.2-4}$$

By differentiating the above formulas with regard to time, one obtains

$$\dot{\bar{x}}_\omega = \begin{bmatrix} \dot{x}_\omega \\ \dot{y}_\omega \end{bmatrix} = an \begin{bmatrix} -\sin[u_o+n(t-t_o)] \\ \cos[u_o+n(t-t_o)] \end{bmatrix} \tag{3.2-5}$$

Two remarks with respect to the above derived equations can be made:

- in celestial mechanics often the time T, denoting the passage of one of the reference axes (line of apsides) is chosen as an orbital parameter instead of the angle u_o. Since this time T might be far outside the time domain of the observational data available preference is given to the angular parameter u_o (one of the polar coordinates). Later in the investigation an appropriate choice for u_o will be developed.
- in the transformation equations (3.2-4) and (3.2-5) only the difference between t and t_o occurs. Consequently, the choice of the reference epoch t_o will be arbitrary and can be set equal to zero. In this case t will denote the time elapsed since the satellite's passage of the reference argument u_o.

Without loss of generality (3.2-4) and (3.2-5) become

$$\bar{x} = \begin{bmatrix} x_\omega \\ y_\omega \end{bmatrix} = an \begin{bmatrix} \cos(u_o+nt) \\ \sin(u_o+nt) \end{bmatrix} \tag{3.2-6}$$

and $$\dot{\bar{x}} = \begin{bmatrix} x_\omega \\ y_\omega \end{bmatrix} = an \begin{bmatrix} -\sin(u_o+nt) \\ \cos(u_o+nt) \end{bmatrix} \tag{3.2-7}$$

A more careful inspection of these transformation formulas reveals that the set of Keplerian orbital elements consists of three independent variables (a, u_o, n) but that the statevector consist of four variables (x_ω, y_ω) and ($\dot{x}_\omega$, $\dot{y}_\omega$). Clearly, the Cartesian elements do not form an independent set which will readily become apparent during the derivation of the reversed transformation formulas. Equation (3.2-6) yields

$$a = \sqrt{x_\omega^2 + y_\omega^2} \tag{3.2-8}$$

and $$\tan(u_o+nt) = y_\omega/x_\omega \tag{3.2-9}$$

Similarly, from (3.2-7) one has

$$an = \sqrt{\dot{x}^2 + \dot{y}_\omega^2} \tag{3.2-10}$$

and $$\tan(u_o+nt) = -\dot{x}_\omega/\dot{y}_\omega \tag{3.2-11}$$

The identity of equations (3.2-9) and (3.2-11) yields the constraint between the four statevector elements which eliminates their dependency.

$$\frac{y_\omega}{x_\omega} = -\frac{\dot{x}_\omega}{\dot{y}_\omega}$$

or $$x_\omega\dot{x}_\omega + y_\omega\dot{y}_\omega = 0 \tag{3.2-12}$$

Geometrically, this can be verified from Figure 3.2. In a circular motion the velocity vector $\dot{\bar{x}}_\omega$ is perpendicular to the radius vector $\bar{x}_\omega$ at any instant of the orbit. This perpendicularity condition is just what the constraint (3.2-12) reflects.

Summarizing, one finds for the direct transformation (Keplerian to statevector) formulas

$$\bar{x}_\omega = \begin{bmatrix} x_\omega \\ y_\omega \end{bmatrix} = a \begin{bmatrix} \cos(u_o+nt) \\ \sin(u_o+nt) \end{bmatrix}$$

$$\dot{\bar{x}}_\omega = \begin{bmatrix} \dot{x}_\omega \\ \dot{y}_\omega \end{bmatrix} = an \begin{bmatrix} -\sin(u_o+nt) \\ \cos(u_o+nt) \end{bmatrix} \tag{3.2-13}$$

with $$x_\omega \dot{x}_\omega + y_\omega \dot{y}_\omega = 0$$

The reversed transformation (statevector to Keplerian) formulas are

$$a = \sqrt{x_\omega^2 + y_\omega^2}$$

$$n = \sqrt{\frac{\dot{x}_\omega^2 + \dot{y}_\omega^2}{x_\omega^2 + y_\omega^2}}$$

$$u_o = \arctan\left(\frac{y_\omega}{x_\omega}\right) - t\sqrt{\frac{\dot{x}_\omega^2 + \dot{y}_\omega^2}{x_\omega^2 + y_\omega^2}} \tag{3.2-14}$$

with $$x_\omega \dot{x}_\omega + y_\omega \dot{y}_\omega = 0$$

3.2.2 GM (or n) Known

Kepler's Third Law describing the inverse proportional relationship between the squared period and the cubed radius of the orbit can be denoted in the following way

$$n^2 a^3 = GM \tag{3.2-15}$$

in which GM is the geocentric gravitational constant of the primary mass (in this relationship the mass of the orbiting particle is being neglected). This dynamical law will eliminate one of the three dependent (Keplerian) parameters (see section 5.2).

Insertion of (3.2-15) into the direct transformation formulas (3.2-13) yields

$$\bar{x}_\omega = \begin{matrix} x_\omega \\ y_\omega \end{matrix} = a \begin{bmatrix} \cos\left(u_o + t\sqrt{\frac{GM}{a^3}}\right) \\ \sin\left(u_o + t\sqrt{\frac{GM}{a^3}}\right) \end{bmatrix} \tag{3.2-16}$$

and

$$\dot{\bar{x}}_\omega = \begin{matrix} \dot{x}_\omega \\ \dot{y}_\omega \end{matrix} = \sqrt{\frac{GM}{a}} \begin{bmatrix} -\sin\left(u_o + t\sqrt{\frac{GM}{a^3}}\right) \\ \cos\left(u_o + t\sqrt{\frac{GM}{a^3}}\right) \end{bmatrix} \tag{3.2-17}$$

However, the sets (3.2-16) and (3.2-17) describe the relationship between two Keplerian elements (a, u_o) and four, thus very dependent, statevector elements (x_ω, y_ω, $\dot{x}_\omega$, $\dot{y}_\omega$). Once again, the development of the reversed transformation formulas reveals the two constraints which need to be carried along with the transformation formulas. Equation (3.2-16) yields

$$a = \sqrt{x_\omega^2 + y_\omega^2} \tag{3.2-18}$$

and

$$\tan\left(u_o + t\sqrt{\frac{GM}{a^3}}\right. = y_\omega / x_\omega \tag{3.2-19}$$

Similarly, from (3.2-17) one has

$$GM/a = \dot{x}_\omega^2 + \dot{y}_\omega^2 \tag{3.2-20}$$

and

$$\tan\left(u_o + t\sqrt{\frac{GM}{a^3}}\right) = -\dot{x}_\omega/\dot{y}_\omega \tag{3.2-21}$$

As in section 3.2.1 the identity of equations (3.2-19) and (3.2-21) produces the constraint,

$$x_\omega\dot{x}_\omega + y_\omega\dot{y}_\omega = 0 \tag{3.2-22}$$

A second constraint is the result of equations (3.218) and (3.2-20) after elimination of the parameter a,

$$(\dot{x}_\omega^2+\dot{y}_\omega^2)\sqrt{x_\omega^2 + y_\omega^2} = GM \tag{3.2-23}$$

The geometrical interpretation of constraint (3.2-22) is already explained in section 3.2.1. The interpretation of constraint (3.2-23) is nothing else than the Kepler's Third Law (3.2-15) but now expressed in statevector elements.

Summarizing, one finds for the direct transformation under enforcement of Kepler's Third Law

$$\bar{x}_\omega = \begin{bmatrix} x_\omega \\ y_\omega \end{bmatrix} = a \begin{bmatrix} \cos\left(u_o + t\sqrt{\frac{GM}{a^3}}\right) \\ \sin\left(u_o + t\sqrt{\frac{GM}{a^3}}\right) \end{bmatrix}$$

$$\dot{\bar{x}}_\omega = \begin{bmatrix} \dot{x}_\omega \\ \dot{y}_\omega \end{bmatrix} = \sqrt{\frac{GM}{a}} \begin{bmatrix} -\sin\left(u_o + t\sqrt{\frac{GM}{a^3}}\right) \\ \cos\left(u_o + t\sqrt{\frac{GM}{a^3}}\right) \end{bmatrix} \tag{3.2-24}$$

with $\quad x_\omega\dot{x}_\omega + y_\omega\dot{y}_\omega = 0$

and $$(\dot{x}_\omega^2+\dot{y}_\omega^2)\sqrt{x_\omega^2 + y_\omega^2} = GM$$

The reversed transformation under Kepler's Third Law is

$$a = \sqrt{x_\omega^2 + y_\omega^2}$$

$$u_o = \arctan\left(\frac{y_\omega}{x_\omega}\right) - t\sqrt{\frac{GM}{(x_\omega^2+y_\omega^2)^{3/2}}} \qquad (3.2\text{-}25)$$

with $$x_\omega\dot{x}_\omega + y_\omega\dot{y}_\omega = 0$$

and $$(\dot{x}_\omega^2+\dot{y}_\omega^2)\sqrt{x_\omega^2 + y_\omega^2} = GM$$

In the latter set the addition of the two constraints is actually superfluous since the velocity components of the statevector are successfully eliminated from the reversed transformation formulas. In other words, the velocity vector of the statevector does not contain any additional information in case of two dimensional circular orbit with GM known.

3.3 Three Dimensional Circular Motion

The generalization to the third dimension will add two angles, describing the orientation of the orbital circle, to the set of Keplerian elements, but also two elements (Z and $\dot{Z}$) to the statevector. It is expected that in the geometrically more free theory (GM or n unknown) one constraint needs to be carried along whereas the case in which GM or n are considered known, eliminates a second parameter from the orbital elements reflected in a second constraint.

3.3.1 GM (or n) Unknown

The following figure illustrates the three dimensional circular motion of a satellite around a primary mass.

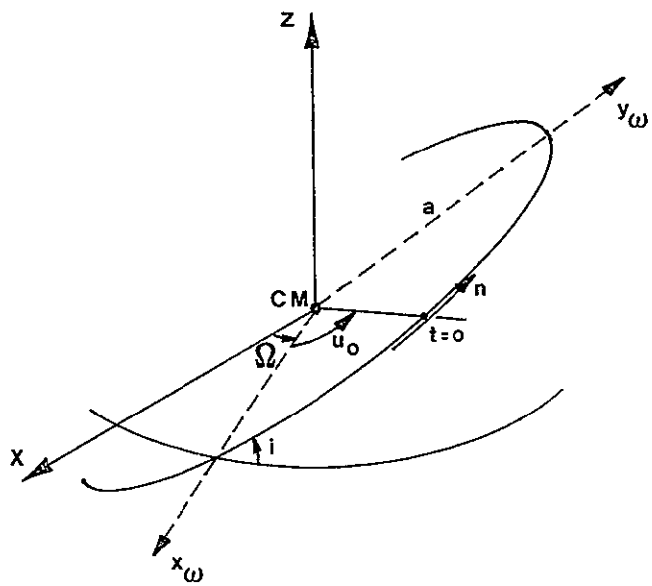

Figure 3.3. 3-D Circular Motion, Keplerian elements and Statevector

In this depiction the conventional Keplerian elements are being approached.

Two rotations $R_1(-i)$ and $R_3(-\Omega)$ of the $\bar{x}_\omega$ system (equations (3,2-6) and (3.2-7)) will immediately furnish the direct transformation formulas

$$\bar{X} = R_3(-\Omega)R_1(-i)\bar{x}_\omega \tag{3.3-1}$$

and after differentiating (3.3-1) with regard to time (Ω and i are time independent)

$$\dot{\bar{X}} = R_3(-\Omega)R_1(-i)\dot{\bar{x}}_\omega \tag{3.3-2}$$

$\bar{x}_\omega$ and $\dot{\bar{x}}_\omega$ are defined as in the equations (3.2-6) and (3.2-7) except for the addition of the third elements z_ω and $\dot{z}_\omega$ (both equal to zero).

Evaluating the rotation matrices $R_3(-\Omega)$ and $R_1(-i)$ and upon insertion of equations (3.2-6) and (3.2-7) into (3.3-1) and (3.3-2) one has

$$\bar{X} = \begin{bmatrix} X \\ Y \\ Z \end{bmatrix} = a \begin{bmatrix} \cos\Omega\cos(u_o+nt) - \sin\Omega\cos i \sin(u_o+nt) \\ \sin\Omega\cos(u_o+nt) + \cos\Omega\cos i \sin(u_o+nt) \\ \sin i \sin(u_o+nt) \end{bmatrix} \tag{3.3-3}$$

and

$$\dot{\bar{X}} = \begin{bmatrix} \dot{X} \\ \dot{Y} \\ \dot{Z} \end{bmatrix} = an \begin{bmatrix} -\cos\Omega\sin(u_o+nt) - \sin\Omega\cos i \cos(u_o+nt) \\ -\sin\Omega\sin(u_o+nt) + \cos\Omega\cos i \cos(u_o+nt) \\ \sin i \cos(u_o+nt) \end{bmatrix} \tag{3.3-4}$$

The reverse transformation (from statevectors to Keplerian orbital elements) will reveal the constraint which has to accompany the six Cartesian orbital elements (X, Y, Z, $\dot{X}$, $\dot{Y}$, $\dot{Z}$) to uniquely transform into the five Keplerian elements (a, i, Ω, u_o, n). From (3.3-3) one obtains

$$a = \sqrt{X^2 + Y^2 + Z^2} \tag{3.3-5}$$

and from (3.3-4)

$$an = \sqrt{\dot{X}^2 + \dot{Y}^2 + \dot{Z}^2}$$

yielding

$$n = \sqrt{\frac{\dot{X}^2 + \dot{Y}^2 + \dot{Z}^2}{X^2 + Y^2 + Z^2}} \tag{3.3-6}$$

The evaluation of the cross product of the positional and velocity parts of the statevector enables the computation of Ω and i

$$\overline{X} \times \dot{\overline{X}} = \begin{bmatrix} Y\dot{Z} - \dot{Y}Z \\ Z\dot{X} - \dot{Z}X \\ X\dot{Y} - \dot{X}Y \end{bmatrix} = a^2 n \begin{bmatrix} \sin\Omega \sin i \\ -\cos\Omega \sin i \\ \cos i \end{bmatrix} \tag{3.3-7}$$

Consequently, one arrives at

$$\Omega = \arctan\left(\frac{Y\dot{Z} - \dot{Y}Z}{X\dot{Z} - \dot{X}Z}\right) \tag{3.3-8}$$

and

$$i = \arctan\left(\frac{\sqrt{(Y\dot{Z}-\dot{Y}Z)^2 + (Z\dot{X}-\dot{Z}X)^2}}{X\dot{Y} - \dot{X}Y}\right) \tag{3.3-9}$$

The last Keplerian element u_o can be obtained from equations (3.3-1) and (3.3-2). Reversing these transformation formulas we have

$$\overline{x}_\omega = R_1(i)R_3(\Omega)\overline{X} \tag{3.3-10}$$

and

$$\dot{\overline{x}}_\omega = R_1(i)R_3(\Omega)\dot{\overline{X}} \tag{3.3-11}$$

From these equations after division of the first two statevector elements one obtains

$$\tan(u_o+nt) = \frac{y_\omega}{x_\omega} = -\frac{\dot{x}_\omega}{\dot{y}_\omega} \tag{3.3-12}$$

This relationship constitutes the constraint which needs to be enforced between the six dependent Cartesian orbital elements.

$$x_\omega\dot{x}_\omega + y_\omega\dot{y}_\omega = 0$$

This might be written as the vector product

$$\bar{x}_\omega^T \dot{\bar{x}}_\omega = 0$$

which gives after substituting (3.3-10) and (3.3-11)

$$\bar{X}^T R_3^T(\Omega) R_1^T(i) R_1(i) R_3(\Omega) \dot{\bar{X}} = 0$$

This reduces to $\bar{X}^T \dot{\bar{X}} = 0$

or
$$X\dot{X} + Y\dot{Y} + Z\dot{Z} = 0 \tag{3.3-13}$$

This condition eliminates the dependency of the six Cartesian elements.

The remaining element u_o can be computed from (3.3-12)

$$u_o = \arctan\left(\frac{y_\omega}{x_\omega}\right) - nt \tag{3.3-14}$$

or after evaluating (3.3-10) and using (3.3-6)

$$u_o = \arctan\left(\frac{-X\sin\Omega\cos i + Y\cos\Omega\cos i + Z\sin i}{X\cos\Omega + Y\sin\Omega}\right) - t\sqrt{\frac{\dot{X}^2 + \dot{Y}^2 + \dot{Z}^2}{X^2 + Y^2 + Z^2}} \tag{3.3-15}$$

Still, we need to compute the sine and cosine terms in expression (3.3-15). Using (3.3-8) and (3.3-9) one has

$$\begin{aligned} \sin\Omega &= \frac{\tan\Omega}{\sqrt{1 + \tan^2\Omega}} = \frac{\dot{Y}Z - Y\dot{Z}}{\sqrt{(Y\dot{Z} - \dot{Y}Z)^2 + (Z\dot{X} - \dot{Z}X)^2}} \\ \cos\Omega &= \frac{1}{\sqrt{1 + \tan^2\Omega}} = \frac{Z\dot{X} - \dot{Z}X}{\sqrt{(Y\dot{Z} - \dot{Y}Z)^2 + (Z\dot{X} - \dot{Z}X)^2}} \end{aligned} \tag{3.3-16}$$

and

$$\sin i = \frac{\tan i}{\sqrt{1 + \tan^2 i}} = \sqrt{\frac{(Y\dot{Z}-\dot{Y}Z)^2 + (Z\dot{X}-\dot{Z}X)^2}{(X^2+Y^2+Z^2)(\dot{X}^2+\dot{Y}^2+\dot{Z}^2)}}$$

$$\cos i = \frac{1}{\sqrt{1 + \tan^2 i}} = \frac{X\dot{Y} - \dot{X}Y}{\sqrt{(X^2+Y^2+Z^2)(\dot{X}^2+\dot{Y}^2+\dot{Z}^2)}} \tag{3.3-17}$$

The substitution of (3.3-16) and (3.3-17) into (3.3-15) will have expressed the variable u_o in terms of all the Cartesian orbital elements.

At this point it has become clear that a simple three dimensional circular motion leads already to very lengthy expressions.

Before summarizing we will clean up our notation by setting

$$\begin{aligned} \bar{r} &= \bar{X} \\ \dot{\bar{r}} &= \dot{\bar{X}} \\ r &= |\bar{X}| = |\bar{x}_\omega| = r_\omega \\ V &= |\dot{\bar{X}}| \end{aligned} \tag{3.3-18}$$

At this point a notation might be added which can be used to one's advantage in a later stage.

View the orbital elements

$$\bar{x}_\omega = a \begin{bmatrix} \cos(u_o+nt) \\ \sin(u_o+nt) \\ 0 \end{bmatrix} \tag{3.3-19}$$

as the result of a rotation of a unit vector $\bar{e}_1$ and a scaling by the satellite's orbital radius a.

$$\bar{x}_\omega = \begin{bmatrix} \cos(u_o+nt) & -\sin(u_o+nt) & 0 \\ \sin(u_o+nt) & \cos(u_o+nt) & 0 \\ 0 & 0 & 1 \end{bmatrix} \begin{bmatrix} a \\ 0 \\ 0 \end{bmatrix} \tag{3.3-20}$$

or

$$\bar{x}_\omega = aR_3(-u_o-nt)\bar{e}_1 \tag{3.3-21}$$

For the velocity part of the statevector one finds after differentiating (3.3-21) with regard to time

$$\dot{\bar{x}}_\omega = a \frac{\partial R_3(-u_o-nt)}{\partial t} \bar{e}_1$$

or

$$= -anR_3(-u_o-nt)L_3\bar{e}_1 \tag{3.3-22}$$

or

$$= -anL_3R_3(-u_o-nt)\bar{e}_1 \tag{3.3-23}$$

or

$$= -nL_3\bar{x}_\omega \tag{3.3-24}$$

with

$$L_3 = \begin{bmatrix} 0 & 1 & 0 \\ -1 & 0 & 0 \\ 0 & 0 & 0 \end{bmatrix} \tag{3.3-25}$$

For an explanation of L_3 see Appendix D.

The direct transformation formulas become

$$\begin{aligned} \bar{r} &= aR_3(-\Omega)R_1(-i)R_3(-u_o-nt)\bar{e}_1 \\ \dot{\bar{r}} &= -anR_3(-\Omega)R_1(-i)R_3(-u_o-nt)L_3\bar{e}_1 \end{aligned} \tag{3.3-26}$$

with

$$\bar{r} \cdot \dot{\bar{r}} = 0$$

The indirect transformation formulas become

$$a = r$$

$$n = V/r$$

$$\tan\Omega = -\frac{(\bar{r} \times \dot{\bar{r}})_1}{(\bar{r} \times \dot{\bar{r}})_2}$$

$$\tan i = \frac{\sqrt{(\bar{r} \times \dot{\bar{r}})_1^{\,2} + (\bar{r} \times \dot{\bar{r}})_2^{\,2}}}{(\bar{r} \times \dot{\bar{r}})_3}$$

$$u_o = \arctan\left[\frac{-r_1 \sin\Omega \cos i + r_2 \cos\Omega \cos i + r_3 \cos i}{r_1 \cos\Omega + r_2 \sin\Omega}\right] \qquad (3.3\text{-}27)$$

$$-\frac{V}{r}t$$

with

$$\sin\Omega = \frac{-(\bar{r} \times \dot{\bar{r}})_1}{\sqrt{(\bar{r} \times \dot{\bar{r}})_1^{\,2} + (\bar{r} \times \dot{\bar{r}})_2^{\,2}}}$$

$$\cos\Omega = \frac{(\bar{r} \times \dot{\bar{r}})_2}{\sqrt{(\bar{r} \times \dot{\bar{r}})_1^{\,2} + (\bar{r} \times \dot{\bar{r}})_2^{\,2}}}$$

$$\sin i = \frac{\sqrt{(\bar{r} \times \dot{\bar{r}})_1^{\,2} + (\bar{r} \times \dot{\bar{r}})_2^{\,2}}}{rV}$$

$$\cos i = \frac{(\bar{r} \times \dot{\bar{r}})_3}{rV}$$

and

$$\bar{r} \cdot \dot{\bar{r}} = 0$$

$(\bar{r} \times \dot{\bar{r}})_i$ denotes the i-th element in the vector $(\bar{r} \times \dot{\bar{r}})$.

3.3.2 GM (or n) Known

Kepler's Third Law will eliminate the variable n from all transformation formulas in section 3.3.1. Now skipping the tedious but relatively simple derivations one arrives directly at

$$\bar{r} = aR_3(-\Omega)R_1(-i)R_3(-u_o - \frac{t}{a}\sqrt{\frac{GM}{a}}\ \bar{e}_1$$

$$\text{and} \qquad \dot{\bar{r}} = \frac{\overline{GM}}{a} R_3(-\Omega)R_1(-i)R_3(-u_o - \frac{t}{a}\sqrt{\frac{GM}{a}}\ L_3\bar{e}_1 \tag{3.3-28}$$

For the reversed transformation formulas one has

$$a = r$$

$$\tan\Omega = -\frac{(\bar{r} \times \dot{\bar{r}})_1}{(\bar{r} \times \dot{\bar{r}})_2}$$

$$\tan i = \frac{\sqrt{(\bar{r} \times \dot{\bar{r}})_1^{\ 2} + (\bar{r} \times \dot{\bar{r}})_2^{\ 2}}}{(\bar{r} \times \dot{\bar{r}})_3} \tag{3.3-29}$$

$$u_o = \arctan\left(\frac{-r_1 \sin\Omega\cos i + r_2\cos\Omega\cos i + r_3\cos i}{r_1\cos\Omega + r_2\sin\Omega}\right) - \frac{t}{r}\sqrt{\frac{GM}{r}}$$

with $\sin\Omega$, $\cos\Omega$, $\sin i$ and $\cos i$ as defined in (3.3-27).

Since we have because of Kepler's Law a transformation between four Keplerian elements (a, i, Ω, u_o) and six Cartesian orbital elements (X, Y, Z, $\dot{X}$, $\dot{Y}$, $\dot{Z}$), two conditions need to be added.

The first condition can be verified from the set of equations (3.3-28)

$$\bar{r}^T\dot{\bar{r}} = \sqrt{aGM}\ \bar{e}_1^T L_3 \bar{e}_1 = 0 \tag{3.3-30}$$

The second condition follows from the lengths of the positional and velocity parts of the statevector

$$|\bar{r}| = r = a$$

$$|\dot{\bar{r}}| = V = \sqrt{GM/a}\,.$$

Eliminating a from the above expressions gives the desired condition

$$rV^2 = GM \tag{3.3-31}$$

Conditions (3.3-30) and (3.3-31) need to be added at all times to the transformation sets (3.3-28) and (3.3-29) to make the sets of orbital parameters uniquely interchangeable.

3.4 Two Dimensional Elliptic Motion

Releasing the restriction of sections 3.2 and 3.3 which dealt with orbits of zero eccentricity at this point the geometry of elliptic orbits will be reviewed as well as the relationship between Keplerian orbital elements and the statevector approach.

3.4.1 GM (or n) Unknown

At any instant the position of a satellite will be determined along its elliptical path by five elements: two parameters describing the size and shape of the ellipse: a, the semimajor axis and e, the eccentricity; the average angular velocity with which the satellite moves along that ellipse as described by the mean motion n; the reference angle at the reference epoch t = 0 as described by either v_o, the true anomaly or M_o, the mean anomaly or E_o, the eccentric anomaly and finally the orientation angle ω which describes the orientation of the ellipse with respect to a reference axis (the argument of perifocus or perigee). These parameters can be illustrated in the following figure.

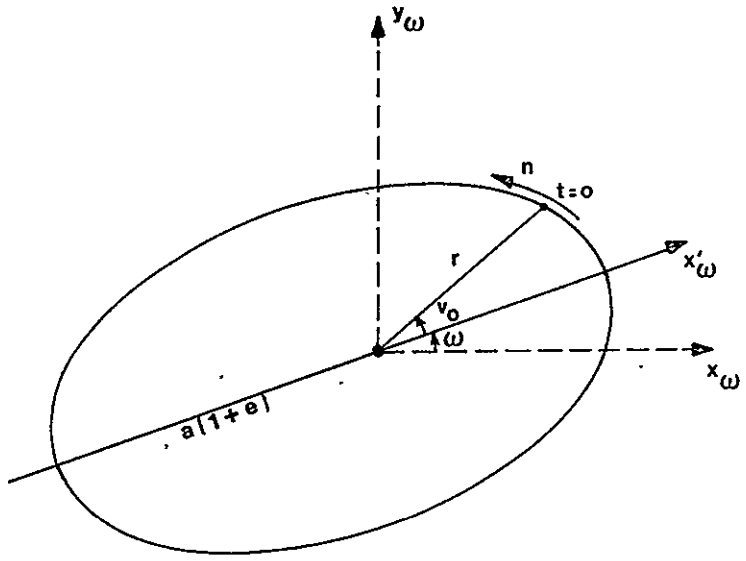

Figure 3.4. 2-D Elliptic Motion, Keplerian elements and Statevector

As explained in section 3.2.1 the often used element T, time of perifocal passage, is not considered in this investigation. The statevector is easily expressed in terms of the eccentric anomaly E because of which E_o became the preferred variable.

From Figure 3.4. one derives

$$\bar{x}'_\omega = \begin{bmatrix} x'_\omega \\ y'_\omega \end{bmatrix} = r \begin{bmatrix} \cos v \\ \sin v \end{bmatrix} \tag{3.4-1}$$

This representation is not convenient at this moment since both r and v are dependent on the chosen orbital parameters a, e, E_o and n. The following well known formulas can be set up

$$\bar{x}' = \begin{bmatrix} x'_\omega \\ y'_\omega \end{bmatrix} = a \begin{bmatrix} \cos E - e \\ \sqrt{1 - e^2}\ \sin E \end{bmatrix} \tag{3.4-2}$$

After differentiation of (3.4-2) with regard to time one obtains

$$\dot{\bar{x}}'_\omega = \begin{bmatrix} \dot{x}'_\omega \\ \dot{y}'_\omega \end{bmatrix} = a\dot{E}\begin{bmatrix} -\sin E \\ \sqrt{1 - e^2}\ \cos E \end{bmatrix} \tag{3.4-3}$$

In these formulas the eccentric anomaly E and its time derivative $\dot{E}$ have to be viewed as intermediate variables which still need to be related to the chosen variables a, e, E_o and n.

The mean anomaly M as defined by

$$M = n(t - T) \tag{3.4-4}$$

is related to E through Kepler's equation as follows

$$M = E - e \sin E \tag{3.4-5}$$

Equating (3.4-4) to (3.4-5) and introducing the reference epoch to (=0) and the corresponding reference anomalies M_o and E_o one has

$$\begin{aligned} n(t - T) &= E - e \sin E \\ n(t-t_o) + n(t_o-T) &= E - e \sin E \\ n(t-t_o) + M_o &= E - e \sin E \\ n(t-t_o) + E_o - e \sin E_o &= E - e \sin E \end{aligned}$$

With $t_o = 0$ the following representation of Kepler's equation is referred to throughout the rest of this investigation

$$(E-E_o) - e(\sin E-\sin E_o) - nt = 0 \tag{3.4-6}$$

This equation expresses the functional relationship between the intermediate variable E and the parameters e, E_o and n. Because of the transcendental nature of equation (3.4-6), no explicit expression for E in terms of e, E_o and n can be obtained. In contrast, an explicit expression for the second intermediate variable $\dot{E}$ can be obtained from (3.4-6)

$$t = \frac{(E-E_o) - e(\sin E - \sin E_o)}{n} \tag{3.4-7}$$

Computing the derivative of (3.4-7) with regard to E one gets

$$\frac{\partial t}{\partial E} = \frac{1 - e\cos E}{n}$$

which yields the required $\dot{E}$

$$\dot{E} = \frac{n}{1 - e\cos E} \tag{3.4-8}$$

The required statevector $(\bar{x}_\omega, \dot{\bar{x}}_\omega)$ still needs to be computed. From Figure 3.4. it is clear that

$$\bar{x}_\omega = \begin{bmatrix} x_\omega \\ y_\omega \end{bmatrix} = \begin{bmatrix} x'_\omega\cos\omega - y'_\omega\sin\omega \\ x'_\omega\sin\omega + y'_\omega\cos\omega \end{bmatrix} \tag{3.4-9}$$

and upon differentiation of (3.4-9) with regard to time

$$\dot{\bar{x}}_\omega = \begin{bmatrix} \dot{x}_\omega \\ \dot{y}_\omega \end{bmatrix} = \begin{bmatrix} \dot{x}'_\omega\cos\omega - \dot{y}'_\omega\sin\omega \\ \dot{x}'_\omega\sin\omega + \dot{y}'_\omega\cos\omega \end{bmatrix} \tag{3.4-10}$$

Using the expressions (3.4-2), (3.4-3), (3.4-6) and (3.4-8) in (3.4-9) and (3.4-10) one arrives at the direct transformation formulas between statevector and Keplerian elements

$$\bar{x}_\omega = a\begin{bmatrix}\cos\omega & -\sin\omega \\ \sin\omega & \cos\omega\end{bmatrix}\begin{bmatrix}\cos E - e \\ \sqrt{1 - e^2}\,\sin E\end{bmatrix} \tag{3.4-11}$$

and

$$\dot{\bar{x}}_\omega = \frac{an}{1 - e\cos E}\begin{bmatrix}\cos\omega & -\sin\omega \\ \sin\omega & \cos\omega\end{bmatrix}\begin{bmatrix}-\sin E \\ \sqrt{1 - e^2}\,\cos E\end{bmatrix} \tag{3.4-12}$$

with $$(E - E_o) - e(\sin E - \sin E_o) - nt = 0$$

Careful inspection of the expressions above reveal that one has four statevector elements as a function of five Keplerian elements. A completely different effect occurs in the elliptic orbit as opposed to the circular orbits. Had one too many Cartesian elements in the case of circular orbits the reverse appears to be true in case of elliptic orbits: one has apparently too many Keplerian elements. Following the same reasoning as developed in the previous sections one tends to search for the condition which brings the five (dependent?) Keplerian elements down to four. This reasoning is false since it was shown at the beginning of this section that five parameters were needed to position a satellite along an elliptic orbit. One has at this point to reach the opposite conclusion: the statevector supplies too few (four instead of five) parameters to successfully represent a satellite in position along an elliptical path. Consequently, the transformation formulas (3.4-11) and (3.4-12) are not allowed to be

used in case of elliptical motions where GM (or n) is considered unknown.

3.4.2 GM (or n) Known

Does one enforce the more restricted behaviour of the elliptical motion of a satellite as expressed by Kepler's Third Law (3.2-15) one arrives at a legitimate set of transformation formulas. Eliminating the mean motion n from (3.4-11) and (3.4-12) by means of (3.2-15) one immediately arrives at

$$\bar{x}_\omega = a\begin{bmatrix}\cos\omega & -\sin\omega \\ \sin\omega & \cos\omega\end{bmatrix}\begin{bmatrix}\cos E - e \\ \sqrt{1-e^2}\,\sin E\end{bmatrix} \tag{3.4-13}$$

and

$$\dot{\bar{x}}_\omega = \frac{\sqrt{GM/a}}{1 - e\cos E}\begin{bmatrix}\cos\omega & -\sin\omega \\ \sin\omega & \cos\omega\end{bmatrix}\begin{bmatrix}-\sin E \\ \sqrt{1-e^2}\,\cos E\end{bmatrix} \tag{3.4-14}$$

with

$$(E-E_o) - e(\sin E - \sin E_o) - \sqrt{GM/a^3}\,t = 0 \tag{3.4-15}$$

Inspection of these formulas reveals the relationship between four statevector elements (x_ω, y_ω, $\dot{x}_\omega$, $\dot{y}_\omega$) and four Keplerian elements (a, e, ω, E_o).

3.5 Three Dimensional Elliptic Motion

As in section 3.3 the generalization to the third dimension will add two angles, describing the orientation of the orbital ellipse, to the set of Keplerian elements but also two elements to the statevector. Once again, it is expected that in the geometrically more free theory (GM (or n) considered unknown) no transformation between Keplerian and Cartesian orbital elements is possible because of the

deficiency in the number of available parameters in the latter set. Only in the case of "GM known" the transformation is a legitimate one.

3.5.1 GM (or n) Unknown

The following figure illustrates the three dimensional elliptic motion of a satellite around a primary mass.

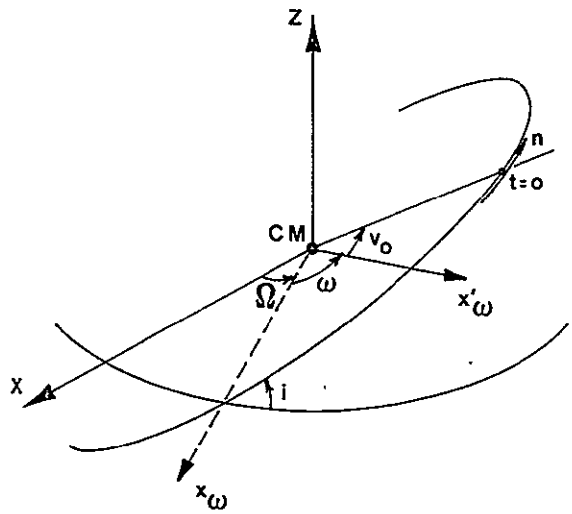

Figure 3.5. 3-D Elliptic Motion, Keplerian elements and Statevector

As in section 3.3.1 the direct transformation formulas are obtained after two rotations $R_1(-i)$ and $R_3(-\Omega)$ of the $\bar{x}_\omega$ system (equations (3.4-11) and (3.4-12)):

$$\bar{X} = R_3(-\Omega)R_1(-i)\bar{x}_\omega \tag{3.5-1}$$

and after differentiating (3.5-1) with regard to time

$$\dot{\bar{X}} = R_3(-\Omega)R_1(-i)\dot{\bar{x}}_\omega \tag{3.5-2}$$

$\bar{x}_\omega$ and $\dot{\bar{x}}_\omega$ are defined as in the equations (3.4-11) and (3.4-12) except for the addition of the third elements z_ω and $\dot{z}_\omega$ (both equal to zero). This addition of the third dimension allows the equations (3.4-11) and (3.4-12) to be rewritten as

$$\bar{x}_\omega = aR_3(-\omega)\begin{bmatrix} \cos E - e \\ \sqrt{1 - e^2}\,\sin E \\ 0 \end{bmatrix} \tag{3.5-3}$$

and

$$\dot{\bar{x}}_\omega = \frac{an}{1 - e\cos E} R_3(-\omega)\begin{bmatrix} -\sin E \\ \sqrt{1 - e^2}\,\cos E \\ 0 \end{bmatrix} \tag{3.5-4}$$

Substituting (3.5-3) and (3.5-4) into (3.5-1) and (3.5-2) and recalling Kepler's equation (3.4-6) one finds

$$\bar{X} = aR_3(-\Omega)R_1(-i)R_3(-\omega)\begin{bmatrix} \cos E - e \\ \sqrt{1 - e^2}\,\sin E \\ 0 \end{bmatrix} \tag{3.5-5}$$

and

$$\dot{\bar{X}} = \frac{an}{1 - e\cos E}\; R_3(-\Omega)R_1(-i)R_3(-\omega)\begin{bmatrix} -\sin E \\ \sqrt{1 - e^2}\,\cos E \\ 0 \end{bmatrix} \tag{3.5-6}$$

with $\quad (E-E_o) - e(\sin E-\sin E_o) - nt = 0$

These two sets of formulas represent the relationships between six Cartesian orbital elements (X, Y, Z, $\dot{X}$, $\dot{Y}$, $\dot{Z}$) and seven Keplerian elements (a, e, i, Ω, ω, E_o, n). These latter ones are the seven elements Gauss is referring to in the quote at the beginning of this chapter. More precisely, he refers to GM instead of n as the seventh required element. As will be shown in later chapters, the seven

parameter orbit allows greater geometrical freedom than the six parameter orbit would do.

3.5.2 GM (or n) Known

Kepler's Third Law will eliminate the variable n from the transformation formulas in section 3.5.1. Without derivation one obtains directly

$$\overline{X} = aR_3(-\Omega)R_1(-i)R_3(-\omega)\begin{bmatrix} \cos E - e \\ \sqrt{1 - e^2}\,\sin E \\ 0 \end{bmatrix} \tag{3.5-7}$$

and

$$\dot{\overline{X}} = \frac{\sqrt{GM/a}}{1 - e\cos E}\; R_3(-\Omega)R_1(-i)R_3(-\omega)\begin{bmatrix} -\sin E \\ \sqrt{1 - e^2}\,\cos E \\ 0 \end{bmatrix} \tag{3.5-8}$$

with $\quad (E-E_o) - e(\sin E-\sin E_o) - \frac{t}{a}\sqrt{\frac{GM}{a}} = 0$

As in section 3.4.2 one has arrived at a legitimate transformation because of the relationship between six statevector elements $(X, Y, Z, \dot{X}, \dot{Y}, \dot{Z})$ and six Keplerian elements $(a, e, i, \Omega, \omega, E_o)$.

3.6 Three Dimensional Secularly Perturbed Elliptic Motion

In this section a simple orbital geometry will be developed in case that secular perturbations change the right ascension of the ascending node, the argument of perigee and mean anomaly in a linear fashion with respect to time. The particular Keplerian elements can be expressed as

$$\Omega_t = \Omega_o + \dot{\Omega}t \tag{3.6-1}$$

$$\omega_t = \omega_o + \dot{\omega}t \tag{3.6-2}$$

$$M_t = M'_o + \dot{M}t \tag{3.6-3}$$

Rather than having $\dot{M}$ as the secular parameter, it is easier to view this rate of change of the mean anomaly to the rate of change M has anyway on basis of its definition

$$M = n(t-T)$$

This correction to the mean motion n which in the case of secular perturbations should be referred to as the mean anomalistic motion (defined between perifocal passages), yields

$$M_t = n(t-t_o) + n(t_o-T) + \dot{M}t$$

$$M_t = (n+\dot{M})t + (E_o - e\sin E_o) \tag{3.6-4}$$

One recognizes that in equation (3.6-4) only the combination $(n + \dot{M})$ appears, consequently making n and $\dot{M}$ not separable. In the geometrical model define

$$n_{(new)} = n_{(old)} + \dot{M} \tag{3.6-5}$$

3.6.1 GM (or n) and J_2 (or $\dot{\omega}$, $\dot{\Omega}$, n) Unknown

A geometrical orbital theory will be developed in this section. This theory does not take any dynamical laws into consideration; however the choice of the geometric parameters is based on the experience given us by dynamical considerations: it will be acknowledged that the satellite's orbit is elliptical, however the

relationship between a, n and GM contains two independent parameters; also it will be acknowledged that the satellite's orbital ellipse changes its orientation in a secular way: two parameters will be added to describe the changing right ascension of the ascending node $\dot{\Omega}$ and the argument of perigee $\dot{\omega}$; the mean motion n will now be simply defined as the mean anomalistic motion (which will differ from the mean nodal motion).

Substituting (3.6-1), (3.6-2) and (3.6-5) in the previously derived expression (3.5-5) the transformation formulas will have the following structure

$$\overline{X} = aR_3(-\Omega-\dot{\Omega}t)R_1(-i)R_3(-\omega-\dot{\omega}t)\begin{bmatrix} \cos E - e \\ \sqrt{1 - e^2}\,\sin E \\ 0 \end{bmatrix} \qquad (3.6\text{-}6)$$

Differentiating (3.6-6) with regard to time yields the velocity part of the statevector. The time dependency of the rotation matrices $R_3(-\Omega-\dot{\Omega}t)$ and $R_3(-\omega-\dot{\omega}t)$ has to be considered

$$\begin{aligned} \frac{\partial R_3(-\Omega-\dot{\Omega}t)}{\partial t} &= -\dot{\Omega}L_3R_3(-\Omega-\dot{\Omega}t) \\ &= -\dot{\Omega}R_3(-\Omega-\dot{\Omega}t)L_3 \end{aligned} \qquad (3.6\text{-}7)$$

and

$$\begin{aligned} \frac{\partial R_3(-\omega-\dot{\omega}t)}{\partial t} &= -\dot{\omega}L_3R_3(-\omega-\dot{\omega}t) \\ &= -\dot{\omega}R_3(-\omega-\dot{\omega}t)L_3 \end{aligned} \qquad (3.6\text{-}8)$$

where L_3 is defined by equation (3.3-25).

The velocity statevector will be

$$\dot{\overline{X}} = \frac{an}{1 - e\cos E} R_3(-\Omega-\dot{\Omega}t)R_1(-i)R_3(-\omega-\dot{\omega}t)\begin{bmatrix} -\sin E \\ \sqrt{1 - e^2}\cos E \\ 0 \end{bmatrix}$$

$$-a\dot{\omega}R_3(-\Omega-\dot{\Omega}t)R_1(-i)R_3(-\omega-\dot{\omega}t)L_3\begin{bmatrix} \cos E - e \\ \sqrt{1 - e^2}\sin E \\ 0 \end{bmatrix} \qquad (3.6\text{-}9)$$

$$-a\dot{\Omega}L_3R_3(-\Omega-\dot{\Omega}t)R_1(-i)R_3(-\omega-\dot{\omega}t)\begin{bmatrix} \cos E - e \\ \sqrt{1 - e^2}\sin E \\ 0 \end{bmatrix}$$

This expression can be simplified by back substitution of equations (3.4-2), (3.4-3) and (3.6-6)

$$\dot{\overline{X}} = R_3(-\Omega-\dot{\Omega}t)R_1(-i)R_3(-\omega-\dot{\omega}t)(\dot{\overline{x}}'_\omega-\dot{\omega}L_3\overline{x}'_\omega) - \dot{\Omega}L_3\overline{X} \qquad (3.6\text{-}10)$$

One has to realize that $\overline{x}'_\omega$ and $\dot{\overline{x}}'_\omega$ have been made three dimensional vectors by amending zeros. Similarly, the expression for $\overline{X}$ can be rewritten as

$$\overline{X} = R_3(-\Omega-\dot{\Omega}t)R_1(-i)R_3(-\omega-\dot{\omega}t)\overline{x}'_\omega \qquad (3.6\text{-}11)$$

Denoting the time dependent rotation matrix as $\mathbb{R}_t$, one can summarize the transformation formulas as follows

$$\overline{X} = \mathbb{R}_t\begin{bmatrix} x'_\omega \\ y'_\omega \\ 0 \end{bmatrix}$$

$$\dot{\overline{X}} = \mathbb{R}_t\begin{bmatrix} \dot{x}'_\omega - \dot{\omega}y'_\omega \\ \dot{y}'_\omega + \dot{\omega}x'_\omega \\ 0 \end{bmatrix} + \dot{\Omega}\begin{bmatrix} -Y \\ X \\ 0 \end{bmatrix} \qquad (3.6\text{-}12)$$

with $$(E-E_o) - e(\sin E-\sin E_o) - nt = 0$$

This set of formulas represents the relationships between six Cartesian orbital elements (X, Y, Z, $\dot{X}$, $\dot{Y}$, $\dot{Z}$) and nine Keplerian elements (a, e, i, Ω, $\dot{\Omega}$, ω, $\dot{\omega}$, E_o, n). The orbital model as represented by (3.6-12) allows even greater geometrical freedom than any previously derived orbit.

3.6.2 GM (or n) and J_2 (or $\dot{\omega}$, $\dot{\Omega}$, n) Known

If one enforces the dynamical law as Kepler's Third Law <u>and</u> considers the gravitational constant GM to be a constant, then one parameter (n) can be eliminated. In a very similar reasoning the dynamical "laws" defining $\dot{\Omega}$, $\dot{\omega}$, and n as a function of J_2 and considering J_2 to be a constant will successfully eliminate two more parameters ($\dot{\Omega}$, $\dot{\omega}$) from the orbital model (3.6-12). Neglecting the secular perturbations caused by J_2^2 and higher order zonal harmonic coefficients (J_n, $n \geq 3$) one has from e.g., [Escobal, 1976],

$$n = n_o \left[1 + \frac{3}{2} \frac{J_2 a_e^2 \sqrt{1 - e^2}}{a^2(1-e^2)^2} (1 - \frac{3}{2} \sin^2 i) \right] \tag{3.6-13}$$

$$\dot{\Omega} = - \frac{3}{2} \frac{J_2 a_e^2}{a^2(1-e^2)^2} n \cos i \tag{3.6-14}$$

$$\dot{\omega} = \frac{3}{2} \frac{J_2 a_e^2}{a^2(1-e^2)^2} n(2 - \frac{5}{2} \sin^2 i) \tag{3.6-15}$$

$$n_o = \sqrt{GM/a^3} \tag{3.6-16}$$

Substituting (3.6-16) into (3.6-13) one has for the mean anomalistic motion

$$n = \sqrt{GM/a^3}\left[1 + \frac{3}{2}\frac{J_2 a_e^2\sqrt{1-e^2}}{a^2(1-e^2)^2}\left(1-\frac{3}{2}\sin^2 i\right)\right] \tag{3.6-17}$$

Inspecting (3.6-14), (3.6-15) and (3.6-17) one has expressed $\dot{\Omega}$, $\dot{\omega}$ and n as functions of the orbital parameters a, e and i. Substitution of these three expressions into the transformation formulas (3.6-12) gives the orbital model with the two dynamical laws enforced. The complete orbital transformation model has to be written as follows.

$$\bar{X} = \mathbb{R}_t \begin{bmatrix} x'_\omega \\ y'_\omega \\ 0 \end{bmatrix}$$

$$\dot{\bar{X}} = \mathbb{R}_t \begin{bmatrix} \dot{x}'_\omega - \dot{\omega} y'_\omega \\ \dot{y}'_\omega + \dot{\omega} x'_\omega \\ 0 \end{bmatrix} + \dot{\Omega}\begin{bmatrix} -Y \\ X \\ 0 \end{bmatrix}$$

with

$$(E-E_o) - e(\sin E - \sin E_o) - nt = 0 \tag{3.6-18}$$

$$\mathbb{R}_t = R_3(-\Omega-\dot{\Omega}t)R_1(-i)R_3(-\omega-\dot{\omega}t)$$

$$n = \sqrt{GM/a^3}\left[1 + \frac{3}{2}\frac{J_2 a_e^2\sqrt{1-e^2}}{a^2(1-e^2)^2}\left(1-\frac{3}{2}\sin^2 i\right)\right]$$

$$\dot{\Omega} = -\frac{3}{2}\frac{J_2 a_e^2}{a^2(1-e^2)^2}\, n\cos i$$

and

$$\dot{\omega} = \frac{3}{2}\frac{J_2 a_e^2}{a^2(1-e^2)^2}\, n\left(2-\frac{5}{2}\sin^2 i\right)$$

The set of formulas (3.6-18) represents the relationships between six Cartesian orbital elements (X, Y, Z, $\dot{X}$, $\dot{Y}$, $\dot{Z}$) and six

Keplerian elements (a, e, i, Ω, ω, E_o). Because of this compatibility a set of reversed transformation formulas might be derived. Several remarks need to be made:

- GM and J_2 are considered to be constants. Not doing so, one has merely replaced one parameter by another parameter (in case of Kepler's Third Law: n by GM).
- Because of the dependency of the mean anomalistic motion on the inclination (3.6-17), the intermediate variable E becomes dependent on the inclination. This fact in turn makes the orbital parameters $\bar{x}'_\omega$ and $\dot{\bar{x}}'_\omega$ dependent on the inclination! This needs to be taken into account when developing the differential relationships (see Appendices A and B).

3.7 Summary

From Table 3.1 the 9 parameter orbital model is the most general one: it retains the highest geometrical freedom which should result in an intermediate orbit which can follow the real orbit accurately for long periods of time. Its flexibility does not only concern the gravitational constant GM but also the secular perturbations. It solves with the help of geometric parameters $\dot{\Omega}$, $\dot{\omega}$ and n for the secular changes in the parameters Ω, ω and M without specifying the cause of these secular perturbations. It is known that terms as J_2^2, J_3, J_4, etc. cause secular perturbations as well in these parameters.

The comparison between the Keplerian and statevector approach was given here because if an orbit determination takes place with the

Table 3.1

The Relationship Between Keplerian Elements and Statevectors for the Various Orbital Models

Orbital Model		Keplerian Elements	No.	Statevector[1]	No.	Compatibility	Constants	Remarks
Circular Motion	2D	a, u_o, n	3	$x_\omega, y_\omega, \dot{x}_\omega, \dot{y}_\omega$	4	no	-	1 condition for statevector
		a, u_o	2	$x_\omega, y_\omega, \dot{x}_\omega, \dot{y}_\omega$	4	no	GM	2 conditions for statevector
	3D	a, i, Ω, u_o, n	5	$X, Y, Z, \dot{X}, \dot{Y}, \dot{Z}$	6	no	-	1 condition for statevector
		a, i, Ω, u_o	4	$X, Y, Z, \dot{X}, \dot{Y}, \dot{Z}$	6	no	GM	2 conditions for statevector
Elliptic Motion	2D	a, e, ω, E_o, n	5	$x_\omega, y_\omega, \dot{x}_\omega, \dot{y}_\omega$	4	no	-	1 deficiency for statevector
		a, e, ω, E_o	4	$x_\omega, y_\omega, \dot{x}_\omega, \dot{y}_\omega$	4	yes	GM	-
	3D	$a, e, i, \Omega, \omega, E_o, n$	7	$X, Y, Z, \dot{X}, \dot{Y}, \dot{Z}$	6	no	-	1 deficiency for statevector
		$a, e, i, \Omega, \omega, E_o$	6	$X, Y, Z, \dot{X}, \dot{Y}, \dot{Z}$	6	yes	GM	-
Secularly Perturbed Elliptic Motion	3D	$a, e, i, \Omega, \dot{\Omega}, \omega, \dot{\omega}, E_o, n$	9	$X, Y, Z, \dot{X}, \dot{Y}, \dot{Z}$	6	no	-	3 deficiencies for statevector
		$a, e, i, \Omega, \omega, E_o$	6	$X, Y, Z, \dot{X}, \dot{Y}, \dot{Z}$	6	yes	GM + J_2	-

[1] GM (and J_2) were considered known in all cases for the statevector.

help of range, range-rate or range difference observations, the statevector approach is often resorted due to the simplicity of the mathematics. As it has been shown in this chapter, there are several hidden constraints or deficiencies among the statevector elements in the various orbital models.

4. ORBIT, OBSERVER AND OBSERVATIONS

"Certainly all these problems can be solved by subjection to the cannonnade of numerical analysis . . . "

P. R. Escobal [1976]

4.1 Introduction

Throughout the literature in celestial mechanics and related sciences chapters on the various orbit determination techniques play important roles. Starting with analytical methods of orbit determination, often having its roots in the Keplerian representation, detailed procedures are worked out on how to update the state of a planet, satellite, etc. Two assumptions are often being made: the first deals with the fact that an initial state of the satellite is known, the second deals with the description of the satellite's environment which is prescribing the satellite's path (e.g. the force field of the primary planet). It is this second item which gives all too often the fatal blow to analytical theories of orbit determination. The complexity of the satellite's environment prescribes a path for the satellite which is very difficult to represent in an analytical way. At this point methods of numerical integration come to help. They solve numerically a set of differential equations according to which the prescribed path can be calculated (iterated, corrected, etc.). The real test comes

only then when the celestial mechanic has a set of observations at his disposal. These observations enable him in addition to the internal checks (for which no observations are necessary) to perform the external check between theory and reality. The position from which the observations are made, is often of second interest to the astronomer and his methods and accuracies are such that this (lack of) knowledge does not influence his orbital theory. In this respect the interest of the celestial geodesist is reversed: the satellite is a nuisance object having in its trail many nuisance parameters. However, the position of the celestial geodesist and the description of the satellite's environment (e.g. the earth's gravity field) are of primary interest to him. Reality must be between these two apparent extremes.

If observational evidence forms the cornerstone of our knowledge, then we have to build on them: a description of the satellite's path, a description of the observer's path and a description of the satellite's and observer's environment. Assuming no a priori knowledge of any of the parameters several questions need to be answered:

(a) Given a certain measurement system can it describe the observer's and satellite's paths as well as some of the environmental parameters?

(b) Given a certain measurement system will any set of parameters be able to perform this task?

(c) Given a certain measurement system can it recover <u>all</u> parameters necessary to describe the satellite's and observer's paths and their environment?

The previous chapter tried to answer question (b) by stressing the care to be exercised in employing Cartesian orbital elements. This chapter will attempt to answer the remaining questions. As an illustration the reader is referred to the following story.

4.2 The Clock Problem

Once upon a time there was a little country named Temporaria. Its reigning king, an enlightened despot, used to punish his subjects by having them take place at the ends of the hands of clocks. This not being an enviable position to be in, the punished ones quickly devised games to alleviate the boredom of their revolutionary stay. The inhabitants of Temporaria were scientifically minded, so it was no surprise that their favorite game was rather intellectual. By calling each other as soon as they came in hearing distance and noting the time it took to get the call returned by his fellow inmate and also the change in pitch of the call, they derived ranges and range-rates. These observations provided them with the puzzle how far they were separated from each other and how they moved with respect to each other. Preferably, they solved their puzzle in an inertial clock-fixed frame (see Figure 4.1).

If one denotes the position and velocity vector of subject A occupying the big hand by X, Y, $\dot{X}$, $\dot{Y}$ and the position and velocity vector of subject B on the short hand by x, y, $\dot{x}$, $\dot{y}$ and the origins of the rotations by x_o, y_o one might believe that making more than ten let say range observations will furnish the principal characters of the story with the required 10 parameters.

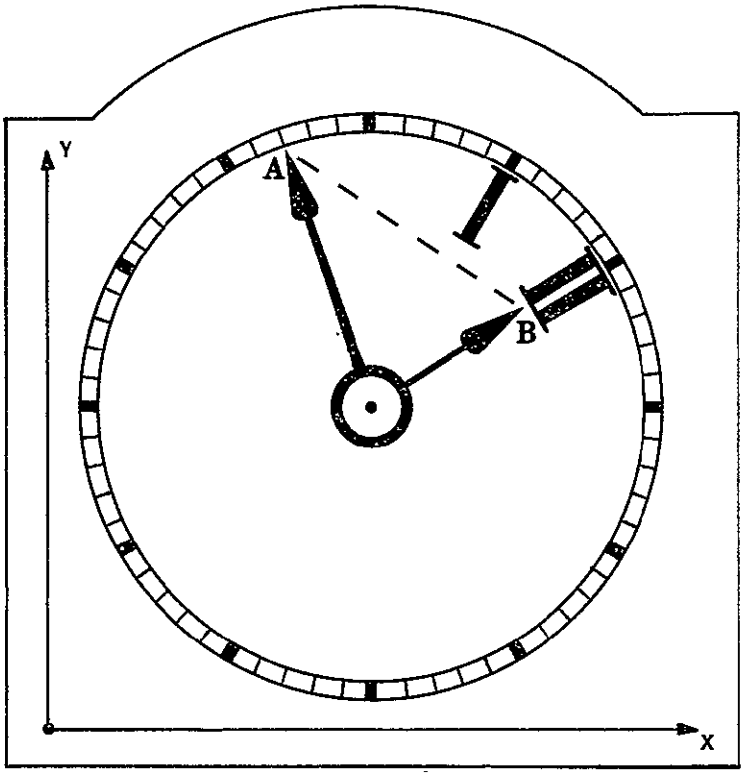

Figure 4.1. Rotations in a Reference Frame

The discussion of section 3.2.1 explained that in case of two dimensional circular motion with constant angular velocity only three out of the four state vector elements are independent. This fact directly reduces our set of parameters to eight.

The orbital elements of subject A are (equation 3.2-13)

$$\overline{X} = \begin{bmatrix} X \\ Y \end{bmatrix} = a \begin{bmatrix} \cos(u_o+nt) \\ \sin(u_o+nt) \end{bmatrix} + \begin{bmatrix} x_o \\ y_o \end{bmatrix} \tag{4.2-1}$$

$$\dot{\overline{X}} = \begin{bmatrix} \dot{X} \\ \dot{Y} \end{bmatrix} = an \begin{bmatrix} -\sin(u_o+nt) \\ \cos(u_o+nt) \end{bmatrix} \tag{4.2-2}$$

with

$$(X-x_o)\dot{X} + (Y-y_o)\dot{Y} = 0 \tag{4.2-3}$$

and for subject B

$$\bar{x} = \begin{bmatrix} x \\ y \end{bmatrix} = R\begin{bmatrix} \cos(ST+\omega_e t) \\ \sin(ST+\omega_e t) \end{bmatrix} + \begin{bmatrix} x_o \\ y_o \end{bmatrix} \tag{4.2-4}$$

$$\dot{\bar{x}} = \begin{bmatrix} -\dot{x} \\ \dot{y} \end{bmatrix} = R\omega_e \begin{bmatrix} -\sin(ST+\omega_e t) \\ \cos(ST+\omega_e t) \end{bmatrix} \tag{4.2-5}$$

with $$(x-x_o)\dot{x} + (y-y_o)\dot{y} = 0 \tag{4.2-6}$$

The new variables a, u_o, n, R, ST and ω_e are illustrated in Figure 4.2.

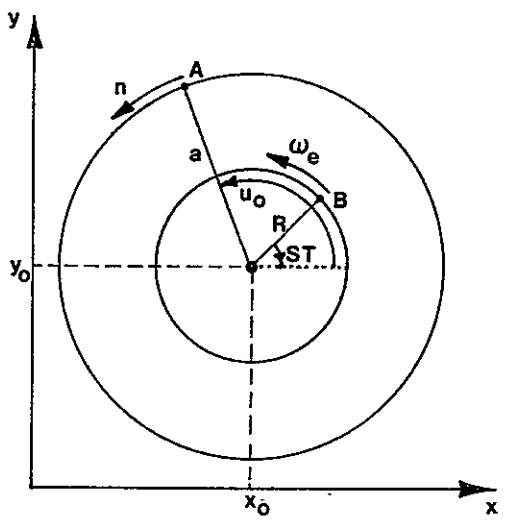

Figure 4.2. Two Dimensional Circular Motions

The range equation will be, from (4.2-1) and (4.2-4)

$$\begin{aligned} r^2 &= (X-x)^2 + (Y-y)^2 \\ &= [a\cos(u_o+nt) - R\cos(ST+\omega_e t)]^2 + \\ &\quad [a\sin(u_o+nt) - R\sin(ST+\omega_e t)]^2 \end{aligned}$$

This equation reduces to

$$r^2 = a^2 + R^2 - 2aR\cos[(u_o - ST) + (n-\omega_e)t] \qquad (4.2\text{-}7)$$

Since the pairs u_o, ST and n, ω_e only appear as differences in equation (4.2-7) only their differences are estimable.

Setting

$$u_o - ST = \alpha_o$$

and

$$n - \omega_e = \dot{\alpha}$$

one obtains

$$r^2 = a^2 + R^2 - 2aR\cos(\alpha_o + \dot{\alpha}t) \qquad (4.2\text{-}8)$$

One hardly has to describe the disappointment of the already so unfortunate inhabitants of Temporaria when upon inspection of equation (4.2-8) they found only four out of the ten parameters to be estimable:

a, the distance of subject A to the center of rotation;

R, the distance of subject B to the center of rotation;

α_o, the angle between the hands of reference epoch t = 0 and

$\dot{\alpha}$, the difference of the angular velocities of the two hands.

In case of range-rate observations one obtains by differentiation of equation (4.2-8) with regard to time

$$2r\frac{dr}{dt} = 2(X-x)\left(\frac{dX}{dt} - \frac{dx}{dt}\right) + 2(Y-y)\left(\frac{dY}{dt} - \frac{dy}{dt}\right)$$

Substitution of equations (4.2-1), (4.2-2), (4.2-4) and (4.2-5) into the equation above yields

$$r\dot{r} = [a\cos(u_o+nt) - R\cos(ST+\omega_e t)][-an\sin(u_o+nt) + R\omega_e\sin(ST+\omega_e t)] +$$
$$[a\sin(u_o+nt) - R\sin(ST+\omega_e t)][an\cos(u_o+nt) - R\omega_e\cos(ST+\omega_e t)]$$

which reduces after some manipulations to

$$r\dot{r} = aR\,\dot{\alpha}\sin(\alpha_o+\dot{\alpha}t) \tag{4.2-9}$$

This <u>range-rate equation</u> can also be written as

$$\dot{r} = \frac{aR\,\dot{\alpha}\sin(\alpha_o+\dot{\alpha}t)}{\sqrt{a^2 + R^2 - 2aR\cos(\alpha_o+\dot{\alpha}t)}} \tag{4.2-10}$$

This equation could have been obtained directly from equation (4.2-8) after differentiation with regard to time. Inspection of the range-rate equation (4.2-10) reveals similar conclusions as far as estimability is concerned: only four parameters a, R, α_o, $\dot{\alpha}$ are estimable. This means that the same variables are estimable from range and range-rate observations.

In case of range-difference observations the <u>range-difference equation</u> can be obtained by differencing two range equations evaluated for epochs $(t + \Delta t)$ and t. From equation (4.2-8) one has

$$\Delta r = r_{t+\Delta t} - r_t = \sqrt{a^2 + R^2 - 2aR\cos[\alpha_o+\dot{\alpha}(t+\Delta t)]} - \sqrt{a^2 + R^2 - 2aR\cos(\alpha_o+\dot{\alpha}t)} \tag{4.2-11}$$

Once again, the same four parameters, a, R, α_o and $\dot{\alpha}$ are estimable.

An alternative for the range-difference equation can be obtained from the original (squared) range equations

$$r^2_{t+\Delta t} - r^2_t = \Delta r(r_{t+\Delta t} + r_t) \tag{4.2-12}$$

$$= -2aR\{\cos[\alpha_o+\dot{\alpha}(t+\Delta t)] - \cos(\alpha_o+\dot{\alpha}t)\} \tag{4.2-13}$$

Combining equations (4.2-12) and (4.2-13) yields

$$\Delta r = \frac{4aR\sin[\alpha_o+\dot{\alpha}(t+\frac{1}{2}\Delta t)]\sin\frac{1}{2}\dot{\alpha}\Delta t}{r_{t+\Delta t} + r_t} \tag{4.2-14}$$

If $1/2\dot{\alpha}\Delta t$ is small one has by approximation

$$\sin\frac{1}{2}\dot{\alpha}\Delta t \simeq \frac{1}{2}\dot{\alpha}\Delta t$$

and

$$r_{t+\Delta t} + r_t \simeq 2r_{t+\frac{1}{2}\Delta t}$$

yielding

$$\Delta r \simeq \frac{aR\dot{\alpha}\sin[\alpha_o+\dot{\alpha}(t+\frac{1}{2}\Delta t)]}{\sqrt{a^2 + R^2 - 2aR\cos[\alpha_o+\dot{\alpha}(t+\frac{1}{2}\Delta t)]}} \tag{4.2-15}$$

which is upon division by Δt equal to the range-rate equation evaluated at half way the time interval between t and $(t + \Delta t)$: the range-rate for epoch $(t + 1/2\Delta t)$. Note that equations (4.2-11) and (4.2-14) are rigorous (and identical).

The difference between range-rate and range-difference observations comes into play only then when the range-differences are considered to be correlated or uncorrelated. For a further discussion see Appendix B, section B.8.

Recapitulating, the moral of this story is:

a. having two points with constant circular motions around a common point in a reference frame leads to three sets of variables
   - the state vector of point A $(X, Y, \dot{X}, \dot{Y})$ in the reference frame

- the state vector of point B (x, y, $\dot{x}$, $\dot{y}$) in the reference frame
- the position of the center of rotation (x_o, y_o) in the reference frame

b. making range, range-rate or range-difference observations between point A and B only four combinations of the ten variables mentioned under a. are estimable:

- parameter 1: the distance between point A and the center of rotation (see equation 3.2-8)

$$\sqrt{X^2 + Y^2} = a \tag{4.2-16}$$

- parameter 2: the distance between point B and the center of rotation (see equation 3.2-8)

$$\sqrt{x^2 + y^2} = R \tag{4.2-17}$$

- parameter 3: the angle between the two radius vectors at reference epoch $t = 0$ (see equations 3.2-10 and 3.2-11)

$$\arctan\left(\frac{Y}{X}\right) - \arctan\left(\frac{y}{x}\right) - t\left(\sqrt{\frac{X^2+Y^2}{\dot{X}^2+\dot{Y}^2}} - \sqrt{\frac{x^2+y^2}{\dot{x}^2+\dot{y}^2}}\right) = u_o - ST = \alpha_o \tag{4.2-18}$$

- parameter 4: the difference between the angular velocities of the two radius vectors (see equation 3.2-10)

$$\sqrt{\frac{X^2 + Y^2}{\dot{X}^2 + \dot{Y}^2}} - \sqrt{\frac{x^2 + y^2}{\dot{x}^2 + \dot{y}^2}} = n - \omega_e = \dot{\alpha} \tag{4.2-19}$$

Transforming the story in a more realistic one, point A will be identified as an earth orbiting satellite and point B will be an

earthbound observer. The clock problem reflects an observer at the equator making range, range-rate or range-difference observations to a satellite in an orbit with an inclination of 0° or 180° and eccentricity equal to zero. From the mentioned observations one can only estimate

- the radius a of the orbit
- the distance R between the observer and the geocenter
- the longitude difference α_o (or difference between right ascensions) between the satellite and the observer at t = 0. A little bit differently stated, the difference between local sidereal time of the observer (hour angle of the vernal equinox) and the right ascension of the satellite at reference epoch t = 0
- the difference $\dot{\alpha}$ between the mean motion n of the satellite and the angular velocity ω_e of the earth.

This rather artificial example should serve as an illustrative warning of the limitations of the observations under discussion. In the coming sections more realistic examples will be handled.

4.3 Satellite, Station and Earth Parameters

In the investigation of the range, range-rate and range-difference observations and their contributions to the recovery of various parameters, the latter have been grouped in three categories: satellite, station and earth parameters.

4.3.1 Satellite Parameters

Keplerian orbital elements referring to the equinox and equator of date have been chosen. The parameters are:

- a: the semimajor axis of the orbit ellipse
- e: the eccentricity of the orbit ellipse
- i: the inclination of the orbit plane
- ω: the argument of perigee
- Ω: the right ascension of the ascending node
- E_o: the eccentric anomaly of the satellite at the reference epoch $t = 0$
- n_o: the mean motion of the satellite
- $\dot{\omega}$: the rate of change in the argument of perigee
- $\dot{\Omega}$: the rate of change in the right ascension of the ascending node
- n: the mean anomalistic motion of the satellite (measured between perigee passages).

The last three variables are used in the secularly perturbed orbits.

In the special orbits as circular and zero inclination orbits certain orbital elements are equal to zero or not defined. In the subsequent study the orbital elements are accordingly redefined or omitted as dictated by the various special circumstances.

4.3.2 Station Parameters

The usual geodetic way of expressing the locations of stations around the globe is with respect to a reference ellipsoid

$$\begin{bmatrix} x \\ y \\ z \end{bmatrix} = \begin{bmatrix} (N+h)\cos\phi\cos\lambda \\ (N+h)\cos\phi\sin\lambda \\ [N(1-e^2) + h]\sin\phi \end{bmatrix} \tag{4.3.1}$$

with N being the radius of curvature in the prime vertical

$$N = \frac{a_e}{\sqrt{1 - e^2\sin^2\phi}} \tag{4.3-2}$$

However, in the investigation at hand the reference ellipsoid is completely immaterial. Consequently, the position of the observer will be expressed in geocentric coordinates as depicted in Figure 4.3

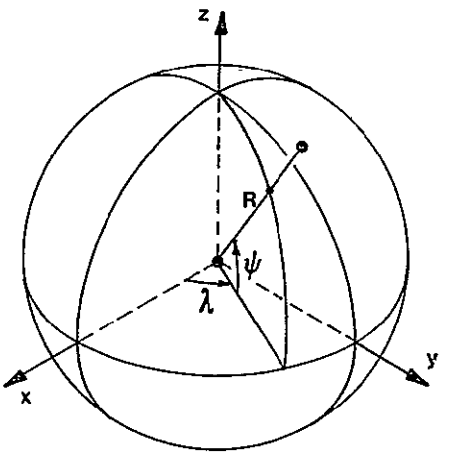

Figure 4.3. Geocentric Reference Frame

From the figure one obviously has

$$\bar{x} = \begin{bmatrix} x \\ y \\ z \end{bmatrix} = R \begin{bmatrix} \cos\psi\cos\lambda \\ \cos\psi\sin\lambda \\ \sin\psi \end{bmatrix} \tag{4.3-3}$$

where R, ψ and λ denote respectively the geocentric radius, the geocentric latitude and the geocentric longitude.

In light of the coming derivations a more unusual representation can be used to one's advantage: one can view the geocentric coordinates of the observer as two consecutive rotations of a unit vector $\bar{e}_1$ scaled by the length R of the radius vector. From equation (4.3-3) one has

$$\bar{x} = R\,R_3(-\lambda)R_2(\psi)\bar{e}_1 \tag{4.3-4}$$

with $\bar{e}_1 = [1,\ 0,\ 0]^T$

or

$$\bar{x} = R_3(-\lambda)R_2(\psi)\begin{bmatrix} R \\ 0 \\ 0 \end{bmatrix} \tag{4.3-5}$$

This representation of the observer's location will mainly be adhered to in the following sections.

4.3.3 Earth Parameters

In the sometimes purely geometrical and other times partly dynamical analysis of orbit, station and earth parameter determination four variables for the earth are included in the (initial) study as presented in this chapter. The parameters are

- ω_e: the instantaneous inertial spin rate of the earth about the instantaneous rotation axis. The variable in this study is simply referred to as the angular velocity of the earth.
- GM: the geocentric gravitational constant of the earth, being the product of the universal gravitational constant G and the mass M of the earth including the atmosphere.
- J_2: the dynamical form factor of the earth, the largest spherical harmonic coefficient (after GM) describing the oblateness of the earth's gravity field.
- $GAST_o$: the Greenwich Apparent Sidereal Time at reference epoch t = 0 describing the orientation of the Greenwich Meridian with respect to the equinox of date, as measured along the equator of date.

Refinements of these simple (i.e. crude) models will be treated in Chapter 5:

polar motion, precession, nutation, non-coincidence of the spin axis and the axis of figure are discussed in section 5.4.

4.4 The Circular Intermediate Orbit, Station and Earth Rotation/Orientation Determination from Range Observations

The ground work for this section has been laid in Chapter 3, sections 3.2 and 3.3.

4.4.1 Two Dimensional Case with GM (or n) Unknown

The two dimensional circular motion with Kepler's Third Law containing two independent parameters has been discussed in section 4.2 as an introductory illustration. From equation (4.2-8) one had the following range equation.

$$r^2 = a^2 + R^2 - 2aR\cos(\alpha_o + \dot{\alpha}t) \tag{4.4-1}$$

The interpretation of the four estimable parameters is given at the end of section 4.2. The third estimable parameter α_o is illustrated in Figure 4.4. From the figure one has the interpretation

$$\alpha_o = \lambda + GAST_o - u_o = \lambda + GAST_o - \Omega - \omega - E_o \tag{4.4-2}$$

and

$$\dot{\alpha} = n - \omega_e \tag{4.4-3}$$

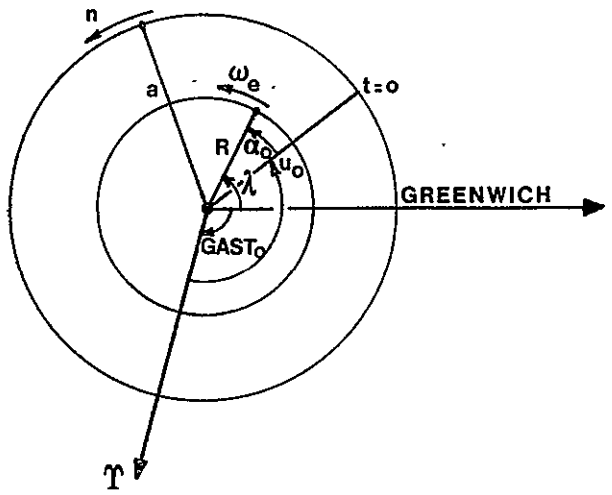

Figure 4.4. The Equator and Orbit Plane

4.4.2 Two Dimensional Case with GM (or n) Known

If one considers the geocentric gravitational constant GM to be a constant, one has for the range equation

$$r^2 = a^2 + R^2 - 2aR\cos\left[\alpha_o + \left(\sqrt{\frac{GM}{a^3}} - \omega_e\right) t\right] \tag{4.4-4}$$

with $\alpha_o = \lambda + GAST_o - u_o = \lambda + GAST_o - \Omega - \omega - E_o$

Once again four estimable parameters are the result with a, R and α_o having the definition as explained in section 4.2. However, the fourth estimable parameter is the angular velocity ω_e of the earth.

It is worth noting that although the consideration of GM being known reduced the number of estimable orbital parameters from three to two as explained in sections 3.2.1 and 3.2.2, the number of estimable parameters in the range equation is not reduced.

4.4.3 Three Dimensional Case with GM (or n) Unknown

The three dimensional circular motion results in a still simple range equation. Initially, a geometric derivation is given with the help of Figure 4.5.

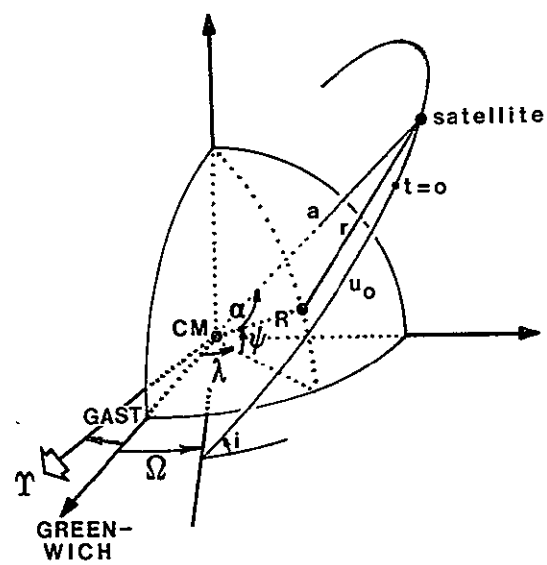

Figure 4.5. Three Dimensional Circular Motion

The angle α can be obtained from the projection of Figure 4.5 onto the celestial sphere. The following relations can be set up from spherical trigonometry (Figure 4.6):

$$\Delta PRS: \quad \cos\alpha = \cos u \cos y + \sin u \sin y \cos(i - i_\psi) \tag{4.4-5}$$

$$\Delta PQR: \quad \cos\psi = \cos(\lambda + GAST_o - \Omega)\cos y + \sin(\lambda + GAST_o - \Omega)\sin y \cos i_\psi \tag{4.4-6}$$

$$\cos y = \cos\psi \cos(\lambda + GAST_o - \Omega) \tag{4.4-7}$$

$$\sin\psi = \sin y \sin i_\psi \tag{4.4-8}$$

Substituting (4.4-7) into (4.4-5) and writing out (4.4-5) one has

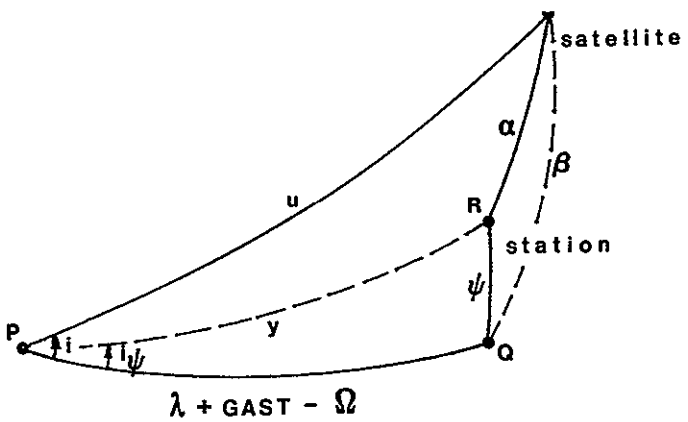

Figure 4.6. The Celestial Sphere and the Fundamental Triangles of Satellite Geodesy

$$\cos\alpha = \cos u \cos\psi \cos(\lambda + GAST - \Omega) + \sin u \sin y \cos i \cos i_\psi + \sin u \sin y \sin i \sin i_\psi \tag{4.4-9}$$

Substituting into equation (4.4-9) expressions for $\sin y \cos i_\psi$ (from 4.4-6) and $\sin y \sin i_\psi$ (from 4.4-8) one gets

$$\cos\alpha = \cos u \cos(\lambda + GAST - \Omega)\cos\psi + \sin u \sin(\lambda + GAST - \Omega)\cos\psi \cos i + \sin u \sin\psi \sin i \tag{4.4-10}$$

Substituting the expression (4.4-10) for $\cos\alpha$ into the range equation (see Figure 4.6) one obtains

$$r^2 = a^2 + R^2 - 2aR\cos\alpha \tag{4.4-11}$$

with $\cos\alpha = \cos\psi\cos\beta + \sin\psi\sin u \sin i$

$$\cos\beta = \cos\Delta\lambda\cos u + \sin\Delta\lambda\sin u \cos i$$

$$\Delta\lambda = \lambda + GAST - \Omega = \lambda + GAST_o - \Omega + \omega_e t$$

$$u = u_o + nt = \omega + E_o + nt$$

Evaluation of the range equation yields the following eight estimable parameters

- satellite parameters : a, i, $\omega + E_o$, n
- station parameters : R, ψ
- earth parameter : ω_e
- mixed station/earth/satellite parameter: $\lambda + GAST_o - \Omega$

4.4.4 Three Dimensional Case with GM (or n) Known

If one considers GM in Kepler's Third Law to be a constant one obtains for the range equation

$$r^2 = a^2 + R^2 - 2aR\cos\alpha \qquad (4.4\text{-}12)$$

with $\cos\alpha = \cos\psi\cos\beta + \sin\psi\sin u \sin i$

$$\cos\beta = \cos\Delta\lambda\cos u + \sin\Delta\lambda\sin u \cos i$$

$$\Delta\lambda = \lambda + GAST - \Omega = \lambda + GAST_o - \Omega + \omega_e t$$

$$u = u_o + \sqrt{GM/a^3}\, t = \omega + E_o + \sqrt{GM/a^3}\, t$$

Evaluation of the range equation yields the following seven estimable parameters:

- satellite parameters : a, i, $\omega + E_o$
- station parameters : R, ψ

- earth parameter : ω_e
- mixed station/earth/satellite parameter: $\lambda + GAST_o - \Omega$

4.4.5 Three Dimensional Case, Alternate Approach

The limitations of the estimability of the various parameters can be arrived at along more algebraic ways rather than the geometrical approach presented above.

The starting point will be the Cartesian orbital elements, X, Y, Z, $\dot{X}$, $\dot{Y}$, $\dot{Z}$ and the Cartesian coordinates for the station (x, y, z). The range equation can be written directly as

$$r^2 = (X-x)^2 + (Y-y)^2 + (Z-z)^2 \tag{4.4-13}$$

assuming that X, Y, Z are the coordinates of the satellite in the station's reference frame.

Equation (4.4-13) can be written as

$$\begin{aligned} r^2 &= (\overline{X}-\overline{x}) \cdot (\overline{X}-\overline{x}) \\ &= (\overline{X}^T\overline{X} + \overline{x}^T\overline{x} - 2\overline{x}^T\overline{X} \end{aligned} \tag{4.4-14}$$

Recalling from equation (4.3-5) that

$$\overline{x} = R_3(-\lambda)\overline{x}' \tag{4.4-15}$$

with

$$\overline{x}' = R_2(\psi)\begin{bmatrix} R \\ 0 \\ 0 \end{bmatrix}$$

and from equation (3.3-1) that

$$\overline{X}' = R_3(-\Omega)R_1(-i)\overline{x}_\omega \tag{4.4-16}$$

with $$\bar{x}_\omega = a \begin{bmatrix} \cos u \\ \sin u \\ 0 \end{bmatrix}$$

the satellite coordinates $\bar{X}'$ defined in the instantaneous inertial frame (equator and vernal equinox, true of date) have to be transformed into the station's reference frame:

$$\bar{X} = R_3(GAST_o + \omega_e t)\bar{X}' \tag{4.4-17}$$

Equation (4.4-17) can be expressed in a similar way as is done for the station coordinates:

$$\bar{X} = R_3(GAST_o - \Omega)R_3(\omega_e t)\bar{X}'' \tag{4.4-18}$$

with $$\bar{X}'' = R_1(-i)\bar{x}_\omega$$

In evaluating the range equation (4.4-14) one finds directly for the first two terms, because of the orthogonality of the rotation matrices,

$$\bar{X}^T\bar{X} = x^2_\omega + y^2_\omega = a^2 \tag{4.4-19}$$

and $$\bar{x}^T\bar{x} = R^2 \tag{4.4-20}$$

Upon substitution of (4.4-15) and (4.4-18) into the third term of (4.4-14) one gets

$$\begin{aligned} -2\bar{x}^T\bar{X} &= -2\bar{x}'^T R_3(\lambda)R_3(GAST_o - \Omega)R_3(\omega_e t)\bar{X}'' \\ &= -2\bar{x}'^T R_3(\lambda + GAST_o - \Omega)R_3(\omega_e t)\bar{X}'' \end{aligned} \tag{4.4-21}$$

The range equation (4.4-14) becomes upon substitution of (4.4-19), (4.4-20) and (4.4-21)

$$r^2 = a^2 + R^2 - 2\overline{x}'^T R_3(\lambda + GAST_o - \Omega + \omega_e t)\overline{X}'' \tag{4.4-22}$$

with
$$\overline{x}'^T = [R\cos\psi \quad 0 \quad R\sin\psi] \tag{4.4-23}$$

and
$$\overline{X}'' = a \begin{bmatrix} \cos u \\ \sin u \cos i \\ \sin u \sin i \end{bmatrix} \tag{4.4-24}$$

$$u = \omega + E_o + nt$$

From this range equation it becomes clear too that a, i, $\omega + E_o$, n, R, ψ, ω_e and $\lambda + GAST_o - \Omega$ are the only eight estimable quantities.

Upon substitution of (4.4-23) and (4.4-24) into equation (4.4-22) the very same result is obtained as reflected by equation (4.4-11).

Some remarks concerning the parameter u need to be made. The parameter has been equated to $\omega + E_o + nt$ ($= u_o + nt$). The constant part u_o of this parameter can be viewed in a more conventional way as

$$u_o = \omega + v_o$$

whereby ω is the argument of perigee and v_o the true anomaly of the satellite at reference epoch t = 0. u (and u_o) is one of the Hill variables and known as the argument of latitude. Because of the zero eccentricity of the orbit the true anomaly, mean anomaly and eccentric anomaly are equal. With an eye upon future derivations the argument of latitude has been set equal to $\omega + E_o + nt$ rather than $\omega + v_o + nt$.

4.5 The Elliptic Intermediate Orbit, Station and Earth Rotation/Orientation Determination from Range Observations

The ground work for this section has been laid in Chapter 3, sections 3.4 and 3.5.

4.5.1 Two Dimensional Case with GM (or n) Unknown

Figure 4.7 illustrates the geometry involved in a two dimensional Keplerian orbit.

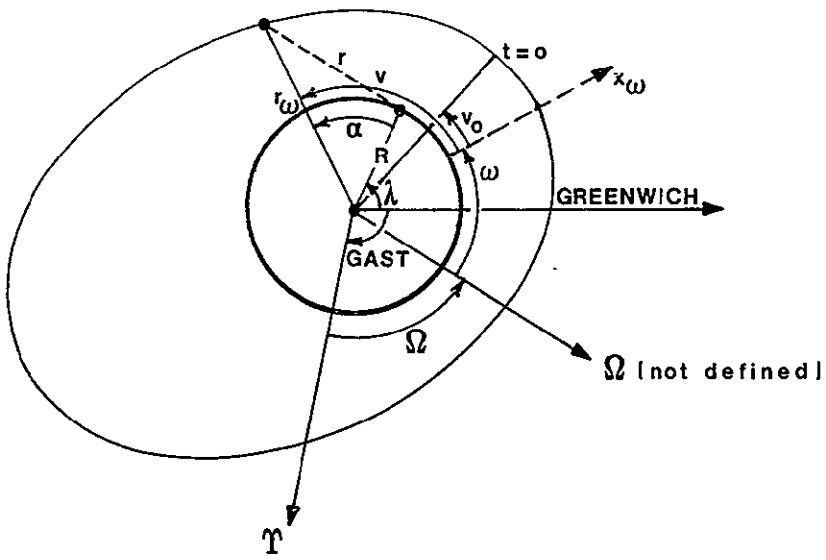

Figure 4.7. Two Dimensional Elliptic Motion

From Figure 4.7 one has the range equation

$$r^2 = r_\omega^2 + R^2 - 2r_\omega R\cos\alpha \tag{4.5-1}$$

with

$$\alpha = \lambda + GAST - \Omega - \omega - v$$

$$= \lambda + GAST_o - \Omega - \omega - v + \omega_e t$$

and $$r_\omega = a(1-e\cos E)$$

from equation (A.2-1) in Appendix A.

In the elliptic motion the true anomaly v does not vary linearly with time so one has to write the range equation as

$$\begin{aligned} r^2 &= r_\omega^2 + R^2 - 2r_\omega R\cos[(\lambda+GAST-\Omega-\omega) - v] \\ &= r_\omega^2 + R^2 - 2r_\omega R[\cos(\lambda+GAST-\Omega-\omega)\cos v + \\ &\qquad \sin(\lambda+GAST-\Omega-\omega)\sin v] \end{aligned} \tag{4.5-2}$$

Recalling from equation (A.2-1) that

$$r_\omega \cos v = x_\omega$$

and $$r_\omega \sin v = y_\omega$$

the range equation (4.5-1) becomes

$$\begin{aligned} r^2 = r_\omega^2 + R^2 - 2R\{&x_\omega\cos[(\lambda+GAST_o-\Omega-\omega) + \omega_e t] + \\ &y_\omega\sin[(\lambda+GAST_o-\Omega-\omega) + \omega_e t]\} \end{aligned} \tag{4.5-3}$$

with x_ω, y_ω, r_ω and their functional relationships as described in Appendix A, sections A.2, A.3.1, A.4.1 and A.5.1.

Evaluation of the range equation yields the following seven estimable parameters:

- satellite parameters : a, e, E_o, n (see section A.5.1)
- station parameter : R
- earth parameter : ω_e
- mixed station/earth/satellite parameter: $\lambda + GAST_o - \Omega - \omega$

The generalization from the two dimensional circular motion to the two dimensional elliptic motion increased the number of estimable

quantities from four to seven. This increase by three can be explained easily: the first additional parameter is needed to describe the eccentricity of the orbit; the second parameter is needed to position the satellite in the ellipse, the latter having now a defined orientation in the reference frame; the third added parameter deals with the separability of the angular velocities: the satellite's variable angular velocity is separable from the assumed constant angular velocity of the earth.

4.5.2 Two Dimensional Case with GM (or n) Known

The case with GM known in Kepler's Third Law yields the same range equation as in section 4.3.1

$$r^2 = r_\omega^2 + R^2 - 2R\{x_\omega \cos[(\lambda+GAST_o-\Omega-\omega) + \omega_e t] + y_\omega \sin[(\lambda+GAST_o-\Omega-\omega) + \omega_e t]\} \qquad (4.5\text{-}4)$$

with x_ω, y_ω, r_ω and their functional relationships as described in Appendix A, sections A.2, A.3.2, A.41. and A.5.2.

Evaluation of the range equation yields the following six estimable parameters:

- satellite parameters : a, e, E_o (see section A.5.2)
- state parameter : R
- earth parameter : ω_e
- mixed station/earth/satellite parameter: $\lambda + GAST_o - \Omega - \omega$

Note that in the case of the elliptic motion with GM known in Kepler's Third Law reduces the number of estimable quantities with one in contrast to the circular motion (see section 4.4.2).

4.5.3 Three Dimensional Case with GM (or n) Unknown

The three dimensional elliptic motion can be directly derived from the three dimensional circular motion. In Figure 4.8 (similar to Figure 4.5) one has to split up the argument of latitude u into the argument of perigee ω and the true anomaly v and to replace a by r_ω.

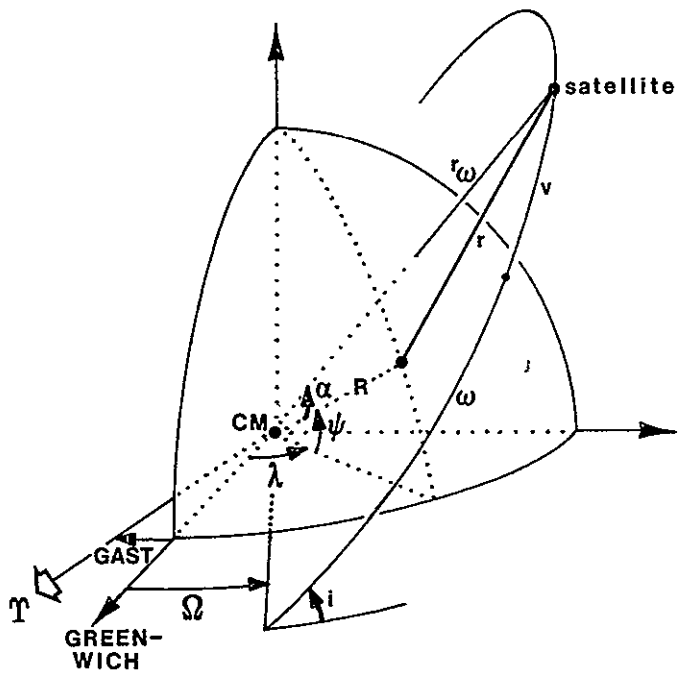

Figure 4.8. Three Dimensional Elliptic Motion

From Figure 4.8 one has the following range equation

$$r^2 = r_\omega^2 + R^2 - 2r_\omega R\cos\alpha \qquad (4.5\text{-}5)$$

Figure 4.6 and the relations from spherical trigonometry in the two fundamental triangles of satellite geodesy (ΔPRS and ΔPQR, Figure 4.6) yield

$$\cos\alpha = \cos\psi\cos\beta + \sin\psi\sin(\omega+v)\sin i \qquad (4.5\text{-}6)$$

with $\cos\beta = \cos(\lambda+GAST-\Omega)\cos(\omega+v) + \sin(\lambda+GAST-\Omega)\sin(\omega+v)\cos i$

Writing out the sine and cosine terms with argument $(\omega + v)$ in equation (4.5-6) one gets

$$\cos\alpha = \cos\psi\cos(\lambda+GAST-\Omega)\cos\omega\cos v - \cos\psi\cos(\lambda+GAST-\Omega)\sin\omega\sin v + \cos\psi\sin(\lambda+GAST-\Omega)\sin\omega\cos i\cos v + \cos\psi\sin(\lambda+GAST-\Omega)\cos\omega\cos i\sin v + \sin\psi\sin i\sin\omega\cos v + \sin\psi\sin i\cos\omega\sin v \qquad (4.5\text{-}7)$$

Recalling from equation (A.2-1) that

$$x_\omega = r_\omega\cos v$$

and

$$y_\omega = r_\omega\sin v$$

the range equation (4.5-5) becomes

$$r^2 = r_\omega^2 + R^2 - 2R(Px_\omega + Qy_\omega) \qquad (4.5\text{-}8)$$

with

$$P = P_c\cos\psi + P_s\sin\psi$$

$$Q = Q_c\cos\psi + Q_s\sin\psi$$

$$P_c = \cos\Delta\lambda\cos\omega + \sin\Delta\lambda\sin\omega\cos i$$

$$P_s = \sin\omega\sin i$$

$$Q_c = -\cos\Delta\lambda\sin\omega + \sin\Delta\lambda\cos\omega\cos i$$

$$Q_s = \cos\omega\sin i$$

$$\Delta\lambda = \Delta\lambda_o + \omega_e t = \lambda + GAST_o - \Omega + \omega_e t$$

and x_ω, y_ω, r_ω and their functional relationships as described in Appendix A, sections A.2, A.3.1, A.4.1 and A.5.1.

Evaluation of the range equation yields the following ten estimable parameters:

- satellite parameters : a, e, i, ω, E_o, n (see section A.5.1)
- station parameters : R, ψ

- earth parameters : ω_e
- mixed station/earth/satellite parameter: $\lambda + GAST_o - \Omega$

4.5.4 Three Dimensional Case with GM (or n) Known

The case with GM known in Kepler's Third Law yields the same range equation as in section 4.5.3

$$r^2 = r_\omega^2 + R^2 - 2R(Px_\omega + Qy_\omega) \tag{4.5-9}$$

with

$$P = P_c \cos\psi + P_s \sin\psi$$

$$Q = Q_c \cos\psi + Q_s \sin\psi$$

$$P_c = \cos\Delta\lambda \cos\omega + \sin\Delta\lambda \sin\omega \cos i$$

$$P_s = \sin\omega \sin i$$

$$Q_c = -\cos\Delta\lambda \sin\omega + \sin\Delta\lambda \cos\omega \cos i$$

$$Q_s = \cos\omega \sin i$$

$$\Delta\lambda = \Delta\lambda_o + \omega_e t = \lambda + GAST_o - \Omega + \omega_e t$$

and x_ω, y_ω, r_ω and their functional relationships as described in Appendix A, sections A.2, A.3.2, A.4.1 and A.5.2.

Evaluation of the range equation yields the following nine estimable parameters:

- satellite parameters : a, e, i, ω, E_o (see section A.5.2)
- station parameters : R, ψ
- earth parameters : ω_e
- mixed station/earth/satellite parameter: $\lambda + GAST_o - \Omega$

4.6 The Secularly Perturbed Elliptic Intermediate Orbit, Station and Earth Rotation/Orientation Determination from Range Observations

The ground work for this section has been laid in Chapter 3, section 3.6. From theory and experience the most dominant effects of the oblateness of the earth's gravity field as expressed by the spherical harmonic coefficient J_2 (better GM $J_2 a_e^2$, section 5.4.3) are the secular changes in the ascending node, the argument of perigee and the mean anomaly other than one would expect from Kepler's Third Law. The secular change of the latter one is usually attributed to a revised mean motion of the satellite: the satellite moves differently from perigee to perigee as one might conclude from Kepler's Third Law.

Section 4.6.1 describes how a pure geometrical orbit is able to handle these secular perturbations as derived from range observations, whereas section 4.6.2 includes the functional relationships between GM, J_2 (both considered constants) and the secular perturbations.

4.6.1 GM (or n) and J_2 (or $\dot{\omega}$, $\dot{\Omega}$, n) Unknown

From the range equation of section 4.5.3 one obtains directly, incorporating the secular perturbations in the ascending node and the argument of perigee

$$r^2 = r_\omega^2 + R^2 - 2R(Px_\omega + Qy_\omega) \qquad (4.6\text{-}1)$$

Before evaluating P and Q one has as the range equation using a similar approach as in section 4.4.5

$$r^2 = \overline{X}^T\overline{X} + \overline{x}^T\overline{x} - 2\overline{x}^T\overline{X} \qquad (4.6\text{-}2)$$

with $$\bar{x} = R_3(-\lambda)R_2(\psi)\begin{bmatrix} R \\ 0 \\ 0 \end{bmatrix} = R_3(-\lambda)\bar{x}' \tag{4.6-3}$$

and $$\bar{X} = R_3(GAST)R_3(-\Omega_o-\dot{\Omega}t)R_1(-i)R_3(-\omega_o-\dot{\omega}t)\bar{x}_\omega \tag{4.6-4}$$

with $\bar{x}_\omega$ as defined in Appendix A, section A.2.

Substitution of (4.6-3) and (4.6-4) into the range equation (4.6-2) yields

$$r^2 = r^2_\omega + R^2 - 2\bar{x}'^T R_3(\lambda+GAST_o-\Omega_o)R_3[(\omega_e-\dot{\Omega})t]\bar{X}'' \tag{4.6-5}$$

with $$\bar{x}'^T = [R\cos\psi \quad 0 \quad R\sin\psi] \tag{4.6-4}$$

and $$\bar{X}'' = R_1(-i)R_3(-\omega_o-\dot{\omega}t)\bar{x}_\omega \tag{4.6-7}$$

Equating the corresponding terms in the range equations (4.6-1) and (4.6-5) one obtains

$$r^2 = r^2_\omega + R^2 - 2R(Px_\omega+Qy_\omega) \tag{4.6-8}$$

with
$$P = P_c\cos\psi + P_s\cos\psi$$
$$Q = Q_c\cos\psi + Q_s\sin\psi$$
$$P_c = \cos\Delta\lambda\cos\omega + \sin\Delta\lambda\sin\omega\cos i$$
$$P_s = \sin\omega\sin i$$
$$Q_c = -\cos\Delta\lambda\sin\omega + \sin\Delta\lambda\cos\omega\cos i$$
$$Q_s = \cos\omega\sin i$$
$$\Delta\lambda = \lambda + GAST_o - \Omega_o + (\omega_e-\dot{\Omega})t$$
$$\omega = \omega_o + \dot{\omega}t$$

and x_ω, y_ω, r_ω and their functional relationships as described in Appendix A, sections A.1, A.3.1, A.4.1 and A.5.1.

Evaluation of the range equation yields the following eleven estimable parameters:

- satellite parameters : a, e, i, ω_o, $\dot{\omega}$, E_o, n (see section A.5.1)
- station parameters : R, ψ
- mixed station/earth/satellite parameter: $\lambda + GAST_o - \Omega_o$
- mixed earth/satellite parameter : $\omega_e - \dot{\Omega}$

Note that n is the mean anomalistic motion (perigee to perigee) without changing the expressions for x_ω, y_ω, r_ω!

At this point of the secularly perturbed orbit one looses the capability of earth rotation (UT 1) determination: one can only recover the--what might be called--effective earth's angular velocity with respect to the regressing orbital plane. Consequently, the J_2 term cannot be determined from the secular perturbation in the ascending node (only one satellite is considered). The mean motion n plays in the range equation the same mathematical role as in the unperturbed case. Consequently from the mean (anomalistic) motion J_2 cannot be determined either. The only difference in geometry between the unperturbed (section 4.5.3) and the secularly perturbed (this section) orbit is the motion of the perigee $\dot{\omega}$. This secular rate furnishes us with the only source for a J_2 determination.

The range model as described in this section should be considered a very powerful one since it includes <u>all</u> secular perturbations in ω, Ω and n due to J_2, J_2^2, J_3, J_4, etc! The model solves for the full secular perturbations in the three elements, not being able to differentiate between sources of the various secular perturbations.

4.6.2 GM (or n) and J_2 (or $\dot{\omega}$, $\dot{\Omega}$, n) Known

Enforcing the four dynamical relationships between the mean motion n, the argument of perigee ω, the ascending node Ω, the gravitational constant GM and the dynamical form factor of the earth J_2 two of the eleven estimable parameters of the range model of section 4.6.1 will be eliminated.

The four dynamical relationships are

$$n_o^2 a^3 = GM \tag{4.6-9}$$

$$n = n_o[1 + \frac{J_2 a_e^2 \sqrt{1-e^2}}{a^2(1-e^2)^2}(1 - \frac{3}{2}\sin^2 i)] \tag{4.6-10}$$

$$\Omega = \Omega_o + \dot{\Omega}t$$

with

$$\dot{\Omega} = -\frac{3}{2}\frac{J_2 a_e^2}{a^2(1-e^2)^2} n \cos i \tag{4.6-11}$$

$$\omega = \omega_o + \dot{\omega}t$$

with

$$\dot{\omega} = \frac{3}{2}\frac{J_2 a_e^2}{a^2(1-e^2)^2} n(2 - \frac{5}{2}\sin^2 i) \tag{4.6-12}$$

The range equation is as in section 4.6.1

$$r^2 = r_\omega^2 + R^2 - 2R(Px_\omega + Qy_\omega) \tag{4.6-13}$$

with P, Q, P_c, P_s, Q_c, Q_s as described in section 4.6.1.

n_o, n, $\dot{\Omega}$, $\dot{\omega}$ as described in equations (4.6-9) through (4.6-12) and x_ω, y_ω, r_ω and their functional relationships as described in Appendix A, sections A.2, A.3.3, A.4.1 and A.5.3.

C - L

Evaluation of the range equation yields the following nine estimable parameters:

- satellite parameters : a, e, i, ω_o, E_o (see section A.5.3)
- station parameters : R, ψ
- earth parameter : ω_e

mixed station/earth/satellite parameter: $\lambda + GAST_o - \Omega_o$

In this version of the range model it should be realized as in every other section where GM was considered known (sections 4.4.2, 4.4.4, 4.5.2, 4.5.4 and 4.6.2) a value for GM has been kept constant. Not doing so, by considering GM a parameter, the models of the five sections mentioned above "degenerate" into the (geometric) models which are described in the sections which precede those five sections. In this section not only GM but also J_2 is considered constant. This may put unwanted strains on the model, especially for UT 1 determinations from low inclination orbits (see section 6.10). It might also be expected that a slight "wrong" value for J_2 will cause an erroneous earth rotation (UT 1) determination since it was shown in section 4.6.1 that in the range model with "everything loose" the only estimable quantity was the difference between the earth's angular velocity ω_e and the secular change in the ascending node $\dot{\Omega}$: $\omega_e - \dot{\Omega}$. In other words, a small change in $\dot{\Omega}$ will change the recovery of ω_e directly! The argumentation for "more geometrically free" orbital models becomes even more apparent since it is suggested in [Kozai, 1970] that certain time variations (e.g., seasonal variations) in UT 1 and J_2 are of the same frequency and consequently difficult to separate.

4.7 The Intermediate Orbit, Station and Earth Rotation/ Orientation Determination from Range-Rate Observations

In section 4.2 the range-rate observations were already introduced for a simple model: the two dimensional circular motion. The range-rate equation is directly obtained from the differentiation of the range equation with regard to time. The derivation followed in that section will be similar for all the different cases treated in the sections 4.3 through 4.6. To avoid overduplication only the three most general cases will be discussed: the three dimensional circular, elliptic and secularly perturbed elliptic orbits with GM and J_2 as unknown parameters.

4.7.1 Three Dimensional Circular Intermediate Orbit

The corresponding range equation for this case was given in section 4.4.3, equation (4.4-11). Taking the time derivative of the range equation (4.4-11) one obtains

$$2r\frac{dr}{dt} = -2aR\frac{d\cos\alpha}{dt} \tag{4.7-1}$$

with

$$\frac{d\cos\alpha}{dt} = \cos\psi\frac{d\cos\beta}{dt} + n\sin\psi\cos u\sin i \tag{4.7-2}$$

and

$$\frac{d\cos\beta}{dt} = -\omega_e\sin\Delta\lambda\cos u + \omega_e\cos\Delta\lambda\sin u\cos i - n\cos\Delta\lambda\sin u + n\sin\Delta\lambda\cos u\cos i \tag{4.7-3}$$

Upon substitution of (4.7-2) and (4.7-3) into the range-rate equation (4.7-1) one obtains

$$r\dot{r} = aR[\cos\psi\sin\Delta\lambda\cos u\,(\omega_e - n\cos i) + \cos\psi\cos\Delta\lambda\sin u\,(n - \omega_e\cos i) + \sin\psi\cos u\,(-n\sin i)] \tag{4.7-4}$$

with r as given by equation (4.4-11).

Evaluation of the range-rate equation yields the following eight estimable parameters:

- satellite parameters : a, i, $\omega + E_o$, n
- station parameters : R, ψ
- earth parameter : ω_e
- mixed station/earth/satellite parameter: $\lambda + GAST_o - \Omega$

Considering GM known will eliminate the parameter n reducing the set to seven estimable parameters.

4.7.2 Three Dimensional Elliptic Intermediate Orbit

The corresponding range equation for this case was given in section 4.5.3, equation (4.5-8). Taking the time derivative of the range equation (4.6-8) one obtains

$$2r\frac{dr}{dt} = 2r_\omega\frac{dr_\omega}{dt} - 2R\left(\frac{dP}{dt}\dot{x}_\omega + \frac{dQ}{dt}\dot{y}_\omega + P\frac{dx_\omega}{dt} + Q\frac{dy_\omega}{dt}\right) \qquad (4.7\text{-}5)$$

with

$$\frac{dP}{dt} = \frac{dP_c}{dt}\cos\psi \qquad (4.7\text{-}6)$$

$$\frac{dQ}{dt} = \frac{dQ_c}{dt}\cos\psi \qquad (4.7\text{-}7)$$

$$\frac{dP_c}{dt} = \omega_e(-\sin\Delta\lambda\cos\omega + \cos\Delta\lambda\sin\omega\cos i) \qquad (4.7\text{-}8)$$

$$\frac{dQ_c}{dt} = \omega_e(\sin\Delta\lambda\sin\omega + \cos\Delta\lambda\cos\omega\cos i) \qquad (4.7\text{-}9)$$

Upon substitution of (4.7-6), (4.7-7), (4.7-8) and (4.7-9) into the range-rate equation (4.7-5) one obtains

$$r\dot{r} = r_\omega\dot{r}_\omega - R(P\dot{x}_\omega + Q\dot{y}_\omega) + R\omega_e\cos\psi(P'x_\omega - Q'y_\omega) \qquad (4.7\text{-}10)$$

with r, P, Q, x_ω, y_ω, r_ω as described in section 4.5.3

$\dot{x}_\omega$, $\dot{y}_\omega$, $\dot{r}_\omega$ and their functional relationships as described in Appendix A, sections A.2, A.3.1, A.4.2 and A.5.1.

and

$$P' = \sin\Delta\lambda\cos\omega - \cos\Delta\lambda\sin\omega\cos i \tag{4.7-11}$$

$$Q' = \sin\Delta\lambda\sin\omega + \cos\Delta\lambda\cos\omega\cos i \tag{4.7-12}$$

Evaluation of the range-rate equation yields the following ten estimable parameters:

- satellite parameters : a, e, i, ω, E_o, n
- station parameters : R, ψ
- earth parameter : ω_e
- mixed station/earth/satellite parameter: $\lambda + GAST_o - \Omega$

Considering GM known will eliminate the parameter n reducing the set to nine estimable parameters.

4.7.3 Three Dimensional Secularly Pertubed Elliptic Intermediate Orbit

The corresponding range equation for this case was given in section 4.6.1, equation (4.6-8). Taking the time derivative of the range equation (4.6-8) one obtains

$$2r\frac{dr}{dt} = 2r_\omega\frac{dr_\omega}{dt} - 2R\left(\frac{dP}{dt}x_\omega + \frac{dQ}{dt}y_\omega + P\frac{dx_\omega}{dt} + Q\frac{dy_\omega}{dt}\right) \tag{4.7-13}$$

with $$\frac{dP}{dt} = \frac{dP_c}{dt}\cos\psi + \frac{dP_s}{dt}\sin\psi \tag{4.7-14}$$

$$\frac{dQ}{dt} = \frac{dQ_c}{dt}\cos\psi + \frac{dQ_s}{dt}\sin\psi \tag{4.7-15}$$

$$\begin{aligned}\frac{dP_c}{dt} &= (\omega_e-\dot{\Omega})(-\sin\Delta\lambda\cos\omega + \cos\Delta\lambda\sin\omega\cos i) + \\ &\quad \dot{\omega}(-\cos\Delta\lambda\sin\omega + \sin\Delta\lambda\cos\omega\cos i) \\ &= (\omega_e-\dot{\Omega})(-\sin\Delta\lambda\cos\omega + \cos\Delta\lambda\sin\omega\cos i) + \dot{\omega}Q_c\end{aligned} \tag{4.7-16}$$

$$\frac{dP_s}{dt} = \dot{\omega}\cos\omega\sin i = \dot{\omega}Q_s \tag{4.7-17}$$

$$\begin{aligned}\frac{dQ_c}{dt} &= (\omega_e-\dot{\Omega})(\sin\Delta\lambda\sin\omega + \cos\Delta\lambda\cos\omega\cos i) + \\ &\quad \dot{\omega}(-\cos\Delta\lambda\cos\omega - \sin\Delta\lambda\sin\omega\cos i) \\ &= (\omega_e-\dot{\Omega})(\sin\Delta\lambda\sin\omega + \cos\Delta\lambda\cos\omega\cos i) - \dot{\omega}P_c\end{aligned} \tag{4.7-18}$$

$$\frac{dQ_s}{dt} = -\dot{\omega}\sin\omega\sin i = -\dot{\omega}P_s \tag{4.7-19}$$

Upon substitution of (4.7-16) through (4.7-19) into the equations (4.7-14) and (4.7-15) one obtains

$$\frac{dP}{dt} = (\omega_e-\dot{\Omega})(-\sin\Delta\lambda\cos\omega + \cos\Delta\lambda\sin\omega\cos i)\cos\psi + \dot{\omega}Q \tag{4.7-20}$$

$$\frac{dQ}{dt} = (\omega_e-\dot{\Omega})(\sin\Delta\lambda\sin\omega + \cos\Delta\lambda\cos\omega\cos i)\cos\psi - \dot{\omega}P \tag{4.7-21}$$

Upon substitution of (4.7-20) and (4.7-21) into the range-rate equation (4.7-13) one obtains

$$r\dot{r} = r_\omega\dot{r}_\omega - R(P\dot{x}_\omega+Q\dot{y}_\omega) - \dot{\omega}R(Qx_\omega-Py_\omega) + R(\omega_e-\dot{\Omega})\cos\psi(P'x_\omega-Q'y_\omega) \tag{4.7-22}$$

with r, P, Q, x_ω, y_ω, r_ω as described in section 4.6.1

$\dot{x}_\omega$, $\dot{y}_\omega$, $\dot{r}_\omega$ and their functional relationships as described in Appendix A, sections A.2, A.3.1, A.4.2 and A.5.1.

and $$P' = \sin\Delta\lambda\cos\omega - \cos\Delta\lambda\sin\omega\cos i \tag{4.7-23}$$

$$Q' = \sin\Delta\lambda\sin\omega + \cos\Delta\lambda\cos\omega\cos i \tag{4.7-24}$$

$$\omega = \omega_o + \dot{\omega}t \tag{4.7-25}$$

An alternate range-rate equation might be written as

$$r\dot{r} = r_\omega\dot{r}_\omega - R(P\dot{x}_\omega + Q\dot{y}_\omega) - R\{[\dot{\omega}Q - (\omega_e - \dot{\Omega})P'\cos\psi]x_\omega + [-\dot{\omega}P + (\omega_e - \dot{\Omega})Q'\cos\psi]y_\omega\} \tag{4.7-26}$$

Evaluation of the range-rate equation yields the following eleven estimable parameters

- satellite parameters : a, e, i, ω_o, $\dot{\omega}$, E_o, n
- station parameters : R, ψ
- mixed station/earth/satellite parameter: $\lambda + GAST - \Omega_o$
- mixed earth/satellite parameter : $\omega_e - \dot{\Omega}$

Considering GM and J_2 known will eliminate the parameters $\dot{\omega}$ and n reducing the set to nine estimable parameters.

The sections (4.7.1), (4.7.2) and (4.7.3) confirm the general principle that the simple example of "The Clock Problem" (section 4.2) already revealed: range and range-rate observations yield the same results as far as the estimability of the parameters is concerned.

4.8 The Intermediate Orbit, Station and Earth Rotation/Orientation Determination from Range-Difference Observations

In section 4.2 the range-difference observations were already introduced for a simple model: the two dimensional circular motion.

The range-difference equation can be obtained in two ways: the first approach is to take the square root of the (quadratic) range equations and subsequently, to subtract them for epochs $t + \Delta t$ and t; the second approach is to derive the range-difference equation from differencing the original quadratic range equations. The latter method enabled an easy comparison between range-rate and range-difference observations: a range-difference observation is about equal to a range-rate observation taken half way the time interval between epochs t and $t + \Delta t$. Since no difference between range and range-rate observations exists as far as the estimability of the various parameters is concerned, the same properties of estimability must hold for range-difference observations. The first approach of deriving range-difference observations confirms these properties: taking the difference of two (square rooted) range equations evaluated for epochs $t + \Delta t$ and t none of the parameters will be either eliminated or appear in a linear combination with any other parameter. This is true for all cases discussed in sections 4.3 through 4.6. Consequently, all the conclusions drawn for the estimability of parameters in case of range and range-rate observations apply also to range-difference observations. At this point no statements have been made how well certain parameters are estimable in the various measurement systems. This item is addressed in Chapter 6.

4.9 Summary

Chapter 4 dealt mainly with the investigation of the estimability of the various parameters in ten orbital models and for three measurement systems: range, range-rate and range-difference observations.

The most general (and geometrically free) model developed is the 11 parameter model which is able to account for secular perturbations in the mean motion, the argument of perigee and the ascending node due to J_2, J_2^2, J_3, J_4, etc.

Often in the literature the question of rank deficiency is addressed. In the philosophy of this investigation the answer to that question must simply be: that just depends on how erroneous the initial set of parameters is!

Despite all of this in Table 4.1 the followed approach in Chapter 4 is compared to the widely (used) Cartesian treatment in case of the three measurement systems. The Cartesian treatment concerns not only the satellite's orbit (statevector representation) but also the station position.

For a detailed description of the partial derivatives needed for the observation equations in the various orbital models and measurement systems one is referred to Appendix B.

Table 4.1

The Estimable Parameters and Rankdeficiencies of the Measurement Systems: Range, Range-Rate and Range-Difference Observations (Non-Simultaneous)

Orbital Model		Estimable Parameters	No.	Cartesian Representation 1)	No.	Rank Deficiency	Constants
Circular Motion	2D	$a, n-\omega_e, R, \lambda+GAST_o-\Omega-\omega-E_o$	4	$X, Y, \dot{X}\ \dot{Y}, GM, \omega_e, GAST_o, x, y$	9	5	-
		$a, \omega_e, R, \lambda+GAST_o-\Omega-\omega-E_o$	4	$X, Y, \dot{X}, \dot{Y}, \omega_e, GAST_o, x, y$	8	4	GM
	3D	$a, i, \omega+E_o, n, \omega_e, R, \psi, \lambda+GAST_o-\Omega$	8	$X, Y, Z, \dot{X}, \dot{Y}, \dot{Z}, GM, \omega_e, GAST_o, x, y, z$	12	4	-
		$a, i, \omega+E_o, \omega_e, R, \psi, \lambda+GAST_o-\Omega$	7	$X, Y, Z, \dot{X}, \dot{Y}, \dot{Z}, \omega_e, GAST_o, x, y, z$	11	4	GM
Elliptic Motion	2D	$a, e, E_o, n, \omega_e, R, \lambda+GAST_o-\Omega-\omega$	7	$X, Y, \dot{X}, \dot{Y}, GM, \omega_e, GAST_o, x, y$	9	2	-
		$a, e, E_o, \omega_e, R, \lambda+GAST_o-\Omega-\omega$	6	$X, Y, \dot{X}, \dot{Y}, \omega_e, GAST_o, x, y$	8	2	GM
	3D	$a, e, i, \omega, E_o, n, \omega_e, R, \psi, \lambda+GAST_o-\Omega$	10	$X, Y, Z, \dot{X}, \dot{Y}, \dot{Z}, GM, \omega_e, GAST_o, x, y, z$	12	2	-
		$a, e, i, \omega, E_o, \omega_e, R, \psi, \lambda+GAST_o-\Omega$	9	$X, Y, Z, \dot{X}, \dot{Y}, \dot{Z}, \omega_e, GAST_o, x, y, z$	11	2	GM
Secularly Perturbed Elliptic Motion	3D	$a, e, i, \omega_o, \dot{\omega}, E_o, n, \omega_e-\dot{\Omega}, R, \psi, \lambda+GAST_o-\Omega_o$	11	$X, Y, Z, \dot{X}, \dot{Y}, \dot{Z}, GM, J_2, \omega_e, GAST_o, x, y, z$	13	2	-
		$a, e, i, \omega_o, E_o, \omega_e, R, \psi, \lambda+GAST_o-\Omega_o$	9	$X, Y, Z, \dot{X}, \dot{Y}, \dot{Z}, \omega_e, GAST_o, x, y, z$	11	2	$GM + J_2$

1) Capital letters refer to the satellite, small letters to the station.

5. VALIDATION OF AND REFINEMENTS TO THE OBSERVATION MODELS

"Nevertheless, the construction of increasingly more accurate analytical theories remains the central task of celestial mechanics."

J. Kovalevsky [1967]

5.1 Introduction

Starting in the late forties a large series of articles have appeared (e.g. in The Astronomical Journal) treating the equations of motion of a satellite around an oblate spheroid analytically. Now, names of scientists as Brouwer, Garfinkel, Hori, Iszak, Kozai, Vinti are connected to the development of analytical theories. The name of one which should have headed this alphabetical list is mentioned last (but not least): K. Aksnes. An extensive list of references can be found in [Gaposchkin, 1973]. In a series of articles from 1965 Aksnes has showed a way to be taken: once the literal computer algebra is developed to its fullest extent one of the main obstacles in the analytical perturbation theories, the almost unsurmountable quantity of tedious algebraic work, can be handled with his theories which belong to the most elegant ones to treat analytically satellite perturbations. In [Aksnes, 1972] his first-order theory (the intermediate orbit is a fixed ellipse) based on Brouwer's first-order theory claims an accuracy (as compared to the numerically integrated solution) of 60 meters for a six day orbit

(100 revolutions, terms up to J_4 were included in the gravity model). In [Aksnes, 1970] a second-order theory (the intermediate orbit is a rotating ellipse) shows an accuracy of 1 meter for a six day orbit. In comparison, presently (1978) the numerical analysis of laser range measurements to STARLETTE shows r.m.s. fits for five arcs in the 1-2 meter range [Marsh and Williamson, 1978].

The theory presented in Chapters 3 and 4 includes as the most general model the rotating intermediate orbit. It is this secularly perturbed ellipse which forms the basis for Aksnes' second-order theory. Not so much from the perturbational point of view but from the point of view of system definition the validation (why unweighted parameters and why a secularly perturbed orbit?) and the refinements (the nature of the influences of polar motion, gravity field, timing, etc.) on these models will be discussed in this chapter.

5.2 The Influence of Weighting on Parameter Estimation

It has become common geodetic practice (and not only geodetic) to add to "clean" models as the observation equations model $La = F(X_a)$, following the notation of [Uotila, 1967], or the condition equations model with parameters $F(L_a, X_a) = 0$ accuracy (precision) estimates for the parameters. The mathematical model (e.g., $L_a = F(X_a)$) does not then only include accuracy estimates for the observations Σ_{L_b} but also for the parameters Σ_X. Since not all parameters are usually weighted one can write

$$\Sigma_X = \left[\begin{array}{c|c} \Sigma_{X_1} & 0 \\ \hline 0 & 0 \end{array}\right] \qquad (5.2\text{-}1)$$

where Σ_{X_1} represents the variance/covariance matrix of the subset of parameters X_1. From the mathematical (and statistical) point of view one simply has changed parameters into observations!

Two main cases can be differentiated at the outset: the weighting of parameters when the original set of parameters is estimable and the weighting of parameters when the original set of parameters is not estimable. In both cases it will be shown that the application of weighted parameters (Bayesian estimation) may lead to too optimistic or even unrealistic standard deviations for the weighted parameters. Two subgroups of parameters weighting will be differentiated: the first deals with the heavy weighting of parameters or in the limit the absolute constraining of parameters, the second deals with the weighting of parameters where the a priori accuracy estimates of the parameters do not exceed the a posteriori accuracy estimates of the parameters of the unweighted case (non-Bayesian estimation).

5.2.1 Strongly Weighting or Absolute Constraining of Estimable Parameters

The strongly or absolute weighting of parameters has to be exercised with care in that sense that in general the a priori estimate of the variance-of-unit-weight can increase to such an extent (as reflected by the a posteriori variance-of-unit-weight) that it leads to an unacceptable statistical test and rejection (better, non-acceptance) of the added (strong or absolute) constraints. This test as described in [Hamilton, 1964, p. 136] is a tool which gives the scientist/systems analyst a clear indication of the legitimacy of the added information. A failing test will lead to a search almost immediately for different ways of analyzing (developing models for) the

observations since the added constraints corrupted in a convincing way the accuracy and internal consistency of the observations. This particular case will not be elaborated upon because of its self-evident repercussions. The subtleness and its repercussions of weighting parameters will be the subject of subsequent sections.

5.2.2 Moderate Weighting of Estimable Parameters

Since the title of this (and the previous) section describes the estimability of the parameters, this feature (of estimability) needs to be elaborated on a little bit further. In general, the estimability of a parameter is a way of saying that the expected value of a parameter is equal to the value of that parameter

$$E(X) = X \tag{5.2-2}$$

It is not so much this statistical property as much as its implication in the estimation algorithm we are interested in. Restricting one self to an estimation procedure as the method of least squares the estimability of parameters is reflected directly in the invertability of the normal matrix. A more precise discussion concerning estimability and its necessary and sufficient conditions can be found for example in [Rao, 1973, p. 224]. The familiar definition of the normal matrix is adhered to

$$N = A^T P A \tag{5.2-3}$$

where P is the weight matrix of the observations L_b as reflected by

$$P = Q_{L_b}^{-1} = \sigma_o^2 \Sigma_{L_b}^{-1} \tag{5.2-4}$$

and A is the design matrix of the linearized model

$$A = \frac{\partial F}{\partial X_a} \tag{5.2-5}$$

A second issue raised in the title of this section is the moderacy of the parameter weighting: the average value of the a priori weight estimates of the parameters are not higher than the a posteriori ones of the parameters of the unweighted case.

$$(P_X)_{ij} \leq (A^T PA)_{ij} \tag{5.2-6}$$

The following notation of [Uotila, 1967 and 1973] one has as the model (observation equations)

$$\begin{aligned} L_a &= F(X_a) \\ L_x &= X_{1,a} \end{aligned} \tag{5.2-7}$$

and the variance/covariance matrix

$$\Sigma = \left[\begin{array}{c|c} \Sigma_{L_b} & 0 \\ \hline 0 & \Sigma_{X_1} \end{array}\right] = \sigma_o^2 \left[\begin{array}{c|c} P^{-1} & 0 \\ \hline 0 & P_{X_1}^{-1} \end{array}\right] \tag{5.2-8}$$

The solution for the parameters, after minimizing $V^T PV + X^T P_X X$, is

$$X = -(A^T PA + P_X)^{-1} A^T PL \tag{5.2-9}$$

with

$$P_X = A_X^T P_{X_1} A_X \tag{5.2-10}$$

where A_X is a $u_1 \times u$ matrix and u is the total number of parameters out of which u_1 are weighted. Equation (5.2-9) assumes that the "observed" values of the parameters is equal to the used approximate values.

Denoting the (Bayesian) solution solution vector of the parameters after weighting by X^W and the (non-Bayesian) solution of the parameters before weighting by X and similar notations for their weight coefficient matrices, one has

$$X^W = -(A^TPA+P_X)^{-1}A^TPL = -N_W^{-1}U \tag{5.2-11}$$

$$X = -(A^TPA)^{-1}A^TPL = -N^{-1}U \tag{5.2-12}$$

$$Q_X^W = (A^TPA+P_X)^{-1} = N_W^{-1} \tag{5.2-13}$$

$$Q_X = (A^TPA)^{-1} = N^{-1} \tag{5.2-14}$$

Rather than following the approach as described in [Uotila, 1973] which expresses the newly obtained estimates as functions of the unweighted estimates and some additive corrections

$$X^W = X + \Delta X \tag{5.2-15}$$

$$Q_X^W = Q_X + \Delta Q_X \tag{5.2-16}$$

it will be shown that the comparison between weighted and unweighted estimates can be viewed as a scaling process.

$$X^W = \Lambda_1 X \tag{5.2-17}$$

$$Q_X^W = \Lambda_2 Q_X \tag{5.2-18}$$

The additional advantage of this approach is that the scaling matrices Λ_1 and Λ_2 are identical for the parameters as well as their weight coefficient matrix.

It was assumed that the parameters are known worse a priori (in terms of their variances) than the parameters a posteriori in the unweighted case. This implies that one might view the addition of P_X to A^TPA as a differential one. The individual element of P_X (under which

many zeros for the unweighted parameters) are in general smaller than the normal matrix N of the unweighted parameters (see equation 5.2-6). In this light the matrix N_W can be viewed as having the form

$$B + \Delta B \tag{5.2-19}$$

The inversion of such a matrix (see Appendix D, section D.2) retaining only first-order terms is

$$(B + \Delta B)^{-1} \simeq B^{-1} - B^{-1}\Delta B B^{-1} \tag{5.2-20}$$

Recognizing that

$$B = A^T P A$$

and

$$\Delta B = P_X$$

one finds for the inversion of the normal matrix N_W

$$(A^T P A + P_X)^{-1} \simeq (A^T P A)^{-1} - (A^T P A)^{-1} P_X (A^T P A)^{-1} \tag{5.2-21}$$

or

$$N_W^{-1} \simeq N^{-1} - N^{-1} P_X N^{-1} \tag{5.2-22}$$

At this point it needs to be stressed that this relationship only holds for estimable parameters otherwise N^{-1} is an invalid expression.

Substituting (5.2-22) in (5.2-11) one obtains a solution to a fair amount of accuracy (terms as $N^{-1}P_X N^{-1} P_X N^{-1} - \ldots$ are omitted in 5.2-22)

$$X^W \simeq (N^{-1} - N^{-1}P_X N^{-1})U$$
$$\simeq (I - N^{-1}P_X)X \tag{5.2-23}$$

The result is
$$X^W = \Lambda_1 X \tag{5.2-24}$$

with
$$\Lambda_1 = I - N^{-1}P_X \tag{5.2-25}$$

Similarly, for the weight coefficient matrix one has

$$Q_X^W \simeq N^{-1} - N^{-1}P_X N^{-1}$$
$$\simeq (I - N^{-1}P_X)Q_X \tag{5.2-26}$$

The result is
$$Q_X^W = \Lambda_2 X \tag{5.2-27}$$

with
$$\Lambda_2 = I - N^{-1}P_X \tag{5.2-28}$$

Combining the results of (5.2-23) through (5.2-28) and recognizing the similarity of the two scaling matrices Λ_1 and Λ_2 one can write symbolically

$$\begin{Bmatrix} X^W \\ Q_X^W \end{Bmatrix} = (I - N^{-1}P_X) \begin{Bmatrix} X \\ Q_X \end{Bmatrix} \tag{5.2-29}$$

The repercussions of these derived relationships is that the weighting of parameters leads to smaller variances of the estimated parameters. Equation (5.2-22) shows that every diagonal element in the weight coefficient matrix Q_X^W will be smaller than the corresponding value in Q_X because of the semi-positive definite nature of the matrices N^{-1} and P_X. Consequently, a characteristic result of the weighted parameter approach is that the method lowers the variances of the parameters. In other

words, without adding any observations to a given set of data one may obtain too optimistic statistics for those parameters which were weighted. Except for the exposure of the possible danger of weighted parameter techniques (Bayesian estimation) a recommendation is clearly that every scientist publishing an analysis of a measurement system clearly has to indicate how the weighting procedure influenced (= improved!) the statistics of the parameters analyzed the non-Bayesian way (unweighted). An even more dangerous case will be discussed in the next section.

5.2.3 Weighting of Non-Estimable Parameters

The approach followed in the previous section which was primarily designed to investigate the influence of weighting procedures, cannot be followed here because the non-estimability of the parameters leads to a rank deficient normal matrix:

$$N_W^{-1} \neq N^{-1} - N^{-1} P_X N^{-1}$$

because $$|N| = 0$$

If one analyzes a given measurement system and expresses the observations (homogeneous in nature and precision) as a function of parameters which are also homogeneous in nature but non-estimable because of the very nature of the observations, the weighting of a subset of these parameters to make the complete set of parameters estimable will have the following two effects. First of all, it will be misleading as far as the usefulness of a certain measurement

system is concerned. A measurement might contribute nothing to the recovery of certain parameters. However, the weighting procedures mask this fact by the mere inclusion of inadmissable parameters. Secondly, the weighting of the subset of parameters will have a direct impact on the overall statistics of the complete set of parameters. This statement can be illustrated with a simple example: measuring height differences (the measurement system is leveling) every geodesist knows that the heights are non-estimable. However, weighting the height of only one station makes the complete level network estimable (misleading) but worse, the weighting of the station will have a dominant influence on the overall precision of the heights of the other stations. A short numerical example will be illustrative.

Imagine three height stations between which in each possible way a levelling took place. (See Figure 5.1.)

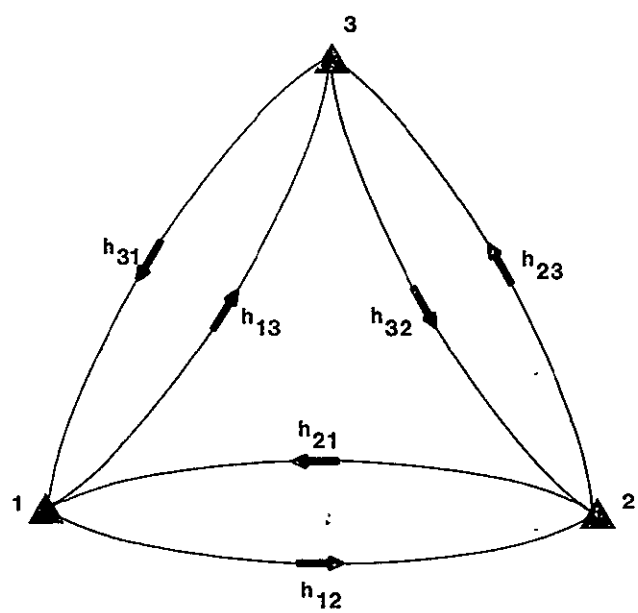

Figure 5.1. Levelling between Three Stations

The following model can be set up as a function of the (non-estimable) heights

$$\begin{bmatrix} h_{12} \\ h_{13} \\ h_{21} \\ h_{23} \\ h_{31} \\ h_{32} \end{bmatrix} = \begin{bmatrix} -1 & 1 & 0 \\ -1 & 0 & 1 \\ 1 & -1 & 0 \\ 0 & -1 & 1 \\ 1 & 0 & -1 \\ 0 & 1 & -1 \end{bmatrix} \begin{bmatrix} H_1 \\ H_2 \\ H_3 \end{bmatrix} \tag{5.2-30}$$

The non-invertible normal matrix is

$$N = A^T P A = \begin{bmatrix} 4 & -2 & -2 \\ -2 & 4 & -2 \\ -2 & -2 & 4 \end{bmatrix} \tag{5.2-31}$$

The precision for the observation was assumed to be

$$\Sigma_{h_{ij}} = \sigma^2 I$$

Assume the height of station 1 to be "known" with the following accuracy

$$\Sigma_H = \sigma^2_{H_1} = \sigma^2 \frac{\sigma^2_{H_1}}{\sigma^2} = \sigma^2 p_X^{-1} \tag{5.2-32}$$

With the help of equation (5.2-9) the following normal matrix is obtained

$$N_W = A^T A + P_X = \begin{bmatrix} 4 + p_X & -2 & -2 \\ -2 & 4 & -2 \\ -2 & -2 & 4 \end{bmatrix} \tag{5.2-33}$$

The inversion of N_W becomes

$$N_W^{-1} = Q_X^W = \frac{1}{6p_X}\begin{bmatrix} 6 & 6 & 6 \\ 6 & 2p_X+6 & p_X+6 \\ 6 & p_X+6 & 2p_X+6 \end{bmatrix} \tag{5.2-34}$$

Assuming that the adjustment procedure did not change the a priori variance-of-unit-weight appreciably (if it did, there is no problem present and the reader is referred to the discussion in section 5.2.1), one might write

$$\Sigma_X^W = \sigma^2 Q_X^W \tag{5.2-35}$$

Replacing P_X by $\sigma^2/\sigma_{H_1}^2$ in (5.2-34) one obtains as a variance/covariance matrix:

$$\Sigma_X^W = \begin{bmatrix} \sigma_{H_1}^2 & \sigma_{H_1}^2 & \sigma_{H_1}^2 \\ \sigma_{H_1}^2 & \sigma_{H_1}^2 + \frac{1}{3}\sigma^2 & \sigma_{H_1}^2 + \frac{1}{6}\sigma^2 \\ \sigma_{H_1}^2 & \sigma_{H_1}^2 + \frac{1}{6}\sigma^2 & \sigma_{H_1}^2 + \frac{1}{3}\sigma^2 \end{bmatrix} \tag{5.2-36}$$

The structure of this variance/covariance matrix shows the overpowering influence of weighting (non-estimable parameters), especially if one computes some numerical examples. With a levelling precision of 1 cm^2 (which is not going to be changed in the two following examples) assume that H_1 is determined first with the low precision (moderate weighting) of 1 m^2, then with a high precision of 1 mm^2. Substitution of these values into (5.2-36) reveals for the precision estimates for H_2 and H_3:

$$\sigma_{H_1}^2 = 1\,m^2 \quad \text{then} \quad \sigma_{H_2}^2 = \sigma_{H_3}^2 = 1.00003\ m^2!$$

$$\sigma^2_{H_1} = 1 \text{ mm}^2 \quad \text{then} \quad \sigma^2_{H_2} = \sigma^2_{H_3} = 0.31 \text{ cm}^2!$$

Without adding one observation one could have manipulated one's results any imaginable way.

It should be noted that the estimable parameters, the height differences, are not influenced by the weighting procedure:

$$H_{32} = H_2 - H_3 = [0 \quad 1 \quad -1] \begin{bmatrix} H_1 \\ H_2 \\ H_3 \end{bmatrix} \tag{5.2-37}$$

This leads immediately to

$$\sigma^2_{H_{32}} = [0 \quad 1 \quad -1] \begin{bmatrix} \sigma^2_{H_1} & \sigma^2_{H_1} & \sigma^2_{H_1} \\ \sigma^2_{H_1} & \sigma^2_{H_1} + \frac{1}{3}\sigma^2 & \sigma^2_{H_1} + \frac{1}{6}\sigma^2 \\ \sigma^2_{H_1} & \sigma^2_{H_1} + \frac{1}{6}\sigma^2 & \sigma^2_{H_1} + \frac{1}{3}\sigma^2 \end{bmatrix} \begin{bmatrix} 0 \\ 1 \\ -1 \end{bmatrix}$$

$$= \frac{1}{3}\sigma^2$$

This necessary mapping-back-into-estimable-quantities is explained in [Grafarend and Schaffrin, 1974] and applied for example in [Mueller et al., 1975].

A typical example in satellite geodesy is the geometric mode (e.g., simultaneous range observations). Such an analysis indicates directly that the coordinates of the stations are non-estimable (the only estimable quantities are the baselines/angles between the stations, see section 6.8 or Appendix C). If one weights six coordinates distributed over three stations in order to guarantee a coordinate system

definition all other stations in the network will be recovered with a precision about equal to the weighted stations no matter how good or bad the quality of the observations.

Consequently, it cannot be emphasized enough that in basic research attention should be devoted to the non-Bayesian investigation of models (i.e., models which do not assume any a priori knowledge as far as the parameters are concerned) before one ventures into the Bayesian world in which the influence of the weighting processis often forgotten.

The recommendation given above stems from the differences between the foundations on which Bayesian and non-Bayesian statistics are built. As stated by a Bayesian statistician [Phillips, 1973, p. 5]:

> "Opinions are expressed in probabilities, data are collected, and these data change the prior probabilities, through the operation of Bayes' theorem, to yield posterior probabilities.
>
> That is the essence of Bayesian methods."

The view expressed in this investigation is that as long as these "opinions" are not based on observational evidence to its fullest extent (i.e., the correlations between the weighted parameters are considered and the weighted parameters would also have been estimable in the unweighted case) it is preferred to restrict oneself to non-Bayesian estimation methods, especially in analyses as measurement system validations.

In section 6.7.3 the (improving effect on the variance analysis of some short arc mode experiments due to the application of (unnecessary) constraints (quasi-minimum constraints) is clearly demonstrated.

5.3 Is Kepler's Third Law a Law?

A question which might have arisen from the geometric modelling of the equations of motion of satellites in the previous two chapters, concerns the validity of the relationship between the geocentric gravitational constant GM, the semi-major axis a of the orbit and the mean motion n of the satellite. The well-known formula is (Kepler's Third Law)

$$GM = n^2 a^3 \tag{5.3-1}$$

In dynamic analyses of satellite observations often a GM is adopted (or weighted) as based on the results of, for example, the Deep Space Network observations by the Jet Propulsion Laboratories. A recent recommended estimate for GM (earth including the atmosphere) is (IAG, 1975):

$$398600.5 \pm 0.3 \text{ km}^3/\text{sec}^2$$

Having then a as a parameter in the model n is not solved for but is computable from the adopted (weighted) value of GM and the recovered value of a. In the more geometrical analysis of the dynamic mode (Chapter 3) the physical law (Kepler's Third Law) has been "omitted" for the following two reasons:

- the mean motion of a satellite and the semi major axis of its orbit can be more accurately determined from precise range observations than one would believe from an adopted GM and its precision. In section 6.10 this is illustrated with some numerical examples.
- Since Kepler's Third Law is a relationship between three parameters, still two are independent and can be recovered from observations.

The set a,n was preferred above the set a,GM because it is probably not realistic to assume that GM can be precisely determined

from observations to a satellite which orbits the earth relatively closely. In other words, GM determined in this way is thought to be physically less meaningful (although the future might contradict this statement!)

If only this reasoning is extended to the inclusion of all secular perturbations (due to J_2, etc.) the recovered mean motion n neither reflects the anomalistic period (equation 3.6-13) which is the period between perigee crossings nor the nodal period which is the period between equator crossings. A secular theory (based on secular perturbations in the orbital elements) assumes a rotating ellipse of which the spin rate is dictated by the value of J_2. The average speed (mean motion) with which the satellite travels along this rotating ellipse is much more complex than for instance a formula for the anomalistic period lets us believe. This argument is illustrated with the same examples in section 6.10: the mean motion is a very good recoverable geometric parameter, no matter what its physical cause is for its (numerical) value.

Considering GM now the third dependent variable, differentiation of (5.3-1) leads to

$$dGM = 2na^3\,dn + 3n^2a^2\,da \tag{5.3-2}$$

yielding

$$\sigma_{GM}^2 = 4n^2a^6\sigma_n^2 + 9n^4a^4\sigma_a^2 + 12n^3a^5\sigma_{an} \tag{5.3-3}$$

Substituting (5.3-1) back into (5.3-3) one obtains

$$\sigma^2_{GM} = GM^2\left(\frac{4\sigma_n^2}{n^2} \quad \frac{9\sigma_a^2}{a^2} \quad \frac{12\sigma_{an}}{an}\right) \tag{5.3-4}$$

This formula forms the base for the discussion of section 6.10.

For similar reasons the geometrical parameter $\dot{\omega}$, the rate of change in the argument of perigee, was included in the orbital models. Also here it was assumed that range analyses of up to one day would result in a physically less meaningful value for J_2 (although the future might conclude otherwise in this case too!)

5.4 The Influence of the Gravity Field and Polar Motion on Satellite Orbits

In the discussion of the various reference frames (Chapter 2) factors influencing a satellite's orbit such as precession, nutation, polar motion, etc. surfaces. The stand was taken in section 2.2 that the influence of precession and nutation in this simulation was assumed to be known or corrected for in the observations: the nature of a measurement system as laser ranging to artificial satellites from the earth is such that the observations will be very biased in this earth-satellite system. Conclusions based on such observations tend to be very earth-satellite dependent or earth-oriented.

Especially the description of the earth's behavior in inertial space might be very difficult since the satellite's behavior in that inertial space is not earth independent at all. Similar reservations are expressed concerning the UT/length-of-day/angular velocity determinations in section 6.9.1. Consequently, the influence of the gravity field and polar motion are left to be discussed in conjunction with the reference frames used in the simulation study. Perturbations due to

atmospheric drag, solar radiation pressure, etc., although important, are considered beyond the scope of this investigation.

As far as polar motion is concerned the more geometric aspects of polar motion are discussed in section 5.4.1, the dynamical aspects in section 5.4.2.

5.4.1 Polar Motion

Three types of polar motion can be differentiated. The motion of the instantaneous spin axis with respect to the Conventional International Origin (C.I.O.), with respect to the principal axis of the maximum moment of inertia and with respect to the position of the instantaneous spin axis at an earlier epoch (differential polar motion). As will become evident from the subsequent discussion the first type of polar motion (w.r.t the C.I.O.) is non-estimable but is based on convention: a set of station latitudes.

Range equations developed in Chapter 4, sections 4.4 and 4.5, were of the following type:

$$r^2 = r_\omega^2 + R^2 - 2\overline{x}'^T R_3(\lambda + GAST_o - \Omega) R_3(\omega_e t)\overline{X}'' \qquad (5.4\text{-}1)$$

where $\overline{x}'^T$ and $\overline{X}''$ are for instance represented by equations (4.4-23) and (4.4-24). The important feature to realize from equation (5.4-1) is that these vectors refer to reference frames which have the z-axes in common. Since the inertial frame is true of date the station vector $\overline{x}'^T$ refers to the instantaneous spin axis (better the instantaneous angular moment axis, but the difference between the two axes is neglected in this simulation study, see section 2.3). Consequently, the geocentric coordinates ψ, λ, R of the (changing) station positions are better

expressed as Ψ, Λ, R, "satellite observed coordinates", similarly to the observed astronomic coordinates in geodetic astronomy. It should be noted that the similarity between these observed coordinates stops here, e.g., the "satellite observed coordinates" do not refer to the direction of the local gravity vector at all (in case of range observations). Comparing the observed geocentric station coordinates at different epochs, the change in latitude and longitude (-difference) can be explained as differential polar motion. (See Figure 5.2.)

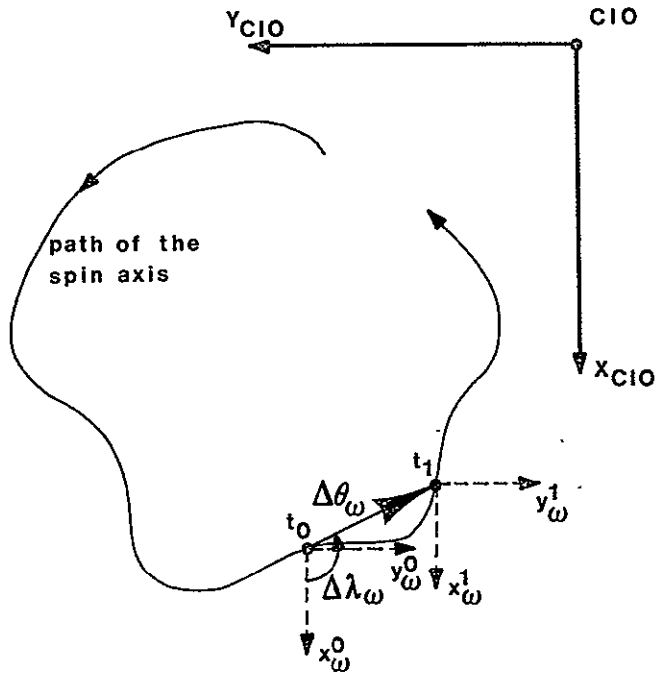

Figure 5.2. Differential Polar Motion

Denoting the two instantaneous reference frames at epochs t_0 and t_1 by $\bar{x}^0_{\omega_e}$ and $\bar{x}^1_{\omega_e}$ respectively, one obtains the following, at first sight remarkable, transformation between the two reference frames

$$\bar{x}^1_{\omega_e} = R_3(-\Delta\lambda_\omega)R_2(\Delta\theta_\omega)R_3(\Delta\lambda_\omega)\bar{x}^0_{\omega_e} \qquad (5.4\text{-}2)$$

Since the maximum change in the spin axis at the pole is around 12 cm per day, one has for $\Delta\theta_\omega$

$$\Delta\theta_\omega \leq \frac{0.12}{6356775} \simeq 2 * 10^{-8} \text{ rad}$$

Approximating $\sin \Delta\theta_\omega$ by $\Delta\theta_\omega$ and $\cos \Delta\theta_\omega$ by 1 is allowed in GM-geodesy since the error committed is less than $2 * 10^{-16}$ (for $\cos \Delta\theta_\omega$: $\cos \Delta\theta_\omega = 1 - 1/2\ \Delta\theta^2 + \ldots$). Carrying out the transformation (5.4-2) one has

$$\bar{x}^1_{\omega_e} = \begin{bmatrix} 1 & 0 & -\Delta\theta_\omega \cos \Delta\lambda_\omega \\ 0 & 1 & -\Delta\theta_\omega \sin \Delta\lambda_\omega \\ \Delta\theta_\omega \cos \Delta\lambda_\omega & \Delta\theta_\omega \sin \Delta\lambda_\omega & 1 \end{bmatrix} \bar{x}^0_{\omega_e} \qquad (5.4\text{-}3)$$

Having

$$\bar{x}^1_{\omega_e} = R \begin{bmatrix} \cos \Psi^1 \cos \Lambda^1 \\ \cos \Psi^1 \sin \Lambda^1 \\ \sin \Psi^1 \end{bmatrix} \qquad (5.4\text{-}4)$$

and

$$\bar{x}^0_{\omega_e} = R \begin{bmatrix} \cos \Psi^0 \cos \Lambda^0 \\ \cos \Psi^0 \sin \Lambda^0 \\ \sin \Psi^0 \end{bmatrix} \qquad (5.4\text{-}5)$$

the changes in the latitudes and longitudes (-differences) will yield the parameters $\Delta\theta_\omega$ and $\Delta\lambda_\omega$ of the differential polar motion. Setting

$$\Delta\Psi = \Psi^1 - \Psi^0 \qquad (5.4\text{-}6)$$

and

$$\Delta\Lambda = \Lambda^1 - \Lambda^0 \qquad (5.4\text{-}7)$$

the goal is to find the transformations which relate $\Delta\Psi$, $\Delta\Lambda$ to $\Delta\theta_\omega$ and $\Delta\lambda_\omega$ and vice versa. It should be noted that $\Delta\Lambda$ is the difference

between longitude differences (e.g., $\Lambda^1 = \lambda^1 + \text{GAST}-\Omega$) and that $\Delta\lambda_\omega$ is not a differentially small angle. Writing out (5.4-3) one gets

$$\cos \Psi^1 \cos \Lambda^1 = \cos \Psi^0 \cos \Lambda^0 - \Delta\theta_\omega \cos \Delta\lambda_\omega \sin \Psi^0 \quad (5.4\text{-}8)$$

$$\cos \Psi^1 \sin \Lambda^1 = \cos \Psi^0 \sin \Lambda^0 - \Delta\theta_\omega \sin \Delta\lambda_\omega \sin \Psi^0 \quad (5.4\text{-}9)$$

$$\sin \Psi^1 = \sin \Psi^0 + \Delta\theta_\omega \cos \Psi^0 (\cos \Lambda \cos \Delta\lambda_\omega + \sin \Lambda \sin \Delta\lambda_\omega) \quad (5.4\text{-}10)$$

The last expression leads immediately to

$$\frac{\sin \Psi^1 - \sin \Psi^0}{\cos \Psi^0} = \Delta\theta_\omega \cos(\Lambda - \Delta\lambda_\omega)$$

or

$$\Delta\Psi = \Psi^1 - \Psi^0 = \Delta\theta_\omega \cos(\Lambda - \Delta\lambda_\omega) \quad (5.4\text{-}11)$$

Equations (5.4-8) and (5.4-9) can be written as

$$\cos \Lambda^0 - \cos \Lambda^1 = \Delta\theta_\omega \cos \Delta\lambda_\omega \tan \Psi$$

$$\sin \Lambda^0 - \sin \Lambda^1 = \Delta\theta_\omega \sin \Delta\lambda_\omega \tan \Psi$$

or

$$2 \sin \Lambda \sin \tfrac{1}{2}(\Lambda^0 - \Lambda^1) = -\Delta\theta_\omega \cos \Delta\lambda_\omega \tan \Psi \quad (5.4\text{-}12)$$

$$2 \cos \Lambda \sin \tfrac{1}{2}(\Lambda^0 - \Lambda^1) = \Delta\theta_\omega \sin \Delta\lambda_\omega \tan \Psi \quad (5.4\text{-}13)$$

After multiplying (5.4-12) by $\sin\Lambda$ and (5.4-13) by $\cos\Lambda$ the addition of the two equations gives

$$\Delta\Lambda = \Lambda^1 - \Lambda^0 = \Delta\theta_\omega \sin(\Lambda - \Delta\lambda_\omega) \tan \Psi \quad (5.4\text{-}14)$$

Combining the results of (5.4-11) and (5.4-14) a differential polar motion of $\Delta\theta_\omega$, $\Delta\lambda_\omega$ results in changes in the latitudes and longitude-differences as given by

$$\Delta\Psi = \Delta\theta_\omega \cos(\Lambda - \Delta\lambda_\omega)$$
$$\Delta\Lambda \operatorname{cotan} \Psi = \Delta\theta_\omega \sin(\Lambda - \Delta\lambda_\omega) \tag{5.4-15}$$

This set of equations forms the basis on which some numerical results are reported in section 6.9.2.

Conversely, the differential polar motion $\Delta\theta_\omega$, $\Delta\lambda_\omega$ is given as a function of the changes in latitudes $\Delta\Psi_i$ and longitude-differences $\Delta\Lambda_i$ of station i by the following set of equations

$$\Delta\theta_\omega = \sqrt{(\Delta\Psi_i)^2 + (\Delta\Lambda_i \operatorname{cotan} \Psi_i)^2}$$
$$\Delta\lambda_\omega = \Lambda_i - \arctan \frac{\Delta\Lambda_i \operatorname{cotan} \Psi_i}{\Delta\Psi_i} \tag{5.4-16}$$

Until so far the geometrical aspects of polar motion were discussed. The dynamical aspects of polar motion will lead to a different type of polar motion.

5.4.2 Polar Motion and the Gravity Field

The spherical harmonic representation of the potential of the earth's gravity field is including terms up to degree and order two:

$$V = \frac{GM}{r}\left\{1 - \left[\left(\frac{a_e}{r^2}\right)(C_{10}z + C_{11}x + S_{11}y) + \left(\frac{a_e^2}{r^4}\right)\left(C_{20}(z^2 - \frac{1}{2}x^2 - \frac{1}{2}y^2) + C_{21}(3xz) + S_{21}(3yz) + C_{22}(3x^2 - 3y^2) + S_{22}(6xy)\right)\right]\right\} \tag{5.4-17}$$

If the center of the coordinate system coincides with the center of mass of the earth and the z-axis lies along the principal axis of the maximum moment of inertia, the equation (5.4-17) simplifies to [Heiskanen and

Moritz, 1967]

$$V = \frac{GM}{r}\left\{1-\left(\frac{a_e^2}{r^4}\right)\left[C_{20}(z^2-\frac{1}{2}x^2-\frac{1}{2}y^2)+C_{22}(3x^2-3y^2)+ + S_{22}(6xy)\right]\right\} \qquad (5.4\text{-}18)$$

In Chapter 2, sections 2.3 and 2.4, a distinction was made between the instantaneous spin axis and the axis of figure frame. Because of the definitions of these reference frames one might view equation (5.4-17) as the potential expressed in the instantaneous terrestrial system and equation (5.4-18) as the potential expressed in the axis of figure system. For this reason the first potential equation will be supplied with the sub- and superscript ω for the coordinates and potential coefficients respectively. Likewise, the second potential equation with the sub- and superscript I.

This leads us to the dynamical aspects of polar motion: polar motion here is the difference between the instantaneous spin axis and the principal axis of maximum moment of inertia. (See Figure 5.3.)

Very similarly as in the previous section one obtains a transformation between the two terrestrial systems:

$$\bar{x}_{\omega_e} = R_3(-\lambda_\omega)R_2(\theta_\omega)R_3(\lambda_\omega)\bar{x}_I \qquad (5.4\text{-}19)$$

Since the maximum amplitude of the Chandler wobble is in the order of 8 meters, one has for

$$\theta_\omega \leq \frac{8}{6356775} \simeq 1.3 * 10^{-6} \text{ rad}$$

Approximating sin θ_ω by θ_ω and cos θ_ω by 1 is still allowed in CM-geodesy since the error committed is less than $8 * 10^{-13}$ (for cos θ_ω:

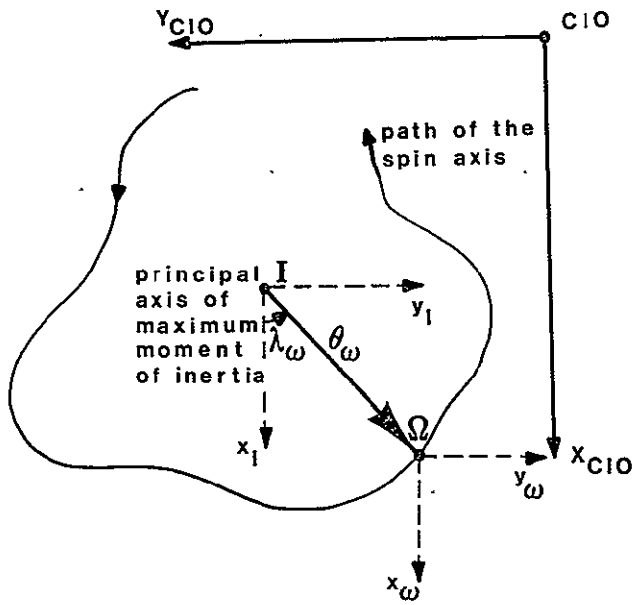

Figure 5.3. Polar Motion

$\cos\theta_\omega = 1 - \theta^2/2 + \ldots$). Carrying out the transformation (5.4-19) one has

$$\bar{x}_{\omega_e} = \begin{bmatrix} 1 & 0 & -\theta_\omega \cos\lambda_\omega \\ 0 & 1 & -\theta_\omega \sin\lambda_\omega \\ \theta_\omega \cos\lambda_\omega & \theta_\omega \sin\lambda_\omega & 1 \end{bmatrix} \bar{x}_I \qquad (5.4\text{-}20)$$

or reversely,

$$\bar{x}_I = \begin{bmatrix} 1 & 0 & \theta_\omega \cos\lambda_\omega \\ 0 & 1 & \theta_\omega \sin\lambda_\omega \\ -\theta_\omega \cos\lambda_\omega & -\theta_\omega \sin\lambda_\omega & 1 \end{bmatrix} \bar{x}_{\omega_e} \qquad (5.4\text{-}21)$$

The axis of figure reference frame has five "inadmissible" potential coefficients because of the coincidence of its origin with the center of mass and because of the alignment of its z-axis with the principal axis of the maximum moment of inertia. However, in the

previous section and section 4.3.1 it was argued that the range equation and the equations of motion are expressed in the instantaneous terrestrial system. This causes not only certain inadmissible coefficients to become admissible but also makes the gravity field time dependent. Implications will be studied below.

At the outset it can be noted that both the instantaneous spin axis and the axis of figure systems were assumed to coincide as far as their origins were concerned (sections 2.3 and 2.4). Consequently, the first degree coefficients stay inadmissible.

The computation of the transformation formulas between the potential coefficients as expressed in both reference systems needs the following equalities, from (5.4-21)

$$\begin{aligned} x_I &= x_\omega + \theta_\omega \cos \lambda_\omega z_\omega \\ y_I &= y_\omega + \theta_\omega \sin \lambda_\omega z_\omega \\ z_I &= z_\omega - \theta_\omega \cos \lambda_\omega x_\omega - \theta_\omega \sin \lambda_\omega y_\omega \end{aligned} \tag{5.4-22}$$

and, dropping second order terms as θ_ω^2,

$$\begin{aligned} x_I^2 &= x_\omega^2 + 2\theta_\omega \cos \lambda_\omega x_\omega z_\omega \\ y_I^2 &= y_\omega^2 + 2\theta_\omega \sin \lambda_\omega y_\omega z_\omega \\ z_I^2 &= z_\omega^2 - 2\theta_\omega \cos \lambda_\omega x_\omega z_\omega - 2\theta_\omega \sin \lambda_\omega y_\omega z_\omega \end{aligned} \tag{5.4-23}$$

These six equations will be substituted in equation (5.4-18) but now with the added sub- and superscripts:

$$V_I = \frac{GM}{r}\left\{1 - \left(\frac{a_e^2}{r^4}\right)\left[C_{20}^I(z_I^2 - \frac{1}{2}x_I^2 - \frac{1}{2}y_I^2) + C_{22}^I(3x_I^2 - 3y_I^2) + S_{22}^I\ (6x_I y_I)\right]\right\} \tag{5.4-24}$$

As said earlier equation (5.4-17) needs to be viewed as

$$V_\omega = V\left\{x_\omega,\ y_\omega,\ z_\omega,\ldots,GM,C_{10}^\omega,C_{11}^\omega,S_{11}^\omega,C_{20}^\omega,C_{21}^\omega,S_{21}^\omega,\ldots\right\} \qquad 5.4\text{-}25)$$

The three terms of (5.4-24) between the square brackets become upon substitution of (5.4-22) and (5.4-23):

$$\begin{aligned}
[z_I^2-\tfrac{1}{2}(x_I^2+y_I^2)]C_{20}^I &= [z_\omega^2-\tfrac{1}{2}(x_\omega^2+y_\omega^2) - 3\theta_\omega \cos\lambda_\omega x_\omega z_\omega \\
&\quad - 3\theta_\omega \sin\lambda_\omega y_\omega z_\omega]C_{20}^I \\
[3x_I^2-3y_I^2]C_{22}^I &= [3x_\omega^2-3y_\omega^2+6\theta_\omega \cos\lambda_\omega x_\omega z_\omega \\
&\quad - 6\theta_\omega \sin\lambda_\omega y_\omega z_\omega]C_{22}^I \\
[6x_I y_I]S_{22}^I &= [6x_\omega y_\omega+6\theta_\omega \sin\lambda_\omega x_\omega z_\omega \\
&\quad + 6\theta_\omega \cos\lambda_\omega y_\omega z_\omega]S_{22}^I
\end{aligned} \qquad (5.4\text{-}26)$$

Now equating terms of equal identity of [5.4-25] and the right hand side of [5.4-26] one gets (term by term),

for $$x_\omega^2: \quad -\frac{1}{2}C_{20}^\omega + 3C_{22}^\omega = -\frac{1}{2}C_{20}^I + 3C_{22}^I \qquad (5.4\text{-}27)$$

$$y_\omega^2: \quad -\frac{1}{2}C_{20}^\omega - 3C_{22}^\omega = -\frac{1}{2}C_{20}^I - 3C_{22}^I \qquad (5.4\text{-}28)$$

$$z_\omega^2: \quad C_{20}^\omega = C_{20}^I \qquad (5.4\text{-}29)$$

$$x_\omega y_\omega: \quad 6S_{22}^\omega = 6S_{22}^I \qquad (5.4\text{-}30)$$

for $\quad x_\omega z_\omega: \quad 3C_{21}^\omega = -3\theta_\omega \cos \lambda_\omega C_{20}^I + 6\theta_\omega \cos \lambda_\omega C_{22}^I$

$$+ 6\theta_\omega \sin \lambda_\omega S_{22}^I \tag{5.4-31}$$

$$y_\omega z_\omega: \quad 3S_{21}^\omega = -3\theta_\omega \sin \lambda_\omega C_{20}^I - 6\theta_\omega \sin \lambda_\omega C_{22}^I$$

$$+ 6\theta_\omega \cos \lambda_\omega S_{22}^I \tag{5.4-32}$$

The first four equations (5.4-27) through (5.4-30) lead to

$$C_{20}^\omega = C_{20}^I \tag{5.4-33}$$

$$C_{22}^\omega = C_{22}^I \tag{5.4-34}$$

$$S_{22}^\omega = S_{22}^I \tag{5.4-35}$$

The last two equations (5.4-31) and (5.4-32) lead to

$$C_{21}^\omega = -\theta_\omega \cos \lambda_\omega C_{20}^I + 2\theta_\omega \cos \lambda_\omega C_{22}^I + 2\theta_\omega \sin \lambda_\omega S_{22}^I \tag{5.4-36}$$

$$S_{21}^\omega = -\theta_\omega \sin \lambda_\omega C_{20}^I - 2\theta_\omega \sin \lambda_\omega C_{22}^I + 2\theta_\omega \cos \lambda_\omega S_{22}^I \tag{5.4-37}$$

The implications of equations (5.4-33) through (5.4-37) are

- the already admissible gravitational coefficients are virtually the same in both reference frames and time independent (terms of θ_ω^2 are neglected).
- two inadmissible coefficients C_{21} and S_{21} become admissible in the instantaneous terrestrial reference frame (in which the equations of

motion are defined). Only the first terms in equations (5.4-36) and (5.4-37) are not negligible (terms including $\theta_\omega C_{22}$ and $\theta_\omega S_{22}$ are of second order). The two coefficients C_{21}^ω and S_{21}^ω are fully dependent on the Chandler wobble: the amplitude of C_{21}^ω and S_{21}^ω in phase with the Chandler wobble (θ_ω) and as well as their periods (main periods about 12 and 14 months). The maximum magnitudes of C_{21}^ω and S_{21}^ω are in the order of

$$\begin{Bmatrix} C_{21}^\omega \\ S_{21}^\omega \end{Bmatrix} \simeq \theta_\omega C_{20}^I = 1.3 * 10^{-6} * 1082.6 * 10^{-6}$$
$$= 0.0014 * 10^{-6}$$

Although these (maximum) values are seven times smaller than the current precision estimates for J_2 [IAG, 1975]

$$J_2 = -C_{20} = 1082.63 \pm 0.01 * 10^{-6}$$

it is safe to say that the time dependency and the admission of certain gravity potential coefficients cannot be avoided depending on the choice of the reference coordinate system. However, in this simulation study the gravity field was assumed to be constant in time and to be referred to the instantaneous terrestrial frame. For similar conclusions the reader is referred to [Lambeck, 1971] or [Newton, 1974].

Does this discussion lead to the conclusion that this type of polar motion (non-coincidence of the instantaneous spin axis and the axis of figure) is not estimable, contrary to the differential polar motion (section 5.4.1)? To answer this question one has to return to the

range equation (5.4-1). This equation has been expressed in the instantaneous terrestrial frame, so one has to add the subscript ω_e to the vector $\overline{x}'^T$:

$$r^2 = r_\omega^2 + R^2 - 2\overline{x}'^T_{\omega_e} R_3(\lambda+GAST_o-\Omega)R_3(\omega_e t)\overline{X}'' \qquad (5.4\text{-}38)$$

The station vector $\overline{x}_I$ is related to the "instantaneous" station vector $\overline{x}_{\omega_e}$ by equation (5.4-20). Using it in (5.4-38) and setting

$$\overline{X}''' = R_3(\omega_e t)\overline{X}'' \qquad (5.4\text{-}39)$$

the range equation (5.4-38) in the average terrestrial system becomes

$$\begin{aligned} r^2 = r_\omega^2 + R^2 - 2R\{ & [\cos\psi\cos(\lambda+GAST_o-\Omega) - \theta_\omega \sin\psi\cos(\lambda+GAST_o-\Omega)]X''' + \\ & [\cos\psi\sin(\lambda+GAST_o-\Omega) - \theta_\omega\sin\psi\sin(\lambda+GAST_o-\Omega)]Y''' + \\ & [\sin\psi \qquad\qquad + \theta_\omega\cos\psi\cos(\lambda-\lambda_\omega)]Z'''\} \end{aligned} \qquad (5.4\text{-}40)$$

From this equation one sees that in theory the positional parameters of the spin axis $\theta_\omega, \lambda_\omega$ are separable from the geocentric coordinates of the stations. Thus, the geocentric coordinates and the "polar motion" are estimable quantities with the following provisions: θ_ω and ψ are in principal estimable but of the four parameters λ, λ_ω, $GAST_o$, and Ω, only the following two are estimable (because of their combinations in the range equation (5.4-40):

$$(\lambda+GAST_o-\Omega) \quad \text{and} \quad (\lambda_\omega+GAST_o-\Omega)$$

More careful inspection of the range equation (5.4-40) reveals that the coefficients of X''', Y''' and Z''' consist of a sum of which the first term is equal to about one, but the second term is in the order of θ_ω which is $1.3 * 10^{-6}$. The numerical value of θ_ω causes weakly differentiable parameters. For this reason one has to prefer range equations as expressed in the instantaneous terrestrial frame above those expressed in the average terrestrial frame. In addition, one would have to wait until θ_ω and λ_ω have gone through an appreciable part of their cycle (12-14 months) in order to become well estimable. Consequently, the idea is to solve for the instantaneous geocentric latitude and longitude difference of the observing stations and to make the "polar motion" indirectly estimable.

5.4.3 Estimability of the Potential Coefficients

In a more precise evaluation of the two-body equations of motion

$$\frac{d^2\overline{X}}{dt^2} = \nabla V \tag{5.4-41}$$

where $\overline{X}$ and V represent the position of the satellite and in an inertial frame of reference and potential of the gravity field, one recognizes from equation (5.4-17) that the spherical harmonic coefficients C_{nm}, S_{nm} are not estimable. Collecting constants in (5.4-17) one obtains

$$
\begin{aligned}
V = \frac{GM}{r} &- (GMa_e C_{10})\frac{z}{r^3} - (GMa_e C_{11})\frac{x}{r^3} - (GMa_e S_{11})\frac{y}{r^3} + \\
&-(GMa_e^2 C_{20})\frac{z^2 - \frac{1}{2}x^2 - \frac{1}{2}y^2}{r^5} - (GMa_e^2 C_{21})\frac{3xz}{r^5} + \\
&-(GMa_e^2 S_{21})\frac{3yz}{r^5} - (GMa_e^2 C_{22})\frac{3x^2 - 3y^2}{r^5} + \\
&- (GMa_e^2 S_{22})\frac{6xy}{r^5} + \ldots
\end{aligned}
\tag{5.4-42}
$$

From the analysis of satellite orbits by means of laser ranging the coefficients A_{nm} and B_{nm} [Heiskanen and Moritz, 1967, p. 60] are the only estimable quantities,

$$
\begin{aligned}
A_{nm} &= -GMa_e^n C_{nm} \\
B_{nm} &= -GMa_e^n S_{nm}
\end{aligned}
\tag{5.4-43}
$$

As already stated in section 4.3.2 when the station parametrization was discussed, the ellipsoid of revolution is virtually immaterial in case of laser ranging to a satellite. This agrees with the result of equation (5.4-43) too: the close to the moments of inertia related quantities A_{nm} and B_{nm} are theoretically the only estimable quantities in the representation of the earth's gravity field from satellite observations. A connecting link might be studies of various satellite orbits which all tend to generate their own gravity field. The remarkable effect occurs when a gravity field generated from countless gravimetric data, terrestrial as well as from satellites, not necessarily generates optimum orbit predictions. In [Marsh and Williamson, 1978] it is again reported that a well determined gravity field as GEM 7 generates a prediction error of 8 to 10

meters over 5 days, whereas a gravity field specially suited to STARLETTE reduced this precision estimate to 1-2 meters in the same time span (5 days). Future studies of this phenomena are therefore a must.

5.5 Time, Time Synchronization and Estimability

In the simulation studies it was tacitly assumed that the observations made at the various sites refer to the same time scale. This of course requires very stringent requirements for the time standards kept by the various clocks at the observing sites. In principle, one could introduce parameters in the mathematical models which describe the clock-offsets. If not, to what precision need clocks to be synchro- at the various sites? In section 6.2.4 it is indicated that ranges to LAGEOS vary between 5900 and 8500 kilometers. This corresponds to a maximum rate of change of about 3 km/sec at an altitude of 20°. If one decides that due to timing errors the distance may not be in error by more than 1 centimeter (the standard deviation of the range measurements was set at 5 cm) then the accuracy of the (relative) time kept at the various sites should be 1 part per million (1 μsec). The proceedings of the meeting on Precise Timing and Time Intervals (PTTI, 1977) indicate that relative clock errors are easily kept within 1 μsec.

A similar reasoning from the satellite's position point of view leads to an identical requirement of relative timing. If a satellite needs to be positioned with an accuracy of 10 mm (its velocity is around 10 km/sec) a relative timing error of around 1 μsec will suffice.

In previous sections it was neglected to mention that laser ranging to a satellite is rather a timing than a ranging measurement system: the time a photon needs for travelling between the laser equipment, satellite and back is recorded. Officially, this leads to a relative station recovery, for instance expressed in terms of baselines, but the unit of length in which the latter are expressed, is time rather than distance. However, recent determinations of the velocity of light have become so accurate that the velocity of light might become the standard for the meter rather than the other way around [IAG, 1975, p. 399]. This was reason enough for this study to consider the range as measured in meters rather than seconds. However, it should be brought to one's attention that light travel time variations as well as deviations from a "straight" light path (refraction) makes that the adaptation of the speed of light as a scale factor should be approached with extreme caution. Techniques as introducing a scale factor per observatory and/or observational time span [Baarda, 1975, p. 46] are serious candidates for modelling highly precise range measurements to satellites. However, they did not form a part of this study.

6. NUMERICAL EXPERIMENTS AND RESULTS

"It should be apparent that judicious use of two-body analysis is of paramount importance . . . "

P. R. Escobal [1976]

6.1 Introduction

In early 1976 a Satellite Laser Ranging Working Group was initiated by Goddard Space Flight Center. Their proposed charter was to " . . . review the progress of the satellite laser validation program and provide guidance on the accomplishment of the validation objectives and on the application of the methods and techniques that are developed" [GSFC, 1976].

One of the objectives was the verification whether " . . . dynamical techniques of satellite geodesy can measure intersite distances of several hundred to several thousand kilometers and polar motion with a precision of about five centimeters" [GSFC, 1976]. One of the suggested analyses was a comparison between the results of the dynamical techniques against those of geometrical techniques. In the first half of 1976 a series of experiments was performed at Ohio State University using geometrical techniques. The logical follow-up, a series of experiments using dynamical techniques became the nucleus around which this report eventually grew. The numerical experiments reported below

mainly concern the geometric aspects (orbit and station configuration, estimability of parameters, etc.) of dynamical techniques in satellite geodesy. The focus is not only on range measurements but also on range-rate and range-difference observations because of the similarity between the three measurement systems. In certain cases the dynamical approach is compared to an equivalent geometrical approach. Under the dynamical approach is understood the parametrization of the behavior of the satellite irrespect whether the observations are simultaneous or not. Under the geometrical approach is understood the technique which takes geometrically advantage of the simultaneity of the observations only. In other words, the dynamic behavior of the satellite is not parametrized and the stations only in a very limited way. As one can see later, the advantages of this technique are very limited.

6.2 The Experiments

6.2.1 The Satellite and Types of Orbit

On May 3, 1976, the satellite LAGEOS was launched in a near circular orbit. A dream come true for many (satellite) goedesists who had pushed the idea of a high flying, low area-to-mass satellite for many years. Originally known under the name Cannonball the concept of the satellite is to minimize the hard-to-model perturbations as atmospheric drag, solar radiation pressure, earth shine, etc. The most important motive was highly precise, hopefully accurate station positioning not corrupted by many perturbing factors to take full advantage of very precise laser range measurements. The satellite should be high enough to be observable from many stations at the same time and to minimize

perturbations (e.g., because of atmospheric drag), low enough neither to loose all information on the earth's gravity field nor to create instrumental problems and at the proper altitude to avoid problems arising from resonance.

The orbital elements of LAGEOS based on long range predictions [Vonbun, 1976] were

semi-major axis (a)	12267.6926 km
eccentricity (e)	0.003845
inclination (i)	109°.85396
right ascension of the ascending node (Ω)	43°.95923
argument of perigee (ω)	245°.07169
mean anomaly (M_o)	55°.20345

The epoch of the orbital elements is August 18, 1976, 0^hUT. An orbit was generated over a two-day period starting August 16, 1976, 23^hUT and ending August 18, 1976, 23^hUT.

Several experiments were performed to Lageos-type satellites: the satellites have some but not all orbital elements with LAGEOS in common. The types of orbit can be classified as follows:

Type 1: a Lageos orbit except for two elements: $e = 0$ and $i = 0°$ (a circular orbit in the equatorial plane). To reduce the situation to a complete two-dimensional case the stations were assumed to be in the equatorial plane as well ($\phi = 0°$). This case was referred to as "The Clock Problem" in Chapter 4, section 4.2.

Type 2: a Lageos orbit except for one element: $e = 0$ (a circular orbit).

Type 3: a Lageos orbit except one element: $i = o°$ (an elliptic orbit in the equatorial plane). As for Type 1 the stations also were thought to be in the equatorial plane.

Type 4: LAGEOS in an elliptic (Keplerian) orbit with elements as reported above.

Type 5: LAGEOS in an elliptic orbit but with secular perturbations in three elements: Ω, ω and n because of the non-sphericity of the earth's gravity field mainly due to J_2.

In the actual reporting of the experiments the designation of the type of orbit is combined with the designation for the type of observation (see section 6.2.5).

6.2.2 The Stations and Observation Campaigns

The stations used in the simulations are those originally planned for the validation, phase 1 in the summer of 1976 [GSFC, 1976]. The six stations, and inter-station distances are represented in Table 6.1. The coordinates of the stations are approximate only. The simulated experiments mainly were to verify the claims of the preceding chapters. The geodetic coordinates were only to give a good approximation of the station geometry.

Many simulations have been performed with subsets of the six stations. To make identification easier the different combinations have received codes. For brevity only the first two letters of the station names are used.

Representative four station configurations are the ones reported in the literature as the San Andreas Fault Experiment [Agreen and Smith, 1973]. One experiment called SAFE 4 consists of the four stations all

TABLE 6.1

STATION COORDINATES AND INTERSTATION DISTANCES

Identification		Geodetic Coordinates[1]							Baseline Lengths in km				
Station	Number	Latitude			Longitude			Height	QU	RA	SA	ST	UT
		°	'	"	°	'	"	m					
Hopkins	1977011	31	41	3.0	249	7	19.0	2350	1290	2912	572	3148	1126
Quincy	1977012	39	58	24.0	239	3	38.0	1060	-	3845	896	3703	828
Ramlas	1977013	28	13	41.0	279	23	39.0	- 30	-	-	3455	1245	3135
San Diego	1977014	32	36	3.0	243	9	33.0	990	-	-	-	3606	1130
Stalas	1977015	39	1	13.0	283	10	20.0	20	-	-	-	-	2907
Utah	1977016	41	50	3.0	248	35	0.0	1980	-	-	-	-	-

[1] a_e = 6378.160 km and f^{-1} = 298.247 167 427 [IAG, 1971].

located in the western part of the United States: HO, QU, SA and UT. In the other four station experiment SAFE 1 station HO was replaced by a station in the eastern part of the United States ST. Experiments which are two and three station subsets of SAFE 4 have been designated respectively SAFE 2 and SAFE 3. Since the bulk of the experiments are analyses using dynamic techniques the prefix SAFE also designates the dynamic nature of the data analysis. The geometric experiments corresponding to SAFE 1 and SAFE 4 have been denoted respectively by GRAM 1 and GRAM 4. Table 6.2 is a summary of the above.

TABLE 6.2

STATION CONFIGURATIONS

Station Combination	Stations
SAFE 4/GRAM 4	HO, QU, SA, UT
SAFE 3	QU, SA, UT
SAFE 2	QU, SA
SAFE 1/GRAM 1	QU, SA, UT, ST

Two simulations will be reported where no more than one or two stations observe each pass of the satellite but in the total observation campaign all four stations (SAFE 4) are involved. The station combination names are respectively SAFE 4(1) and SAFE 4(2).

Before specifying the exact observation schemes of the various combinations, it should be noted that during the 48 hour period of investigation the satellite LAGEOS is observable by the six laser stations in 11 passes. By observable is meant that the satellite is above a specified minimum altitude. In all simulations, but the ones reported

in section 6.7.4, this minimum altitude has been set to 20°. If one looks at the pattern of observability for a local region in the mid-latitudes, one recognizes the following pattern: LAGEOS is observable in groups of five passes. The passes, which are consecutive (!) are at 2-1/2 hour intervals. The interval between groups of consecutive passes is around 8 hours. This seemingly nice pattern might not be very favorable for the monitoring of the local geophysical phenomena. For the specified orbital elements and time span the Table 6.3 lists the observable passes during the two days.

The average length of a pass as seen by at least one station is about 55 minutes. The average length of a pass as seen by at least four stations is around 30 minutes which means a 45% reduction of available measurement time in case of a geometrical analyses. Two other factors will further reduce the amount of data in a geometric analysis. First of all, complete passes will be lost when four or more stations have to observe the satellite. In our example 11 passes were observable by at least one station, however only 10 passes by at least 4 stations. Secondly, the probability that the satellite will be observed by four or more stations is simply small due to unfavorable weather conditions at the various sites [Mao and Mohr, 1976], instrumental breakdowns, etc. These latter factors are not considered in this investigation. Corrections to the reported numbers can easily be made considering certain quotas for loss of passes (data groups). The percentage of 33 [GSFC, 1976] is the ratio of actual observed passes over all possible passes a station could have observed under ideal conditions (no cloud coverage,

TABLE 6.3

OBSERVABLE PASSES DURING TWO DAYS

Pass	Interval between Passes	LAGEOS as seen by at least 1 station Start[1]	End[1]	Duration	4 stations Start[1]	End[1]	Duration
1		$-24^h\ 38^m$	$-23^h\ 42^m$	54^m	$-24^h\ 26^m$	$-23^h\ 50^m$	36^m
	$2^h\ 36^m$						
2		-21 06	-20 10	56	-20 54	-20 16	38
	2 22						
3		-17 48	-16 54	54	-17 24	-17 08	16
	2 26						
4		-14 28	-13 28	60	-14 12	-13 34	38
	2 44						
5		-10 44	-09 54	50	-10 36	-10 04	32
	7 54						
6		-02 00	-01 08	52	-01 40	-01 26	14
	2 40						
7		01 32	02 30	58	01 42	02 24	42
	2 26						
8		04 56	05 50	54	05 18	05 38	20
	2 22						
9		08 12	09 10	58	08 30	09 02	32
	2 38						
10		11 48	12 42	54	11 56	12 36	40
	7 56						
11		20 38	21 24	46	-	-	-

[1]All times are with respect to August 18, 1976, 0^h UT.

instrumental problems, etc.). For simultaneous range observations this means a chance of 1 in 80, whereas for a dynamical analysis the chance is 1 in 10 for the two station configuration.

The ground tracks (observable by at least one station) of LAGEOS in the area of interest is shown in Figure 6.1. The segments between the dots on each groundtrack denote the positions of LAGEOS between which it can be observed by at least four stations.

6.2.3 Modes of Analysis

Three modes have been analyzed for various time spans:

a. the geometric mode using the station combinations GRAM 1 and GRAM 4 (see section 6.2.2) for the time span of 1 day (4 or 5 passes depending on the four stations involved) and 2 days (10 passes).

b. the long arc dynamic mode for the duration of 1 day (6 passes of which 5 are consecutive) and the "short" long arc dynamic mode for the duration of 4-1/2 hours (2 passes). The latter mode approaches very closely the next mode.

c. the short arc dynamic mode (for the duration of 1 hour). This (extreme) short arc mode solves for all parameters every time a group of observations becomes available. The long arc mode considers all parameters to be constant for the time span under investigation. Some (compromise) short arc mode simulations have been made using two and three passes (only interstation distances were considered constant during the time of investigation).

The observability per station plus the various modes can be represented in the following table.

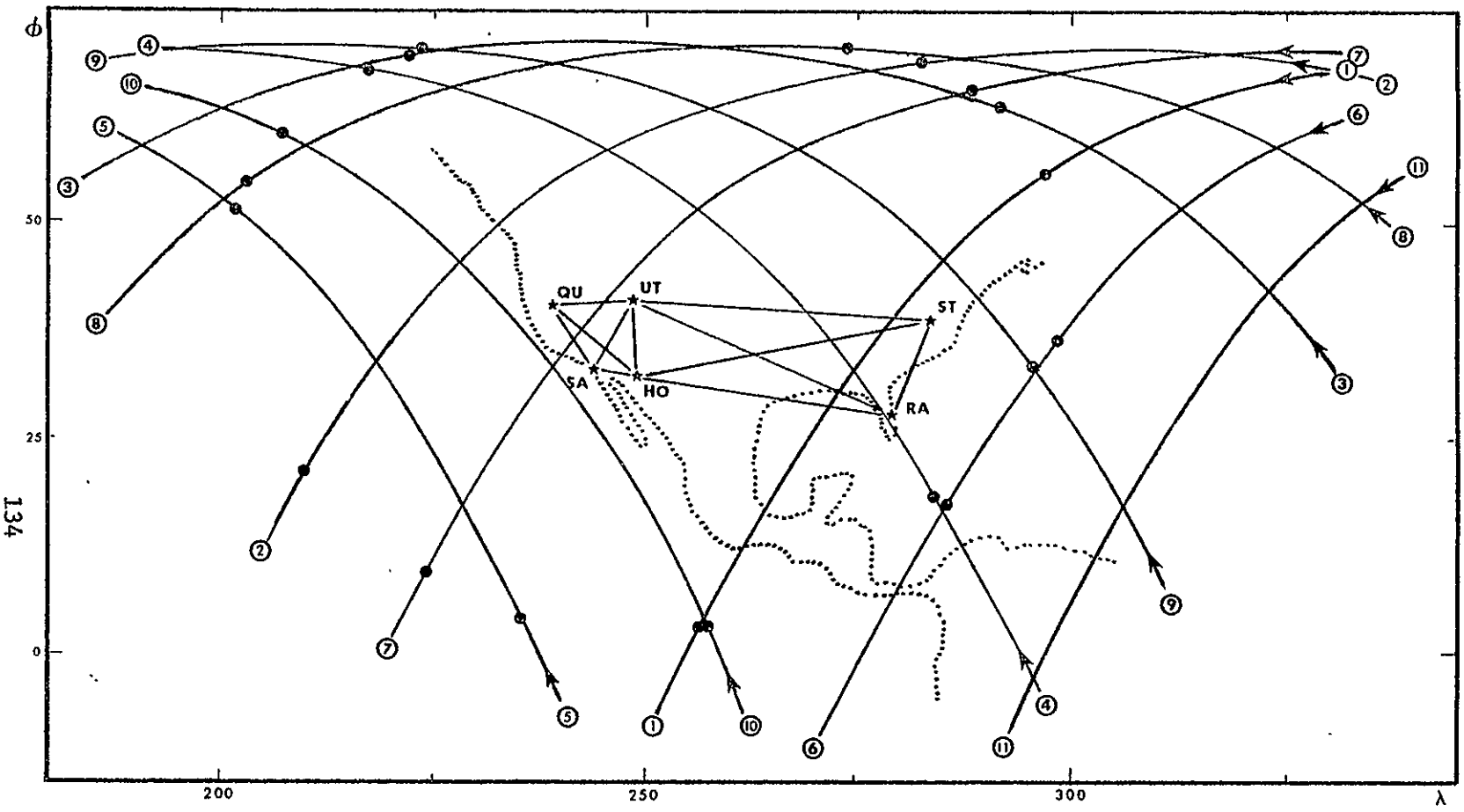

Figure 6.1. Ground Tracks[1] of LAGEOS (Two Days)

[1]Ground track segments between dots (●) denote observability from at least 4 stations, between pass numbers (ⓘ) denote observability from at least 1 station.

TABLE 6.4

STATIONS AND THEIR OBSERVABLE PASSES

Pass	As seen by	Geometric mode	Geometric and dynamic mode (long arc)	Dynamic mode (long arc)	Dynamic mode (short arc)
		For the period of			
1	HO QU RA SA ST UT				1 hr.
2	HO QU RA SA ST UT				
3	HO QU RA SA ST UT				
4	HO QU RA SA ST UT				
5	HO QU SA UT				
6	HO RA ST UT	2 days			
7	HO QU RA SA ST UT			4-1/2 hrs.	1 hr.
8	HO QU SA ST UT		1 day		
9	HO QU RA SA ST UT				
10	HO QU RA SA ST UT			1 hr.	1 hr.
11	RA ST				

The two special cases (see section 6.2.2) where less than four stations made observations to each pass can be represented in the following table.

TABLE 6.5

4 STATIONS WITH 1 OR 2 OBSERVING EACH PASS
(1 day, long arc mode)

Pass	SAFE 4(1)[1]	SAFE 4(2)[1]
5	ho qu SA ut	HO qu SA ut
6	ho UT	HO UT
7	ho qu SA ut	ho qu SA UT
8	ho QU sa ut	ho QU SA ut
9	HO qu sa ut	HO QU sa ut
10	ho QU sa ut	ho QU sa UT

[1]Capital letters denote that observations were made from that station.

6.2.4 The Observations and Their Accuracies

Different Lageos-type satellites are considered not only because of their different orbital geometries (circular, elliptic, secularly perturbed orbits) but also because of the different type of observations. LAGEOS being a passive satellite equipped with corner cube reflectors allows only laser range measurements and with some effort camera observations. However, the range models developed in Chapter 4 easily make a comparison possible with models based on range-rate and range-difference observations. To verify claims concerning estimability made in Chapter 4 the two measurement systems (range-rate and range-difference) have been compared to an equivalent simulation with range observations. The three measurement systems have been coded as RANGE n, RRATE n and RDIFF n, where n is an integer

denoting the type of orbit (see section 6.2.1). The last two measurement systems have been merely included in the discussion to clarify problems of estimability in case of Doppler measurements either in long or short arc analyses.

The interval between the observations in each simulation has been (arbitrarily) set to one minute. In the geometric analysis the ranges were, of course, simultaneous. In the dynamic analysis each set of observations was offset by an amount of seconds to avoid even one pair of simultaneous observations. As an example, in the four station solution the observations of one station were offset by 15, 30 and 45 seconds with respect to the observations at the other three stations.

The precision of the individual range observations was set at 5 cm, a goal envisioned to be reached in 1978/79 [GSFC, 1976]. Comparable precision estimates for the range-rate and range-difference observations are not easily arrived at. First of all, one has to settle the question concerning the relativity of 5 cm precision range measurements to a satellite as LAGEOS. The observable ranges to LAGEOS (the satellite is within 70° from the zenith!) vary between 5900 and 8500 kilometers. The observable range-rate to a Lageos-type satellite will range between -2.94 and 2.94 km/sec. One may sketch the range and range-rate as a function of time as in Figure 6.2.

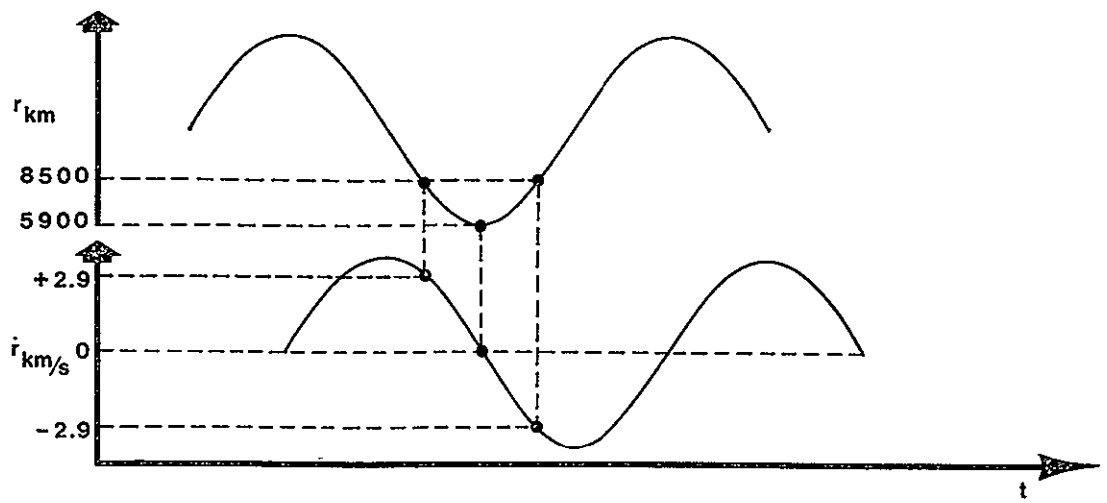

Figure 6.2. Range and Range-Rate as a Function of Time

Probably the best way to estimate the standard deviation of an observable is to compare it to the range of values over which the observable varies rather than to the value of the observable itself.

Reasonings comparing the standard deviation of an observable to the average value (common practice!) or the smallest absolute value of that observable cannot be used here since the range-rate observable fluctuates around the value of zero.

$$\frac{\sigma_r}{r_{max} - r_{min}} \quad \frac{5 \text{ cm}}{(8500 - 5900)_{km}} = 1{:}50{,}000{,}000$$

To find the standard deviation of the range-rate one has

$$\sigma_{\dot{r}} = (\dot{r}_{max} - \dot{r}_{min}) * (1{:}50{,}000{,}000) \simeq 0.1 \text{ mm/sec}$$

In section 6.11 it will become clear that this reasoning leads already to a close approximation (it is overestimated by a factor of two) if one tries to answer the question: How accurately does one have to perform range-rate observations (at the same observational intervals) to a Lageos-type satellite in order to recover the relative station positions among other parameters with the same precision as ranging with a specified precision would have done?

Once the standard deviation of the range-rate observations has been chosen, the compatible precision of the range-difference observables can be computed from

$$\Delta r \simeq \dot{r}\Delta t$$

leading to

$$\sigma_r = \sigma_{\dot{r}}\Delta t$$

Having observations spaced at 60 seconds interval, one obtains with a $\sigma_{\dot{r}}$ of 0.1 mm

$$\sigma_{\Delta r} = 6 \text{ mm} .$$

In section 6.11 it also will become clear that this precision is underestimated by a factor of two since $\sigma_{\dot{r}}$ was overestimated by the same factor.

In all simulations the standard deviation of the observables have been kept constant independently of the value of the observable itself. This might be a little unrealistic since for

the longer ranges the satellite is nearer to the horizon. A constant ranging precision would imply the refraction correction to be of the same uncertainty through the range of admissable zenith distances.

6.2.5 The Earth

All data were simulated using a set of data as adopted by the International Association of Geodesy in Moscow, 1971, during the XVth General Assembly of the I.U.G.G. [IAG, 1971]. The values for the four parameters are:

gravitational constant (GM)	398603 km^3/sec^2
equatorial radius (a_e)	6378.160 km
dynamical form factor (J_2)	0.0010827
angular velocity of the earth (ω_e)	$7.292\ 115\ 1467 * 10^{-5}$ rad/sec

The Greenwich Apparent Sidereal Time for the reference epoch August 18, 1976, 0^hUT has been taken from the American Ephemeris and Nautical Almanac [AENA, 1976, p. 17].

$$GAST_o = 21^h\ 45^m\ 56^s.302$$

Throughout the investigation the principle was to consider all possible parameters unknown. Two of the most important earth parameters, the gravitational constant of the earth and the dynamical form factor are often the subject of some kind of (weighted) constraints. To study the influence of these constraints, the values of these parameters were purposely changed: in the data generation the in 1971 adopted values were used while in the data analysis the in 1975 recommended values by

the XVIth General Assembly of the I.U.G.G. in Grenoble [IAG, 1975] were used

$$GM = 398600.5 \pm .3 \ km^3/sec^2$$

$$J_2 = 108263 \pm 1 * 10^{-8}$$

For a further discussion, the reader is referred to section 6.10.

6.3 Testing Procedure

Simulation studies, which can be characterized by you-get-out-what-you-put-in, make several statistical tests superfluous. Still, a testing procedure for the a posteriori variance-of-unit-weight $\hat{\sigma}^2$ was performed during each simulation mainly for the two following reasons:

1. It is one of the tests which gives an internal check on the computational procedures, e.g., the linearization process. Each simulation was performed in two steps: first of all, the "adjustment" was carried out with observations fitting the model perfectly. In other words, no noise was added to the observations. This procedure should result in an a posteriori variance-of-unit-weight close to zero as compared to the a priori variance. Secondly, the adjustment was performed using observations with a noise of a specified level. This second procedure should result in an a posteriori variance close to the a priori variance. In principle, a variance analysis can take place without the second step but it was found that in borderline cases where the mathematical model was weakly determined by a set of observations the normal matrix was invertible with the

"noiseless" observations but non-invertible with the "noisy" observations. The second step was consequently the safeguard against erroneous conclusions.

2. in several numerical experiments a bias was introduced in the model. The sensitivity of the observations to the introduced bias is nicely reflected in the behavior of the a posteriori variance.

The a posteriori variances $\hat{\sigma}^2$ are tested with the χ^2-test:

$$P\left\{\frac{\chi^2_{DF,1-\alpha/2}}{DF} < \frac{\hat{\sigma}^2}{\sigma^2} < \frac{\chi^2_{DF,\alpha/2}}{DF}\right\} = 1 - \alpha$$

where DF and α denote the degrees of freedom and the level of significance respectively. A failure of the test in case of introduced biases indicates that the model was conditioned enough that the observations could detect the bias. The non-failure of the test could form a warning that the observations were insensitive to the bias introduced and left it undetected possibly causing a biased parameter recovery. In most cases it is unjustified to speak of biased observations or removing a bias from observations. From a philosophical standpoint observations are never biased (excluding instrumental errors, blunders, etc.): it is the model, uncapable of representing reality, which is biased.

Since the majority of the experiments were performed with degrees of freedom between 100 and 1000 and statistical tables often stop at 100 degrees of freedom, a table was constructed with approximate χ^2-values for various large degrees of freedom. An accurate

approximation is given in [Kreyszig, 1970]. For degrees larger than 100 one has for $\alpha = 5\%$

$$\chi^2_{m,\alpha/2} = \frac{1}{2}(h-1.96)^2$$

with $$h = \sqrt{2DF - 1}$$

Rewriting the two equations above, one has

$$\sqrt{2\chi^2_{m,\alpha/2}} - \sqrt{2DF - 1} = -1.96$$

which means that χ^2 can be found by treating the variable $\sqrt{2\chi^2} - \sqrt{2DF - 1}$ as a normally distributed variable with unit variance. Similarly for the lower bound, one has

$$\chi^2_{m,1-\alpha/2} = \frac{1}{2}(h+1.96)^2$$

In general, for $\alpha = 5\%$ one obtains

$$\frac{\chi^2_{DF}}{DF} = 1 + \frac{1.42 + 1.96\sqrt{2DF - 1}}{DF}$$

in which the positive sign denotes the upper bound and the negative sign the lower bound.

As an example for DF = 100, one obtains for

$$\chi^2_{100,97-1/2\%} = 73.77 \ (74.22)$$

and

$$\chi^2_{100,2-1/2\%} = 129.07 \ (129.56)$$

which result in errors of only .6% and .4% (the numbers between brackets are tabulated values, e.g. [Hamilton, 1964]). The upper and lower bounds for degrees of freedom between 100 and 1000 are represented in Table 6.6.

TABLE 6.6

LOWER AND UPPER BOUNDS FOR THE RATIO BETWEEN THE A POSTERIORI AND A PRIORI VARIANCES-OF-UNIT-WEIGHT FOR LARGE DEGREES OF FREEDOM.
Testing level of significance α = 5%.

DF	Lower Bound	$< \hat{\sigma}^2/\sigma^2 <$	Upper Bound
100	0.74		1.29
200	0.81		1.20
300	0.84		1.16
400	0.87		1.14
500	0.88		1.13
600	0.89		1.12
700	0.90		1.11
800	0.90		1.10
900	0.91		1.09
1000	0.91		1.09

6.4 Standard Deviations of the Parameters as a Function of the Number of Observations per Pass and the Precision of the Single Range Measurements

Because of the "non-Bayesness" (no weighted parameters, see section 6.5) of the reported simulation studies the following two properties hold:

a. the standard deviations of the parameters are reduced by a factor of $\sqrt{n}$ when the number of observations per pass are increased by a factor of n. This not too surprising remark was (unnecessarily!) checked by a simulation in which the time interval between observations was reduced from 60 sec to 15 sec: the standard deviations of the parameters were reduced by a factor of 2. Obviously, this reasoning cannot be followed for increasingly denser observations,

e.g., observations measured 0.1 seconds apart cannot be considered uncorrelated anymore.

b. the standard deviations of the recovered parameters have a constant ratio to the standard deviations of the observations (assuming of course that in case of a change the standard deviations of all observations are changed by the same factor). This also rather trivial remark is left to the reader to proof.

The correct way of reporting the results of these studies is to mention the weight coefficients of the parameters rather than their variances or standard deviations (see e.g., Aardoom, 1971). Having second and third generation lasers in mind a single shot precision of 5 cm had been chosen and consequently, the (dimensioned) standard deviations of the recovered parameters are reported rather than the square root of their weight coefficients.

6.5 Baseline Precision as a Function of the Orbital Geometry (Shape and Length)

A variance analysis of the relative station position recovery, in particular the interstation distance recovery, is performed varying the shape of the orbit, i.e., circular, elliptic and secularly perturbed elliptic orbits. The observations were laser range measurements (σ_r = 5 cm, Δt = 60 sec), thus the three solutions were coded RANGE 2, 4 and 5 (see sections 6.2.1 and 6.2.4). A second variable, the length of the analyzed orbit, was also investigated. First it was assumed that the observatories measured ranges during all available (6) passes during 1 day. Secondly, only 2 passes were observed during 1 day. The observatories belonged to the SAFE 4 group (HO, QU, SA, UT). No constraints were applied initially: GM and J_2 were left free which meant that in this

dynamical analysis in the cases of RANGE 2 and RANGE 4 the mean motion was also solved for and in the case of RANGE 5 the mean anomalistic motion and the secular perturbation in perigee were the (unweighted, of course) parameters. As a comparison two simulations were performed having GM constrained (compatible with six orbital elements, rather than seven in case of RANGE 4).

6.5.1 Long Arc Analysis (1 day, 6 passes, 4 stations)

The standard deviations of the interstation distances, expressed in centimeters are listed in Table 6.7.

TABLE 6.7

LONG ARC ANALYSIS (1 DAY, 6 PASSES, 4 STATIONS) FOR CIRCULAR, ELLIPTIC AND SECULARLY PERTURBED ELLIPTIC ORBITS

Interstation Distance Recovery with Standard Deviation in cm. No Constraints for GM and J_2. $\sigma_r = 5$ cm, $\Delta t = 60$ sec

SAFE 4	RANGE 2	RANGE 4	RANGE 5
HO-QU	1.0 cm	1.0 cm	1.0 cm
HO-SA	1.1	1.2	1.2
HO-UT	0.8	0.8	0.8
QU-SA	0.9	0.9	0.9
QU-UT	1.0	1.0	1.0
SA-UT	0.8	0.8	0.9
$\tilde{\sigma}^2/\sigma^2$ 1)	.956	.963	.962
Observations	864	871	872
DF	847	852	852

1) $\tilde{\sigma}^2$ is the a posteriori variance-of-unit-weight in case of simulated observations.

A first inspection of Table 6.7 reveals the small standard deviations for the recovered interstation distances. This is the result of the

more or less unrealistic feature that all stations observed all passes for one day (later more realistic examples are discussed). Still, it means that one day of nice weather in the western part of the United States may result in a highly precise baseline recovery. But this was not the objective of this section. The main purpose of this section, namely investigating the influence of the shape of the orbital geometry is clearly illustrated in Table 6.7. As one might intuitively have expected, the influence between a circular, elliptic and secularly perturbed elliptic orbit on the precision of interstation distance geometry is virtually negligible. This is very important insofar that not very complicated orbital models need be employed to investigate the geodetic potentials of laser ranging to artificial satellites. In the rest of this chapter repeatedly advantage is taken from this feature.

If one considers GM (or n) known the same conclusions hold as Table 6.8 shows.

TABLE 6.8

LONG ARC ANALYSIS (1 DAY, 6 PASSES, 4 STATIONS) FOR CIRCULAR AND ELLIPTIC ORBITS

Interstation Distance Recovery with Standard Deviation in cm. Constraint on GM (or mean motion). $\sigma_r = 5$ cm, $\Delta t = 60$ sec.

SAFE 4	RANGE 2	RANGE 4
HO-QU	1.0 cm	1.0 cm
HO-SA	1.1	1.1
HO-UT	0.8	0.8
QU-SA	0.9	0.9
QU-UT	1.0	1.0
SA-UT	0.8	0.8
$\tilde{\sigma}^2/\sigma^2$	.957	.964
Observations	864	871
DF	848	853

6.5.2 Long Arc Analysis (4-1/2 hours, 2 passes, 4 stations)

Once again the SAFE 4 group of stations observed LAGEOS but now with a reduced set of observations. All observatories observed only 2 passes during a 4-1/2 hour period. The geometry of the stations with respect to the two (consecutive) passes was such that the first pass could be observed only by HO and UT while the next pass was observed by all four stations (see Table 6.4). The standard deviations of the interstation distances (in centimeters) are found in Table 6.9.

TABLE 6.9

LONG ARC ANALYSIS (4-1/2 HOURS, 2 PASSES, 4 STATIONS)
FOR ELLIPTIC AND SECULARLY PERTURBED ORBITS

Interstation Distance Recovery with Standard Deviation in cm.
No Constraints on GM and J_2. σ_r = 5 cm, Δt = 60 sec.

SAFE 4	RANGE 4	RANGE 5
HO-QU	116 cm	135 cm
HO-SA	30	35
HO-UT	9	11
QU-SA	85	95
QU-UT	77	86
SA-UT	6	7
$\tilde{\sigma}^2/\sigma^2$	1.015	1.008
Observations	238	238
DF	219	218

This example, which starts to approach a short arc analysis, shows clearly the influence of the bad geometry (only 2, better 1-1/2 pass is observed). Still, this more realistic simulation (LAGEOS could be observed on a particular day for only 4-1/2 hours, just enough to be

observed twice by two stations and once by two other stations) has implications for the daily monitoring of geophysical phenomena. Assume that one wants to monitor the baseline between Hopkins and Quincy with a precision not exceeding 5 cm. Table 6.9 shows that the standard deviation needs a reduction by a factor of 25, implying an increase in the single-shot frequency by a factor of 600. Since all simulations were performed with a frequency of one shot per minute, it means that range measurements to LAGEOS with a single-shot precision of 5 cm and a frequency of 10 shots per second would be necessary. Alternatively, one may have a single shot precision of 2 cm reducing the precision of the recovered baseline HO-QU (RANGE 5) to 54 cm. In this case the single-shot frequency has to be only $(54 \div 5)^2 = 120$ per minute or 2 shots per second. On the correctness of both reasonings has been elaborated in the previous section (e.g., increasing frequency implies increasing correlation between observations!)

A similar experiment with the "short" long arc but with GM constrained (known) shows identical results (Table 6.10).

The general conclusion of section 6.5 is that while the variances of the baselines are virtually independent of the orbital models (circular, elliptic, etc.), the time-span of the observations is of great importance.

In section 6.7 two other geometrically significant aspects are discussed. First of all (sections 6.7.1 through 6.7.3), the shortest dynamical long arc analysis, the short arc mode is investigated. Secondly (section 6.7.4), the influence of the minimum altitude, above which the satellite is allowed to be observed, is investigated.

TABLE 6.10

LONG ARC ANALYSIS (4-1/2 HOURS, 2 PASSES, 4 STATIONS)
FOR ELLIPTIC ORBIT

Interstation Distance Recovery with Standard
Deviation in cm. Constraint on GM.
σ_r = 5 cm, Δt = 60 sec.

SAFE 4	RANGE 4
HO-QU	115 cm
HO-SA	30
HO-UT	9
QU-SA	85
QU-UT	76
SA-UT	6
$\tilde{\sigma}^2/\sigma^2$	1.011
Observations	238
DF	220

6.6 Baseline Precision as a Function of the Number of Stations

In contrast to a geometric analysis of laser range measurements which require four or more stations observing simultaneously, in a dynamic analysis this stringent requirement is not present. Two cases can be differentiated: the first where a group of stations observes each pass in a specified time span and the second where a subset of a group of stations observes each pass. The experiments reported in the next two sections are with the station group SAFE 4 and its subsets.

6.6.1 All Stations Observing Each Pass

A long arc analysis (1 day, 6 passes) is performed on LAGEOS in the RANGE 2 mode (circular orbit, no constraints on GM). The baseline precision for four, three and two stations is reflected in Table 6.11.

TABLE 6.11

LONG ARC ANALYSIS (1 DAY, 6 PASSES, 4, 3 AND 2 STATIONS) FOR CIRCULAR ORBIT

Interstation Distance Recovery with Standard Deviation in cm. No Constraints on GM. σ_r = 5 cm, Δt = 60 sec.

RANGE 2	SAFE 4	SAFE 3	SAFE 2
HO-QU	1.0 cm	-	-
HO-SA	1.1	-	-
HO-UT	0.8	-	-
QU-SA	0.9	0.9 cm	0.9 cm
QU-UT	1.0	1.0	-
SA-UT	0.8	0.8	-
$\tilde{\sigma}^2/\sigma^2$	.956	.936	.952
Observations	864	647	413
DF	847	633	402

Table 6.11 shows clearly the independence of the number of stations on the relative position recovery in a dynamic analysis when the geometry of the orbit is good (arc of 1 day long). However, when the long arc starts to approach the short arc, the degeneration is very drastic if one reduces the number of observing stations. This is illustrated in Table 6.12.

TABLE 6.12

LONG ARC ANALYSIS (4-1/2 HOURS, 2 passes, 4, 3 and 2 STATIONS) FOR CIRCULAR ORBIT.

Interstation Distance Recovery with Standard Deviation in cm. No Constraints on GM. σ_r = 5 cm, Δt = 60 sec.

RANGE 2	SAFE 4	SAFE 3	SAFE 2
HO-QU	116 cm	-	-
HO-SA	30	-	-
HO-UT	9	-	-
QU-SA	85	206 cm	8966 cm
QU-UT	77	153	-
SA-UT	6	7	-
$\tilde{\sigma}^2/\sigma^2$	1.015	1.108	1.041
Observations	238	166	97
DF	219	152	86

As recalled from Table 6.4 passes 6 and 7 are the ones used for the "short" long arc analyses. From this table it can be seen that pass 6 cannot be observed by the SAFE 2 group (QU and SA) of stations. So the baseline, with a precision of 90 meters, is the result of range observations to a single arc (pass 7). In section 6.7 more attention will be given to the short arc mode.

6.6.2 Some Stations Observing Each Pass

Whereas in the previous section all stations of the SAFE 4 group observed each pass, two experiments have been performed with only one and two stations (out of the possible four) observing each pass. It should be realized that now the subsets of the SAFE 4 group changed

from pass to pass (see section 6.2.3, Table 6.5). The results are as follows.

TABLE 6.13

LONG ARC ANALYSIS (1 DAY, 6 PASSES, 4, 2 AND 1 STATION) FOR ELLIPTIC ORBIT.

Interstation Distance Recovery with Standard Deviation in cm. No Constraints on GM. σ_r = 5 cm, Δt = 60 sec.

RANGE 4	SAFE 4(4)	SAFE 4(2)	SAFE 4(1)
HO-QU	1.0 cm	1.7 cm	7 cm
HO-SA	1.2	2.0	48
HO-UT	0.8	1.8	100
QU-SA	0.9	1.7	58
QU-UT	1.0	1.8	47
SA-UT	0.8	1.5	23
$\tilde{\sigma}^2/\sigma^2$	.963	.997	1.012
Observations	871	462	234
DF	852	443	215

Two important results may be drawn from this table:

1. It is almost a necessity that each arc (pass) is observed by more than one station. Arcs observed by a single station do not contribute very much to the total recovery of a group of stations.
2. In case arcs are observed by single stations the best results are obtained from consecutively observed arcs: as Table 6.5 shows passes 5, 6 and 7 are observed by SA, UT and SA respectively and passes 8, 9 and 10 by QU, HO and QU. Indeed, the baselines SA-UT and HO-QU are determined with the highest precision. Even the fact

that QU and SA are the only two stations which observed two arcs each, their baseline (QU-SA) is the one but worst determined.

Expanding on these results one has to recognize the implications for LAGEOS as a tool for the establishment of a global reference frame. As the distances between stations increase, the chance that arcs are co-observed by two or more stations, decreases. Especially, the monitoring of phenomena with high frequency (periods of 1 day or shorter) might be difficult to realize with the help of satellites. However, in local areas chances are that monitoring by satellites is more successful. The future role of satellites might be seen as an interpolating one as opposed to a measurement system as Very Long Baseline Interferometry.

6.7 Short Arc Mode

In the last ten years the short arc mode analyses of satellite observations have become increasingly popular. As will be explained later, the short arc mode can take various identities.

In Chapters 3 and 4 models have been developed for the dynamic analysis of mainly range observations. Since the equations of these mathematical models do not dictate any specifications regarding the minimum time span of the observation campaign, one might expect that there is no fundamental difference between long and short arc analyses of satellite data. The conclusion must then be that the same parameters are estimable in the short arc mode as in the long arc mode. Of course, because of the unfavorable geometry of the short arc mode (recall the effect of shortening the long arcs as described in section 6.5), the various parameters in the short arc mode will be determined

worse than in the long arc mode. In this respect the "inner constraints" for origin and orientation applied in the short arc mode, e.g., by [Brown and Trotter, 1973] must be qualified as "over constraints" (see section 6.7.3). As it follows from the detailed discussions in Chapter 4 the only inner constraint to be applied stems from the lack of system definition in longitude. Consequently, only one (not six) inner constraint is needed if one has as one's parameters the orbital elements and the station coordinates (two inner constraints if also the orientation of the earth at some epoch was entered as a parameter, see e.g., section 4.9).

6.7.1 Short Arc Mode, One Pass at a Time

The different identities a short arc mode can have is based on the time span certain parameters are kept constant. It follows from the line of the discussion presented here that with the (geophysical) applications in mind the parameters should not be considered constant longer than the time in which a phenomena to be monitored varies appreciably. A satellite geodesist who has a set of observed arcs at his disposal, which are somewhat spaced in time and who wants to analyze the data in the short arc mode, might have to resort to this extreme: resolve all parameters for each pass. A different compromise type of short arc mode will be discussed later.

The first experiments were performed with the SAFE 4 group of stations with three passes: pass 1, 7 and 10 (see Table 6.3). Between pass 1 and 7 is a time lapse of about 25 hours, between pass 7 and 10 about 9 hours. The three passes have the following geometrical characteristics:

pass 1: this pass is low at the horizon for all four stations.

pass 7: this pass reaches a high altitude for all four stations and the (short) arc is parallel to the interstation baseline SA-UT (see Figure 6.1).

pass 10: this pass also reaches a high altitude for all four stations but its arc is parallel to the baseline QU-SA

The standard deviations of the six interstation distances are reported below.

TABLE 6.14

SHORT ARC ANALYSIS (2 DAYS, 3 PASSES, 4 STATIONS)
FOR ELLIPTIC ORBIT

Interstation Distance Recovery with Standard
Deviations in cm. No Constraints on GM.
σ_r = 5 cm, Δt = 60 sec.

RANGE 4 SAFE 4	Pass 1	Pass 7	Pass 10
HO-QU	1578 cm	1111 cm	187 cm
HO-SA	1331	204	327
HO-UT	194	200	206
QU-SA	296	750	13
QU-UT	1013	565	690
SA-UT	59	19	429
$\tilde{\sigma}^2/\sigma^2$	1.116	1.042	1.033
Observations	166	192	194
DF	147	173	175

From this table the following conclusions can readily be drawn:

- the overall precision of the relative positioning of the short arc mode is very disappointing if restricted to the one-pass-analysis.

In general, the standard deviations of the interstation distances are far above the one meter level. As an example, the standard deviation of the baseline HO-UT is in the order of 2 meters in all three passes. One only has to recall the shortest long arc analysis reported in section 6.5.2 (in 1-1/2 passes the standard deviation of this baseline is 9 cm) in order to appreciate the superiority of long arc analyses no matter how short they may be!

the influence of the geometry is felt as strongly in the short arc mode as in the geometric mode (see section 6.8): if an arc is "parallel" to a baseline a very precise recovery of that baseline is made. This phenomena is easily explained geometrically. One does not have to have a great geometrical insight to see that a distance between two points is determined the best if distance measurements are made from the two end points to a third point which is situated on a line through those two points. Consequently, a satellite which flies "parallel" to the direction of an interstation distance and preferably reaches a high altitude provides a good recovery of that baseline, especially when it enters and leaves the cone of observability (the points of intersection of the orbit with this cone are situated the closest to that most ideal "third point" as described earlier). In this respect the minimum altitude above which a satellite is allowed to be observed, plays an important role (section 6.7.4).

6.7.2 Short Arc Mode, Several Passes at a Time

To return to the definition of "short arc analyses" one has to compare the already reported long, "short" long and short arc solutions

for one particular case (Table 6.15). In all these three solutions all parameters have been kept constant for the time span under investigation. In this light one has to classify the short arc algorithms as in [Brown and Trotter, 1969, 1973] as a compromise between the long and short arc methods as reported above. Instead of going to the extremes of solving for all parameters for each pass, one could for instance consider certain parameters as the latitude, longitude-difference (!) and the distance of the earth's center-of-mass of the participating stations constant during, let's say, 1 day but solve for the orbital parameters in each pass. Good reasons for the (compromise) short arc

TABLE 6.15

DYNAMIC ANALYSES FOR ELLIPTIC ORBIT

Interstation Distance Recovery with Standard Deviations in cm. No Constraints on GM. σ_r = 5 cm, Δt = 60 sec.

RANGE 4 SAFE 4	Long Arc (1 day, 6 passes)	Short Long Arc (4-1/2 hrs., 1-1/2 passes)	Short Arc (1 hr., 1 pass)
HO-QU	1.0 cm	116 cm	1111 cm
HO-SA	1.2	30	204
HO-UT	0.8	9	200
QU-SA	0.9	85	750
QU-UT	1.0	77	565
SA-UT	0.8	6	19
$\tilde{\sigma}^2/\sigma^2$	.963	1.015	1.042
Observations	871	238	192
DF	852	219	173

method exist: basically the station parameters can be classified as slowly varying parameters, whereas the orbital parameters are often rapidly varying parameters due to various secular and periodic perturbations (please note: in case of a Keplerian orbit the orbital parameters do not vary). The catch is, of course, that the compromise short arc mode cannot be applied limitless in time, especially viewing the future goals of satellite ranging. The method will defeat itself with highly precise measurements. In a short campaign of a week the latitude of a station may vary more than half a meter due to polar motion, thus clearly coming in conflict with one of its assumptions: the station parameters are considered constant during the campaign. Obviously, the (compromise) short arc method has to be used with great care not to introduce biases in the solution as result of its assumptions.

A different type of (compromise) short arc method is analyzed here: instead of considering the station coordinates ($R, \bar{\psi}, \Delta\lambda$) constant only the baselines are assumed to be time invariant. This method allows for a larger geometrical freedom because it reduces the number of invariant parameters. In case of 4 stations only 6 instead of 12 station parameters are assumed to be constant in time. Geometrically, it implies that the size and shape of the station polyhedron does not vary with time but its orientation is allowed to change (e.g., due to polar motion).

Instead of results reported for individual passes (Table 6.14, passes 1, 7 and 10) the standard deviations of the baselines from the four possible combinations between these passes are reported (Table 6.16).

TABLE 6.16

SHORT ARC ANALYSIS FOR ELLIPTIC ORBIT
(2 DAYS, 2 AND 3 PASS SOLUTIONS, 4 STATIONS)

Interstation Distance Recovery with Standard Deviations in cm. No Constraint on GM. σ_r = 5 cm, Δt = 60 sec.

RANGE 4 SAFE 4	Passes			
	1 + 7	1 + 10	7 + 10[1)]	1 + 7 + 10
HO-QU	91 cm	73 cm	46 cm (10 cm)	36 cm
HO-SA	46	85	43 (11)	34
HO-UT	44	30	23 (5)	18
QU-SA	47	9	9 (2)	9
QU-UT	52	120	57 (15)	43
SA-UT	14	35	15 (3)	13

1) The standard deviations between brackets from the comparable long arc analysis.

Comparison with Table 6.14 reveals that the standard deviations of the baselines reduce more than one would initially expect from the results of the individual passes. This effect is due to the correlations between the baselines from the one-pass solutions. The results of Table 6.16 are computed with the following relationship

$$\Sigma_{combination} = \Sigma^{-1}_{pass\ 1} + \Sigma^{-1}_{pass\ 2} + \ldots + \Sigma^{-1}_{pass\ n}{}^{-1}$$

where each Σ denotes a full variance/covariance matrix.

The best short arc solution using only two passes (passes 7 and 10 cross each other almost perpendicularly over the area under investigation, see Figure 6.1) cannot compete with the comparable long arc solution: the standard deviations of the baselines range between 9 and

57 cm for the short arc analysis but between 2 and 15 cm for the long arc analysis. This means as far as the organization of observation campaigns is concerned, that full advantage should be taken of the consecutive character of LAGEOS' passes (five consecutive passes per day, see section 6.2.2). Data analyzed in the long arc mode (arcs up to 1 day) are capable of making more precise "snap shorts" of ground networks than multiple short arcs would do. The gain in precision by evaluating the satellite parameters over longer periods of time (long arc mode) is apparently much higher than by evaluating only the (constant) station parameters over long periods (short arc mode).

6.7.3 The Influence of Weighting in the Short Arc Mode

In section 5.2 it was argued that weighting of parameters may result in too optimistic precision estimates. In a series of tables it is shown that weighting of parameters (in this case, the station parameters) will yield optimistic standard deviations not only for the baseline recoveries (Tables 6.17 through 6.19) but also for the other station, satellite and earth parameters (Table 6.20).

The first case (Table 6.17) deals with the weighting of one station (HO). In the literature it has been suggested that the lack of coordinate system definition of the short arc mode finds mainly its cause in the "lack-of-origin." The constraint may be viewed as a "quasi-minimum-constraint" since it has been shown (Chapter 4) that the set of estimable quantities is already established.

TABLE 6.17

SHORT ARC ANALYSIS FOR ELLIPTIC ORBIT (2 DAYS, 3 PASS SOLUTION, 4 STATIONS) WITH VARYING WEIGHTS ON ONE STATION (HO: R, ψ, $\Delta\lambda$)

Interstation Distance Recovery with Standard Deviations in cm. No Constraint on GM. σ_r = 5 cm, Δt = 60 sec.

RANGE 4 SAFE 4	Weighting (σ)			
	∞	10 m	1 m	10 cm
HO-QU	36 cm	26 cm	20 cm	19 cm
HO-SA	34	23	18	17
HO-UT	18	13	9	9
QU-SA	9	8	7	6
QU-UT	43	30	24	23
SA-UT	13	11	10	10

The reduction in the standard deviations of the baselines proves that a lack of origin definition is not present in the short arc mode solution. It should be noted that estimable quantities are not affected by weighting of (non-estimable) parameters (see section 5.2.3).

Another quasi-minimum-constraint is the five parameter constraint. This constraint might be compared to similar minimum constraints which are used in the geometric mode analyses of simultaneous range observations to satellites. Not six but five quasi minimum constraints (HO: R, ψ, $\Delta\lambda$ and QU: R, ψ) are needed since the longitudinal rank defect has already been eliminated from the model (Chapter 4). This case (Table 6.18) and the case whereby all four stations are weighted (Table 6.19) are merely included to demonstrate the (dangerous) influence of (over-) weighting.

TABLE 6.18

SHORT ARC ANALYSIS FOR ELLIPTIC ORBIT (2 DAYS, 3 PASS SOLUTION, 4 STATIONS) WITH VARYING WEIGHTS ON TWO STATIONS (HO: R, ψ, $\Delta\lambda$ AND QU: R, ψ)

Interstation Distance Recovery with Standard Deviations in cm. No Constraint on GM. σ_r = 5 cm, Δt = 60 sec.

RANGE 4 SAFE 4	Weighting (σ)			
	∞	10 m	1 m	10 cm
HO-QU	36 cm	23 cm	18 cm	16 cm
HO-SA	34	19	14	12
HO-UT	18	11	8	6
QU-SA	9	8	6	6
QU-UT	43	24	18	16
SA-UT	13	11	9	6

TABLE 6.19

SHORT ARC ANALYSIS FOR ELLIPTIC ORBIT (2 DAYS, 3 PASS SOLUTION, 4 STATIONS) WITH VARYING WEIGHTS ON FOUR STATIONS (HO, QU, SA, UT: R, ψ, $\Delta\lambda$)

Interstation Distance Recovery with Standard Deviations in cm. No Constraint on GM. σ_r = 5 cm, Δt = 60 sec.

RANGE 4 SAFE 4	Weighting (σ)			
	∞	10 m	1 m	10 cm
HO-QU	36 cm	21 cm	17 cm	7 cm
HO-SA	34	16	13	5
HO-UT	18	10	8	4
QU-SA	9	8	6	3
QU-UT	43	21	17	6
SA-UT	13	11	9	5

So far only the influence of weighting has been investigated on the quantities which are dependent on the (weighted) station parameters: the baselines. However, the influence varies from parameter group to parameter group. Table 6.20 shows the impact on the various parameters in the case of a short arc mode analysis using only one pass (7).

The influence of the weighting procedure is the strongest for the latitudes and longitude differences and the weakest for the geocentric radii as far as the station parameters are concerned. Similarly, a latitude related satellite parameter, the inclination of the orbit, is strongly influenced by the weighting. The largest factors by which the standard deviations decreased, are 400 for UT's latitude (UT is almost exactly north of HO) and 75 for SA's longitude (SA is almost exactly west of HO). The standard deviation of the inclination reduced by a factor of 8. The strong dependency of the precision of these three types of parameters (ψ_i, $\Delta\lambda_i$, i) might indicate the largest weaknesses in the short arc mode.

6.7.4 The Influence of the Cut Off Angle

In section 6.7.1 the most ideal geometry to determine the length of a baseline very precisely has been elaborated upon. In Table 6.21 this is once more illustrated by the overpowering influence of the minimum altitude above which range observations to a satellite are permissable.

TABLE 6.20

SHORT ARC ANALYSIS FOR ELLIPTIC ORBIT (1 PASS, 4 STATIONS) WITH VARYING WEIGHTS ON ONE STATION (HO: R, ψ, $\Delta\lambda$)

Interstation Distance, Station, Satellite and Earth Parameters Recovery. No Constraint on GM. σ_r = 5 cm, Δt = 60 sec.

SAFE 4		Weighting (σ) ∞	10 m	1 m	10 cm
HO-QU		1111 cm	494 cm	372 cm	369 cm
HO-SA		204	89	74	73
HO-UT		200	112	76	74
QU-SA		750	341	252	248
QU-UT		565	234	182	181
SA-UT		19	17	13	12
HO	R	771 cm	407 cm	100 cm	10 cm
	ψ	8".1	0".3	0".03	0".003
	$\Delta\lambda$	3".9	0".4	0".04	0".004
QU	R	773 cm	693 cm	461 cm	442 cm
	ψ	5".6	0".9	0".42	0".37
	$\Delta\lambda$	7".9	1".2	0".60	0".55
SA	R	568 cm	238 cm	210 cm	209 cm
	ψ	6".7	0".6	0".26	0".23
	$\Delta\lambda$	4".6	0".4	0".07	0".06
UT	R	545 cm	238 cm	213 cm	212 cm
	ψ	8".0	0".3	0".04	0".02
	$\Delta\lambda$	7".9	1".5	0".72	0".64
a		1448 cm	1295 cm	833 cm	795 cm
e		$9.9 * 10^{-7}$	$8.5 * 10^{-7}$	$4.2 * 10^{-7}$	$3.8 * 10^{-7}$
i		17"	5"	2".5	2".2
ω		50"	32"	21"	20"
E_o		47"	35"	23"	22"
n		0.00140 "/sec	0.00068 "/sec	0.00035 "/sec	0.00032 "/sec
ω_e		0.00071 "/sec	0.00040 "/sec	0.00020 "/sec	0.00018 "/sec
Observations		192	192 + 3	192 + 3	192 + 3
DF		173	173 + 3	173 + 3	173 + 3

TABLE 6.21

SHORT ARC ANALYSIS FOR ELLIPTIC ORBIT (HALF A DAY, 2 PASS SOLUTION, 4 STATIONS) WITH VARYING MAXIMUM ZENITH ANGLE

Interstation Distance Recovery with Standard Deviations in cm. No Constraint on GM. σ_r = 5 cm, Δt = 60 sec.

RANGE 4 SAFE 4	Maximum Zenith Angle		
	70°	60°	50°
HO-QU	46 cm	101 cm	211 cm
HO-SA	43	96	197
HO-UT	23	52	120
QU-SA	9	23	59
QU-UT	57	127	260
SA-UT	15	35	81

Table 6.21 seems to indicate the following rule of thumb: for every 10° decrease in the maximum zenith angle the precision (standard deviation) decreases by a factor of two. Since the frequency of the observations has not been varied during these experiments, this seems to imply that the frequency of the observations has to be increased by a factor of four to compensate for the worsening geometry. This increase in the number of observations is much larger than actually was lost in observations by raising the minimum altitude, clearly showing the negative power of the worsened satellite-station geometry.

6.8 Geometric Mode

Before discussing some variations on the theme of the dynamic mode (application of constraints, usage of different measurement systems

and evaluation of other than station parameters) it may be worthwhile to compare the various dynamic experiments with the geometric mode, especially because of the similar nature and quality of their parameters. In the geometric mode the interstation baselines are the only estimable quantities whereas in the dynamic mode these are the best estimable quantities (see section 6.11).

Of the six stations many combinations of four stations can be formed. Before discussing the results for the station groups SAFE 1 and SAFE 4 (or GRAM 1 and GRAM 4 as they are called in the geometric analysis), other combinations of stations are worth noting because many of them form critical or near critical configurations [Blaha, 1971b]. The stations HO, RA, ST and UT and also the stations SA, RA, ST and QU form roughly trapezoids with equal sides. Since a plane can almost be fitted through the four stations, the geometric recovery of the interstation distances proves to be impossible. The GRAM 1 and GRAM 4 groups turn out to be more representative station combinations. GRAM 4 (or SAFE 4) consists of four relatively close stations in the western United States, capable of generating "many" simultaneous observations (because of their closeness) but with the danger of being close to a critical configuration. GRAM 1 (or SAFE 1) breaks up this "closeness" by exchanging one station (HO) in the West for a station (ST) in the eastern United States. This GRAM 1 combination proves to be far from "critical" but has fewer observations (events) because of its spaced-out geometry. As in all other experiments the data acquisition was one range measurement per minute with a standard deviation of 5 cm. Because of its lower ability to collect large quantities of data, a one and a two day solution have

been performed. Although this experiment is completely unrealistic (every possible simultaneous event in the one or two day time span is being used!) it clearly shows the very severe limitations of the geometric analysis even in this over-idealized situation (i.e., reality is worse!). The results as compared to the long arc analyses of 4-1/2 hours and 1 day, are as follows.

TABLE 6.22

GEOMETRIC AND DYNAMIC ANALYSES

Interstation Distance Recovery with Standard Deviation in cm. (Dynamic Mode: Elliptic Orbit, no Constraints on GM.) σ_r = 5 cm, Δt = 60 sec.

GRAM 1 or SAFE 1	GRAM 4 or SAFE 4	Geometric Mode				Dynamic Mode SAFE 4	
		GRAM 1		GRAM 4			
		1 day	2 days	1 day	2 days	4-1/2 hrs.	1 day
	HO-QU	-	-	66 cm	48 cm	116 cm	1.0 cm
	HO-SA	-	-	55	36	30	1.2
	HO-UT	-	-	142	90	9	0.8
QU-SA		10 cm	6 cm	80	53	85	0.9
QU-ST		56	42	-	-	-	-
QU-UT		11	8	111	72	77	1.0
SA-ST		63	41	-	-	-	-
SA-UT		17	9	185	117	6	0.8
ST-UT		43	32	-	-	-	-
$\tilde{\sigma}^2/\sigma^2$		0.858	0.936	1.128	0.981	1.015	.963
Observations		376	772	676	1180	238	871
DF		88	187	163	289	219	852
Passes		5	9	4	8	2 (1-1/2)	6

From Table 6.22 the following conclusions can be drawn:

- The geometry of GRAM 1 is superior to that of GRAM 4, e.g., the standard deviation of the baseline Quincy-San Diego is reduced five times (from 53 cm to 10 cm) with less than one third of the observations (!) if recovered in a good geometry.
- Not only is the geometric mode limited in terms of estimable quantities the analysis shows clearly that it is also limited as far as the precision of the baseline recovery is concerned: 4-1/2 hours of dynamic analysis (2 or better 1-1/2 pass) does an equivalent job as two days of geometric analysis (8 passes). Keep also in mind, 1-1/2 pass per day in the dynamic mode is feasible, 2 days with (all!) 8 passes in a geometric analysis is completely unrealistic.
- The previous conclusion leads to the inefficiency of the geometric mode: in two days the GRAM 4/SAFE 4 group collected 1180 range observations but in the geometric analysis the model has only 289 degrees of freedom. The same group collects only 238 range observations in 4-1/2 hours but still has 219 degrees of freedom in case of a dynamic analysis.

6.9 Precision of Parameters not Directly Related to Station Positioning

At the end of Chapter 4, Table 4.1 gives a detailed discussion of the estimability of the various parameters in dynamic analyses. So far our discussion has been limited to best estimable quantities, the interstation distances. Other estimable quantities are the orbital parameters, the station coordinates ψ, $\Delta\lambda$, R and the angular

velocity of the earth ω_e. The estimability of these parameters indicates the possible monitoring of the following important phenomena the length of day/UT1 determination from the angular velocity ω_e and polar motion determination from the (variation in the) latitudes of the stations.

6.9.1 Length of Day/UT1 Determination

Striving for relative accuracies of 10^{-9} implies a length-of-day determination with a precision of about 0.086 msec (per day) or an angular velocity determination of $7.3 * 10^{-14}$ rad/sec (ω_e = 7.292 115 1467 * 10^{-5} rad/sec).

Concerning the above apparently stringent requirement of determining the length-of-day to about 0.086 msec/day one only has to remember that the largest short periodic variations in the spinrate are in the order of 0.15 msec/day [Rochester, 1973]. The standard deviation being hardly half of that value is not an exaggerated requirement. See also section 2.5.

If limited to the discussion of secular perturbations of the gravity field, the estimable quantity in case of range observations is $(\omega_e - \dot{\Omega})$ (see Chapter 4, section 4.7.3). Since the rate of change in the argument of perigee is also estimable, J_2 is estimable and ω_e and $\dot{\Omega}$ can be determined separately. (In Chapter 4 the two geometrical parameters $\omega_e - \dot{\Omega}$ and $\dot{\omega}$ were preferred over the set ω_e and J_2; similarly, the parameter n (mean motion) was preferred over GM.) Does this mean that J_2 also has to be known with a relative accuracy (precision) of 10^{-9}? The answer to this question will be given in the following discussion.

To be on the safe side, let the uncertainty of the contribution of J_2 to the parameter $(\omega_e - \dot{\Omega})$ be half of the specifications mentioned above. This means that $\dot{\Omega}$ should be known with a relative precision of $3.5 * 10^{-14}$ rad/sec. However, for a satellite as LAGEOS ($a \cong 12.000$ km) the rate of change in the ascending node is around $^{\circ}.34$/day or $6.9 * 10^{-8}$ rad/sec. This yields a relative accuracy for $\dot{\Omega}$ of

$$\frac{3.5 * 10^{-14}}{6.9 * 10^{-8}} \cong 5 * 10^{-7}$$

Since $\dot{\Omega}$ is proportional to J_2 the dynamical form factor needs also to be known with a relative accuracy of $5 * 10^{-7}$. The recommended value of the XVI General Assembly of the IUGG (1975) for J_2 is

$$J_2 = 108263 \pm 1 * 10^{-8} \qquad \text{[IAG, 1975]}$$

which indicates a relative accuracy of about 10^{-5}. The conclusion is that J_2 needs to be known with an accuracy at least 200 times better than the currently recommended value. This seems to make UT1 determinations by means of satellite ranging to LAGEOS very difficult. For lower satellites as STARLETTE ($a \simeq 7000$ km) the rate of change in the ascending node is much larger. For example, $\dot{\Omega} = -3^{\circ}.9$/day for STARLETTE which is ten times larger than LAGEOS' node rate. This in turn implies that for UT1 determinations from range observations to STARLETTE J_2 needs to known 2000 times better than the recommended value of 1975.

If one expresses the spinrate in arcseconds per time seconds the requirement for spin rate determinations is $15 * 10^{-9}$ "/sec. Several experiments are grouped in the following table.

TABLE 6.23

EARTH'S SPIN RATE DETERMINATIONS WITH STANDARD DEVIATIONS IN ARCSECONDS PER TIMESECONDS

$\sigma_r = 5$ cm, $\Delta t = 60$ sec

Stations	Orbit	Time Span	$\sigma_{\omega_e, \omega_e - \dot{\Omega}}$
SAFE 4(1)	elliptic	1 day	$370 * 10^{-9}$ "/sec
SAFE 4(2)	"	"	$16 * 10^{-9}$
SAFE 4	"	"	$8 * 10^{-9}$
"	"	4-1/2 hrs.	$5118 * 10^{-9}$
"	elliptic with sec. perturb.	1 day	$18 * 10^{-9}$
"	"	4-1/2 hrs.	$8286 * 10^{-9}$

The results of this table are in apparent contradiction to the reasoning at the beginning of this section. If the geometry of orbit and station configuration is not too bad (more than one station, long arc not too short), the spin rate of the earth can indeed be determined with a precision of 0.1 msec/day. The earlier reasoning told us that J_2 is insufficiently known to guarantee proper UT 1 determinations. The one but last experiment in Table 6.23 shows that if 4 stations observe LAGEOS for 1 day (6 passes) with a ranging precision of 5 cm (and $\Delta t = 60$ sec) the spin rate not only can be determined with a relative precision of 10^{-9} but also must have inherently determined J_2 with a higher precision than currently known. Reasoning further, this implies that eight orbital parameter models are not only preferable

but also a necessity (see also section 6.10). In this investigation simple analytic expressions are used for the dynamical analysis: the eight parameter model consists of a, e, i, ω, $\dot{\omega}$, Ω, E_o and n. As the fourth example in Table 6.23 shows: all eight parameters are estimable even from a long arc as short as 4-1/2 hours (which was 1-1/2 pass: four stations observed one pass (#7) two stations the other pass (#6)). The above mentioned model is capable of incorporating all secular perturbations (due to J_2, J_2^2, J_3, J_4, etc.) in ω, $\dot{\Omega}$ (better $\omega_e-\dot{\Omega}$) and n (or E_o). If one would have opted for the orbit determination by numerical integration the eight parameters could be: a, e, i, ω, Ω, E_o, GM and J_2. The advantage of this approach is that it includes all perturbations due to J_2 (long and short periodic) but it does not include any other perturbations as the analytic eight parameter model does.

However, one should not forget that in the next to last experiment (of Table 6.23) the recovery of the spin rate was a little above the set requirements (18×10^{-9} "/sec instead of 15×10^{-9} "/sec) whereas the very same simulation recovered the baselines with an average precision of less than 1 cm! (see Table 6.7). This might also serve as an example why in the dynamic mode the interstation distances are called the best estimable quantities. Consequently, these optimistic but still marginal results leads to the following opinion: length-of-day/UT1/earth rotation determinations are preferably to be derived from Very Long Baseline Interferometry as long as a blind system such as laser ranging to a satellite cannot successfully separate the rotation of the satellite's orbit with respect to the earth into two

components: the (inertial) angular velocity of the earth and the (inertial) fluctuating rotations of the orbit caused by the non-central gravity field of the primary. Other phenomena, as tides, will cause similar fluctuating effects both in the angular velocity of the earth and in the rotations of the orbit. Future research has to show how well these effects are separable from satellite laser ranging.

6.9.2 Polar Motion Determination

Limiting our discussion to polar motion determinations in short time spans the only estimable polar motion is the differential one: the change in latitude and longitude difference of the observing stations determines the change in position of the instantaneous rotation axis (see Figure 6.3).

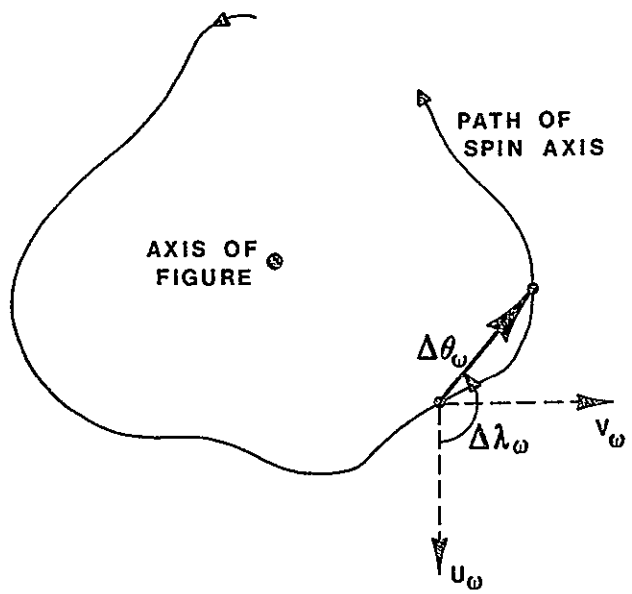

Figure 6.3. Differential Polar Motion

Derivations in section 5.4.1 gave for the changes in latitude and longitude difference

$$\Delta\psi = \Delta\theta_\omega \cos(\lambda-\Delta\lambda_\omega) \tag{6.9-1}$$

$$\Delta\lambda \operatorname{cotan}\phi = \Delta\theta_\omega \sin(\lambda-\Delta\lambda_\omega) \tag{6.9-2}$$

At maximum amplitude of the Chandler wobble the pole might displace some 10-12 cm/day. Opting for standard deviations of the latitudes less than 3 cm or 0".001 (10^{-9} relative accuracy) is not unrealistic. For the same experiments as used for the spin rate determination one finds the results in Table 6.18. Even in the cases of good geometry (the second, third and fifth experiments) the ability of polar motion estimation seems to be marbinal. This is only apparent since Table 6.24 reflects only the range of precision for the four stations individually. The differential polar motion parameters $\Delta\theta_\omega$ and $\Delta\lambda_\omega$ will be determined from several stations, consequently their precision estimates will be lower than the ones from the individual stations. From equations (6.9-1) and (6.9-2) it can be derived that

$$\Delta\theta_\omega = \left[(\Delta\psi_i)_i^2 + (\Delta\lambda_i \operatorname{cotan}\psi_i)^2\right]^{1/2} \tag{6.9-3}$$

and

$$\Delta\lambda_\omega = \lambda_i - \arctan\left(\frac{\Delta\lambda_i \operatorname{cotan}\psi_i}{\Delta\psi_i}\right) \tag{6.9-4}$$

where $i = 1, \ldots, n$.

From formulas (6.9-1) and (6.9-2) it can be seen that the contribution from the changes in longitude difference to polar motion is negligible for stations in the low latitudes: polar motion is mainly determined from latitude changes. However, in the mid-latitude or

TABLE 6.24

DIFFERENTIAL POLAR MOTION DETERMINATIONS WITH STANDARD DEVIATION FOR LATITUDE AND LONGITUDE DIFFERENCES (TIMES cotanψ) IN ARCSECONDS AND cm

σ_r = 5 cm, Δt = 60 sec.

Stations	Orbit	Time Span	σ_ψ	$\sigma_{\Delta\lambda.\mathrm{cotan}\psi}$
SAFE 4(1)	elliptic	1 day	(34 cm) 0".011 < σ_ψ < 0".027 (83 cm)	(28 cm) 0".009 < $\sigma_{\Delta\lambda.\mathrm{cotan}\psi}$ < 0".029 (90 cm)
SAFE 4(2)	"	"	(5.3) 0.0017 < < 0.0020 (6.2)	(1.0) 0".0006 < < 0.0012 (3.7)
SAFE 4	"	"	(3.7) 0.0012 < < 0.0013 (4.0)	(0.9) 0.0003 < < 0.0006 (1.9)
"	"	4-1/2 hrs.	(136) 0.044 < < 0.076 (235)	(442) 0.143 < < 0.157 (485)
"	elliptic with sec. perturb.	1 day	(4.3) 0.0014 < < 0.0017 (5.3)	(1.5) 0.0005 < < 0.0009 (2.8)
"	"	4-1/2 hrs.	(284) 0.092 < < 0.186 (575)	(1301) 0.421 < < 0.487 (1505)

higher regions the changes in longitude difference and latitude are equally important for the polar motion determination.

It may be concluded that differential polar motion determination from range measurements to LAGEOS is feasible depending again on the geometry. Not only needs the geometry of orbit and station configuration be of high quality, the relative geometry of the stations with respect to the path of the spin axis is important too. For example, θ_ω is best determined by the changes in latitude of stations in the path of the spin axis, whereas stations in a direction perpendicular to the path ($\lambda-\Delta\lambda_\omega = 90°$ or $270°$, see equation 6.9-2) contribute to the polar motion through their changes in longitude difference. Having 14 months as a main period of the Chandler wobble stations in a local region (as the experiments with the stations in the United States) will every 3-1/2 months alternate the nature of polar motion determining quantities. For consistent polar determinations world wide stations equally spaced in longitude are desirable.

6.10 The Influence of Constraints on GM (and J_2)

The seven (a, e, i, Ω, ω, E_o, n) and eight (a, e, i, Ω, ω, $\dot{\omega}$, E_o, n) parameter models introduced in Chapter 4 to represent the orbit of a satellite had the purpose to allow for greater geometric freedom in the orbit determination. In algorithms using numerical integration the equivalent models are: a, e, i, Ω, ω, E_o, GM and a, e, i, Ω, ω, E_o, GM and J_2. The advantage of the analytic seven and eight parameter models was briefly touched upon in section 6.9.1: the analytic models allow for <u>all</u> secular perturbations in Ω, ω and n and if used

over short time spans short and long periodic perturbations in the seven or eight elements are taken care of as well.

The subtle differences between the six and seven parameters will now be elaborated on (the eighth parameter J_2 was the subject already of some extensive discussion in section 6.9.1).

In principle there is hardly any difference between the six and seven orbital parameter model if "one had constrained GM to the proper value." In the first model one parameter has been simply eliminated changing the degrees of freedom by one and consequently the standard deviation of the recovered parameters (recall Tables 6.7 through 6.10), see Table 6.25.

TABLE 6.25

LONG ARC ANALYSIS (ELLIPTIC ORBIT) WITHOUT AND WITH A PROPERLY CONSTRAINED GM

Interstation distance and spin rate recovery with standard deviations in cm and "/sec. σ_r = 5 cm and Δt = 60 sec.

RANGE 4	SAFE 4, 1 day		SAFE 4, 4-1/2 hours	
	GM free	GM constrained	GM free	GM constrained
HO-QU	1.0 cm	1.0 cm	116 cm	115 cm
HO-SA	1.2	1.1	30	30
HO-UT	0.8	0.8	9	9
QU-SA	0.9	0.9	85	85
QU-UT	1.0	1.0	77	76
SA-UT	0.8	0.8	6	6
ω_e	$8 * 10^{-9}$ "/sec	$7 * 10^{-9}$ "/sec	$5118 * 10^{-9}$ "/sec	$1348 * 10^{-9}$ "/sec
$\tilde{\sigma}^2/\sigma^2$	.963	.964	1.015	1.011
Observa.	871	871	238	238
DF	852	853	219	220

In reality, of course, one does not know the right value of GM. In the following experiment it was assumed that the constrained value of GM is as far from the truth as the latest recommended value of GM [IAG, 1975] from the one but latest recommended value [IAG, 1971].

$$GM_{1971} = 398603 \qquad km^3/sec^2$$

$$GM_{1975} = 398600.5 \pm .3 \ km^3/sec^2$$

The latest value claims a precision of 1 part per million. The difference between the values is around 6 parts per million. In the past scientists have proved often to be much farther away from the truth than one might have concluded from their precision estimates: e.g., in [Deutsch, 1963] a value and a precision for J_2 was estimated to be

$$J_2 = 108219 \pm 2 * 10^{-8}$$

Compare this against the [IAG, 1975] value of

$$J_2 = 108263 \pm 1 * 10^{-8}$$

The 1963 value was different from the 1975 value by a factor of about 25 times its precision estimate. In fairness, in [O'Keefe et al., 1959, p. 248] and [Kozai, 1964] the reported values were respectively $108260 \pm 6 * 10^{-8}$ and $108264.5 \pm 0.6 * 10^{-8}$!

In Table 6.26 the same experiments are repeated but now GM is constrained to the 1975 value whereas the orbit and range were generated with the 1971 value (it does not matter whether GM_{1975} is actually better than GM_{1971}):

C-3

TABLE 6.26

LONG ARC ANALYSIS (ELLIPTIC ORBIT) WITH A WRONGLY CONSTRAINED GM[1]

Interstation Distance and Spin Rate Recovery with Standard Deviation in cm and "/sec. σ_r = 5 cm and Δt = 60 sec.

	SAFE 4, 1 day	SAFE 4, 4-1/2 hrs
HO-QU	66 cm	180 cm
HO-SA	77	47
HO-UT	57	14
QU-SA	62	133
QU-UT	69	120
SA-UT	58	9
ω_e	$483 * 10^{-9}$ "/sec	$2109 * 10^{-9}$ "/sec
$\tilde{\sigma}^2/\sigma^2$	4577	2.474
Observations	871	238
DF	853	220

[1] $GM_{\text{data generation}} = 398603\ km^3/sec^2$; $GM_{\text{recovery}} = 398600.5\ km^3/sec^2$

From this table it becomes clear that a long arc analysis of one day is geometrically conditioned enough to detect the erroneously constrained GM: the χ^2-test on $\hat{\sigma}^2/\sigma^2$ fails without looking up the statistical tables. However, a 4-1/2 hour long arc analysis barely fails the χ^2-test. In reality, a satellite geodesist might be tempted to think that he underestimated his ranging precision: a small increase from σ_r = 5 cm to 7 cm will make $\tilde{\sigma}^2/\sigma^2$ pass the χ^2 test. To illustrate the danger, the change in GM introduced a bias in the San Diego-Utah baseline of 45 cm, its standard deviation still being only 9 cm!

This experiment hopes to show two features: first of all, the importance to have a very accurate estimate of the ranging precision, secondly at a ranging precision of 5 cm a short long arc analysis is already long enough to include either GM or the mean motion n as a parameter.

In this respect the short arc mode (Table 6.27) has the advantage to be insensitive to a "wrongly applied constraint" as was done with GM.

TABLE 6.27

SHORT ARC ANALYSIS (ELLIPTIC ORBIT) WITHOUT AND WITH A WRONGLY CONSTRAINED GM

Interstation Distance Recovery with Standard Deviation in cm. σ_r = 5 cm and Δt = 60 sec.

	GM free			GM wrongly constrained		
	Pass 1	Pass 7	Pass 10	Pass 1	Pass 7	Pass 10
HO-QU	1578 cm	1111 cm	187 cm	1188 cm	1107 cm	186 cm
HO-SA	1331	204	327	1015	203	324
HO-UT	194	200	206	150	200	204
QU-SA	296	750	13	223	747	13
QU-UT	1013	565	690	796	563	691
SA-UT	59	19	429	58	19	429
$\tilde{\sigma}^2/\sigma^2$	1.116	1.042	1.033	1.110	1.036	1.036
Observa.	166	192	194	166	192	194
DF	147	173	175	148	174	176

The short arc mode is so elastic, which is not in the last place reflected by its large standard deviations (a sign of weakness), that the introduced wrong value of GM causes in pass 10 an "error" in the

baseline Quincy-San Diego of only 17 cm, whereas its standard deviation was 13 cm. In the unconstrained case the "error" was 15 cm, so an increase of only 2 cm in a baseline of 896 km because of a GM which was "in error" by 6 parts per million.

The conclusions following Table 6.23 (section 6.9.1) included one concerning the recovery of J_2: based on the highly precise recovery of the spin rate of the earth inherently J_2 must have been determined with a higher precision than currently estimated. The basis for this remark is illustrated with some examples. Because of the attention already paid to J_2 two examples concerning the recovery of GM will follow.

First, one can similarly say on behalf of GM: based on the highly precise recoverable parameters a (semi major axis) and n (mean motion) the gravitational constant GM must have been determined with a higher precision than currently estimated.

From section 5.3 Kepler's Third Law led to the following statistic for GM

$$\sigma_{GM}^2 = GM^2 \left(\frac{4\sigma_n^2}{n^2} + \frac{9\sigma_a^2}{a^2} + \frac{12\ \sigma_{an}}{an} \right)$$

Range observations from 4 stations (SAFE 4) during 1 day (6 passes) led to the following result

$$\sigma_{GM} = 0.0012\ km^3/sec^2$$

Even a 4-1/2 hour (2, or better 1-1/2, passes) long arc analysis recovers "a" GM with a high precision

$$\sigma_{GM} = 0.14 \text{ km}^3/\text{sec}^2$$

These two examples clearly show the importance of seven parameter (or including J_2, eight) orbital analyses or in general, the inclusion of parameters as GM, J_2, etc., is a necessity in orbital analyses (using numerical integration techniques) no matter how short the time span of the precise data is. One should not give too much physical significance to the value of GM determined in such a way: e.g., perturbations in the semi-major axis and mean motion would cause a rapid varying value of GM, which is of course nonsense.

A last example shows the influence of constraining GM on low inclination satellites. The "Clock Problem" (Chapter 4, section 4.2) forms an excellent example of wrongly applied constraints, and best estimable parameters. One pass of ranges was measured to a Lageos-type satellite in an elliptic equatorial orbit ($i = 0°$). Two equatorial stations with a difference in longitude of 25° measured ranges with a precision of 5 cm and at an interval of 60 sec (Table 6.28).

Despite the flexibility of the short arc it cannot absorb the "wrong" GM constraint in the spin rate recovery. Geometrically, this has a simple explanation: by constraining an "erroneous" GM the satellite is forced around its orbit with the wrong mean motion due to Kepler's Third Law. Because the orbit is equatorial and blind range measurements recover the earth's spin rate against the satellite's orbit, the only way the "wrong" mean motion can be compensated for is by the spin rate. This is the reason for the very large discrepancy in the recovery of the earth's spin rate. In general, it should be concluded that for low

TABLE 6.28

SHORT ARC ANALYSIS (ELLIPTIC EQUATORIAL ORBIT)
WITH A PROPERLY AND WRONGLY CONSTRAINED GM

σ_r = 5 cm, Δt = 60 sec.

RANGE 3 (i=0°)		GM properly constrained		GM wrongly constrained	
Parameter	Value	σ	Δ[1]	σ	Δ"
R_1	6378.140 km	232 cm	-47.0 cm	232 cm	-84.6 cm
λ_1	-12°.5	1".23	0".29	1".23	-0".22
R_2	6379.140 km	233 cm	-45.6 cm	233 cm	-73.8 cm
λ_2	12°.5	1".24	0".30	1".24	-0".21
ω_e	$.72921151467*10^{-4}$ rad/sec	$4767*10^{-9}$"/sec	$<5*10^{-13}$ rad/sec	$4765*10^{-9}$"/sec	$-144806*10^{-14}$ rad/sec
a	12267.6926 km	252 cm	-56.2 cm	252 cm	-39.7 cm
e	0.003845	$34 * 10^{-9}$	$-5.7 * 10^{-9}$	$34 * 10^{-9}$	$40.1 * 10^{-9}$
E_o	55°.20345	1".24	0".30	1".24	-2".22
R_{12}	2761.181 km	21.8 cm	-4.5 cm	24.6 cm	-4.2 cm
$\tilde{\sigma}^2/\sigma^2$		1.116		1.115	
Observa.		120		120	
DF		112		112	

[1] Δ = recovered parameter - "true" parameter.

inclination satellites the UT1 determinations are very vulnerable for constraints affecting the satellite's mean motion, argument of perigee, mean anomaly, etc.

A second feature which is only shown here but could have been added as a conclusion almost to all experiments is that despite the fact that the distance between the stations and the earth's center-of-mass cannot be determined with a high precision (Table 6.28, $\sigma_R > 2$ meters!) the distances between the stations are very well recoverable (Table 6.22, $\sigma_{R_{12}} = 22$ cm!) and therefore often referred to as "best-estimable-parameters."

6.11 Range, Range-Rate and Range-Difference Observations

With the help of a very simple geometrical example, the Clock Problem, the predictions were made that as far as estimability of parameters is concerned the three measurement systems range, range-rate and range-difference observations are equivalent. The following experiments not only verify this but also give some insight in the precision standards one has to impose on these three systems in order to arrive at similarly precise results. In section 6.2.4 the standard deviations $\sigma_r = 5$ cm, $\sigma_{\dot{r}} = 0.1$ mm/sec and $\sigma_{\Delta r} = 6$ mm were estimated to be equivalent. The first test concerned the range-rate observations (Table 6.29).

Since the standard deviations of the baselines recovered with range-rate observations are twice the standard deviations of those recovered with range observations, it is concluded that the following standard deviations are equivalent for a Lageos-type satellite (Table 6.30).

TABLE 6.29

LONG ARC ANALYSIS (CIRCULAR ORBIT, 1 DAY) WITH RANGE (σ_r = 5 cm) AND RANGE-RATE OBSERVATIONS ($\sigma_{\dot{r}}$ = 0.1 mm/sec). Δt = 60 sec.

SAFE 4	RANGE 2	RRATE 2
HO-QU	1.0 cm	2.0
HO-SA	1.1	2.3
HO-UT	0.8	1.8
QU-SA	0.9	1.8
QU-UT	1.0	2.2
SA-UT	0.8	2.0
$\tilde{\sigma}^2/\sigma^2$	.956	.965
Observa.	864	862
DF	847	845

TABLE 6.30

LONG ARC ANALYSIS (CIRCULAR ORBIT, 1 DAY) WITH RANGE, RANGE-RATE AND RANGE DIFFERENCE OBSERVATIONS Δt = 60 sec.

SAFE 4	RANGE 2 σ_r = 5 cm	RRATE 2 $\sigma_{\dot{r}}$ = 0.05 mm/sec	RDIFF 2 $\sigma_{\Delta r}$ = 3 mm
HO-QU	1.0 cm	1.0 cm	1.0
HO-SA	1.1	1.1	1.1
HO-UT	0.8	0.9	0.9
QU-SA	0.9	0.9	0.9
QU-UT	1.0	1.1	1.1
SA-UT	0.8	1.0	1.0
$\tilde{\sigma}^2/\sigma^2$	.956	.959	.941
Observa.	864	864	864
DF	847	847	847

$$\sigma_r = 5 \text{ cm}$$

$$\sigma_{\dot{r}} = 0.05 \text{ mm/sec}$$

$$\sigma_{\Delta r} = 3 \text{ mm}$$

Not only the interstation distances but all other estimable parameters (e.g., orbital parameters) were recovered with the same precision.

7. SUMMARY AND CONCLUSIONS

"Episodic determinations of UT_o and/or the variation in latitude have been obtained by VLBI, artificial satellite ranging, and LLR, ... True, there are sensitivity studies and projections for several of them, but most of these are believed at most by their authors."

[J. D. Mulholland and O. Calame, 1977]

Simple dynamical models have been analyzed from the non-Bayesian point of view (no a priori weighting of parameters, models expressed in (the maximum number of unconditional) estimable parameters only) in the cases of range (LAGEOS), range-rate and range-difference observations.

The parameters which are estimable from a dynamical analysis of laser range observations to artificial satellites are also estimable in case of range-rate or range-difference observations. The different nature of these three types of observations does not influence the estimability of any of the parameters.

The rank deficiency of the three measurement systems (range, range-rate and range-difference) in case of simple dynamical analyses of Keplerian orbits is equal to <u>two.</u> The most general set of parameters consists of twelve parameters: 6 satellite parameters a, e, i, Ω, ω, E_o (or X, Y, Z, $\dot{X}$, $\dot{Y}$, $\dot{Z}$), 3 station parameters R, ψ, λ (or x, y, z) and 3 earth parameters GM, ω_e and $GAST_o$. Of these parameters ten parameters

are estimable: a, e, i, ω, E_o, R, ψ, GM, ω_e and $(\lambda + GAST_o - \Omega)$. For (secularly) perturbed orbits due to J_2 the rank deficiency is still two. In this case the most general set of parameters consists of thirteen parameters: a, e, i, Ω, ω, E_o, R, ψ, λ, GM, J_2, ω_e and $GAST_o$. Of these parameters eleven are estimable: a, e, i, ω, E_o, R, ψ, GM, J_2, ω_e and $(\lambda + GAST_o - \Omega)$.

Since rapidly changing dynamical phenomena are to be monitored (periods as short as half a day, for example) preference was given to a more geometric approach of the dynamical analysis of satellite data. In the Keplerian model GM was replaced by the mean motion n and in the secularly perturbed case J_2 was replaced by the rate of the argument of perigee $\dot{\omega}$. It has been argued that very short analyses might yield unrealistic values for GM and J_2. However, n and $\dot{\omega}$ have been shown to be very well recoverable parameters. The additional advantage is that the now anomalistic mean motion, $\dot{\omega}$ and $\dot{\Omega}$ are capable of modelling all secular perturbations (due to J_2^2, J_3, J_4, J_2J_3, etc.). A disadvantage is the possible loss in capability to determine UT. In the secularly perturbed case it is clearly shown that because of the estimability of $(\omega_e - \dot{\Omega})$ instead of ω_e variations in UT might be hard to separate from any variations in the right ascension of the ascending node. Worse, the variations might have the same frequencies (e.g., seasonal variations in J_2 and UT).

Although in a geometric mode analysis (simultaneous range measurements) called the only estimable quantities, the baselines are still the best estimable quantities in a dynamic mode analysis. It is expected that this is also true for more complicated dynamical models

in which more perturbations (due to the earth's gravity field, atmosphere, etc.) are included.

In the dynamic mode the estimability of the various parameters is in theory independent of the length of the arcs under investigation. This results in a rank deficiency of two also for the short arc mode. Obviously, because of the deteriorating geometry the parameters in the short arc mode are determined much worse than in the long arc mode. This (relative) deterioration of the strength of the geometry in case of short arc analyses is to such an extent that its future usefulness needs to be reconsidered. In those cases whereby a baseline has a short arc overhead and parallel to itself, the relative station recovery (the length of that particular baseline) is the best. It is shown that more in accuracy is gained by analyzing satellite observations over longer time spans (e.g., a short long-arc of two passes).

With the help of some short-arc experiments it was shown that weighting of parameters (Bayesian estimation) may lead to too optimistic statistics.

Another geometric effect, the maximum zenith angle (cut off angle) plays an important role: for every 10° decrease in the maximum zenith angle (70°, 60°, 50°) the standard deviations of the recovered parameters increase by a factor of two.

The consecutiveness of passes of LAGEOS (in average one set of five consecutive passes per day for a local area) provides an excellent opportunity of relative station position to a high degree of precision. Because of the nature of the various reference systems, the instantaneous geocentric latitudes of the stations are precisely recoverable.

This makes in turn day-to-day monitoring of (differential) polar motion easily possible.

Because of the closeness in the earth-satellite relationship and the excellent capabilities of relative station positioning, the role of LAGEOS must mainly be seen as an interpolating one. A measurement system as VLBI has to provide the absolute (external) angular orientation of satellite networks because it lacks the biases which are so inherent to an earth-satellite system. However, satellite systems will provide the positioning of networks with respect to the earth's center-of-mass.

Because of the longitudinal rank deficiency satellite networks determined by laser range and/or Doppler measurements will even in the most ideal case (perfect internal and external consistency) be related by an one-parameter similarity transformation (one rotation in longitude).

Even in short time spans (two consecutive passes) GM and J_2 (or n and $\dot{\omega}$) are easily recoverable. The high precision range measurements require the inclusion of these parameters. Although erroneous constraints on GM and J_2 in longer arc analyses are easier to detect, a short arc analysis is very insensitive to these. It was shown that a bias in a baseline (1130 km) of 45 cm was statistically undetectable despite the fact that the baseline was recovered with an estimated precision of 9 cm.

Whereas the geometric mode analyses of (simultaneous) range observations requires at least four stations the minimum number of stations in dynamically analyzed range observations seems to be two.

For simulation studies it is worth to note that identical results from a variance analysis on the relative station positioning are obtained if just simple orbital models as the circular one are used, provided that: a. proper care is taken of introduced rank deficiencies ($e = 0$, ω and E_o are not separable, etc.), b. the (proposed) satellite has a near-circular orbit as not to deviate too much from the geometric structure of orbit and observations.

Recommendations for future studies may include the investigations (centered around the question of estimability) of the effects of a. an extended gravity field (coefficients higher in degree and order than J_2, b. other non-gravitational perturbations, c. correlated observations (in case of dense range observations, e.g., 10 measurements per second), d. the earth's orientation (precession, nutation) and its influence on the satellite's orbit.

APPENDIX A

DIFFERENTIAL FORMULAS IN ORBIT DETERMINATION IN THE ORBIT PLANE

A.1 Introduction

In the determination of orbits one often makes use of geocentric coordinate systems which refer to the focus of the orbit and whose orientation is referred to the line of apsides. In Chapter 4 and Appendix B repeatedly the same differential formulas are needed for the setup of observation equations necessary in the various range, range-rate and range-difference models.

The reader is also referred to references as Brouwer and Clemence [1961, Chapter IV], Escobal [1976, Chapter 3] and Dubyago [1961, Chapter 11].

A.2 Geocentric Orbital Coordinates

The coordinates x_ω, y_ω as well as the radius r_ω and their time derivatives can be deduced from Figure A.1

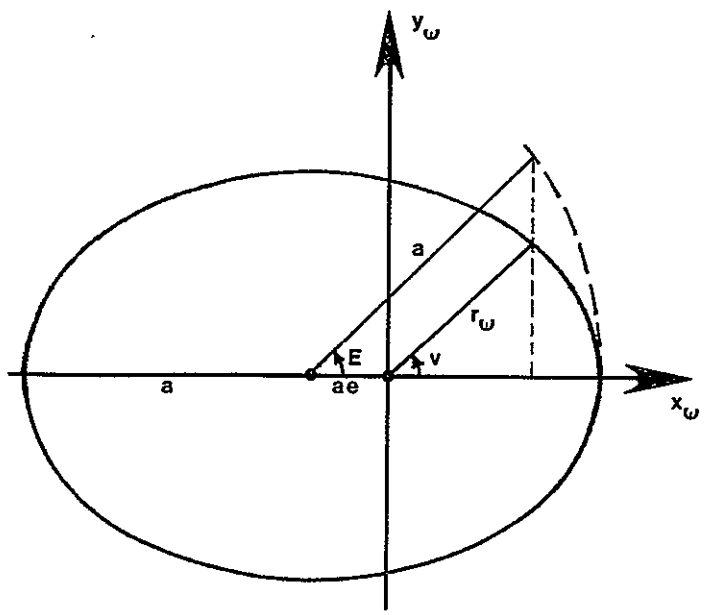

Figure A.1. Keplerian Orbital Geometry

One finds

$$\begin{bmatrix} x_\omega \\ y_\omega \\ r_\omega \end{bmatrix} = \begin{bmatrix} r_\omega \cos v \\ r_\omega \sin v \\ x_\omega^2 + y_\omega^2 \end{bmatrix} = a \begin{bmatrix} \cos E - e \\ \sqrt{1 - e^2}\, \sin E \\ 1 - e \cos E \end{bmatrix} \tag{A.2-1}$$

and

$$\begin{bmatrix} \dot{x}_\omega \\ \dot{y}_\omega \\ \dot{r}_\omega \end{bmatrix} = a\dot{E} \begin{bmatrix} -\sin E \\ \sqrt{1 - e^2}\, \cos E \\ e \sin E \end{bmatrix} \tag{A.2-2}$$

These six quantities are functions of a, e and two intermediate variables E and $\dot{E}$ which are related to time through Kepler's equation.

A.3 Kepler's Equation and the Intermediate Variables E and $\dot{E}$

The eccentric anomaly E is related to time through Kepler's equation. Three cases have to be distinguished: the free geometric

orbit where two out of the three parameters in Kepler's Third Law are independent, the semi-major axis a, the mean motion n and the gravitational constant GM, the case where GM is considered known (in Kepler's Third Law) and the case whereby the mean anomaly is secularly perturbed by the dynamical form factor of the earth J_2.

A.3.1 GM (or n) Unknown

Kepler's equation was derived in section 3.4.1. From equation (3.4-6) one had

$$(E-E_o) - e(\sin E-\sin E_o) - nt = 0 \tag{A.3-1}$$

The intermediate variable $\dot{E}$ was given by equation (3.4-8)

$$\dot{E} = \frac{n}{1 - e\cos E} = \frac{an}{r_\omega} \tag{A.3-2}$$

In evaluating the functional dependencies of E and $\dot{E}$ one has from (A.3-1) and (A.3-2)

$$E = f(e,E_o,n) \tag{A.3-3}$$

and

$$\dot{E} = g(e,E,n) = g[e,f(e,E_o,n),n] \tag{A.3-4}$$

or in differential matrix form

$$dE = \begin{bmatrix} \frac{\partial E}{\partial e} & \frac{\partial E}{\partial E_o} & \frac{\partial E}{\partial n} \end{bmatrix} \begin{bmatrix} de \\ dE_o \\ dn \end{bmatrix} \tag{A.3-4}$$

and

$$d\dot{E} = \begin{bmatrix} \frac{\partial \dot{E}}{\partial e} & \frac{\partial \dot{E}}{\partial E} & \frac{\partial \dot{E}}{\partial n} \end{bmatrix} \begin{bmatrix} de \\ dE \\ dn \end{bmatrix} \tag{A.3-5}$$

With substitution of (A.3-4) into (A.3-5) one has

$$d\dot{E} = \left[\frac{\partial \dot{E}}{\partial e} + \frac{\partial \dot{E}}{\partial E}\frac{\partial E}{\partial e} \quad \frac{\partial \dot{E}}{\partial E}\frac{\partial E}{\partial E_o} \quad \frac{\partial \dot{E}}{\partial n} + \frac{\partial \dot{E}}{\partial E}\frac{\partial E}{\partial n} \right] \begin{bmatrix} de \\ dE_o \\ dn \end{bmatrix} \tag{A.3-6}$$

<u>The Evaluation of $\frac{\partial E}{\partial e}$</u>

From equation (A.3-1) one obtains

$$e = \frac{(E-E_o) - nt}{\sin E - \sin E_o}$$

and

$$\frac{\partial e}{\partial E} = \frac{(\sin E - \sin E_o) - \cos E(E-E_o-nt)}{(\sin E - \sin E_o)^2}$$

$$= \frac{r_\omega}{a(\sin E - \sin E_o)} \tag{A.3-7}$$

Consequently, one has from (A.3-7)

$$\frac{\partial E}{\partial e} = \frac{a(\sin E - \sin E_o)}{r_\omega} \tag{A.3-8}$$

<u>The Evaluation of $\frac{\partial E}{\partial E_o}$</u>

From equation (A.3-1) one obtains

$$nt = (E-E_o) - e(\sin E - \sin E_o)$$

and

$$\frac{\partial nt}{\partial E} = 1 - e\cos E = \frac{r_\omega}{a} \tag{A.3-9}$$

and

$$\frac{\partial nt}{\partial E_o} = -1 + e\cos E_o = -\frac{r_o}{a} \tag{A.3-10}$$

whereby

$$r_o = a(1-e\cos E_o) \tag{A.3-11}$$

Consequently, one has from (A.3-9) and (A.3-10)

$$\frac{\partial E}{\partial E_o} = -\frac{\partial(nt)}{\partial E_o} \Big/ \frac{\partial(nt)}{\partial E} = \frac{r_o}{r_\omega} \tag{A.3-12}$$

<u>The Evaluation of $\frac{\partial E}{\partial n}$</u>

From equation (A.3-1) one obtains

$$n = \frac{(E-E_o) - e(\sin E - \sin E_o)}{t}$$

and

$$\frac{\partial n}{\partial E} = \frac{1 - e\cos E}{t} = \frac{r_\omega}{at} \tag{A.3-13}$$

Consequently, one has from (A.3-13)

$$\frac{\partial E}{\partial n} = \frac{at}{r_\omega} \tag{A.3-14}$$

Combining the results of (A.3-8), (A.3-12) and (A.3-14) in the differential equation (A.3-4) one has

$$dE = \frac{a}{r_\omega}\,[\sin E - \sin E_o;\ 1 - e\cos E_o;\ t]\begin{bmatrix} de \\ dE_o \\ dn \end{bmatrix} \tag{A.3-15}$$

The above derived expressions are needed for the observation equations in the case of range and range-difference observations. Range-rate observations require the partial derivatives of $\dot{E}$ in addition.

The expressions for these partial derivatives require the additional partial derivative $\frac{\partial \dot{E}}{\partial E}$. From equations (A.3-2), (A.2-1) and (A.2-2) one finds

$$\frac{\partial \dot{E}}{\partial E} = -\frac{en \sin E}{(1 - e \cos E)^2} = -\frac{\dot{r}_\omega}{r_\omega} \tag{A.3-16}$$

<u>The Evaluation of $\frac{\partial \dot{E}}{\partial e}$</u>

From equation (A.3-6) one obtains

$$\frac{\partial \dot{E}}{\partial e} = \frac{\partial \dot{E}}{\partial e} + \frac{\partial \dot{E}}{\partial E}\frac{\partial E}{\partial e} \tag{A.3-17}$$

Substituting (A.3-16) and (A.3-8) into (A.3-17) and from (A.3-2) one has

$$\frac{\partial \dot{E}}{\partial e} = \frac{a^2 n \cos E}{r_\omega^2} - \frac{a\dot{r}_\omega(\sin E - \sin E_o)}{r_\omega^2}$$

$$= \frac{a}{r_\omega^2}[an \cos E - \dot{r}_\omega(\sin E - \sin E_o)] \tag{A.3-18}$$

<u>The Evaluation of $\frac{\partial \dot{E}}{\partial E_o}$</u>

From equation (A.3-6) one obtains

$$\frac{\partial \dot{E}}{\partial E_o} = \frac{\partial \dot{E}}{\partial E}\frac{\partial E}{\partial E_o} \tag{A.3-19}$$

Substituting (A.3-16) and (A.3-12) into (A.3-19) one has

$$\frac{\partial \dot{E}}{\partial E_o} = -\frac{\dot{r}_\omega}{r_\omega} \cdot \frac{r_o}{r_\omega} = -\frac{r_o \dot{r}_\omega}{r_\omega^2} \tag{A.3-20}$$

<u>The Evaluation of $\frac{\partial \dot{E}}{\partial n}$</u>

From equation (A.3-6) one obtains

$$\frac{\partial \dot{E}}{\partial n} = \frac{\partial \dot{E}}{\partial n} + \frac{\partial \dot{E}}{\partial E}\frac{\partial E}{\partial n} \tag{A.3-21}$$

Substituting (A.3-16) and (A.3-14) into (A.3-21) and from (A.3-2) one has

$$\frac{\partial \dot{E}}{\partial n} = \frac{a}{r_\omega} - \frac{\dot{r}_\omega}{r_\omega} \cdot \frac{at}{r_\omega}$$

$$= \frac{a}{r_\omega^2} (r_\omega - \dot{r}_\omega t) \qquad \text{(A.3-22)}$$

Combining the results of (A.3-18), (A.3-20) and (A.3-22) in the differential equation (A.3-6) one has

$$d\dot{E} = \frac{a}{r_\omega^2} [an \cos E - \dot{r}_\omega(\sin E - \sin E_o); -\dot{r}_\omega(1 - e \cos E_o); r_\omega - \dot{r}_\omega t] \begin{bmatrix} de \\ dE_o \\ dn \end{bmatrix} \qquad \text{(A.3-23)}$$

A.3.2 GM (or n) Known

Kepler's equation was derived in section 3.4.2. From equation (3.4-15) one had

$$(E - E_o) - e(\sin E - \sin E_o) - nt = 0 \qquad \text{(A.3-24)}$$

The intermediate variable $\dot{E}$ was given by

$$\dot{E} = \frac{n}{1 - e \cos E} = \frac{an}{r_\omega} \qquad \text{(A.3-25)}$$

But the variable n in equations (A.3-24) and (A.3-25) has become an intermediate variable as well and is given by (Kepler's Third Law)

$$n = \sqrt{GM/a^3} \qquad \text{(A.3-26)}$$

In evaluating the functional dependencies of n, E and $\dot{E}$ one has from (A.3-24), (A.3-25) and (A.3-26)

$$n = f(a) \tag{A.3-27}$$

$$E = g(n,e,E_o) = g[f(a),e,E_o] \tag{A.3-28}$$

$$\dot{E} = h(n,e,E) = h\{f(a),e,g[f(a),e,E_o]\} \tag{A.3-29}$$

or in differential matrix form

$$dn = \frac{\partial n}{\partial a}\, da \tag{A.3-30}$$

$$dE = \begin{bmatrix} \frac{\partial E}{\partial n} & \frac{\partial E}{\partial e} & \frac{\partial E}{\partial E_o} \end{bmatrix} \begin{bmatrix} dn \\ de \\ dE_o \end{bmatrix} \tag{A.3-31}$$

$$d\dot{E} = \begin{bmatrix} \frac{\partial \dot{E}}{\partial n} & \frac{\partial \dot{E}}{\partial e} & \frac{\partial \dot{E}}{\partial E} \end{bmatrix} \begin{bmatrix} dn \\ de \\ dE \end{bmatrix} \tag{A.3-32}$$

With substitution of (A.3-30) into (A.3-31) one has

$$dE = \begin{bmatrix} \frac{\partial E}{\partial n}\frac{\partial n}{\partial a} & \frac{\partial E}{\partial e} & \frac{\partial E}{\partial E_o} \end{bmatrix} \begin{bmatrix} da \\ de \\ dE_o \end{bmatrix} \tag{A.3-33}$$

With substitution of (A.3-30) and (A.3-33) into (A.3-32) one has

$$d\dot{E} = \left[\left(\frac{\partial \dot{E}}{\partial n} + \frac{\partial \dot{E}}{\partial E}\frac{\partial E}{\partial n}\right)\frac{\partial n}{\partial a};\ \frac{\partial \dot{E}}{\partial e} + \frac{\partial \dot{E}}{\partial E}\frac{\partial E}{\partial e};\ \frac{\partial \dot{E}}{\partial E}\frac{\partial E}{\partial E_o}\right] \begin{bmatrix} da \\ de \\ dE_o \end{bmatrix} \tag{A.3-34}$$

<u>The Evaluation of $\frac{\partial n}{\partial a}$</u>

Differentiating (A.3-26) with regard to a, one has

$$\frac{\partial n}{\partial a} = -\frac{3}{2}\frac{n}{a} \tag{A.3-35}$$

The Evaluation of $\frac{\partial E}{\partial a}$

From Equation (A.3-33) one obtains

$$\frac{\partial E}{\partial a} = \frac{\partial E}{\partial n}\frac{\partial n}{\partial a} \tag{A.3-36}$$

Substituting (A.3-14) and (A.3-35) into (A.3-36) one has

$$\frac{\partial E}{\partial a} = -\frac{3}{2}\frac{nt}{r_\omega} \tag{A.3-37}$$

with $$n = \sqrt{GM/a^3}$$

The Evaluation of $\frac{\partial E}{\partial e}$ and $\frac{\partial E}{\partial E_o}$

The partial derivatives of E with regard to e and E_o yield the same results as the case whereby Kepler's Third Law is not constrained (see section A.3.1). Consequently, one has directly from (A.3-8) and (A.3-12)

$$\frac{\partial E}{\partial e} = \frac{a(\sin E - \sin E_o)}{r_\omega} \tag{A.3-38}$$

and $$\frac{\partial E}{\partial E_o} = \frac{r_o}{r_\omega} \tag{A.3-39}$$

Combining results of (A.3-37), (A.3-38) and (A.3-39) in the differential equation (A.3-33) one has

$$dE = \frac{1}{r_\omega}\begin{bmatrix} -\frac{3}{2}nt & a(\sin E - \sin E_o) & r_o \end{bmatrix}\begin{bmatrix} da \\ de \\ dE_o \end{bmatrix} \tag{A.3-40}$$

with $$n = \sqrt{GM/a^3}$$

The above derived expressions are needed for the observation equations in the case of range and range-difference observations. Range-rate observations require the partial derivatives of $\dot{E}$ in addition.

<u>The Evaluation of $\frac{\partial \dot{E}}{\partial a}$</u>

From equation (A.3-34) one obtains

$$\frac{\partial \dot{E}}{\partial a} = \left(\frac{\partial \dot{E}}{\partial a} + \frac{\partial \dot{E}}{\partial E}\frac{\partial E}{\partial n}\right)\frac{\partial n}{\partial a} \tag{A.3-41}$$

Substituting (A.3-21) (from equation (A.3-21) and (A.3-35) into (A.3-41) one has

$$\frac{\partial \dot{E}}{\partial a} = -\frac{3}{2}\frac{n}{r_\omega^2}(r_\omega - \dot{r}_\omega t) \tag{A.3-42}$$

with $$n = \sqrt{GM/a^3}$$

<u>The Evaluation of $\frac{\partial \dot{E}}{\partial e}$ and $\frac{\partial \dot{E}}{\partial E_o}$</u>

The partial derivatives of $\dot{E}$ with regard to e and E_o yield the same results as the case where GM is unknown (see section A.3.1). Consequently, one has directly from (A.3-18) and (A.3-20)

$$\frac{\partial \dot{E}}{\partial e} = \frac{a}{r_\omega^2}\left[an \cos E - \dot{r}_\omega(\sin E - \sin E_o)\right] \tag{A.3-43}$$

and $$\frac{\partial \dot{E}}{\partial E_o} = -\frac{r_o \dot{r}_\omega}{r_\omega^2} \tag{A.3-44}$$

with $$n = \sqrt{GM/a^3}$$

Combining the results of (A.3-42), (A.3-43) and (A.3-44) in the differential equation (A.3-34) one has

$$d\dot{E} = \frac{1}{r_\omega^2}\left[-\frac{3}{2}n\,(r_\omega - \dot{r}_\omega t);\ a^2 n\,\cos E - a\dot{r}_\omega(\sin E - \sin E_o);\ -r_o\dot{r}_\omega\right]\begin{bmatrix} da \\ de \\ dE_o \end{bmatrix} \qquad \text{(A.3-45)}$$

A.3.3 Secular Perturbations due to J_2 (GM and J_2 Known)

Kepler's equation was derived in section 3.6.2. From equation (3.4-6) one had

$$(E - E_o) - e(\sin E - \sin E_o) - nt = 0 \qquad \text{(A.3-46)}$$

The intermediate variable $\dot{E}$ was given by

$$\dot{E} = \frac{n}{1 - e\cos E} = \frac{an}{r_\omega} \qquad \text{(A.3-47)}$$

But the variable n in equations (A.3-46) and (A.3-47) has become an intermediate variable and is given by the modified Kepler's Third Law

$$n = \sqrt{GM/a^3}\left[1 + \frac{3}{2}\,\frac{J_2 a_e^2\sqrt{1 - e^2}}{a^2(1-e^2)^2}\,(1 - \frac{3}{2}\sin^2 i)\right] \qquad \text{(A.3-48)}$$

$$= n_o(1 + \Delta_n) = n_o\left[1 + \Delta_i(1 - \frac{3}{2}\sin^2 i)\right] \qquad \text{(A.3-49)}$$

with

$$n_o = \sqrt{GM/a^3} \qquad \text{(A.3-50)}$$

$$\Delta_n = \frac{3}{2}\,\frac{J_2 a_e^2\sqrt{1 - e^2}}{a^2(1-e^2)^2}\,(1 - \frac{3}{2}\sin^2 i) \qquad \text{(A.3-51)}$$

and

$$\Delta_i = \frac{3}{2}\,\frac{J_2 a_e^2\sqrt{1 - e^2}}{a^2(1-e^2)^2} \qquad \text{(A.3-52)}$$

In evaluating the functional dependencies of n, E and $\dot{E}$ one has from (A.3-46), (A.3-47) and (A.3-48)

$$n = f(a,e,i) \tag{A.3-53}$$

$$E = g(n,e,E_o) = g[f(a,e,i),e,E_o] \tag{A.3-54}$$

$$\begin{aligned}\dot{E} &= h(n,e,E) = h[f(a,e,i),e,g(n,e,E_o)] \\ &= h\{f(a,e,i),e,g[f(a,e,i),e,E_o]\}\end{aligned} \tag{A.3-55}$$

or in differential matrix form

$$dn = \begin{bmatrix} \frac{\partial n}{\partial a} & \frac{\partial n}{\partial e} & \frac{\partial n}{\partial i} \end{bmatrix} \begin{bmatrix} da \\ de \\ di \end{bmatrix} \tag{A.3-56}$$

$$dE = \begin{bmatrix} \frac{\partial E}{\partial n} & \frac{\partial E}{\partial e} & \frac{\partial E}{\partial E_o} \end{bmatrix} \begin{bmatrix} dn \\ de \\ dE_o \end{bmatrix} \tag{A.3-57}$$

$$d\dot{E} = \begin{bmatrix} \frac{\partial \dot{E}}{\partial n} & \frac{\partial \dot{E}}{\partial e} & \frac{\partial \dot{E}}{\partial E} \end{bmatrix} \begin{bmatrix} \partial n \\ \partial e \\ \partial E \end{bmatrix} \tag{A.3-58}$$

With substitution of (A.3-56) into (A.3-57) one has

$$dE = \begin{bmatrix} \frac{\partial E}{\partial n}\frac{\partial n}{\partial a}; & \frac{\partial E}{\partial e} + \frac{\partial E}{\partial n}\frac{\partial n}{\partial e}; & \frac{\partial E}{\partial n}\frac{\partial n}{\partial i}; & \frac{\partial E}{\partial E_o} \end{bmatrix} \begin{bmatrix} da \\ de \\ di \\ dE_o \end{bmatrix} \tag{A.3-59}$$

With substitution of (A.3-56) and (A.3-59) into (A.3-58) one has

$$d\dot{E} = \begin{bmatrix} \partial_1 & \partial_2 & \partial_3 & \partial_4 \end{bmatrix} \begin{bmatrix} da \\ de \\ di \\ dE_o \end{bmatrix} \tag{A.3-60}$$

with

$$\partial_1 = \left(\frac{\partial \dot{E}}{\partial n} + \frac{\partial \dot{E}}{\partial E}\frac{\partial E}{\partial n}\right)\frac{\partial n}{\partial a} \tag{A.3-61}$$

$$\partial_2 = \frac{\partial \dot{E}}{\partial e} + \frac{\partial \dot{E}}{\partial E}\frac{\partial E}{\partial e} + \left(\frac{\partial \dot{E}}{\partial n} + \frac{\partial \dot{E}}{\partial E}\frac{\partial E}{\partial n}\right)\frac{\partial n}{\partial e} \tag{A.3-62}$$

$$\partial_3 = \left(\frac{\partial \dot{E}}{\partial n} + \frac{\partial \dot{E}}{\partial E}\frac{\partial E}{\partial n}\right)\frac{\partial n}{\partial i} \tag{A.3-63}$$

$$\partial_4 = \frac{\partial \dot{E}}{\partial E}\frac{\partial E}{\partial E_o} \tag{A.3-64}$$

In the evaluations of (A.3-59) and (A.3-60) one needs the partial derivatives of n with regard to a, e and i respectively.

<u>The Evaluation of $\frac{\partial n}{\partial a}$</u>

Differentiating (A.3-48) with regard to a, one has

$$\begin{aligned}\frac{\partial n}{\partial a} &= \frac{\partial n_o}{\partial a}(1+\Delta_n) + n_o\frac{\partial \Delta_n}{\partial a} \\ &= -\frac{3}{2}\frac{n_o(1+\Delta_n)}{a} + n_o\Delta_n \cdot \frac{-2}{a} \\ &= \frac{1}{a}\left(2n_o - 3\tfrac{1}{2}n\right)\end{aligned} \tag{A.3-65}$$

<u>The Evaluation of $\frac{\partial n}{\partial e}$</u>

$$\begin{aligned}\frac{\partial n}{\partial e} &= n_o\frac{\partial \Delta_n}{\partial e} \\ &= n_o \cdot -\frac{3}{2} \cdot \frac{\Delta_n}{(1-e^2)} \cdot -2e \\ &= \frac{3e}{1-e^2}(n-n_o)\end{aligned} \tag{A.3-66}$$

<u>The Evaluation of $\frac{\partial n}{\partial i}$</u>

$$\begin{aligned}\frac{\partial n}{\partial i} &= n_o\Delta_i \cdot -3\sin i\cos i \\ &= -3n_o\Delta_i\sin i\cos i\end{aligned} \tag{A.3-67}$$

The Evaluation of $\frac{\partial E}{\partial a}$

From equation (A.3-59) one obtains

$$\frac{\partial E}{\partial a} = \frac{\partial E}{\partial n}\frac{\partial n}{\partial a} \tag{A.3-68}$$

Substituting (A.3-14) and (A.3-65) into (A.3-68) one has

$$\frac{\partial E}{\partial a} = \frac{t}{r_\omega}\left(2n_o - 3\tfrac{1}{2}n\right) \tag{A.3-69}$$

The Evaluation of $\frac{\partial E}{\partial e}$

From equation (A.3-59) one obtains

$$\frac{\partial E}{\partial e} = \frac{\partial E}{\partial e} + \frac{\partial E}{\partial n}\frac{\partial n}{\partial e} \tag{A.3-70}$$

Substituting (A.3-8), (A.3-14) and (A.3-66) into (A.3-70) one has

$$\frac{\partial E}{\partial e} = \frac{a(\sin E - \sin E_o)}{r_\omega} + \frac{at}{r_\omega}\cdot\frac{3e}{1-e^2}(n-n_o)$$

$$= \frac{a(1-e^2)(\sin E - \sin E_o) + 3aet(n-n_o)}{r_\omega(1-e^2)} \tag{A.3-71}$$

The Evaluation of $\frac{\partial E}{\partial i}$

From equation (A.3-59) one obtains

$$\frac{\partial E}{\partial i} = \frac{\partial E}{\partial n}\frac{\partial n}{\partial i} \tag{A.3-72}$$

Substituting (A.3-14) and (A.3-67) into (A.3-73) one has

$$\frac{\partial E}{\partial i} = \frac{-3atn_o\Delta_I \sin i \cos i}{r_\omega} \tag{A.3-73}$$

The Evaluation of $\frac{\partial E}{\partial E_o}$

The partial derivative of E with regard to E_o yields the same result as section A.3.1 or A.3.2. Consequently, one has directly from (A.3-12) or (A.3-39)

$$\frac{\partial E}{\partial E_o} = \frac{r_o}{r_\omega} \tag{A.3-74}$$

Combining the results of (A.3-69), (A.3-71), (A.3-73) and (A.3-74) in the differential equation (A.3-59) one has

$$dE = \frac{1}{r_\omega}\left[(2n_o - 3\tfrac{1}{2}n)t;\ \frac{a(1-e^2)(\sin E-\sin E_o) + 3aet(n-n_o)}{r_\omega(1-e^2)};\right.$$
$$\left. - 3atn_o\Delta_i \sin i \cos i;\ r_o\right]\begin{bmatrix} da \\ de \\ di \\ dE_o \end{bmatrix} \tag{A.3-75}$$

with n, n_o and Δ_i given by (A.3-48), (A.3-50) and (A.3-52) respectively.

The above derived expressions are needed for the observation equations in the case of range and range-difference observations. Range-rate observations require the partial derivatives of $\dot{E}$ in addition.

The Evaluation of $\frac{\partial \dot{E}}{\partial a}$

From equation (A.3-60) and (A.3-61) one obtains

$$\frac{\partial \dot{E}}{\partial a} = \left(\frac{\partial \dot{E}}{\partial n} + \frac{\partial \dot{E}}{\partial E}\frac{\partial E}{\partial n}\right)\frac{\partial n}{\partial a} \tag{A.3-76}$$

Substituting (A.3-22) (from equation A.3-21) and (A.3-65) into (A.3-76) one has

$$\frac{\partial \dot{E}}{\partial a} = \frac{1}{r_\omega^2}(r_\omega - \dot{r}_\omega t)(2n_o - 3\tfrac{1}{2}n) \tag{A.3-77}$$

<u>The Evaluation of $\frac{\partial \dot{E}}{\partial e}$</u>

From equation (A.3-60) and (A.3-62) one obtains

$$\frac{\partial \dot{E}}{\partial e} = \frac{\partial \dot{E}}{\partial e} + \frac{\partial \dot{E}}{\partial E}\frac{\partial E}{\partial e} + \left(\frac{\partial \dot{E}}{\partial n} + \frac{\partial \dot{E}}{\partial E}\frac{\partial E}{\partial n}\right)\frac{\partial n}{\partial e} \tag{A.3-78}$$

Substituting (A.3-18) from equation (A.3-17), (A.3-22) and (A.3-66) into (A.3-78) one has

$$\frac{\partial \dot{E}}{\partial e} = \frac{a}{r_\omega^2}\left[an\ \cos E - \dot{r}_\omega(\sin E - \sin E_o)\right] + \frac{a}{r_\omega^2}(r_\omega - \dot{r}_\omega t)\frac{3e}{1 - e^2}(n - n_o)$$

$$= \frac{a}{r_\omega^2}\left[an\ \cos E - \dot{r}_\omega(\sin E - \sin E_o) + \frac{3e}{1 - e^2}(r_\omega - \dot{r}_\omega t)(n - n_o)\right] \tag{A.3-79}$$

<u>The Evaluation of $\frac{\partial \dot{E}}{\partial i}$</u>

From equation (A.3-60) and (A.3-63) one obtains

$$\frac{\partial \dot{E}}{\partial i} = \left(\frac{\partial \dot{E}}{\partial n} + \frac{\partial \dot{E}}{\partial E}\frac{\partial E}{\partial n}\right)\frac{\partial n}{\partial i} \tag{A.3-80}$$

Substituting (A.3-22) and (A.3-67) into (A.3-80) one has

$$\frac{\partial \dot{E}}{\partial i} = \frac{-3an_o\Delta_i \sin i \cos i\ (r_\omega - \dot{r}_\omega t)}{r_\omega^2} \tag{A.3-81}$$

<u>The Evaluation of $\frac{\partial \dot{E}}{\partial E_o}$</u>

The partial derivative of $\dot{E}$ with regard to E_o yields the same result as section A.3.1 or A.3.2. Consequently, one has directly from (A.3-19) or (A.3-44)

$$\frac{\partial \dot{E}}{\partial E_o} = -\frac{r_o \dot{r}_\omega}{r_\omega^2} \tag{A.3-82}$$

Combining the results of (A.3-77), (A.3-79), (A.3-81) and (A.3-82) in the differential equation (A.3-60) one has

$$d\dot{E} = \frac{1}{r_\omega^2}\Big[(2n_o - 3\tfrac{1}{2}n)(r_\omega - \dot{r}_\omega t); a^2 n \cos E - a\dot{r}_\omega(\sin E - \sin E_o) + \frac{3ae}{1-e^2}(n-n_o)(r_\omega - \dot{r}_\omega t);$$

$$-3an_o\Delta_i \sin i \cos i\,(r_\omega - \dot{r}_\omega t); -r_o\dot{r}_\omega\Big]\begin{bmatrix} da \\ de \\ di \\ dE_o \end{bmatrix} \tag{A.3-82}$$

A.4 Cartesian Orbital Elements and the Intermediate Variables E and $\dot{E}$

A.4.1 Range and Range-Difference Observations

In case of range and range-difference observations the partial derivatives of x_ω, y_ω and r_ω are needed with regard to E.

$$\frac{\partial}{\partial E}\begin{bmatrix} x_\omega \\ y_\omega \\ r_\omega \end{bmatrix} = a\begin{bmatrix} -\sin E \\ \sqrt{1-e^2}\cos E \\ e\sin E \end{bmatrix} \tag{A.4-1}$$

Back substituting (A.2-2) into (A.4-1) one has

$$\frac{\partial}{\partial E}\begin{bmatrix} x_\omega \\ y_\omega \\ r_\omega \end{bmatrix} = \dot{E}^{-1}\begin{bmatrix} \dot{x}_\omega \\ \dot{y}_\omega \\ \dot{r}_\omega \end{bmatrix} = \frac{r_\omega}{an}\begin{bmatrix} \dot{x}_\omega \\ \dot{y}_\omega \\ \dot{r}_\omega \end{bmatrix} \tag{A.4-2}$$

A.4.2 Range-Rate Observations

In case of range-rate observations the partial derivatives of $\dot{x}_\omega$, $\dot{y}_\omega$ and $\dot{r}_\omega$ are needed with regard to E and $\dot{E}$. In addition the partial derivatives of section A.4.1 are needed

$$\frac{\partial}{\partial E}\begin{bmatrix}\dot{x}_\omega\\ \dot{y}_\omega\\ \dot{r}_\omega\end{bmatrix} = -a\dot{E}\begin{bmatrix}\cos E\\ \sqrt{1-e^2}\,\sin E\\ -e\cos E\end{bmatrix} \tag{A.4-3}$$

Back su stituting (A.2-1) into (A.4-3) one has

$$\frac{\partial}{\partial E}\begin{bmatrix}\dot{x}_\omega\\ \dot{y}_\omega\\ \dot{r}_\omega\end{bmatrix} = -\frac{an}{r_\omega}\begin{bmatrix}x_\omega + ae\\ y_\omega\\ r_\omega - a\end{bmatrix} \tag{A.4-4}$$

$$\frac{\partial}{\partial \dot{E}}\begin{bmatrix}\dot{x}_\omega\\ \dot{y}_\omega\\ \dot{r}_\omega\end{bmatrix} = a\begin{bmatrix}-\sin E\\ \sqrt{1-e^2}\,\cos E\\ e\sin E\end{bmatrix} \tag{A.4-5}$$

Backsubstituting (A.2-2) into (A.4-5) one has

$$\frac{\partial}{\partial \dot{E}}\begin{bmatrix}\dot{x}_\omega\\ \dot{y}_\omega\\ \dot{r}_\omega\end{bmatrix} = \dot{E}^{-1}\begin{bmatrix}\dot{x}_\omega\\ \dot{y}_\omega\\ \dot{r}_\omega\end{bmatrix} = \frac{r_\omega}{an}\begin{bmatrix}\dot{x}_\omega\\ \dot{y}_\omega\\ \dot{r}_\omega\end{bmatrix} \tag{A.4-6}$$

Note that

$$\frac{\partial}{\partial E}\begin{bmatrix}x_\omega\\ y_\omega\\ r_\omega\end{bmatrix} = \frac{\partial}{\partial \dot{E}}\begin{bmatrix}\dot{x}_\omega\\ \dot{y}_\omega\\ \dot{r}_\omega\end{bmatrix} \tag{A.4-7}$$

A.5 Cartesian Orbital Elements

With the development of the partial derivatives E and $\dot{E}$ with respect to the various parameters the differential equations for the Cartesian orbital elements (A.2-1) and (A.2-2) can be derived.

A.5.1 GM (or n) Unknown (Parameters a, e, E_o, n)

From (A.2-1) and (A.3-4) the functional relationships for range and range-difference observations can be set up

$$(x_\omega, y_\omega, r_\omega) = f_i(a,e,E) = f_i[a,e,g(e,E_o,n)] \tag{A.5-1}$$

with $\qquad i = 1,2,3$

or in differential matrix form

$$d\begin{bmatrix} x_\omega \\ y_\omega \\ r_\omega \end{bmatrix} = \frac{\partial}{\partial a}\begin{bmatrix} x_\omega \\ y_\omega \\ r_\omega \end{bmatrix} da + \frac{\partial}{\partial e}\begin{bmatrix} x_\omega \\ y_\omega \\ r_\omega \end{bmatrix} de + \frac{\partial}{\partial E}\begin{bmatrix} x_\omega \\ y_\omega \\ r_\omega \end{bmatrix}\left(\frac{\partial E}{\partial e} de + \frac{\partial E}{\partial E_o} dE_o + \frac{\partial E}{\partial n} dn\right) \tag{A.5-2}$$

<u>The Evaluation of the p.d.'s with Regard to a</u>

From equations (A.5-2) and (A.2-1) one has

$$\frac{\partial}{\partial a}\begin{bmatrix} x_\omega \\ y_\omega \\ r_\omega \end{bmatrix} = \begin{bmatrix} \cos E - e \\ \sqrt{1 - e^2}\ \sin E \\ 1 - e \cos E \end{bmatrix} = \frac{1}{a}\begin{bmatrix} x_\omega \\ y_\omega \\ r_\omega \end{bmatrix} \tag{A.5-3}$$

<u>The Evaluation of the p.d.'s with Regard to e</u>

From equation (A.5-2) one obtains

$$\frac{\partial}{\partial e}\begin{bmatrix} x_\omega \\ y_\omega \\ r_\omega \end{bmatrix} = \frac{\partial}{\partial e}\begin{bmatrix} x_\omega \\ y_\omega \\ r_\omega \end{bmatrix} + \frac{\partial}{\partial E}\begin{bmatrix} x_\omega \\ y_\omega \\ r_\omega \end{bmatrix}\frac{\partial E}{\partial e} \tag{A.5-4}$$

Substituting (A.4-2) and (A.3-8) into (A.5-4) and developing the derivative of (A.2-1) with regard to e one has

$$\frac{\partial}{\partial e}\begin{bmatrix} x_\omega \\ y_\omega \\ r_\omega \end{bmatrix} = -a\begin{bmatrix} \dfrac{e}{\sqrt{1-e^2}} \\ \sin E \\ \cos E \end{bmatrix} + \frac{r_\omega}{an}\begin{bmatrix} x_\omega \\ y_\omega \\ r_\omega \end{bmatrix}\frac{a(\sin E - \sin E_o)}{r_\omega}$$

$$= -a\begin{bmatrix} \dfrac{e}{\sqrt{1-e^2}} \\ \sin E \\ \cos E \end{bmatrix} + \frac{\sin E - \sin E_o}{n}\begin{bmatrix} x_\omega \\ y_\omega \\ r_\omega \end{bmatrix} \tag{A.5-5}$$

This expression (A.5-5) can also be written as

$$\frac{\partial}{\partial E}\begin{bmatrix} x_\omega \\ y_\omega \\ r_\omega \end{bmatrix} = A\begin{bmatrix} x_\omega \\ y_\omega \\ r_\omega \end{bmatrix} + B\begin{bmatrix} \dot{x}_\omega \\ \dot{y}_\omega \\ \dot{r}_\omega \end{bmatrix} \tag{A.5-6}$$

with

$$A = -\frac{\cos E + e}{1 - e^2} \tag{A.5-7}$$

$$B = \frac{(E-E_o)-(M-M_o)}{en} + \frac{\sin E}{\dot{E}(1-e^2)} \tag{A.5-8}$$

and $\dot{E}$ given by equation (A.3-2).

The reader is referred for similar expressions to Brouwer and Clemence [1961, Chapter IX].

<u>The Evaluation of the p.d.'s with Regard to E_o</u>

From equation (A.5-2) one obtains

$$\frac{\partial}{\partial E_o}\begin{bmatrix} x_\omega \\ y_\omega \\ r_\omega \end{bmatrix} + \frac{\partial}{\partial E}\begin{bmatrix} x_\omega \\ y_\omega \\ r_\omega \end{bmatrix}\frac{\partial E}{\partial E_o} \tag{A.5-9}$$

Substituting (A.4-2) and (A.3-12) into (A.5-9) one has

$$\frac{\partial}{\partial E_o}\begin{bmatrix} x_\omega \\ y_\omega \\ r_\omega \end{bmatrix} = \frac{r_o}{an}\begin{bmatrix} \dot{x}_\omega \\ \dot{y}_\omega \\ \dot{r}_\omega \end{bmatrix} \tag{A.5-10}$$

<u>The Evaluation of the p.d.'s with Regard to n</u>

From equation (A.5-2) one obtains

$$\frac{\partial}{\partial n}\begin{bmatrix} x_\omega \\ y_\omega \\ r_\omega \end{bmatrix} = \frac{\partial}{\partial E}\begin{bmatrix} x_\omega \\ y_\omega \\ r_\omega \end{bmatrix}\frac{\partial E}{\partial n} \tag{A.5-11}$$

Substituting (A.4-2) and (A.3-14) into (A.5-11) one has

$$\frac{\partial}{\partial n}\begin{bmatrix} x_\omega \\ y_\omega \\ r_\omega \end{bmatrix} = \frac{t}{n}\begin{bmatrix} \dot{x}_\omega \\ \dot{y}_\omega \\ \dot{r}_\omega \end{bmatrix} \tag{A.5-12}$$

Note that from (A.5-10) and (A.5-12) the following relationship holds

$$\frac{\partial}{\partial n}\begin{bmatrix} x_\omega \\ y_\omega \\ r_\omega \end{bmatrix} = \frac{at}{r_o}\frac{\partial}{\partial E_o}\begin{bmatrix} x_\omega \\ y_\omega \\ r_\omega \end{bmatrix} \tag{A.5-13}$$

From (A.2-2) and (A.3-6) the functional relationships for range-rate observations can be set up

$$\begin{aligned}(\dot{x}_\omega,\dot{y}_\omega,\dot{r}_\omega) &= f_i(a,e,E,\dot{E}) = f_i[a,e,g_1(e,E_o,n),g_2(e,E,n)] = \\ &= f_i\{a,e,g_1(e,E_o,n),g_2[e,h(e,E_o,n),n]\}\end{aligned} \tag{A.5-14}$$

with $\qquad i = 1,2,3$

or in differential matrix form

$$\begin{aligned} d\begin{bmatrix} \dot{x}_\omega \\ \dot{y}_\omega \\ \dot{r}_\omega \end{bmatrix} &= \frac{\partial}{\partial a}\begin{bmatrix} \dot{x}_\omega \\ \dot{y}_\omega \\ \dot{r}_\omega \end{bmatrix} da + \frac{\partial}{\partial e}\begin{bmatrix} \dot{x}_\omega \\ \dot{y}_\omega \\ \dot{r}_\omega \end{bmatrix} + \\ &\frac{\partial}{\partial E}\begin{bmatrix} \dot{x}_\omega \\ \dot{y}_\omega \\ \dot{r}_\omega \end{bmatrix}\left(\frac{\partial E}{\partial e}de + \frac{\partial E}{\partial E_o}dE_o + \frac{\partial E}{\partial n}dn\right) + \\ &\frac{\partial}{\partial \dot{E}}\begin{bmatrix} \dot{x}_\omega \\ \dot{y}_\omega \\ \dot{r}_\omega \end{bmatrix}\left[\frac{\partial \dot{E}}{\partial e}de + \frac{\partial \dot{E}}{\partial E}\left(\frac{\partial E}{\partial e}de + \frac{\partial E}{\partial E_o}dE_o + \frac{\partial E}{\partial n}dn\right) + \frac{\partial \dot{E}}{\partial n}dn\right] \end{aligned} \tag{A.5-15}$$

<u>The Evaluation of the p.d.'s with Regard to a</u>

From equations (A.5-15) and (A.2-2) one has

$$\frac{\partial}{\partial a}\begin{bmatrix} \dot{x}_\omega \\ \dot{y}_\omega \\ \dot{r}_\omega \end{bmatrix} = \dot{E}\begin{bmatrix} -\sin E \\ \sqrt{1-e^2}\cos E \\ e\sin E \end{bmatrix} = \frac{1}{a}\begin{bmatrix} \dot{x}_\omega \\ \dot{y}_\omega \\ \dot{r}_\omega \end{bmatrix} \tag{A.5-16}$$

The Evaluation of the p.d.'s with Regard to e

From equation (A.5-15) one obtains

$$\frac{\partial}{\partial e}\begin{bmatrix}\dot{x}_\omega\\ \dot{y}_\omega\\ \dot{r}_\omega\end{bmatrix} = \frac{\partial}{\partial e}\begin{bmatrix}\dot{x}_\omega\\ \dot{y}_\omega\\ \dot{r}_\omega\end{bmatrix} + \frac{\partial}{\partial E}\begin{bmatrix}\dot{x}_\omega\\ \dot{y}_\omega\\ \dot{r}_\omega\end{bmatrix}\frac{\partial E}{\partial e} + \frac{\partial}{\partial \dot{E}}\begin{bmatrix}\dot{x}_\omega\\ \dot{y}_\omega\\ \dot{r}_\omega\end{bmatrix}\left(\frac{\partial \dot{E}}{\partial e} + \frac{\partial \dot{E}}{\partial E}\frac{\partial E}{\partial e}\right) \qquad \text{(A.5-17)}$$

Substituting (A.4-4), (A.3-8), (A.4-6) and (A.3-18) into (A.5-17) and developing the derivative of (A.2-2) with regard to e one has

$$\frac{\partial}{\partial e}\begin{bmatrix}\dot{x}_\omega\\ \dot{y}_\omega\\ \dot{r}_\omega\end{bmatrix} = \frac{a^2 n}{r_\omega}\begin{bmatrix}0\\ -\dfrac{e}{\sqrt{1-e^2}}\cos E\\ \sin E\end{bmatrix} - \frac{a^2 n(\sin E - \sin E_o)}{r_\omega^2}\begin{bmatrix}x_\omega + ae\\ y_\omega\\ r_\omega - a\end{bmatrix} +$$

$$\frac{an\cos E - \dot{r}_\omega(\sin E - \sin E_o)}{n r_\omega}\begin{bmatrix}\dot{x}_\omega\\ \dot{y}_\omega\\ \dot{r}_\omega\end{bmatrix} \qquad \text{(A.5-18)}$$

The Evaluation of the p.d.'s with Regard to E_o

From equation (A.5-15) one obtains

$$\frac{\partial}{\partial E_o}\begin{bmatrix}\dot{x}_\omega\\ \dot{y}_\omega\\ \dot{r}_\omega\end{bmatrix} = \frac{\partial}{\partial E}\begin{bmatrix}\dot{x}_\omega\\ \dot{y}_\omega\\ \dot{r}_\omega\end{bmatrix}\frac{\partial E}{\partial E_o} + \frac{\partial}{\partial \dot{E}}\begin{bmatrix}\dot{x}_\omega\\ \dot{y}_\omega\\ \dot{r}_\omega\end{bmatrix}\frac{\partial \dot{E}}{\partial E}\frac{\partial E}{\partial E_o} \qquad \text{(A.5-19)}$$

Substituting (A.4-4), (A.3-12), (A.4-6) and (A.3-20) into (A.5-19) one has

$$\frac{\partial}{\partial E_o}\begin{bmatrix}\dot{x}_\omega\\ \dot{y}_\omega\\ \dot{r}_\omega\end{bmatrix} = -\frac{an\, r_o}{r_\omega^2}\begin{bmatrix}x_\omega + ae\\ y_\omega\\ r_\omega - a\end{bmatrix} - \frac{r_o \dot{r}_\omega}{an\, r_\omega}\begin{bmatrix}\dot{x}_\omega\\ \dot{y}_\omega\\ \dot{r}_\omega\end{bmatrix} \qquad \text{(A.5-20)}$$

The Evaluation of the p.d.'s with Regard to n

From equation (A.5-15) one obtains

$$\frac{\partial}{\partial n}\begin{bmatrix}\dot{x}_\omega\\ \dot{y}_\omega\\ \dot{r}_\omega\end{bmatrix} = \frac{\partial}{\partial E}\begin{bmatrix}\dot{x}_\omega\\ \dot{y}_\omega\\ \dot{r}_\omega\end{bmatrix}\frac{\partial E}{\partial n} + \frac{\partial}{\partial \dot{E}}\begin{bmatrix}\dot{x}_\omega\\ \dot{y}_\omega\\ \dot{r}_\omega\end{bmatrix}\left(\frac{\partial \dot{E}}{\partial n} + \frac{\partial \dot{E}}{\partial E}\frac{\partial E}{\partial n}\right) \qquad \text{(A.5-21)}$$

Substituting (A.4-4), (A.3-14), (A.4-6) and (A.3-22) into (A.5-21) one has

$$\frac{\partial}{\partial n}\begin{bmatrix}\dot{x}_\omega\\ \dot{y}_\omega\\ \dot{r}_\omega\end{bmatrix} = -\frac{a^2 nt}{r_\omega^2}\begin{bmatrix}x_\omega + ae\\ y_\omega\\ r_\omega - a\end{bmatrix} + \frac{r_\omega - \dot{r}_\omega t}{nr_\omega}\begin{bmatrix}\dot{x}_\omega\\ \dot{y}_\omega\\ \dot{r}_\omega\end{bmatrix} \qquad \text{(A.5-22)}$$

Note that from (A.5-20) and (A.5-22) the following relationship holds

$$\frac{\partial}{\partial n}\begin{bmatrix}\dot{x}_\omega\\ \dot{y}_\omega\\ \dot{r}_\omega\end{bmatrix} = \frac{at}{r_\omega}\frac{\partial}{\partial E_o}\begin{bmatrix}\dot{x}_\omega\\ \dot{y}_\omega\\ \dot{r}_\omega\end{bmatrix} + \frac{1}{n}\begin{bmatrix}\dot{x}_\omega\\ \dot{y}_\omega\\ \dot{r}_\omega\end{bmatrix} \qquad \text{(A.5-23)}$$

A.5.2 GM (or n) Known (Parameters a, e, E_o)

From (A.2-1) and (A.3-33) the functional relationship for range and range-difference observations can be set up

$$(x_\omega, y_\omega, r_\omega) = f_i(a,e,E) = f_i[a,e,g(a,e,E_o)] \qquad \text{(A.5-24)}$$

with $\qquad i = 1,2,3$

or in differential matrix form

$$d\begin{bmatrix}x_\omega\\ y_\omega\\ r_\omega\end{bmatrix} = \frac{\partial}{\partial a}\begin{bmatrix}x_\omega\\ y_\omega\\ r_\omega\end{bmatrix}da = \frac{\partial}{\partial e}\begin{bmatrix}x_\omega\\ y_\omega\\ r_\omega\end{bmatrix}de + \frac{\partial}{\partial E}\begin{bmatrix}x_\omega\\ y_\omega\\ r_\omega\end{bmatrix}\left(\frac{\partial E}{\partial a}da + \frac{\partial E}{\partial e}de + \frac{\partial E}{\partial E_o}dE_o\right) \qquad \text{(A.5-25)}$$

<u>The Evaluation of the p.d.'s with Regard to a</u>

From equation (A.5-25) one obtains

$$\frac{\partial}{\partial a}\begin{bmatrix}x_\omega\\ y_\omega\\ r_\omega\end{bmatrix} = \frac{\partial}{\partial a}\begin{bmatrix}x_\omega\\ y_\omega\\ r_\omega\end{bmatrix} + \frac{\partial}{\partial E}\begin{bmatrix}x_\omega\\ y_\omega\\ r_\omega\end{bmatrix}\frac{\partial E}{\partial a} \qquad \text{(A.5-26)}$$

Substituting (A.4-2) and (A.3-37) into (A.5-26) and developing the derivative of (A.2-1) with regard to a, one has

$$\frac{\partial}{\partial a}\begin{bmatrix} x_\omega \\ y_\omega \\ r_\omega \end{bmatrix} = \frac{1}{a}\begin{bmatrix} x_\omega \\ y_\omega \\ r_\omega \end{bmatrix} - \frac{3}{2}\frac{t}{a}\begin{bmatrix} \dot{x}_\omega \\ \dot{y}_\omega \\ \dot{r}_\omega \end{bmatrix} \tag{A.5-27}$$

<u>The Evaluation of the p.d.'s with Regard to e</u>

From equation (A.5-25) one obtains

$$\frac{\partial}{\partial e}\begin{bmatrix} x_\omega \\ y_\omega \\ r_\omega \end{bmatrix} = \frac{\partial}{\partial e}\begin{bmatrix} x_\omega \\ y_\omega \\ r_\omega \end{bmatrix} + \frac{\partial}{\partial E}\begin{bmatrix} x_\omega \\ y_\omega \\ r_\omega \end{bmatrix}\frac{\partial E}{\partial e} \tag{A.5-28}$$

Substituting (A.4-2) and (A.3-38) into (A.5-28) and developing the derivative of (A.2-1) with regard to e one has

$$\frac{\partial}{\partial e}\begin{bmatrix} x_\omega \\ y_\omega \\ r_\omega \end{bmatrix} = -a\begin{bmatrix} 1 \\ \frac{e}{\sqrt{1-e^2}}\sin E \\ \cos E \end{bmatrix} + \frac{\sin E - \sin E_o}{n}\begin{bmatrix} \dot{x}_\omega \\ \dot{y}_\omega \\ \dot{r}_\omega \end{bmatrix} \tag{A.5-29}$$

which, as in section A.5.1, can be written as

$$\frac{\partial}{\partial e}\begin{bmatrix} x_\omega \\ y_\omega \\ r_\omega \end{bmatrix} = A\begin{bmatrix} x_\omega \\ y_\omega \\ r_\omega \end{bmatrix} + B\begin{bmatrix} \dot{x}_\omega \\ \dot{y}_\omega \\ \dot{r}_\omega \end{bmatrix} \tag{A.5-30}$$

with

$$A = -\frac{\cos E + e}{1 - e^2} \tag{A.5-31}$$

$$B = \frac{(E-E_o) - (M-M_o)}{en} + \frac{\sin E}{\dot{E}(1-e^2)} \tag{A.5-32}$$

and

$$\dot{E} = \frac{an}{r_\omega}$$

but now $$n = \sqrt{GM/a^3}$$

<u>The Evaluation of the p.d.'s with Regard to E_o</u>

From equation (A.5-25) one obtains

$$\frac{\partial}{\partial E_o}\begin{bmatrix} x_\omega \\ y_\omega \\ r_\omega \end{bmatrix} = \frac{\partial}{\partial E}\begin{bmatrix} x_\omega \\ y_\omega \\ r_\omega \end{bmatrix}\frac{\partial E}{\partial E_o} \tag{A.5-33}$$

Substituting (A.4-2) and (A.3-39) into (A.5-33) one has

$$\frac{\partial}{\partial E_o}\begin{bmatrix} x_\omega \\ y_\omega \\ r_\omega \end{bmatrix} = \frac{r_o}{an}\begin{bmatrix} \dot{x}_\omega \\ \dot{y}_\omega \\ \dot{r}_\omega \end{bmatrix} \tag{A.5-34}$$

with $$n = \sqrt{GM/a^3}$$

From (A.2-2) and (A.3-34) the functional relationships for range-rate observations can be set up

$$\begin{aligned}(\dot{x}_\omega,\dot{y}_\omega,\dot{r}_\omega) &= f_i(a,e,E,\dot{E}) = f_i[a,e,g_1(a,e,E_o),g_2(a,e,E)] \\ &= f_i\{a,e,g_1(a,e,E_o),g_2[a,e,h(a,e,E_o)]\}\end{aligned} \tag{A.5-35}$$

with $$i = 1,2,3$$

or in differential matrix form

$$\begin{aligned} d\begin{bmatrix} \dot{x}_\omega \\ \dot{y}_\omega \\ \dot{r}_\omega \end{bmatrix} &= \frac{\partial}{\partial a}\begin{bmatrix} \dot{x}_\omega \\ \dot{y}_\omega \\ \dot{r}_\omega \end{bmatrix} da + \frac{\partial}{\partial e}\begin{bmatrix} \dot{x}_\omega \\ \dot{y}_\omega \\ \dot{r}_\omega \end{bmatrix} de + \frac{\partial}{\partial E}\begin{bmatrix} \dot{x}_\omega \\ \dot{y}_\omega \\ \dot{r}_\omega \end{bmatrix}\left(\frac{\partial E}{\partial a}da + \frac{\partial E}{\partial e}de + \frac{\partial E}{\partial E_o}dE_o\right) \\ &\frac{\partial}{\partial \dot{E}}\begin{bmatrix} \dot{x}_\omega \\ \dot{y}_\omega \\ \dot{r}_\omega \end{bmatrix}\left[\frac{\partial \dot{E}}{\partial a}da + \frac{\partial \dot{E}}{\partial e}de + \frac{\partial \dot{E}}{\partial E}\left(\frac{\partial E}{\partial a}da + \frac{\partial E}{\partial e}de + \frac{\partial E}{\partial E_o}dE_o\right)\right] \end{aligned} \tag{A.5-36}$$

<u>The Evaluation of the p.d.'s with Regard to a</u>

From equation (A.5-36) one obtains

$$\frac{\partial}{\partial a}\begin{bmatrix}\dot{x}_\omega\\ \dot{y}_\omega\\ \dot{r}_\omega\end{bmatrix} = \frac{\partial}{\partial a}\begin{bmatrix}\dot{x}_\omega\\ \dot{y}_\omega\\ \dot{r}_\omega\end{bmatrix} + \frac{\partial}{\partial E}\begin{bmatrix}\dot{x}_\omega\\ \dot{y}_\omega\\ \dot{r}_\omega\end{bmatrix}\frac{\partial E}{\partial a} + \frac{\partial}{\partial \dot{E}}\begin{bmatrix}\dot{x}_\omega\\ \dot{y}_\omega\\ \dot{r}_\omega\end{bmatrix}\left(\frac{\partial \dot{E}}{\partial a} + \frac{\partial \dot{E}}{\partial E}\frac{\partial E}{\partial a}\right) \quad \text{(A.5-37)}$$

Substituting (A.4-4), (A.3-37), (A.4-6) and (A.3-42) into (A.5-37) and developing the derivative of (A.2-2) with regard to a, one has

$$\frac{\partial}{\partial a}\begin{bmatrix}\dot{x}_\omega\\ \dot{y}_\omega\\ \dot{r}_\omega\end{bmatrix} = \frac{1}{a}\begin{bmatrix}\dot{x}_\omega\\ \dot{y}_\omega\\ \dot{r}_\omega\end{bmatrix} + \frac{3}{2}\frac{a\,n^2 t}{r_\omega^2}\begin{bmatrix}x_\omega + ae\\ y_\omega\\ r_\omega - a\end{bmatrix} - \frac{3}{2}\frac{r_\omega - \dot{r}_\omega t}{a r_\omega}\begin{bmatrix}\dot{x}_\omega\\ \dot{y}_\omega\\ \dot{r}_\omega\end{bmatrix}$$

$$= \frac{3}{2}\frac{a n^2 t}{r_\omega^2}\begin{bmatrix}x_\omega + ae\\ y_\omega\\ r_\omega - a\end{bmatrix} - \frac{r_\omega - 3\dot{r}_\omega t}{2 a r_\omega}\begin{bmatrix}\dot{x}_\omega\\ \dot{y}_\omega\\ \dot{r}_\omega\end{bmatrix} \quad \text{(A.5-38)}$$

<u>The Evaluation of the p.d.'s with Regard to e</u>

From equation (A.5-36) one obtains

$$\frac{\partial}{\partial e}\begin{bmatrix}\dot{x}_\omega\\ \dot{y}_\omega\\ \dot{r}_\omega\end{bmatrix} = \frac{\partial}{\partial e}\begin{bmatrix}\dot{x}_\omega\\ \dot{y}_\omega\\ \dot{r}_\omega\end{bmatrix} + \frac{\partial}{\partial E}\begin{bmatrix}\dot{x}_\omega\\ \dot{y}_\omega\\ \dot{r}_\omega\end{bmatrix}\frac{\partial E}{\partial e} + \frac{\partial}{\partial \dot{E}}\begin{bmatrix}\dot{x}_\omega\\ \dot{y}_\omega\\ \dot{r}_\omega\end{bmatrix}\left(\frac{\partial \dot{E}}{\partial e} + \frac{\partial \dot{E}}{\partial E}\frac{\partial E}{\partial e}\right) \quad \text{(A.5-39)}$$

Substituting (A.4-4), (A.3-38), (A.4-6) and (A.3-43) into (A.5-39) and developing the derivative of (A.2-2) with regard to e one has

$$\frac{\partial}{\partial e}\begin{bmatrix}\dot{x}_\omega\\ \dot{y}_\omega\\ \dot{r}_\omega\end{bmatrix} = \frac{a^2 n}{r_\omega}\begin{bmatrix}0\\ \dfrac{-e}{\sqrt{1-e^2}}\cos E\\ \sin E\end{bmatrix} - \frac{a^2 n(\sin E - \sin E_o)}{r_\omega^2}\begin{bmatrix}x_\omega + ae\\ y_\omega\\ r_\omega - a\end{bmatrix} +$$

$$\frac{a n \cos E - \dot{r}_\omega(\sin E - \sin E_o)}{n r_\omega}\begin{bmatrix}\dot{x}_\omega\\ \dot{y}_\omega\\ \dot{r}_\omega\end{bmatrix} \quad \text{(A.5-40)}$$

<u>The Evaluation of the p.d.'s with Regard to E_o</u>

From equation (A.5-36) one obtains

$$\frac{\partial}{\partial E_o}\begin{bmatrix}\dot{x}_\omega\\ \dot{y}_\omega\\ \dot{r}_\omega\end{bmatrix} = \frac{\partial}{\partial E}\begin{bmatrix}\dot{x}_\omega\\ \dot{y}_\omega\\ \dot{r}_\omega\end{bmatrix}\frac{\partial E}{\partial E_o} + \frac{\partial}{\partial \dot{E}}\begin{bmatrix}\dot{x}_\omega\\ \dot{y}_\omega\\ \dot{r}_\omega\end{bmatrix}\frac{\partial \dot{E}}{\partial E}\frac{\partial E}{\partial E_o} \tag{A.5-41}$$

Substituting (A.4-4), (A.3-39), (A.4-6) and (A.3-44) into (A.5-41) one has

$$\frac{\partial}{\partial E_o}\begin{bmatrix}\dot{x}_\omega\\ \dot{y}_\omega\\ \dot{r}_\omega\end{bmatrix} = -\frac{anr_o}{r_\omega^2}\begin{bmatrix}x_\omega + ae\\ y_\omega\\ r_\omega - a\end{bmatrix} - \frac{r_o\dot{r}_\omega}{anr_\omega}\begin{bmatrix}\dot{x}_\omega\\ \dot{y}_\omega\\ \dot{r}_\omega\end{bmatrix} \tag{A.5-42}$$

Note that every n in section A.5.2 is given by Kepler's Third Law.

A.5.3 Secular Perturbations due to J_2 (GM and J_2 Known) (Parameters a, e, i, E_o)

From (A.2-1) and (A.3-59) the functional relationship for range and range-difference observations can be set up

$$(x_\omega, y_\omega, r_\omega) = f_i(a,e,E) = f_i[a,e,g(a,e,i,E_o)] \tag{A.5-43}$$

with $\qquad i = 1,2,3$

or in differential matrix form

$$d\begin{bmatrix}x_\omega\\ y_\omega\\ r_\omega\end{bmatrix} = \frac{\partial}{\partial a}\begin{bmatrix}x_\omega\\ y_\omega\\ r_\omega\end{bmatrix}da + \frac{\partial}{\partial e}\begin{bmatrix}x_\omega\\ y_\omega\\ r_\omega\end{bmatrix} + \frac{\partial}{\partial E}\begin{bmatrix}x_\omega\\ y_\omega\\ r_\omega\end{bmatrix}\left(\frac{\partial E}{\partial a}da + \frac{\partial E}{\partial e}de + \frac{\partial E}{\partial i}di + \frac{\partial E}{\partial E_o}dE_o\right) \tag{A.5-44}$$

<u>The Evaluation of the p.d.'s with Regard to a</u>

From equation (A.5-44) one obtains

$$\frac{\partial}{\partial a}\begin{bmatrix}x_\omega\\ y_\omega\\ r_\omega\end{bmatrix} = \frac{\partial}{\partial a}\begin{bmatrix}x_\omega\\ y_\omega\\ r_\omega\end{bmatrix} + \frac{\partial}{\partial E}\begin{bmatrix}x_\omega\\ y_\omega\\ r_\omega\end{bmatrix}\frac{\partial E}{\partial a} \tag{A.5-45}$$

Substituting (A.4-2) and (A.3-69) into (A.5-45) and developing the derivative of (A.2-1) with regard to a, one has

$$\frac{\partial}{\partial a}\begin{bmatrix} x_\omega \\ y_\omega \\ r_\omega \end{bmatrix} = \frac{1}{a}\begin{bmatrix} x_\omega \\ y_\omega \\ r_\omega \end{bmatrix} + \frac{(2n_o - 3\frac{1}{2}n)\,t}{an}\begin{bmatrix} \dot{x}_\omega \\ \dot{y}_\omega \\ \dot{r}_\omega \end{bmatrix} \tag{A.5-46}$$

<u>The Evaluation of the p.d.'s with Regard to e</u>

From equation (A.5-44) one obtains

$$\frac{\partial}{\partial e}\begin{bmatrix} x_\omega \\ y_\omega \\ r_\omega \end{bmatrix} = \frac{\partial}{\partial e}\begin{bmatrix} x_\omega \\ y_\omega \\ r_\omega \end{bmatrix} + \frac{\partial}{\partial E}\begin{bmatrix} x_\omega \\ y_\omega \\ r_\omega \end{bmatrix}\frac{\partial E}{\partial e} \tag{A.5-47}$$

Substituting (A.4-2) and (A.3-71) into (A.5-47) and developing the derivative of (A.2-1) with regard to e, one has

$$\frac{\partial}{\partial e}\begin{bmatrix} x_\omega \\ y_\omega \\ r_\omega \end{bmatrix} = -a\begin{bmatrix} 1 \\ \frac{e}{\sqrt{1-e^2}}\sin E \\ \cos E \end{bmatrix} + \frac{(1-e^2)(\sin E - \sin E_o) + 3et(n-n_o)}{n(1-e^2)}\begin{bmatrix} \dot{x}_\omega \\ \dot{y}_\omega \\ \dot{r}_\omega \end{bmatrix} \tag{A.5-48}$$

<u>The Evaluation of the p.d.'s with Regard to i</u>

From equation (A.5-44) one obtains

$$\frac{\partial}{\partial i}\begin{bmatrix} x_\omega \\ y_\omega \\ r_\omega \end{bmatrix} = \frac{\partial}{\partial E}\begin{bmatrix} x_\omega \\ y_\omega \\ r_\omega \end{bmatrix}\frac{\partial E}{\partial i} \tag{A.5-49}$$

Substituting (A.4-2) and (A.3-73) into (A.5-49) one has

$$\frac{\partial}{\partial i}\begin{bmatrix} x_\omega \\ y_\omega \\ r_\omega \end{bmatrix} = -\frac{3n_o t\Delta_i \sin i \cos i}{n}\begin{bmatrix} \dot{x}_\omega \\ \dot{y}_\omega \\ \dot{r}_\omega \end{bmatrix} \tag{A.5-50}$$

The Evaluation of the p.d.'s with Regard to E_o

From equation (A.5-44) one obtains

$$\frac{\partial}{\partial E_o}\begin{bmatrix} x_\omega \\ y_\omega \\ r_\omega \end{bmatrix} = \frac{\partial}{\partial E}\begin{bmatrix} x_\omega \\ y_\omega \\ r_\omega \end{bmatrix}\frac{\partial E}{\partial E_o} \tag{A.5-51}$$

Substituting (A.4-2) and (A.3-74) into (A.5-51) one has

$$\frac{\partial}{\partial E_o}\begin{bmatrix} x_\omega \\ y_\omega \\ r_\omega \end{bmatrix} = \frac{r_o}{an}\begin{bmatrix} \dot{x}_\omega \\ \dot{y}_\omega \\ \dot{r}_\omega \end{bmatrix} \tag{A.5-52}$$

with n, n_o and Δ_i given by equations (A.3-48), (A.3-50) and (A.3-52).

From (A.2-2) and (A.3-60) the functional relationships for range-rate observations can be set up

$$\begin{aligned}(\dot{x}_\omega,\dot{y}_\omega,\dot{r}_\omega) &= f_i[a,e,g_1(a,e,i,E_o),g_2(a,e,i,E)] \\ &= f_i\{a,e,g_1(a,e,i,E_o),g_2[a,e,i,\\ &\qquad h(a,e,i,E_o)]\}\end{aligned} \tag{A.5-53}$$

with $\qquad i = 1,2,3$

or in differential matrix form

$$\begin{aligned} d\begin{bmatrix} \dot{x}_\omega \\ \dot{y}_\omega \\ \dot{r}_\omega \end{bmatrix} &= \frac{\partial}{\partial a}\begin{bmatrix} \dot{x}_\omega \\ \dot{y}_\omega \\ \dot{r}_\omega \end{bmatrix} da + \frac{\partial}{\partial e}\begin{bmatrix} \dot{x}_\omega \\ \dot{y}_\omega \\ \dot{r}_\omega \end{bmatrix} de + \frac{\partial}{\partial E}\begin{bmatrix} \dot{x}_\omega \\ \dot{y}_\omega \\ \dot{r}_\omega \end{bmatrix}\left(\frac{\partial E}{\partial a}\, da + \frac{\partial E}{\partial e}\, de + \frac{\partial E}{\partial i}\, di + \frac{\partial E}{\partial E_o} dE_o\right) \\ &+ \frac{\partial}{\partial \dot{E}}\begin{bmatrix} \dot{x}_\omega \\ \dot{y}_\omega \\ \dot{r}_\omega \end{bmatrix}\left[\frac{\partial \dot{E}}{\partial a}da + \frac{\partial \dot{E}}{\partial e}de + \frac{\partial \dot{E}}{\partial i}di + \frac{\partial \dot{E}}{\partial E}\left(\frac{\partial E}{\partial a}da + \frac{\partial E}{\partial e}de + \frac{\partial E}{\partial i}di + \frac{\partial E}{\partial E_o}dE_o\right)\right] \end{aligned} \tag{A.5-54}$$

The Evaluation of the p.d.'s with Regard to a

From equation (A.5-54) one obtains

$$\frac{\partial}{\partial a}\begin{bmatrix} \dot{x}_\omega \\ \dot{y}_\omega \\ \dot{r}_\omega \end{bmatrix} = \frac{\partial}{\partial a}\begin{bmatrix} \dot{x}_\omega \\ \dot{y}_\omega \\ \dot{r}_\omega \end{bmatrix} + \frac{\partial}{\partial E}\begin{bmatrix} \dot{x}_\omega \\ \dot{y}_\omega \\ \dot{r}_\omega \end{bmatrix}\frac{\partial E}{\partial a} + \frac{\partial}{\partial \dot{E}}\begin{bmatrix} \dot{x}_\omega \\ \dot{y}_\omega \\ \dot{r}_\omega \end{bmatrix}\left(\frac{\partial \dot{E}}{\partial a} + \frac{\partial \dot{E}}{\partial E}\frac{\partial E}{\partial a}\right) \tag{A.5-55}$$

Substituting (A.4-4), (A.3-69), (A.4-6) and (A.3-77) into (A.5-55) and developing the derivative of (A.2-2) with regard to a, one has

$$\frac{\partial}{\partial a}\begin{bmatrix}\dot{x}_\omega\\ \dot{y}_\omega\\ \dot{r}_\omega\end{bmatrix} = \frac{1}{a}\begin{bmatrix}\dot{x}_\omega\\ \dot{y}_\omega\\ \dot{r}_\omega\end{bmatrix} - \frac{an(2n_o - 3\frac{1}{2}n)\,t}{r_\omega^2}\begin{bmatrix}x_\omega + ae\\ y_\omega\\ r_\omega - a\end{bmatrix}$$

$$+ \frac{(r_\omega - \dot{r}_\omega t)(2n_o - 3\frac{1}{2}n)}{anr_\omega}\begin{bmatrix}\dot{x}_\omega\\ \dot{y}_\omega\\ \dot{r}_\omega\end{bmatrix} \qquad \text{(A.5-56)}$$

$$= \frac{r_\omega n + (r_\omega - \dot{r}_\omega t)(2n_o - 3\frac{1}{2}n)}{anr_\omega}\begin{bmatrix}\dot{x}_\omega\\ \dot{y}_\omega\\ \dot{r}_\omega\end{bmatrix} - \frac{an(2n_o - 3\frac{1}{2}n)\,t}{r_\omega^2}\begin{bmatrix}x_\omega + ae\\ y_\omega\\ r_\omega - a\end{bmatrix}$$

<u>The Evaluation of the p.d.'s with Regard to e</u>

From equation (A.5-54) one obtains

$$\frac{\partial}{\partial e}\begin{bmatrix}\dot{x}_\omega\\ \dot{y}_\omega\\ \dot{r}_\omega\end{bmatrix} = \frac{\partial}{\partial e}\begin{bmatrix}\dot{x}_\omega\\ \dot{y}_\omega\\ \dot{r}_\omega\end{bmatrix} + \frac{\partial}{\partial E}\begin{bmatrix}\dot{x}_\omega\\ \dot{y}_\omega\\ \dot{r}_\omega\end{bmatrix}\frac{\partial E}{\partial e} + \frac{\partial}{\partial \dot{E}}\begin{bmatrix}\dot{x}_\omega\\ \dot{y}_\omega\\ \dot{r}_\omega\end{bmatrix}\left(\frac{\partial \dot{E}}{\partial e} + \frac{\partial \dot{E}}{\partial E}\frac{\partial E}{\partial e}\right) \qquad \text{(A.5-57)}$$

Substituting (A.4-4), (A.3-71), (A.4-6) and (A.3-79) into (A.5-57) and developing the derivative of (A.2-2) with regard to e, one has

$$\frac{\partial}{\partial e}\begin{bmatrix}\dot{x}_\omega\\ \dot{y}_\omega\\ \dot{z}_\omega\end{bmatrix} = \frac{a^2 n}{r_\omega}\begin{bmatrix}0\\ \frac{-e}{\sqrt{1-e^2}}\cos E\\ \sin E\end{bmatrix} - \frac{a^2 n}{r_\omega^2(1-e^2)}\left[(1-e^2)(\sin E - \sin E_o) + 3et(n-n_o)\right]\begin{bmatrix}x_\omega + ae\\ y_\omega\\ r_\omega - a\end{bmatrix}$$

$$+ \frac{1}{nr_\omega}\left[an\cos E - \dot{r}_\omega(\sin E - \sin E_o) + \frac{3e}{1-e^2}(r_\omega - \dot{r}_\omega t)(n-n_o)\right]\begin{bmatrix}\dot{x}_\omega\\ \dot{y}_\omega\\ \dot{r}_\omega\end{bmatrix} \qquad \text{(A.5-58)}$$

<u>The Evaluation of the p.d.'s with Regard to i</u>

From equation (A.5-54) one obtains

$$\frac{\partial}{\partial i}\begin{bmatrix}\dot{x}_\omega\\ \dot{y}_\omega\\ \dot{r}_\omega\end{bmatrix} = \frac{\partial}{\partial E}\begin{bmatrix}\dot{x}_\omega\\ \dot{y}_\omega\\ \dot{r}_\omega\end{bmatrix}\frac{\partial E}{\partial i} + \frac{\partial}{\partial \dot{E}}\begin{bmatrix}\dot{x}_\omega\\ \dot{y}_\omega\\ \dot{r}_\omega\end{bmatrix}\left(\frac{\partial \dot{E}}{\partial i} + \frac{\partial \dot{E}}{\partial E}\frac{\partial E}{\partial i}\right) \tag{A.5-59}$$

Substituting (A.4-4), (A.3-73), (A.4-6) and (A.3-81) into (A.5-59) one has

$$\frac{\partial}{\partial i}\begin{bmatrix}\dot{x}_\omega\\ \dot{y}_\omega\\ \dot{r}_\omega\end{bmatrix} = \frac{3a^2 n_o n t \Delta_i \sin i \cos i}{r_\omega^2}\begin{bmatrix}x_\omega + ae\\ y_\omega\\ r_\omega - a\end{bmatrix} + - \frac{3n_o \Delta_i \sin i \cos i\,(r_\omega - \dot{r}_\omega t)}{n r_\omega}\begin{bmatrix}\dot{x}_\omega\\ \dot{y}_\omega\\ \dot{r}_\omega\end{bmatrix} \tag{A.5-60}$$

<u>The Evaluation of the p.d.'s with Regard to E_o</u>

From equation (A.5-54) one obtains

$$\frac{\partial}{\partial E_o}\begin{bmatrix}\dot{x}_\omega\\ \dot{y}_\omega\\ \dot{r}_\omega\end{bmatrix} = \frac{\partial}{\partial E}\begin{bmatrix}\dot{x}_\omega\\ \dot{y}_\omega\\ \dot{r}_\omega\end{bmatrix}\frac{\partial E}{\partial E_o} + \frac{\partial}{\partial \dot{E}}\begin{bmatrix}\dot{x}_\omega\\ \dot{y}_\omega\\ \dot{r}_\omega\end{bmatrix}\frac{\partial \dot{E}}{\partial E}\frac{\partial E}{\partial E_o} \tag{A.5-61}$$

Substituting (A.4-4), (A.3-74), (A.4-6) and (A.3-82) one has

$$\frac{\partial}{\partial E_o}\begin{bmatrix}\dot{x}_\omega\\ \dot{y}_\omega\\ \dot{r}_\omega\end{bmatrix} = -\frac{a n r_o}{r_\omega^2}\begin{bmatrix}x_\omega + ae\\ y_\omega\\ r_\omega - a\end{bmatrix} - \frac{r_o \dot{r}_\omega}{a n r_\omega}\begin{bmatrix}\dot{x}_\omega\\ \dot{y}_\omega\\ \dot{r}_\omega\end{bmatrix} \tag{A.5-62}$$

Note that every n, n_o and Δ_i in section A.5.3 are given by equations (A.3-48), (A.3-50) and (A.3-52).

APPENDIX B

OBSERVATION EQUATIONS FOR RANGE, RANGE-RATE AND RANGE-DIFFERENCE OBSERVATIONS

B.1 Introduction

In the determination of orbits, station positions and earth parameters the partial derivatives for the observation equations in the various measurement systems follow certain patterns. Special attention will be given to the order in which the partial derivatives will be computed as to take fully advantage of previous calculations. Since in the Chapters 3 and 4 the models were set up in the already estimable quantities no analysis of the partial derivatives and their possible linear combinations needs to take place.

B.2 Two Dimensional Circular Motion in Case of Range Observations

B.2.1 GM (or n) Unknown

The range equation derived in sections 4.2 and 4.4.1 was

$$r^2 = a^2 + R^2 - 2aR\cos(\alpha_o + \dot{\alpha}t) \tag{B.2-1}$$

with

$$\alpha_o = \lambda + GAST_o - \Omega - \omega - E_o$$
$$\dot{\alpha} = n - \omega_e$$

In order to take advantage of certain equalities the range-rate equation as derived in section 4.2 will be used as well

$$r\dot{r} = aR\dot{\alpha}\sin(\alpha_o+\dot{\alpha}t) \tag{B.2-2}$$

<u>The Evaluation of the p.d. with Regard to a</u>

$$2r\frac{\partial r}{\partial a} = 2a - 2R\cos(\alpha_o+\dot{\alpha}t)$$

$$\frac{\partial r}{\partial a} = \frac{a - R\cos(\alpha_o+\dot{\alpha}t)}{r}$$

Substituting the trigonometric part of the range equation (B.2-1) into the equation above yields

$$\frac{\partial r}{\partial a} = \frac{a^2 + r^2 - R^2}{2ar} \tag{B.2-3}$$

<u>The Evaluation of the p.d. with Regard to R</u>

$$\frac{\partial r}{\partial R} = \frac{R - a\cos(\alpha_o+\dot{\alpha}t)}{r}$$

$$= \frac{R^2 + r^2 - a^2}{2Rr} \tag{B-2.4}$$

<u>The Evaluation of the p.d. with Regard to α_o</u>

$$\frac{\partial r}{\partial \alpha_o} = \frac{aR}{r}\sin(\alpha_o+\dot{\alpha}t)$$

Substituting the trigonometric part of the range-rate equation (B.2-2) into the equation above yields

$$\frac{\partial r}{\partial \alpha_o} = \frac{\dot{r}}{\dot{\alpha}} \tag{B.2-5}$$

The Evaluation of the p.d. with Regard to $\dot{\alpha}$

$$\frac{\partial r}{\partial \dot{\alpha}} = \frac{aRt}{r} \sin(\alpha_o + \dot{\alpha} t) = \frac{\dot{r} t}{\dot{\alpha}} = t \frac{\partial r}{\partial \alpha_o} \tag{B.2-6}$$

B.2.2 GM (of n) Unknown

The range equation derived in section 4.4.2 was

$$r^2 = a^2 + R^2 - 2aR \cos[\alpha_o + (n - \omega_e)t] \tag{B.2-7}$$

with $$n = \sqrt{GM/a^3}$$

The range-rate equation is

$$r\dot{r} = aR(n - \omega_e)\sin[\alpha_0 + (n - \omega_e)t] \tag{B.2-8}$$

The Evaluation of the p.d. with Regard to α_o

$$\frac{\partial r}{\partial \alpha_o} = \frac{aR}{r} \sin[\alpha_o + (n - \omega_e)t] = \frac{\dot{r}}{n - \omega_e} \tag{B.2-9}$$

The Evaluation of the p.d. with Regard to ω_e

$$\frac{\partial r}{\partial \omega_e} = -\frac{aRt}{r} \sin[\alpha_o + (n - \omega_e)t] = \frac{-\dot{r}t}{n - \omega_e} = -t \frac{\partial r}{\partial \alpha_o} \tag{B.2-10}$$

The Evaluation of the p.d. with Regard to a

$$\frac{\partial r}{\partial a} = \frac{a^2 + r^2 - R^2}{2ar} + \frac{aR}{r} \sin[\alpha_o + (n - \omega_e)t] \cdot -\frac{3}{2}\frac{nt}{a}$$

$$= \frac{a^2 + r^2 - R^2}{2ar} - \frac{3}{2}\frac{nt}{a}\frac{\partial r}{\partial \alpha_o} \tag{B.2-11}$$

The Evaluation of the p.d. with Regard to R

$$\frac{\partial r}{\partial R} = \frac{R^2 + r^2 - a^2}{2Rr} \tag{B.2-12}$$

In the equations (B.2-8) through (B.2-12) the mean motion n is equal to $\sqrt{GM/a^3}$.

B.3 Three Dimensional Circular Motion in Case of Range Observations

B.3.1 GM (or n) Unknown

The range equation derived in section 4.4.3 was

$$r^2 = a^2 + R^2 - 2aR\cos\alpha \tag{B.3-1}$$

with

$$\cos\alpha = \cos\psi\cos\beta + \sin\psi\sin u \sin i$$

$$\cos\beta = \cos\Delta\lambda\cos u + \sin\Delta\lambda\sin u \cos i$$

$$u = u_o + nt = (\omega + E_o) + nt$$

$$\Delta\lambda = \Delta\lambda_o + \omega_e t = (\lambda + GAST_o - \Omega) + \omega_e t$$

The range-rate equation derived in section 4.7.1 was

$$\begin{aligned} r\dot{r} = aR[&\cos\psi\sin\Delta\lambda\cos u\,(\omega_e - n\cos i) + \\ &\cos\psi\cos\Delta\lambda\sin u\,(n - \omega_e\cos i) + \\ &- n\sin\psi\cos u\sin i] \end{aligned} \tag{B.3-2}$$

$$\begin{aligned} = aRn[&\cos\psi(\cos\Delta\lambda\sin u - \sin\Delta\lambda\cos u\cos i) \\ &- \sin\psi\cos u\sin i] + \\ &aR\omega_e\cos\psi(\sin\Delta\lambda\cos u - \cos\Delta\lambda\sin u\cos i) \end{aligned} \tag{B.3-3}$$

The Evaluation of the p.d. with Regard to a

$$\frac{\partial r}{\partial a} = \frac{a^2 + r^2 - R^2}{2ar} \tag{B.3-4}$$

The Evaluation of the p.d. with Regard to R

$$\frac{\partial r}{\partial R} = \frac{R^2 + r^2 - a^2}{2Rr} \tag{B.3-5}$$

The Evaluation of the p.d. with Regard to i

$$\frac{\partial r}{\partial i} = \frac{aR\sin u}{r} \left(\cos\psi\sin\Delta\lambda\sin i - \sin\psi\cos i\right) \tag{B.3-6}$$

The Evaluation of the p.d. with Regard to ψ

$$\frac{\partial r}{\partial \psi} = \frac{aR}{r} \left(\sin\psi\cos\beta - \cos\psi\sin u \sin i\right) \tag{B.3-7}$$

The Evaluation of the p.d. with Regard to u_o

$$\frac{\partial r}{\partial u_o} = \frac{aR}{r} \left[\cos\psi(\cos\Delta\lambda\sin u - \sin\Delta\lambda\cos u \cos i) - \sin\psi\cos u \sin i\right] \tag{B.3-8}$$

Substituting the trigonometric part of the first term of the range-rate equation (B.3-3) into the equation above yields

$$\frac{\partial \dot{r}}{\partial u} = \frac{\dot{r}}{n} - \frac{aR\omega_e\cos\psi}{nr} \left(\sin\Delta\lambda\cos u - \cos\Delta\lambda\sin u \cos i\right) \tag{B.3-9}$$

The Evaluation of the p.d. with Regard to n

$$\frac{\partial r}{\partial n} = \frac{aRt}{r} [\cos\psi(\cos\Delta\lambda\sin u - \sin\Delta\lambda\cos u \cos i)$$

$$- \sin\psi\cos u \sin i] = t \frac{\partial r}{\partial u_o} \qquad \text{(B.3-10)}$$

The Evaluation of the p.d. with Regard to $\Delta\lambda_o$

$$\frac{\partial r}{\partial \Delta\lambda_o} = \frac{aR\cos\psi}{r} (\sin\Delta\lambda\cos u - \cos\Delta\lambda\sin u \cos i)$$

Substitution of the trigonometric part of equation (B.3-9) into the equation above yields

$$\frac{\partial r}{\partial \Delta\lambda_o} = \frac{\dot{r}}{\omega_e} - \frac{n}{\omega_e}\frac{\partial r}{\partial u_o} = \frac{1}{\omega_e}\left(r - n\frac{\partial r}{\partial u_o}\right) \qquad \text{(B.3-11)}$$

The Evaluation of the p.d. with Regard to ω_e

$$\frac{\partial r}{\partial \omega_e} = \frac{aRt\cos\psi}{r} (\sin\Delta\lambda\cos u - \cos\Delta\lambda\sin u \cos i)$$

$$= t \frac{\partial r}{\partial \Delta\lambda_o} \qquad \text{(B.3-12)}$$

B.3.2 GM (or n) Known

The range equation derived in section 4.4.4 was

$$r^2 = a^2 + R^2 - 2aR\cos\alpha \qquad \text{(B.3-13)}$$

with

$$\cos\alpha = \cos\psi\cos\beta + \sin\psi\sin u \sin i$$

$$\cos\beta = \cos\Delta\lambda\cos u + \sin\Delta\lambda\sin u \cos i$$

$$u = u_o + nt = (\omega + E_o) + \sqrt{GM/a^3}\, t$$

$$\Delta\lambda = \Delta\lambda_o + \omega_e t = (\lambda + GAST_o - \Omega) + \omega_e t$$

The range-rate equation as in section B.3.1 is

$$r\dot{r} = aRn[\cos\psi(\cos\Delta\lambda\sin u - \sin\Delta\lambda\cos u\cos i) - \sin\psi\cos u\sin i] + aR\omega_e\cos\psi(\sin\Delta\lambda\cos u - \cos\Delta\lambda\sin u\cos i) \tag{B.3-14}$$

with $n = \sqrt{GM/a^3}$.

<u>The Evaluation of the p.d. with Regard to u_o</u>

A similar expression as in section B.3.1 applies here

$$\frac{\partial r}{\partial u_o} = \frac{r\dot{r} - aR\omega_e\cos\psi(\sin\Delta\lambda\cos u - \cos\Delta\lambda\sin u\cos i)}{nr} \tag{B.3-15}$$

<u>The Evaluation of the p.d. with Regard to a</u>

$$\frac{\partial r}{\partial a} = \frac{a^2 + r^2 - R^2}{2ar} + \frac{aR}{r}\{\cos\psi(\cos\Delta\lambda\sin u - \sin\Delta\lambda\cos u\cos i) - \sin\psi\cos u\sin i\} \cdot -\frac{3}{2}\frac{nt}{a}$$

Substituting the equation (B.3-8) into the expression above one obtains

$$\frac{\partial r}{\partial a} = \frac{a^2 + r^2 - R^2}{2ar} - \frac{3}{2}\frac{nt}{a}\frac{\partial r}{\partial u_o} \tag{B.3-16}$$

<u>The Evaluation of the p.d.'s with Regard to R, i, ψ, $\Delta\lambda_o$ and ω_e</u>

The partial derivatives with regard to R, i, ψ, $\Delta\lambda_o$ and ω_e are given in section B.3.1 by the equations (B.3-5), (B.3-6), (B.3-7), (B.3-11) and (B.3-12) respectively. Wherever the mean motion n appears in the partial derivatives of this section it needs to be evaluated as $\sqrt{GM/a^3}$.

B.4 Two Dimensional Elliptic Motion in Case of Range Observations

B.4.1 GM (or n) Unknown

The range equation derived in section 4.5.1 was

$$r^2 = r_\omega^2 + R^2 - 2R(x_\omega \cos\Delta\lambda + y_\omega \sin\Delta\lambda) \tag{B.4-1}$$

with $$\Delta\lambda = \Delta\lambda_o + \omega_e t = (\lambda + GAST_o - \Omega - \omega) + \omega_e t$$

and x_ω, y_ω, r_ω as given in Appendix A, sections A.2, A.3.1, A.4.1 and A.5.1.

The range-rate equation is

$$r\dot{r} = r_\omega \dot{r}_\omega - R(\dot{x}_\omega \cos\Delta\lambda + \dot{y}_\omega \sin\Delta\lambda) + R\omega_e (x_\omega \sin\Delta\lambda - y_\omega \cos\Delta\lambda) \tag{B.4-2}$$

with $\dot{x}_\omega$, $\dot{y}_\omega$, $\dot{r}_\omega$ as developed in Appendix A, sections A.2, A.3.1, A.4.2 and A.5.1.

The Evaluation of the p.d. with Regard to a

$$2r \frac{\partial r}{\partial a} = 2r_\omega \frac{\partial r_\omega}{\partial a} - 2R\left(\frac{\partial x_\omega}{\partial a} \cos\Delta\lambda + \frac{\partial y_\omega}{\partial a} \sin\Delta\lambda\right)$$

Using equation (A.5-3) one obtains

$$\frac{\partial r}{\partial a} = \frac{r_\omega^2 - R(x_\omega \cos\Delta\lambda + y_\omega \sin\Delta\lambda)}{ar}$$

$$= \frac{r_\omega^2 + r^2 - R^2}{2ar} \tag{B.4-3}$$

The Evaluation of the p.d. with Regard to E_o

$$2r \frac{\partial r}{\partial E_o} = 2r_\omega \frac{\partial r_\omega}{\partial E_o} - 2R\left(\frac{\partial x_\omega}{\partial E_o} \cos\Delta\lambda + \frac{\partial y_\omega}{\partial E_o} \sin\Delta\lambda\right)$$

Using equation (A.5-10) one obtains

$$\frac{\partial r}{\partial E_o} = \frac{r_o}{anr} [r_\omega \dot{r}_\omega - R(\dot{x}_\omega \cos\Delta\lambda + \dot{y}_\omega \sin\Delta\lambda)] \tag{B.4-4}$$

Using the range-rate equation (B.4-2) one has

$$\frac{\partial r}{\partial E_o} = \frac{r_o}{anr} [r\dot{r} - R\omega_e (x_\omega \sin\Delta\lambda - y_\omega \cos\Delta\lambda)] \tag{B.4-5}$$

<u>The Evaluation of the p.d. with Regard to n</u>

With the help of equation (A.5-13) one obtains

$$\frac{\partial r}{\partial n} = \frac{at}{r_o} \cdot \frac{r_o}{anr} [r_\omega \dot{r}_\omega - R(\dot{x}_\omega \cos\Delta\lambda + \dot{y}_\omega \sin\Delta\lambda)]$$

$$= \frac{at}{r_o} \frac{\partial r}{\partial E_o} \tag{B.4-6}$$

<u>The Evaluation of the p.d. with Regard to e</u>

From equation (A.5-6) one had

$$\frac{\partial}{\partial e} \begin{bmatrix} x_\omega \\ y_\omega \\ r_\omega \end{bmatrix} = A \begin{bmatrix} x_\omega \\ y_\omega \\ r_\omega \end{bmatrix} + B \begin{bmatrix} \dot{x}_\omega \\ \dot{y}_\omega \\ \dot{r}_\omega \end{bmatrix} \tag{B.4-7}$$

Substituting (A.5-3) and (A.5-10) into (B.4-7) one obtains

$$\frac{\partial}{\partial e} \begin{bmatrix} x_\omega \\ y_\omega \\ r_\omega \end{bmatrix} = a \left\{ A \frac{\partial}{\partial a} \begin{bmatrix} x_\omega \\ y_\omega \\ r_\omega \end{bmatrix} + \frac{nB}{r_o} \frac{\partial}{\partial E_o} \begin{bmatrix} \dot{x}_\omega \\ \dot{y}_\omega \\ \dot{r}_\omega \end{bmatrix} \right\} \tag{B.4-8}$$

This relationship plays an important role in the analytical orbit determination theory. With the help of equation (B.4-8) one arrives

directly at the partial derivative of the observed range with regard to e

$$\frac{\partial r}{\partial e} = a\left(A\frac{\partial r}{\partial a} + \frac{nB}{r_o}\frac{\partial r}{\partial E_o}\right) \tag{B.4-9}$$

<u>The Evaluation of the p.d. with Regard to R</u>

$$\frac{\partial r}{\partial R} = \frac{R^2 + r^2 - a^2}{2Rr} \tag{B.4-10}$$

<u>The Evaluation of the p.d. with Regard to $\Delta\lambda_o$</u>

$$\frac{\partial r}{\partial \Delta\lambda_o} = \frac{R}{r}\,(x_\omega \sin\Delta\lambda - y_\omega \cos\Delta\lambda)$$

Substitution of the trigonometric part of equation (B.4-5) into the equation above yields

$$\frac{\partial r}{\partial \Delta\lambda_o} = \frac{\dot{r}}{\omega_e} - \frac{an}{r_o\omega_e}\frac{\partial r}{\partial E_o} = \frac{1}{\omega_e}\left(\dot{r} - \frac{an}{r_o}\frac{\partial r}{\partial E_o}\right) \tag{B.4-11}$$

<u>The Evaluation of the p.d. with Regard to ω_e</u>

$$\frac{\partial r}{\partial \omega_e} = \frac{Rt}{r}\,(x_\omega \sin\Delta\lambda - y_\omega \cos\Delta\lambda)$$

$$= t\,\frac{\partial r}{\partial \Delta\lambda_o} \tag{B.4-12}$$

B.4.2 GM (or n) Known

The range equation derived in section 4.5.2 was

$$r^2 = r_\omega^2 + R^2 - 2R(x_\omega \cos\Delta\lambda + y_\omega \sin\Delta\lambda) \tag{B.4-13}$$

with $\Delta\lambda = \Delta\lambda_o + \omega_e t = (\lambda + GAST_o - \Omega - \omega) + \omega_e t$

and x_ω, y_ω, r_ω as given in Appendix A, sections A.2, A.3.2, A.4.1 and A.5.1.

The range-rate equation is

$$r\dot{r} = r_\omega \dot{r}_\omega - R(\dot{x}_\omega \cos\Delta\lambda + \dot{y}_\omega \sin\Delta\lambda) + R\omega_e (x_\omega \sin\Delta\lambda - y_\omega \cos\Delta\lambda) \quad \text{(B.4-14)}$$

with $\dot{x}_\omega$, $\dot{y}_\omega$, $\dot{r}_\omega$ as developed in Appendix A, sections A.2, A.3.2, A.4.2 and A.5.2.

<u>The Evaluation of the p.d. with Regard to E_o</u>

A similar expression as in section B.4.1 applies here

$$\frac{\partial r}{\partial E_o} = \frac{t_o}{anr} [r_\omega \dot{r}_\omega - R(\dot{x}_\omega \cos\Delta\lambda + \dot{y}_\omega \sin\Delta\lambda)] \quad \text{(B.4-15)}$$

<u>The Evaluation of the p.d. with Regard to a</u>

With the help of equation (A.5-27) one obtains

$$\frac{\partial r}{\partial a} = \frac{r_\omega^2 + r^2 - R^2}{2ar} - \frac{3}{2}\frac{t}{a} [r_\omega \dot{r}_\omega - R(\dot{x}_\omega \cos\Delta\lambda + \dot{y}_\omega \sin\Delta\lambda)]$$

Substituting equation (B.4-15) into the equation above yields

$$\frac{\partial r}{\partial a} = \frac{r_\omega^2 + r^2 - R^2}{2aR} - \frac{3nt}{2r_o}\frac{\partial r}{\partial E_o} \quad \text{(B.4-16)}$$

<u>The Evaluation of the p.d. with Regard to e</u>

From equation (A.5-30) one had

$$\frac{\partial}{\partial e}\begin{bmatrix} x_\omega \\ y_\omega \\ r_\omega \end{bmatrix} = A \begin{bmatrix} x_\omega \\ y_\omega \\ r_\omega \end{bmatrix} + B \begin{bmatrix} \dot{x}_\omega \\ \dot{y}_\omega \\ \dot{r}_\omega \end{bmatrix} \quad \text{(B.4-17)}$$

Substituting (A.5-27) and (A.5-35) into (B.4-17) one obtains

$$\frac{\partial}{\partial e}\begin{bmatrix} x_\omega \\ y_\omega \\ r_\omega \end{bmatrix} = A\left\{ a\frac{\partial}{\partial a}\begin{bmatrix} x_\omega \\ y_\omega \\ r_\omega \end{bmatrix} + \frac{3}{2}\frac{ant}{r_o}\frac{\partial}{\partial E_o}\begin{bmatrix} x_\omega \\ y_\omega \\ r_\omega \end{bmatrix}\right\} + \frac{anB}{r_o}\frac{\partial}{\partial E_o}\begin{bmatrix} x_\omega \\ y_\omega \\ r_\omega \end{bmatrix}$$

$$= a\left\{ A\frac{\partial}{\partial a}\begin{bmatrix} x_\omega \\ y_\omega \\ r_\omega \end{bmatrix} + \frac{n}{2r_o}(3At+2B)\frac{\partial}{\partial E_o}\begin{bmatrix} x_\omega \\ y_\omega \\ r_\omega \end{bmatrix}\right\} \qquad \text{(B.4-18)}$$

This relationship plays a similar role as equation (B.4-8) in the range observation equation with non-enforcement of Kepler's Third Law. With the help of equation (B.4-18) one arrives directly at the partial derivative of the observed range with regard to e.

$$\frac{\partial r}{\partial e} = aA\frac{\partial r}{\partial a} + \frac{an}{2r_o}(3At+2B)\frac{\partial r}{\partial E_o} \qquad \text{(B.4-19)}$$

<u>The Evaluation of the p.d.'s with Regard to R, $\Delta\lambda_o$ and ω_e</u>

The partial derivatives with regard to R, $\Delta\lambda_o$ and ω_e are given in section B.4.1 by the equations (B.4-10), (B.4-11) and (B.4-12). Wherever the mean motion n appears in the partial derivatives of this section it needs to be evaluated as $\sqrt{GM/a^3}$. Similarly; wherever the variables x_ω, y_ω, r_ω, $\dot{x}_\omega$, $\dot{y}_\omega$, $\dot{r}_\omega$ appear in the partial derivatives of this section, they need to be evaluated as in the sections A.2, A.3.2, A.4.1, A.4.2 and A.5.2 of Appendix A.

B.5 Three Dimensional Elliptic Motion in Case of Range Observations

B.5.1 GM (or n) Unknown

The range equation derived in section 4.5.3 was

$$r^2 = r_\omega^2 + R^2 - 2R(Px_\omega + Qy_\omega) \tag{B.5-1}$$

with

$$P = P_c \cos\psi + P_s \sin\psi$$

$$Q = Q_c \cos\psi + Q_s \sin\psi$$

$$P_c = \cos\Delta\lambda\cos\omega + \sin\Delta\lambda\sin\omega\cos i$$

$$P_s = \sin\omega\sin i$$

$$Q_c = -\cos\Delta\lambda\sin\omega + \sin\Delta\lambda\cos\omega\cos i$$

$$Q_s = \cos\omega\sin i$$

$$\Delta\lambda = \Delta\lambda_o + \omega_e t = (\lambda + GAST_o - \Omega) + \omega_e t$$

and x_ω, y_ω, r_ω as given in Appendix A, sections A.2, A.3.1, A.4.1 and A.5.1.

The range-rate equation derived in section 4.7.2 was

$$r\dot{r} = r_\omega \dot{r}_\omega - R(P\dot{x}_\omega + Q\dot{y}_\omega) + R\omega_e \cos\psi(P'x_\omega - Q'y_\omega) \tag{B.5-2}$$

with

$$P' = \sin\Delta\lambda\cos\omega - \cos\Delta\lambda\sin\omega\cos i$$

$$Q' = \sin\Delta\lambda\sin\omega + \cos\Delta\lambda\cos\omega\cos i$$

and $\dot{x}_\omega$, $\dot{y}_\omega$, $\dot{r}_\omega$ as developed in Appendix A, sections A.2, A.3.1, A.4.2 and A.5.1. Several partial derivatives can be taken directly from section B.4.1.

The Evaluation of the p.d. with Regard to a

$$\frac{\partial r}{\partial a} = \frac{r_\omega^2 + r^2 - R^2}{2aR} \tag{B.5-3}$$

The Evaluation of the p.d. with Regard to E_o

$$\frac{\partial r}{\partial E_o} = \frac{r_o}{anr} [r_\omega \dot{r}_\omega - R(Px_\omega + Qy_\omega)] \tag{B.5-4}$$

Using the range-rate equation (B.5-2) one has

$$\frac{\partial r}{\partial E_o} = \frac{r_o}{anr} [r\dot{r} - R\omega_e \cos\psi(P'x_\omega - Q'y_\omega)] \tag{B.5-5}$$

The Evaluation of the p.d. with Regard to n

$$\frac{\partial r}{\partial n} = \frac{at}{r_o} \frac{\partial r}{\partial E_o} \tag{B.5-6}$$

The Evaluation of the p.d. with Regard to e

$$\frac{\partial r}{\partial e} = a \left(A \frac{\partial r}{\partial a} + \frac{nB}{r_o} \frac{\partial r}{\partial E_o} \right) \tag{B.5-7}$$

The Evaluation of the p.d. with Regard to i

$$\frac{\partial r}{\partial i} = \frac{R}{r} (x_\omega \sin\omega + y_\omega \cos\omega)(\cos\psi \sin\Delta\lambda \sin i - \sin\psi \cos i) \tag{B.5-8}$$

The Evaluation of the p.d. with Regard to ω

Since
$$\frac{\partial P_c}{\partial \omega} = Q_c$$
$$\frac{\partial P_s}{\partial \omega} = Q_s$$
$$\frac{\partial Q_c}{\partial \omega} = -P_c$$
and
$$\frac{\partial Q_s}{\partial \omega} = -P_s$$

$$\frac{\partial r}{\partial \omega} = \frac{R}{r}\,(Py_\omega - Qx_\omega) \tag{B.5-9}$$

The Evaluation of the p.d. with Regard to R

$$\frac{\partial r}{\partial R} = \frac{R^2 + r^2 - r_\omega^2}{2Rr} \tag{B.5-10}$$

The Evaluation of the p.d. with Regard to ψ

$$\frac{\partial r}{\partial \psi} = \frac{R}{r}\,[(P_c \sin\psi - P_s \cos\psi)x_\omega + (Q_c \sin\psi - Q_s \cos\psi)y_\omega] \tag{B.5-11}$$

The Evaluation of the p.d. with Regard to $\Delta\lambda_o$

$$\frac{\partial r}{\partial \Delta\lambda_o} = \frac{R\cos\psi}{r}\,[(\sin\Delta\lambda\cos\omega - \cos\Delta\lambda\sin\omega\cos i)\,x_\omega - (\sin\Delta\lambda\sin\omega + \cos\Delta\lambda\cos\omega\cos i)\,y_\omega]$$
$$= \frac{R\cos\psi}{r}\,(P'x_\omega - Q'y_\omega) \tag{B.5-12}$$

Substitution of the second term of equation (B.5-5) into the equation above yields

$$\frac{\partial r}{\partial \Delta\lambda_o} = \frac{\dot{r}}{\omega_e} - \frac{an}{\omega_e r_o}\frac{\partial r}{\partial E_o} = \frac{1}{\omega_e}\left(\dot{r} - \frac{an}{r_o}\frac{\partial r}{\partial E_o}\right) \tag{B.5-13}$$

<u>The Evaluation of the p.d. with Regard to ω_e</u>

$$\frac{\partial r}{\partial \omega_e} = \frac{Rt\cos\psi}{r}(P'x_\omega - Q'y_\omega) = t\frac{\partial r}{\partial \Delta\lambda_o} \tag{B.5-14}$$

B.5.2 GM (or n) Known

The range equation derived in section 4.5.4 is

$$r^2 = r_\omega^2 + R^2 - 2R(Px_\omega + Qy_\omega) \tag{B.5-15}$$

The range-rate equation derived in section 4.7.2 was

$$r\dot{r} = r_\omega\dot{r}_\omega - R(P\dot{x}_\omega + Q\dot{y}_\omega) - R\omega_e\cos\psi(P'x_\omega - Q'y_\omega) \tag{B.5-16}$$

All the variables are as defined in section B.5.1 with the exception of x_ω, y_ω, r_ω. These variables are as developed in Appendix A, sections A.2, A.3.2, A.4.2 and A.5.2.

The evaluation of the partial derivatives of the range with respect to the various parameters is identical to the ones as described in section B.5.1 with the exception of:

- the omission of $\partial r/\partial n$ (not applicable in this case)
- the revised version of $\partial r/\partial a$ and consequently $\partial r/\partial e$
- the replacement of n in all the partial derivatives of section B.5.1 by $\sqrt{GM/a^3}$.

<u>The Evaluation of the p.d. with Regard to a</u>

A similar expression as in section B.4.2 applies here

$$\frac{\partial r}{\partial a} = \frac{r_\omega^2 + r^2 - R^2}{2ar} - \frac{3}{2}\frac{nt}{r_o}\frac{\partial r}{\partial E_o} \qquad \text{(B.5-17)}$$

The Evaluation of the p.d. with Regard to e

A similar expression as in section B.4.2 applies here

$$\frac{\partial r}{\partial e} = aA\frac{\partial r}{a} + \frac{an}{2r_o}(3At+2B)\frac{\partial r}{\partial E_o} \qquad \text{(B.5-18)}$$

The Evaluation of the p.d.'s with Regard to E_o, i, ω, R, ψ, $\Delta\lambda_o$ and ω_e

The partial derivatives with regard to E_o, i, ω, R, ψ, $\Delta\lambda_o$ and ω_e are given in section B.5.1 by the equations (B.5-4), (B.5-8), (B.5-9), (B-5-10), (B.5-11), (B.5-13) and (B.5-14). Wherever the mean motion n appears in the partial derivatives of this section it needs to be evaluated as $\sqrt{GM/a^3}$. Similarly, wherever the variables x_ω, y_ω, r_ω, $\dot{x}_\omega$, $\dot{y}_\omega$, $\dot{r}_\omega$ appear in the partial derivatives of this section, they need to be evaluated as defined in sections A.2, A.3.2, A.4.1, A.4.2 and A.5.2 of Appendix A.

B.6 Three Dimensional Secularly Perturbed Elliptic Motion in Case of Range Observations

The range and range-rate equations for this case were developed in sections 4.6.1 and 4.7.3 respectively. The partial derivatives for the various parameters will be very similar as developed in section B.5 and will not be repeated as the pattern developed in the sections B.2 through B.5 must be clear to the reader by now. The following exceptions to the above mentioned similarities should be noted. Wherever the argument of perigee ω appears in the equations it needs to be evaluated

as $\omega_o + \dot{\omega}t$. Similarly, the longitude difference $\Delta\lambda$ has now to be evaluated as $(\lambda+GAST_o-\Omega) + (\omega_e-\dot{\Omega})t$ and the angular velocity ω_e has to be replaced by $(\omega_e-\dot{\Omega})$. The partial derivative of the only new parameter $\dot{\omega}$ is easily obtained

$$\frac{\partial r}{\partial \dot{\omega}} = t\,\frac{\partial r}{\partial \omega_o} \tag{B.6-1}$$

with $\partial r/\partial\omega_o$ equal to $\partial r/\partial\omega$ as in section B.5.

B.7 Partial Derivatives in Case of Range-Rate Observations

In the sections concerning the partial derivatives in case of range observations (sections B.2 through B.6) the corresponding range-rate equation was always given (to simplify the expressions of the partial derivatives for range observations). With the help of the range equation and the corresponding partial derivatives for the ranges the partial derivatives for range-rate observations are easily obtained. Denoting the parameter for which a partial derivative is computed, by p_i one has

$$\frac{\partial(r\dot{r})}{\partial p_i} = \dot{r}\,\frac{\partial r}{\partial p_i} + r\,\frac{\partial \dot{r}}{\partial p_i} \tag{B.7-1}$$

from which easily is obtained

$$\frac{\partial \dot{r}}{\partial p_i} = \frac{1}{r}\,\frac{\partial(r\dot{r})}{\partial p_i} - \frac{\dot{r}}{r}\,\frac{\partial r}{\partial p_i} \tag{B.7-2}$$

The only term left to be determined is $\partial(r\dot{r})/\partial p_i$ and is left to the reader to derive.

B.8 Range-Difference Observations as Viewed as a Transformation of Range Observations

Large simplifications in the analysis of range-difference observations are obtained if the range-difference model is viewed as a transformation of the range model.

$$\Delta r_i = r_j - r_i \tag{B.8-1}$$

In matrix form (B.8-1) becomes, using the notation as developed in [Uotila, 1967]

$$(L_b)_{\Delta r_i} = G(L_b)_{r_i} \tag{B.8-2}$$

with

$$G = \begin{bmatrix} -1 & 1 & & & & & & \\ & -1 & 1 & & & & 0 & \\ & & -1 & 1 & & & & \\ & & & -1 & 1 & & & \\ & & & & \ddots & \ddots & & \\ & 0 & & & & \ddots & \ddots & \\ & & & & & & -1 & 1 \end{bmatrix} \tag{B.8-3}$$

Similarly, one has

$$(L_o)_{\Delta r_i} = G(L_o)_{r_i} \tag{B.8-4}$$

and

$$\begin{aligned} (L)_{\Delta r_i} &= (L_o)_{\Delta r_i} - (L_b)_{\Delta r_i} \\ &= G[(L_o)_{r_i} - (L_b)_{r_i} \\ &= G(L)_{r_i} \end{aligned} \tag{B-8-5}$$

Assuming uncorrelated range observations

$$\Sigma_{r_i} = \sigma_o^2 I \tag{B.8-6}$$

the variance/covariance matrix for the range-difference observations becomes

$$\Sigma_{\Delta r_i} = G\Sigma_{r_i} G^T = \sigma_o^2 GG^T \tag{B.8-7}$$

The weight coefficient of the range differences is then

$$Q_{\Delta r_i} = \sigma_o^{-2}\Sigma_{\Delta r_i} = GG^T = \begin{bmatrix} 2 & -1 & & & & \\ -1 & 2 & -1 & & 0 & \\ & -1 & 2 & -1 & & \\ & & -1 & 2 & & \\ & 0 & & & 2 & -1 \\ & & & & -1 & 2 \end{bmatrix} \tag{B.8-8}$$

The computation of the weight matrix, the inverse of the weight coefficient matrix, would be time consuming if one does not take advantage of the elegant structure of the matrix $Q_{\Delta r_i}$.

Empirically, it was found that the inverse can be computed in an analytic manner:

$$\left[P_{\Delta r_i}\right]_{r,c} = \frac{r(n+1-c)}{n+1} \quad \text{for } c \geq r \tag{B.8-9}$$

where n, r and c are integers denoting respectively the number of range-difference observations, the row number of the matrix element and the column number of the matrix element.

As an example, assume n = 5.

Then

$$Q_{\Delta r_i} = \begin{bmatrix} 2 & -1 & 0 & 0 & 0 \\ & 2 & -1 & 0 & 0 \\ & & 2 & -1 & 0 \\ & & & 2 & -1 \\ s & & & & 2 \end{bmatrix}$$

and

$$P_{\Delta r_i} = \frac{1}{6}\begin{bmatrix} 5 & 4 & 3 & 2 & 1 \\ & 8 & 6 & 4 & 2 \\ & & 9 & 6 & 3 \\ & & & 8 & 4 \\ s & & & & 5 \end{bmatrix}$$

Not only the observation vector but also the design matrix for the range difference model is obtained by transforming the design matrix for the range model. Without derivation, one clearly has

$$A_{\Delta r_i} = GAr_i \tag{B.8-10}$$

The normal matrix for the range difference observations becomes

$$N_{\Delta r_i} = A^T_{\Delta r_i} P_{\Delta r_i} A_{\Delta r_i} \tag{B.8-11}$$

Using (B.8-8) and (B.8-10) in (B.8-11) one obtains

$$N_{\Delta r_i} = A^T_{r_i} G^T (GG^T)^{-1} GA_{r_i} \tag{B.8-12}$$

which might be written as

$$N_{\Delta r_i} = A^T_{r_i} \overline{P}_{r_i} A_{r_i} \tag{B.8-13}$$

with the special weight matrix $\overline{P}_{r_i}$ being

$$\overline{P}_{r_i} = G^T (GG^T)^{-1} G \tag{B.8-14}$$

Empirically, it was found that

$$[G^T (GG^T)^{-1} G]_{r,c} = \frac{1}{n+1} \begin{cases} n \text{ for } r = c \\ -1 \text{ for } r \neq c \end{cases} \tag{B.8-15}$$

Using the same example for n = 5 one has

$$G(GG^T)^{-1}G = \frac{1}{6}\begin{bmatrix} 5 & -1 & -1 & -1 & -1 \\ & 5 & -1 & -1 & -1 \\ & & 5 & -1 & -1 \\ & & & 5 & -1 \\ s & & & & 5 \end{bmatrix} \qquad \text{(B.8-16)}$$

A similar reasoning for the U-vector in the normal equations leads to

$$U_{\Delta r_i} = A^T_{\Delta r_i} P_{\Delta r_i} L_{\Delta r_i} \qquad \text{(B.8-17)}$$

Substituting (B.8-10), (B.8-8) and (B.8-5) in (B.8-17) one obtains

$$\begin{aligned} U_{\Delta r_i} &= A^T_{r_i} G^T (GG^T)^{-1} G L_{r_i} \\ &= A^T_{r_i} \overline{P}_{r_i} L_{r_i} \end{aligned} \qquad \text{(B.8-18)}$$

This makes the similarity between the range and range-difference models complete:

Range Observations	Range-Difference Observations
r_i	$\Delta r_i = G r_i$
$\Sigma_{r_i} = \sigma_o^2 P_{r_i}^{-1} = \sigma_o^2 I$	$\Sigma_{\Delta r_i} = G \Sigma_{r_i} G^T = \sigma_o^2 G G^T$
$X = -(A_{r_i}^T P_{r_i} A_{r_i})^{-1} A_{r_i}^T P_{\ i} L_{r_i}$	$X = -(A_{r_i}^T \overline{P}_{r_i} A_{r_i})^{-1} A_{r_i}^T \overline{P}_{r_i} L_{r_i}$
$\Sigma_x = \hat{\sigma}_o^2 (A_{r_i}^T P_{r_i} A_{r_i})^{-1}$	$\Sigma_x = \hat{\sigma}_o^2 (A_{r_i}^T \overline{P}_{r_i} A_{r_i})^{-1}$
with	with
$P_{r_i} = I$	$\overline{P}_{r_i} = G^T (G G^T)^{-1} G$
and	and
$[I]_{r,c} = \begin{cases} 1 \text{ for } r = c \\ o \text{ for } r \neq c \end{cases}$	$[G^T (G G^T)^{-1} G]_{r,c} = \frac{1}{n+1} \begin{cases} n \text{ for } r = c \\ -1 \text{ for } r \neq c \end{cases}$

It should be understood that this transformation needs to be applied each time a new pass of ranges/range-differences has been observed.

APPENDIX C

SIMULTANEOUS RANGE OBSERVATIONS AND THE GRAM DETERMINANT

The International Dictionary of Applied Mathematics [IDAM, 1960, p. 412] gives the following definition of a Gram Determinant:

> "The Gram Determinant of n functions (or vectors) $f_1, f_2, \ldots, f_n$ is the determinant of the n x n matrix whose general term is (f_i, f_j), namely the scalar product of f_i and f_j. The vanishing of the Gram Determinant (or Gramian) is necessary and sufficient for linear dependence of the functions (or vectors)."

This definition becomes once clear if one considers the normal rix in least squares methods as a Gram matrix.

Having a design matrix A,

$$A = \begin{bmatrix} a_{11} & a_{12} \\ a_{21} & a_{22} \\ a_{31} & a_{32} \end{bmatrix} \qquad \text{(C-1)}$$

the normal matrix N becomes, omitting weights,

$$N = A^T A = \begin{bmatrix} a_{11}^2 + a_{21}^2 + a_{31}^2 & a_{11}a_{12} + a_{21}a_{22} + a_{31}a_{32} \\ a_{12}a_{11} + a_{22}a_{21} + a_{32}a_{31} & a_{12}^2 + a_{22}^2 + a_{32}^2 \end{bmatrix} \qquad \text{(C-2)}$$

If one considers the design matrix A as built up from two column vectors, (C-1) becomes

$$A = \left[\bar{a}_1, \bar{a}_2\right] \tag{C-3}$$

The normal matrix becomes, written in scalar products,

$$N = \begin{bmatrix} (\bar{a}_1, \bar{a}_1) & (\bar{a}_1, \bar{a}_2) \\ (\bar{a}_2, \bar{a}_1) & (\bar{a}_2, \bar{a}_2) \end{bmatrix} \tag{C-4}$$

The rephrased definition will read as follows:

> "The Gram Determinant (i.e. the determinant of the normal matrix) of u vectors $\bar{a}_1, \bar{a}_2, \ldots, \bar{a}_u$ is the determinant of a u x u matrix whose general term is $(\bar{a}_i, \bar{a}_j)$. The vanishing of the Gramian (the determinant of the normal matrix being zero) is necessary and sufficient for linear dependence of the vectors."

This fact is well known to geodesists: you cannot invert the normal matrix when the columns in the design matrix are linear dependent. Applying this knowledge to geometry: four vectors in three dimensional space are linearly dependent (Fig. C.1), see also [Kowalevsky, 1948].

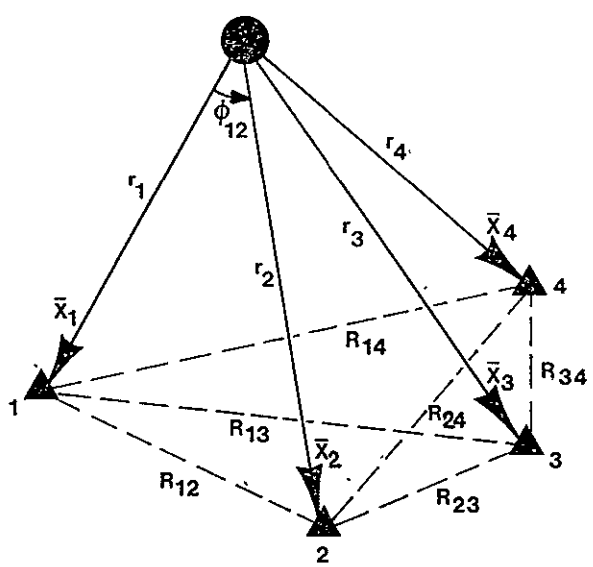

Figure C.1. Four Vectors in Three Dimensional Space

Using the approach followed above the Gram Determinant must be equal to zero for these four vectors

$$|G| = \begin{vmatrix} (\bar{x}_1,\bar{x}_1) & (\bar{x}_1,\bar{x}_2) & (\bar{x}_1,\bar{x}_3) & (\bar{x}_1,\bar{x}_4) \\ & (\bar{x}_2,\bar{x}_2) & (\bar{x}_2,\bar{x}_3) & (\bar{x}_2,\bar{x}_4) \\ & & (\bar{x}_3,\bar{x}_3) & (\bar{x}_3,\bar{x}_4) \\ s & & & (\bar{x}_4,\bar{x}_4) \end{vmatrix} = 0 \qquad \text{(C-5)}$$

Equation (C-5) is exactly the one condition which corresponds to the difference between the ten possible distances and the nine necessary and sufficient distances to determine a polyhedron with five vertices (Figure C.1). Writing out each scalar product in the Gram Determinant in terms of the distances between the five points one has with the help of Figure C.1:

$$(\bar{x}_i,\bar{x}_j) = r_i r_j \cos \phi_{ij} \qquad \text{(C-6)}$$

Using the cosine rule,

$$R_{ij}^2 = r_i^2 + r_j^2 - 2r_i r_j \cos \phi_{ij} \qquad \text{(C-7)}$$

equation (C-6) becomes

$$(\bar{x}_i,\bar{x}_j) = 1/2\ (r_i^2 + r_j^2 - R_{ij}^2) \qquad \text{(C-8)}$$

If $i = j$, then $R_{ij} = 0$ and (C-8) still holds (for the diagonal elements of the Gramian):

$$|G| = \begin{vmatrix} 2r_1^2 & r_1^2+r_2^2-R_{12}^2 & r_1^2+r_3^2-R_{13}^2 & r_1^2+r_4^2-R_{14}^2 \\ & 2r_2^2 & r_2^2+r_3^2-R_{23}^2 & r_2^2+r_4^2-R_{24}^2 \\ & & 2r_3^2 & r_3^2+r_4^2-R_{34}^2 \\ & & & 2r_4^2 \end{vmatrix}_s = 0 \qquad \text{(C-9)}$$

Viewing the origin of the four vectors as a satellite and the end points of the vectors as ground stations, the Gram Determinant forms the mathematical model for simultaneous ranging analyzed in the geometric mode. The model is a function of the measured ranges r_i and the unknown interstation distances R_{ij}. This elegant method, which circumvents the necessity of inner constraints since it consists of estimable parameters, is applied in [Aardoom, 1970 and 1971].

The simulations in the geometric mode as reported in section 6.8 is solely based on this Gramian approach.

One of the disadvantages of this model is its high nonlinearity: the Gramian consists of terms each a function of distances (either observations or unknowns) raised to the eighth power! Despite this the linearized form of the Gramian takes on an easily programmable identity. The partial derivatives of the Gramian with respect to the parameters (R_{ij}) and the observations (r_i) are, using [Uotila, 1967]

$$\frac{\partial F}{\partial X_a} = A \qquad \text{(C-10)}$$

and

$$\frac{\partial F}{\partial X_b} = B \qquad \text{(C-11)}$$

with $$F = F(L_a, X_a) = 0 \tag{C-12}$$

Equation (C-12) becomes in this case

$$|G| = F(L_a, X_a) = F(r_i, R_{ij}) = 0 \tag{C-13}$$

<u>The Evaluation of the p.d. with Regard to R_{ij}</u>

$$\begin{aligned}\frac{\partial|G|}{\partial R_{ij}} = A_p^{ij} = 4R_{ij}(&a_{ij}a_{kk}a_{ll} - a_{ij}a_{kl}a_{kl} + \\ &- a_{ik}a_{jk}a_{ll} + a_{ik}a_{jl}a_{kl} + \\ &+ a_{il}a_{jk}a_{kl} - a_{il}a_{jl}a_{kk})\end{aligned} \tag{C-14}$$

with $$a_{ij} = r_i^2 + r_j^2 - R_{ij}^2 \tag{C-15}$$

For the six parameters the indices in (C-14) go through the following cycle

p	i	j	k	l
1	1	2	3	4
2	1	3	2	4
3	1	4	3	2
4	2	3	1	4
5	2	4	3	1
6	3	4	1	2

The Evaluation of the p.d. with Regard fo r_i

$$
\begin{aligned}
\frac{\partial |G|}{\partial r_i} = B_i = 4r_i(&a_{jj}a_{kk}a_{ll} - a_{jj}a_{kl}a_{kl} + \\
&- a_{jk}a_{jk}a_{ll} + a_{jk}a_{jl}a_{kl} + \\
&+ a_{jk}a_{jl}a_{kl} - a_{jl}a_{jl}a_{kk} + \\
&- a_{ij}a_{kk}a_{ll} + a_{ij}a_{kl}a_{kl} + \\
&+ a_{ik}a_{jk}a_{ll} + a_{ij}a_{jk}a_{ll} + \\
&- a_{ik}a_{jl}a_{kl} - a_{ij}a_{jl}a_{kl} + \\
&- a_{il}a_{jk}a_{kl} - a_{ij}a_{jk}a_{kl} + \\
&+ a_{il}a_{jl}a_{kk} + a_{ij}a_{jl}a_{kk} + \\
&- a_{ik}a_{jj}a_{ll} + a_{il}a_{jj}a_{kl} + \\
&+ a_{ik}a_{jj}a_{kl} + a_{ik}a_{jl}a_{jl} + \\
&- a_{il}a_{jk}a_{jl} - a_{ik}a_{jk}a_{jl} + \\
&- a_{il}a_{jj}a_{kk} + a_{il}a_{jk}a_{jk})
\end{aligned}
\qquad \text{(C-16)}
$$

For the four observations the indices in (C-16) go through the following cycle

i	j	k	l
1	2	3	4
2	1	3	4
3	2	1	4
4	2	3	1

The evaluation of $|G|_o = W = F(L_b, X)$

$$
\begin{aligned}
|G|_o = {} & a_{ii}a_{jj}a_{kk}a_{ll} - a_{ii}a_{jj}a_{kl}a_{kl} + \\
& - a_{ii}a_{jk}a_{jk}a_{ll} - a_{ii}a_{jl}a_{jl}a_{kk} + \\
& - a_{ij}a_{ij}a_{kk}a_{ll} + a_{ij}a_{ij}a_{kl}a_{kl} + \\
& - a_{ik}a_{ik}a_{jj}a_{ll} + a_{ik}a_{ik}a_{jl}a_{jl} + \\
& - a_{il}a_{il}a_{jj}a_{kk} + a_{il}a_{il}a_{jk}a_{jk} + \\
& + 2(a_{ii}a_{jk}a_{jl}a_{kl} + a_{ij}a_{ik}a_{jk}a_{ll} + \\
& \quad - a_{ij}a_{ik}a_{jl}a_{kl} - a_{ij}a_{il}a_{jk}a_{jl} + \\
& \quad + a_{ij}a_{il}a_{jl}a_{kk} + a_{ik}a_{il}a_{jj}a_{kl} + \\
& \quad - a_{ik}a_{il}a_{jk}a_{jl})
\end{aligned}
\qquad \text{(C-17)}
$$

with

$$i = 1$$

$$j = 2$$

$$k = 3$$

$$l = 4$$

In equation (C-16) as well as (C-17) a_{ij} is given by (C-15).

APPENDIX D

SOME MATRIX PROPERTIES

D.1 Differentiation of Rotation Matrices

Designating positive (counter clockwise) rotations of a coordinate system over angles α, β, γ about the x, y, z-axes (as viewed from the positive ends of these axes) by $R_1(\alpha)$, $R_2(\beta)$ and $R_3(\gamma)$ respectively, one has

$$R_1(\alpha) = \begin{bmatrix} 1 & 0 & 0 \\ 0 & \cos\alpha & \sin\alpha \\ 0 & -\sin\alpha & \cos\alpha \end{bmatrix} \tag{D.1-1}$$

$$R_2(\beta) = \begin{bmatrix} \cos\beta & 0 & -\sin\beta \\ 0 & 1 & 0 \\ \sin\beta & 0 & \cos\beta \end{bmatrix} \tag{D.1-2}$$

$$R_3(\gamma) = \begin{bmatrix} \cos\gamma & \sin\gamma & 0 \\ -\sin\gamma & \cos\gamma & 0 \\ 0 & 0 & 1 \end{bmatrix} \tag{D.1-3}$$

For instance, in the development of observation equations it is necessary to differentiate rotation matrices whenever the rotation angles are part of the set of parameters to be estimated. Often simpler formulas can be obtained by viewing the differentiated rotation matrix

as the product of the original matrix and an auxiliary matrix. This transformation matrix is often referred to as the "Lucas matrix" in the geodetic and photogrammetric literature [Lucas, 1963].

Differentiating (D.1-1) with respect to α one has

$$\frac{\partial R_1(\alpha)}{\partial \alpha} = \begin{bmatrix} 0 & 0 & 0 \\ 0 & -\sin\alpha & \cos\alpha \\ 0 & -\cos\alpha & -\sin\alpha \end{bmatrix} \tag{D.1-4}$$

This matrix can be viewed as

$$\begin{bmatrix} 0 & 0 & 0 \\ 0 & -\sin\alpha & \cos\alpha \\ 0 & -\cos\alpha & \sin\alpha \end{bmatrix} = \begin{bmatrix} 0 & 0 & 0 \\ 0 & 0 & 1 \\ 0 & -1 & 0 \end{bmatrix} \begin{bmatrix} 1 & 0 & 0 \\ 0 & \cos\alpha & \sin\alpha \\ 0 & -\sin\alpha & \cos\alpha \end{bmatrix} \tag{D.1-5}$$

$$= \begin{bmatrix} 1 & 0 & 0 \\ 0 & \cos\alpha & \sin\alpha \\ 0 & -\sin\alpha & \cos\alpha \end{bmatrix} \begin{bmatrix} 0 & 0 & 0 \\ 0 & 0 & 1 \\ 0 & -1 & 0 \end{bmatrix} \tag{D.1-6}$$

or in short

$$\frac{\partial R_1(\alpha)}{\partial \alpha} = L_1 R_1(\alpha) = R_1(\alpha) L_1 \tag{D.1-7}$$

with

$$L_1 = \begin{bmatrix} 0 & 0 & 0 \\ 0 & 0 & 1 \\ 0 & -1 & 0 \end{bmatrix} \tag{D.1-8}$$

Similar expressions can be derived for rotations around the y- and z-axes:

$$\frac{\partial R_2(\beta)}{\partial \beta} = L_2 R_2(\beta) = R_2(\beta) L_2 \tag{D.1-9}$$

with

$$L_2 = \begin{bmatrix} 0 & 0 & -1 \\ 0 & 0 & 0 \\ 1 & 0 & 0 \end{bmatrix} \tag{D.1-10}$$

and

$$\frac{\partial R_2(\gamma)}{\partial \gamma} = L_3 R_3(\gamma) = R_3(\gamma) L_3 \tag{D.1-11}$$

with

$$L_3 = \begin{bmatrix} 0 & 1 & 0 \\ -1 & 0 & 0 \\ 0 & 0 & 0 \end{bmatrix} \tag{D.1-12}$$

Two examples will illustrate the advantage of the use of Lucas-matrices:

<u>Example 1</u>: In forming the observation equations during satellite data analyses, what are the partial derivatives of the positional part of the inertial state vector with respect to the right ascension of the ascending node Ω?

The inertial vector $\overline{X}_{in}$ in terms of the coordinates of the satellite in the orbital plane $\overline{x}_\omega$ are (Keplerian case):

$$\overline{X}_{in} = \mathbb{R}\overline{x}_\omega \tag{D.1-13}$$

with

$$\mathbb{R} = R_3(-\Omega) R_1(-i) R_3(-\omega) \tag{D.1-14}$$

Differentiating (D.1-13) with regard to Ω, one gets

$$\frac{\partial \overline{X}_{in}}{\partial \Omega} = \frac{\partial \mathbb{R}}{\partial \Omega} \overline{x}_\omega + \mathbb{R} \frac{\partial \overline{x}_\omega}{\partial \Omega} \tag{D.1-15}$$

Now is

$$\frac{\partial \overline{x}_\omega}{\partial \Omega} = \overline{0} \tag{D.1-16}$$

and

$$\frac{\partial \mathbb{R}}{\partial \Omega} = \frac{\partial R_3(-\Omega)}{\partial(-\Omega)} \frac{\partial(-\Omega)}{\partial \Omega} R_1(-i) R_3(-\omega) \tag{D.1-17}$$

This equation simplifies to, using (D.1-11) and (D.1-12)

$$\frac{\partial \mathbb{R}}{\partial \Omega} = -L_3 \mathbb{R} \tag{D.1-18}$$

Substituting (D.1-16) and (D.1-18) into (D.1-15) one has

$$\frac{\partial \overline{X}_{in}}{\partial \Omega} = -L_3 \mathbb{R} \overline{x}_\omega = -L_3 \overline{X}_{in} = \begin{bmatrix} -Y \\ X \\ 0 \end{bmatrix}_{in} \tag{D.1-19}$$

This is a rather simple expression if one considers the alternative of differentiating each individual element of the $\mathbb{R}$-matrix with regard to $\overline{\Omega}$.

<u>Example 2</u>: Compute the velocity part $\dot{\overline{X}}_{ef}$ of the state vector in an earth-fixed system.

Having

$$\overline{X}_{in} = \mathbb{R} \overline{x}_\omega \tag{D.1-20}$$

and

$$\overline{X}_{ef} = R_3(\theta_o + \omega_e t) \overline{X}_{in} \tag{D.1-21}$$

which neglects precession and nutation, the time derivatives of (D.1-20) become

$$\frac{\partial \bar{X}_{ef}}{\partial t} = \dot{\bar{X}}_{ef} = \frac{\partial R_3(\theta_o+\omega_e t)}{\partial t} \mathbb{R}\bar{x}_\omega + R_3(\theta_o+\omega_e t) \frac{\partial \mathbb{R}}{\partial t}\bar{x}_\omega$$

$$+ R_3(\theta_o+\omega_e t)\mathbb{R}\frac{\partial \bar{x}_\omega}{\partial t} \qquad \text{(D.1-22)}$$

With the help of (D.1-11), (D.1-12) and (D.1-21) and the assumption that the R matrix is time independent, (D.1-22) simplifies to

$$\dot{\bar{X}}_{ef} = \omega_e L_3 \bar{X}_{ef} + R_3(\theta_o+\omega_e t)\mathbb{R}\dot{\bar{x}}_\omega \qquad \text{(D.1-23)}$$

or

$$\dot{\bar{X}}_{ef} = R_2(\theta_o+\omega_e t)\dot{\bar{X}}_{in} + \omega_e \begin{bmatrix} Y \\ -X \\ 0 \end{bmatrix}_{ef} \qquad \text{(D.1-24)}$$

Combining the results of (D.1-20), (D.1-21) and (D.1-24) into a full state vector representation one has

$$\begin{bmatrix} X & \dot{X} \\ Y & \dot{Y} \\ Z & \dot{Z} \end{bmatrix}_{ef} = R_3(\theta_o+\omega_e t) \begin{bmatrix} X & \dot{X} \\ Y & \dot{Y} \\ Z & \dot{Z} \end{bmatrix}_{in} + \omega_e \begin{bmatrix} 0 & Y \\ 0 & -X \\ 0 & 0 \end{bmatrix}_{ef} \qquad \text{(D.1-25)}$$

In computing algorithms, the implication of (D.1-25) is that the left column of the earth-fixed state matrix needs to be computed before the right column because of the appearance of two earth-fixed positional elements at the right hand side of (D.1-25).

<u>Example 3</u>: Lucas matrices can also be applied to rotation matrices in case of differentially small angles.

Applying (D.1-1) to a small angle $\Delta\alpha$:

$$R_1(\Delta\alpha) = \begin{bmatrix} 1 & 0 & 0 \\ 0 & \cos\Delta\alpha & \sin\Delta\alpha \\ 0 & -\sin\Delta\alpha & \cos\Delta\alpha \end{bmatrix} \tag{D.1-26}$$

$$\simeq \begin{bmatrix} 1 & 0 & 0 \\ 0 & 1 & \Delta\alpha \\ 0 & -\Delta\alpha & 1 \end{bmatrix} \tag{D.1-27}$$

Using the Lucas matrix (D.1-8) $R_1(\Delta\alpha)$ can clearly be written as

$$R_1(\Delta\alpha) = I + \Delta\alpha L_1 \tag{D.1-28}$$

Similar expressions can be derived for small rotations around the y- and z-axes

$$R_2(\Delta\beta) = I + \Delta\beta L_2 \tag{D.1-29}$$

and

$$R_3(\Delta\gamma) = I + \Delta\gamma L_3 \tag{D.1-30}$$

D.2 Inversion of a Differentially Changed Matrix

In weighted least-squares procedures it may happen that one only wants to consider the weighting of parameters after one has already solved the unweighted case. Rephrased, what is the new inverted normal matrix (with weighted parameters) expressed in terms of the inverse of the original normal matrix (with unweighted parameters)? The purpose is to avoid a (probably costly) second inversion of the normal matrix.

The problem is to express $(A + \Delta A)^{-1}$ in terms of A^{-1} and ΔA, assuming that A is a (square) invertable matrix.

$$(A+\Delta A)(A^{-1}+\Delta_1 A^{-1}) = I \tag{D.2-1}$$

Multiplying (D.2-1) out, one has

$$AA^{-1} + \Delta AA^{-1} + A\Delta_1 A^{-1} + \Delta A\Delta_1 A^{-1} = I \tag{D.2-2}$$

Assuming $\Delta A\Delta_1 A^{-1} \simeq [0]$, one finds

$$\Delta_1 A^{-1} \simeq -A^{-1}\Delta AA^{-1} \tag{D.2-3}$$

As an example from weighted least squares procedures (A is now the design matrix), one has

$$(A^T PA+P_x)^{-1} \simeq (A^T PA)^{-1} - (A^T PA)^{-1}P_x(A^T PA)^{-1} \tag{D.2-4}$$

$$\simeq N^{-1}(I-P_x N^{-1}) = (I-N^{-1}P_x)N^{-1} \tag{D.2-5}$$

If $\Delta A\Delta_1 A^{-1}$ is not negligibly small, one continues the above followed reasoning once more,

$$(A+\Delta A)^{-1}\ (A^{-1}-A^{-1}\Delta AA^{-1}+\Delta_2 A^{-1}) = I \tag{D.2-6}$$

Multiplying (D.2-6) out and solving for $\Delta_2 A^{-1}$ one finds,

$$\Delta_2 A^{-1} = A^{-1}\Delta AA^{-1}\Delta AA^{-1} \tag{D.2-7}$$

In general, one has

$$(A+\Delta A)(A^{-1}+\Delta A^{-1}) = I \tag{D.2-8}$$

with

$$\Delta A^{-1} = \sum_{i=1}^{\infty} \Delta_i A^{-1} \tag{D.2-9}$$

and

$$\Delta_i A^{-1} = (-1)^i A^{-1}(\Delta A A^{-1})^i \tag{D.2-10}$$

$$= (-1)^i (A^{-1}\Delta A)^i A^{-1} \tag{D.2-11}$$

Consequently,

$$(A+\Delta A)^{-1} = A^{-1} \sum_{i=0}^{\infty} (-\Delta A A^{-1})^i \tag{D.2-12}$$

or

$$= \sum_{i=0}^{\infty} (-A^{-1}\Delta A)^i A^{-1} \tag{D.2-13}$$

The notation used in (D.2-12) and (D.2-13) assumes that a matrix raised to the zero power is equal to the identity matrix.

Similar expressions are derived in [Bodewig, 1959, p. 36] by differentiating the expression $AA^{-1} = I$, obtaining a Taylor series for $(A + \Delta A)^{-1}$.

<u>Example</u>: A small example illustrates the power of the method and in addition it is shown that the addition ΔA to the original matrix A does not necessarily has to have a differential character. However, convergence of the Taylor series still depends on the nature of ΔA [Bodewig, 1959, p. 37].

Invert the matrix B

$$B = \begin{bmatrix} 3 & 1 \\ 1 & 2 \end{bmatrix} \tag{D.2-14}$$

by splitting up B in a matrix B_d and a matrix ΔB with

$$\Delta B = B - B_d \tag{D.2-15}$$

The matrix B_d is assumed to be equal to

$$B_d = \begin{bmatrix} 3 & 1 \\ 1 & 1 \end{bmatrix} \tag{D.2-16}$$

yielding

$$\Delta B = \begin{bmatrix} 0 & 0 \\ 0 & 1 \end{bmatrix} \tag{D.2-17}$$

The solution using (D.2-12) term by term is

- first term $$B_d^{-1} = \begin{bmatrix} \frac{1}{2} & -\frac{1}{2} \\ -\frac{1}{2} & \frac{3}{2} \end{bmatrix}$$

- second term $$-B_d^{-1}(\Delta B B_d^{-1}) = \begin{bmatrix} -\frac{1}{4} & \frac{3}{4} \\ \frac{3}{4} & -\frac{9}{4} \end{bmatrix}$$

- third term $$+B_d^{-1}(\Delta B B_d^{-1})^2 = \begin{bmatrix} \frac{3}{8} & -\frac{9}{8} \\ -\frac{9}{8} & \frac{27}{8} \end{bmatrix}$$

- fourth term $$-B_d^{-1}(\Delta B B_d^{-1})^3 = \begin{bmatrix} -\frac{9}{16} & \frac{27}{16} \\ \frac{27}{16} & -\frac{81}{16} \end{bmatrix}$$

- fifth term $\qquad +B_d^{-1}(\Delta B B_d^{-1})^4 = \begin{bmatrix} \frac{27}{32} & -\frac{81}{32} \\ -\frac{81}{32} & \frac{243}{32} \end{bmatrix}$

- etc.

Setting $\qquad B^{-1} = \begin{bmatrix} b'_{11} & b'_{12} \\ b'_{21} & b'_{22} \end{bmatrix}$

we find for b'_{11}

$$b'_{11} = \frac{1}{2} - \frac{1}{4} + \frac{3}{8} - \frac{9}{16} + \ldots = \frac{1}{2} - \frac{1}{4}(1 - \frac{3}{2} + \frac{9}{4} - \frac{27}{16} + \ldots)$$

The second term in the product is the binomial series

$$(1-x)^{-1} = 1 + x + x^2 + \ldots$$

with $\qquad x = -\frac{3}{2}$

Consequently, $\qquad b'_{11} = \frac{1}{2} - \frac{1}{4}(1 + \frac{3}{2})^{-1} = \frac{2}{5} \qquad$ (D.2-18)

In a similar fashion we find from binomial series with $x = -\frac{3}{2}$

$$b'_{22} = 1 - (1-x)^{-1} = \frac{3}{5} \qquad \text{(D.2-19)}$$

and $\qquad b'_{12} = b'_{21} = -\frac{1}{2}(1-x)^{-1} = -\frac{1}{5} \qquad$ (D.2-20)

Equations (D.2-18) through (D.2-20) yield the following inverse

$$B^{-1} = \begin{bmatrix} \frac{2}{5} & -\frac{1}{5} \\ -\frac{1}{5} & \frac{3}{5} \end{bmatrix} = \frac{1}{5} \begin{bmatrix} 2 & -1 \\ -1 & 3 \end{bmatrix} \tag{D.2-21}$$

which agrees with the "normally" computed inverse of (D.2-14).

REFERENCES

Aardoom, L., 1970. "Geometry from Simultaneous Satellite Ranging," Tellus, Vol. XXII, No. 5, 572-580.

Aardoom, L., 1971. "Geometric Accuracy Obtainable from Simultaneous Range Measurements to Satellites," in The Use of Artificial Satellites for Geodesy, Henriksen, S. W., A. Mancini and B. H. Chovitz (Editors), Geophysical Monograph Series, Vol. 15, American Geophysical Union, Washington, D. C., 9-18.

Agreen, R. W. and D. E. Smith, 1973. "A Simulation of the San Andreas Fault Experiment," GSFC-X-592-73-216, Goddard Space Flight Center, Greenbelt, Maryland.

Aksnes, K., 1970. "A Second-Order Artificial Satellite Theory Based on an Intermediate Orbit," The Astronomical Journal, Vol. 75, No. 9, 1066-1076.

Aksnes, K., 1972. "On the Use of the Hill Variables in Artificial Satellite Theory: Brouwer's Theory," Astronomy and Astrophysics, Vol. 17, No. 1, 70-75.

The American Ephemeris and Nautical Almanac (AENA), 1976. Issued by the Nautical Almanac Offices of the United States Naval Observatory and the Royal Greenwich Observatory, U. S. Government Printing Office, Washington, D. C.

Arur, M. G., 1977. "Experiments for Improved Positioning by Means of Integrated Doppler Satellite Observations and the NNSS Broadcast Ephemeries," Report No. 258, Department of Geodetic Science, The Ohio State University, Columbus, Ohio.

Baarda, W., 1968. "A Testing Procedure for Use in Geodetic Networks," Publications on Geodesy, New Series. Netherlands Geodetic Commission, Vol. 2, No. 5, Delft, Netherlands.

Baarda, W., 1975. "Difficulties in Establishing a Model for Testing Crustal Movements," in Progress in Geodynamics, Borradaile G. J., A. R. Ritsema, H. E. Rondeel and O. J. Simon (Editors), North-Holland Publishing Company, Amsterdam, Netherlands, 45-51.

Bjerhammar, A., 1973. Theory of Errors and Generalized Matrix Inverses. Elsevier Scientific Publishing Company, Amsterdam, Netherlands.

Blaha, G., 1971a. "Inner Adjustment Constraints with Emphasis on Range Observations," Report No. 148, Department of Geodetic Science, The Ohio State University, Columbus, Ohio.

Blaha, G., 1971b. "Investigations of Critical Configurations for Fundamental Range Networks," Report No. 150, Department of Geodetic Science, The Ohio State University, Columbus, Ohio

Bodewig, E., 1959. Matrix Calculus, North-Holland Publishing Company, Amsterdam, Netherlands.

Bossler, J., 1973. "A Note on the Meaning of Generalized Inverse Solutions in Geodesy," Journal of Geophysical Research, Vol. 78, No. 14, 2616-2617.

Brouwer, D. and G. M. Clemence, 1961. Methods of Celestial Mechanics, Academic Press, New York, New York.

Brown, D. C. and J. E. Trotter, 1969. "SAGA, A Computer Program for Short Arc Geodetic Adjustment of Satellite Observations," AFCRL-69-0080, Air Force Cambridge Research Laboratories, Bedford, Massachusetts.

Brown, D. C. and J. E. Trotter, 1973. "Extensions to SAGA for the Geodetic Reduction of Doppler Operations," AFCRL-TR-73-0177, Air Force Cambridge Research Laboratories, Bedford, Massachusetts.

Condon, S. P., 1974. "Sequential Filtering to the Determination of Satellite Tracking Station Locations," AMRL-1059, Applied Mechanics Research Laboratory, The University of Texas at Austin, Austin, Texas

Coolidge, J. L., 1940. A History of Geometrical Methods, Oxford University Press. Republication by Dover Publications, Inc., New York, New York, 1963.

Descartes, R., 1637. La Géométrie or The Geometry of René Descartes, Translated from the French and Latin by Smith, D. E. and M. L. Latham, Open Court Publishing Co. 1925. Republication by Dover Publications, Inc., New York, New York, 1954.

Deutsch, R., 1963. Orbital Dynamics of Space Vehicles, Prentice-Hall, Inc., Englewood Cliffs, New Jersey.

Dubyago, A. D., 1961. The Determination of Orbits, Translated from the Russian by Burke, R. D. et al., The Macmillan Company, New York, New York.

Escobal, P. R., 1976. Methods of Orbit Determination, Robert E. Krieger Publishing Company, Huntington, New York

Fedorov, E. P., 1974. "Magnitudes and Spectra of Important Dynamical Phenomena," in On Reference Coordinate Systems for Earth Dynamics, Kolaczek, B. and G. Weiffenbach (Editors), International Astronomical Union, Colloquium No. 26, Torun, Poland. Institute of Higher Geodesy and Geodetic Astronomy, Warsaw Technical University, Warsaw and The Smithsonian Astrophysical Observatory, Cambridge, Massachusetts, 63-77.

Gaposchkin, E. M., 1973. "1973 Smithsonian Standard Earth (III)," Special Report No. 353, Smithsonian Astrophysical Observatory, Cambridge, Massachusetts.

Gauss, K. F., 1857. Theoria Motus Corporum Coelestium in Sectionibus Conicis Solem Ambientium or Theory of the Motion of the Heavenly Bodies Moving about the Sun in Conic Sections, Translated from the Latin by Davis, C. H. Republication by Dover Publications, Inc., New York, New York, 1963.

Goddard Space Flight Center (GSFC), 1976. "Satellite Laser Ranging Systems Validation Plan." Goddard Space Flight Center, Greenbelt, Maryland.

Grafarend, E. and K. Heinz, 1978. "Rank Defect Analysis of Satellite Geodetic Networks II, Dynamic Mode," Manuscripta Geodetica (in press).

Grafarend, E. and E. Livieratos, 1978. "Rank Defect Analyses of Satellite Geodetic Networks I, Geometric and Semi-Dynamic Mode," Manuscripta Geodetica (in press).

Grafarend, E. and B. Schaffrin, 1974. "Unbiased Free Net Adjustment," Survey Review, Vol. XXII, No. 171, 200-218.

Hamilton, W. C., 1964. Statistics in Physical Sciences (Estimation, Hypothesis Testing, and Least Squares), The Ronald Press Company, New York, New York.

Heiskanen, W. A. and H. Moritz, 1967. Physical Geodesy, W. H. Freeman and Company, San Francisco, California.

International Association of Geodesy (IAG), 1971. "Geodetic Reference System 1967," Special Publication 3, Paris, France.

International Association of Geodesy (IAG), 1975. IAG Resolutions, XVIth General Assemblee, Bulletin Géodésique, No. 118, 363-408.

The International Dictionary of Applied Mathematics (IDAM), 1960. D. van Nostrand Company, Inc., Princeton, New Jersey.

O'Keefe, J. A., A. Eckels and R. K. Squires, 1959. "The Gravitational Field of the Earth," The Astronomical Journal, Vol. 64, No. 7, 245-253.

Kolaczek, B. and G. Weiffenbach (Editors), 1974. On Reference Coordinate Systems for Earth Dynamics, International Astronomical Union, Colloquium No. 26, Torun, Poland. Institute of Higher Geodesy and Geodetic Astronomy, Warsaw Technical University, Warsaw and The Smithsonian Astrophysical Observatory, Cambridge, Massachusetts.

Kovalevsky, J., 1967. Introduction to Celestial Mechanics, Astrophysics and Space Science Library, Vol. 7, D. Reidel Publishing Company, Dordrecht, Netherlands.

Kowalevsky, G., 1948. Einführung in die Determinantentheorie (einschiesslich der Fredholmschen Determinanten), Chelsea Publishing Company, New York, New York.

Kozai, Y., 1960. "Effect of Precession and Nutation on the Orbital Elements of a Close Earth Satellite," The Astronomical Journal, Vol. 64, No. 10, 621-623.

Kozai, Y., 1964. "New Determination of Zonal Harmonics Coefficients of the Earth's Gravitational Potential," Special Report No. 165, Smithsonian Astrophysical Observatory, Cambridge, Massachusetts,

Kozai, Y., 1970. "Seasonal Variations of the Geopotential," Special Report No. 312, Smithsonian Astrophysical Observatory, Cambridge, Massachusetts.

Kozai, Y., 1974. "Hybrid Systems for Use in the Dynamics of Artificial Satellites," in On Reference Coordinate Systems for Earth Dynamics, Kolaczek, B. and G. Weiffenbach (Editors), International Astronomical Union, Colloquium No. 26, Torun, Poland. Institute of Higher Geodesy and Geodetic Astronomy, Warsaw Technical University, Warsaw and the Smithsonian Astrophysical Observatory, Cambridge, Massachusetts, 235-240.

Kozai, Y. and H. Kinoshita, 1973. "Effects of Motion of the Equatorial Plane on the Orbital Elements of an Earth Satellite," Celestial Mechanics, Vol. 7, 356-366.

Kreyszig, E., 1970. Statistische Methoden und ihre Anwendungen, Vandenhoeck & Ruprecht, Göttingen, West Germany.

Lambeck, K., 1971. "Determination of the Earth's Pole of Rotation from Laser Range Observations to Satellites," Bulletin Géodésique, No. 101, 263-281.

Lambeck, K., 1973. "Precession, Nutation and the Choice of Reference System for Close Earth Satellite Orbits," Celestial Mechanics, Vol. 7, 139-155.

Leick, A. and B.H.W. van Gelder, 1975. "On Similarity Transformations and Geodetic Network Distortions Based on Doppler Satellite Observations," Report No. 235, Department of Geodetic Science, The Ohio State University, Columbus, Ohio.

Lucas, J., 1963. "Differentiation of the Orientation Matrix by Matrix Multipliers," Photogrammetric Engineering, Vol. XXIX, No. 4, 708-715.

Mao, N. H. and P. A. Mohr, 1976. "Site Evaluation for Laser Satellite Tracking Stations," Special Report No. 371, Smithsonian Astrophysical Observatory, Cambridge, Massachusetts.

Marsh, J. G. and R. G. Williamson, 1978. "Precision Orbit Computations for Starlette," Bulletin Géodésique, Vol. 52, No. 1, 71-83.

Meissl, P., 1969. "Zusammenfassung und Ausbau der inneren Fehlertheorie eines Punkthaufens," in "Beiträge zur Theorie der geodätischen Netze im Raum," by Rinner, K., K. Killian and P. Meissl, Deutsche Geodätische Kommission, Reihe A, No. 61.

Mueller, I. I., 1969. Spherical and Practical Astronomy (as Applied to Geodesy), Frederick Ungar Publishing Co., New York, New York.

Mueller, I. I., B.H.W. van Gelder and M. Kumar, 1975. "Error Analysis for the Proposed Close Grid Geodynamic Satellite Measurement System (Clogeos)," Report No. 230, Department of Geodetic Science, The Ohio State University, Columbus, Ohio.

Mulholland, J. D. and O. Calame, 1977. "Earth Rotation from Lunar Distances: Basis and Current Status," in Proceedings of the Ninth Annual Precise Time and Time Interval (PTTI) Applications and Planning Meeting, NASA Technical Memorandum 78104, Goddard Space Flight Center, Greenbelt, Maryland.

National Aeronautics and Space Administration (NASA), 1972. "Earth and Ocean Physica Applications Program, Vol. II, Rationale and Program Plans," Washington, D.C.

Newton, R. R., 1974. "Coordinates Used in Range or Range-Rate Systems and Their Extension to a Dynamic Earth," in On Reference Coordinate Systems for Earth Dynamics, Kolaczek, B. and G. Weiffenbach (Editors), International Astronomical Union, Colloquium No. 26, Torun, Poland. Institute of Higher Geodesy and Geodetic Astronomy, Warsaw Technical University, Warsaw and The Smithsonian Astrophysical Observatory, Cambridge, Massachusetts, 181-200.

Phillips, L. D., 1973. Bayesian Statistics for Social Sciences, Thomas Nelson and Sons Ltd., London, England.

Proceedings of the Ninth Annual Precise Time and Time Interval (PTTI) Applications and Planning Meeting, 1977. NASA Technical Memorandum 78104, Goddard Space Flight Center, Greenbelt, Maryland.

Rao, C. R., 1973. Linear Statistical Inference and Its Applications, John Wiley and Sons, New York, New York.

Rinner, K., 1966. "Systematic Investigations of Geodetic Networks in Space," U. S. Army Research and Development Group (Europe).

Rochester, M. G., 1973. "The Earth's Rotation," EOS, Transactions American Geophysical Union, Vol. 54, No. 8, 769-781.

Soler, T., 1977. "Global Plate Tectonics and the Secular Motion of the Pole," Report No. 252, Department of Geodetic Science, The Ohio State University, Columbus, Ohio.

Struik, D. J., 1967. A Concise History of Mathematics, Dover Publications, Inc., New York, New York.

Uotila, U. A., 1967. "Introduction to Adjustment Computations with Matrices," Lecture Notes, Department of Geodetic Science, The Ohio State University, Columbus, Ohio.

Uotila, U. A., 1973. "Sequential Solutions with Observation Equations," Lecture Notes, Department of Geodetic Science, The Ohio State University, Columbus, Ohio.

Vonbun, F. O., 1976. "Table 1. Lageos Orbit Elements," in a letter to COSPAR Committee on Satellite Laser Ranging. Goddard Space Flight Center, Greenbelt, Maryland.